BTN

Final Report

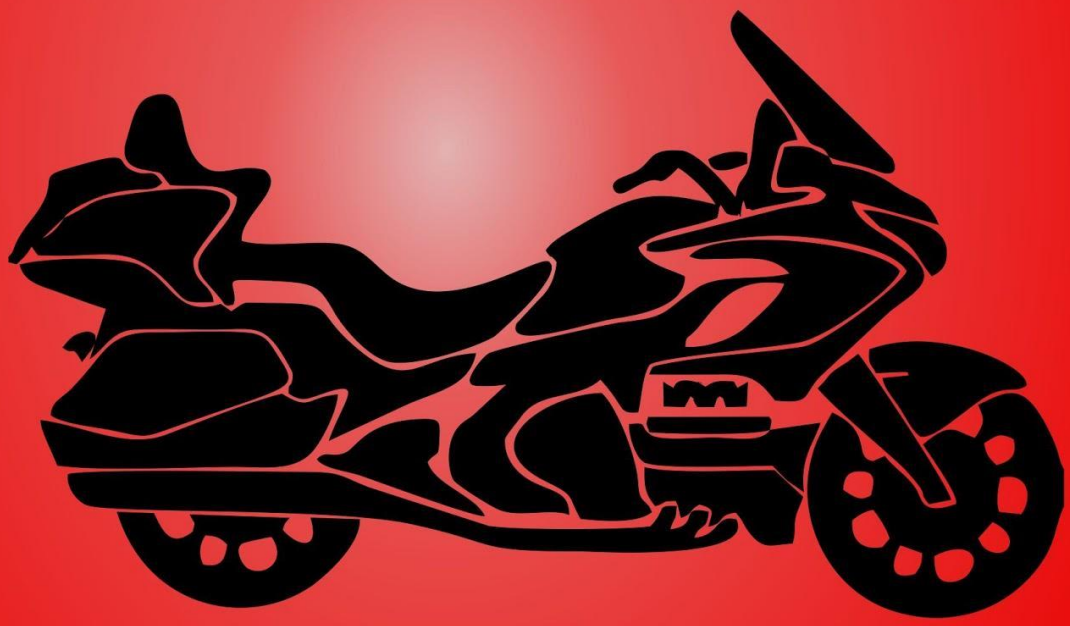

EMAE 360: Design & Manufacturing II

Professor:
Dr. Sunniva Collins

Teaching Assistants:
Genesis Mlakar
Matt Parulski
Alexander Yaney
Rhys Hamlet

Team Lead:
Alex Kushner

Project Manager:
Maja Paar

Group 1 Lead:
Owen Yang

Group 1 Members:
Sharad Mukerji
Sean Jose

Group 2 Lead:
Lydia Sgouros

Group 2 Members:
Peter Welter
Jackson White

Thermo Lead:
Carter Waligura

Thermo Member:
Joel Hauerwas

Table of Contents

1 - Project Introduction

1.1 - Executive Summary

Our team, BTN Performance, has been tasked to design a motorcycle engine for the Spartan Motorcycle Company (SMC). The BTN-1500E is designed for the sport touring market and will outpace competitors in terms of efficiency while maintaining respectable performance through the use of variable valve technology. The engine has an inline 3 cylinder configuration as well as a displacement of 1500 cc. It also has a square bore-to-stroke ratio and a compression ratio of 10:1 in order to maximize power and efficiency. The engine has a maximum power output of 103 kW (138 hp), maximum torque of 168 N-m (124 ft-lbs), and a redline at 8700 rpm.

1.2 - Goals and Objectives

The goal for this project was to design an engine for the Spartan Motorcycle Company's (SMC) new 2021 model. The estimated sales are at 7500 units in the first year, with 12,000 and then 15,000 units in the following two years. The engine brings unique features to the market including its discrete variable valve lift and variable valve timing which maximize efficiency compared to its competitors. The engine is configured to fit the engine envelope of many different sport touring motorcycles so that SMC can easily integrate it into their products.

The deliverables of this project include a detailed design, theory of operations, FMEA and cost estimates. All of these are thoroughly described in this report.

2 - Requirements and Scope

2.1 - Explicit requirements

BTN Performance was tasked with designing an engine that meets the following requirements:

1. 2 or more cylinders, 4-stroke cycle
2. Displacement 1500 to 1800cc
3. Fuel injection, spark ignition
4. Runs on standard gasoline
5. Compression ratio 9:1 to 10:1
6. Capable of 5000 rpm continuous service, idle at 800 rpm
7. Powers a six-speed transmission
8. Must meet all relevant specifications and standards for safety, fuel efficiency, noise and emissions

In addition to these, BTN strived to maximize fuel efficiency, minimize size and weight, and reduce production cost.

2.2 - Derived Requirements

Our derived requirements are listed below:

Assigned Requirements	Derived Requirements	Final Design
The system shall have spark ignition	No HCCI	No HCCI
The system shall run on standard gasoline	Must run on 87 octane	Runs on 87 octane
The system shall have a compression ratio of 9:1 to 10:1	9:1 - 10:1 compression	10:1 compression ratio
The system shall have a displacement of 1500 to 1800cc	1500-1800cc	1500 cc displacement
The system shall have 2 or more cylinders	2+ cylinders	3 cylinders
The system shall have a 4-stroke cycle	Otto/Atkinson Cycle	Otto/Atkinson cycle
The system shall have fuel injection	Direct or port injection	Port Injection
The system shall power a six-speed transmission	Powers a six-speed transmission	Powers a six-speed transmission
The system shall be capable of 5000 rpm continuous service	Redline higher than 5000 rpm	Redline at 8700 rpm
The system shall idle at 800 rpm	Idle at 800 rpm	Idles at 800 rpm
The system shall be safe	Meet NHTSA and SAE standards, ISO TC 70	Meets NHTSA, SAE and ISO TC 70 standards
The system design should minimize noise	CGS § 14-80a - 78 dB going below 35 mph/idle in soft site at 50 ft from centerline	Meets CGS § 14-80a
The system design should minimize emissions	§86.410-2006 - CO 12 g/km - HC + NOx 0.8 g/km	Meets §86.410-2006
The system design should maximize fuel efficiency	Over 17 km/l (40 mpg)	Fuel efficiency of about 50 mpg

The system design should minimize cost	Less than $10,000	$4811 final cost
The system design should minimize overall dimensions	Less than .75m x .75m x .75m	.583 x .466 x .332 m
The system design should minimize weight	Less than 110 kg	59.4kg
The system should be fun to drive	Above 90 kW (120 hp), 150 Nm (110 lb/ft)	103 kW (138 hp) 168 N-m (124 ft-lb)

Table 2.1: Derived Requirements

2.3 - Project Scope

In order to design an engine that meets all of our requirements, both purchased and designed parts have been integrated to form the complete the final product. The make versus buy decisions are as follows:

Make and Design	Design Only	Specify but not Buy	Buy Specifically
● Short block ● Camshaft ● Cylinder head ● Valve cover ● Rocker arms ● Sprockets ● Camshaft caps ● Crankshaft ● Valves ● Connecting rod ● Piston rings ● Etc.	● Valve Springs ● Head Gasket ● Bearings	● Oil Pump ● Oil ● Coolant ● Sensors	● Spark plugs ● Injectors ● Fasteners ● Sprockets ● Chain ● Tensioners ● Linear Actuators ● Coolant Pump ● Catalytic Converter ● Valve stem seals

Table 2.2: Make vs. Buy

The components were split into four categories: “Make and Design,” “Design Only, Specify but not Buy,” and “Buy Specifically.” The “Make and Design” components are designed by BTN and will also be manufactured in house. The “Design Only” parts are designed by us, but the manufacturing will be outsourced. The components that are “Specify but not Buy” have

been chosen by BTN but will not be provided with our engine. These components are also affected by other parts of the motorcycle. The “Buy Specifically” components have been specifically sourced and will be bought from other companies.

The components deemed as out-of-scope are as follows:

- Transmission
- Fuel pump
- Gas tank
- ECU
- TCU
- Chassis
- Production intake and exhaust manifold
- Catalytic converter
- Exhaust

These decisions were made based on time and complexity constraints. Since the project was to be completed within one semester, some components were left out of the scope and others were purchased in order to realistically be able to complete the design.

3 - Design Considerations

3.1 - Regulations

3.1.1 - Company/Road Safety

During the design phase the requirements and standards set by SMC and various United States organizations had to be considered. We will comply with all regulations set by the Occupational Safety and Health Administration (OSHA) as well as the National Highway Transit Safety Administration (NHTSA) and the standards as set forth in the Federal Motor Vehicle Safety Standards (FMVSS) in order to ensure company and road safety. We are also guided by ISO TC 70 for testing, ASTM for lubrication and materials, and JASO for oil standards.

3.1.2 - Emissions

Emissions are regulated by the Environmental Protection Agency (EPA) in the 40 CFR regulation. 40 CFR subpart F outlines the emission test procedures while 40 CFR 86.410-2006 states the emissions standards for vehicles after the year 2006. Our product will be used in a class III vehicle which means that we are restricted to 12 g/km CO emissions and 0.8 g/km (or 1.4 g/km with different averaging) HC + NO_X emissions.

3.1.3 - Noise

Noise is regulated by the EPA and local and state regulations. We decided to use the most restrictive regulations so that the product can be sold in any state in the United States. This means we are using Connecticut's noise regulations in CGS 14-80a of 78 dB going below 35 mph in soft site conditions at a distance of 50 feet from the centerline of the vehicle. Additionally, we meet the Low Noise Emission Product certification standards of 40 CFR 203 and 205 which permit only 71 dB in the same conditions.

3.1.4 - Product Liability

The product shall be sold with a 5 years or 30 thousand kilometers warranty, consistent with the standards of EPA. However, unintended uses of the product shall void this warranty. These may include modification of the engine (and unauthorized maintenance that may result in modification) as well as use of the engine outside of its intended use in a motorcycle. Proper labels about warranty, safety, and liability will be affixed to the product following the standards of 49 CFR Part 567.

4 - Market Identification

The sports touring market has a demand of approximately 75,000 motorcycles every year in the United States. This is based on a total of 500,000 motorcycles sold per year, with sports touring making up 15% of the market. This is a very large demand that is currently being met by competitors such as Harley Davidson, Polaris' Indian Motorcycle, and Honda. These companies have a steady customer base despite downward trends in motorcycle popularity and we believe there is space for competition in this market. The BTN-1500E by BTN Performance will set itself apart with outstanding efficiency and meet sales goals.

5 - Major Design Decisions

The following section describes some of the major design decisions made for the BTN-1500E. These were made early on since they influenced the overall engine design.

5.1 - Bottom End

5.1.1 - Displacement

As the engine name suggests, a displacement of 1500 cc was chosen due to its great size, efficiency and power. The Pugh chart below illustrates our decision process:

Characteristic	Weight (0-1)	1500	1600	1700	1800
Weight	0.15	10	7	4	1
Size	0.15	10	7	4	1
Efficiency	0.4	10	7	4	1
Power	0.3	1	4	7	10
SUM	1	7.3	3.75	4.9	3.7

Table 5.1: Pugh Chart for Engine Displacement

Based on this, we chose a bore and stroke of 86 and 86.1. The ratio decision is covered in the following section.

5.1.2 - Bore to Stroke Ratio

The bore to stroke ratio was chosen to be square since this had the best balance of criteria as listed below:

Characteristic	Weight (0-1)	Undersquare	Square	Oversquare
Efficiency	0.25	7	5	3
Red line	0.2	2	5	7
Thermal Stresses	0.1	7	6	3
Emissions	0.2	5	5	5

Good low end	0.1	8	6	3
Good high end	0.15	3	5	7
SUM	1	5.1	5.2	4.8

Table 5.2: Bore to Stroke Ratio Pugh Chart

5.1.3 - Compression Ratio

We chose a compression ratio of 10:1 because it had the best power and efficiency while minimizing emissions.

Characteristic	Weight (0-1)	9:1	9.5:1	10:1
Power	0.3	1	5	10
Efficiency	0.2	2	5	6
Emissions	0.1	10	4	1
Stress	0.4	7	5	3
SUM	1	4.5	4.9	6

Table 5.3: Compression Ratio Pugh Chart

5.1.4 - Cylinder Configuration

The team decided to go with an inline 3 configuration based on the Pugh chart below:

Characteristic	Weight (0-1)	Inline 2	Inline 3	Inline 4	V twin	V4/5	V6	Flat 2	Flat 4	Flat 6
Smoothness	0.18	1	7	5	2	4	6	7	8	10
Efficiency	0.25	7	5	3	7	3	1	7	3	1
Footprint	0.07	10	7	5	8	4	2	7	3	1
Design Complexity	0.04	9	8	7	6	5	4	3	2	1

Manufacturing Complexity	0.13	8	7	6	7	6	5	7	5	3
Performance factor	0.18	1	7	8	3	5	6	5	6	8
Cooling	0.05	3	5	7	4	6	7	4	6	8
Serviceability	0.1	7	7	7	5	5	5	3	3	3
SUM	1	8.28	9.54	8.64	7.56	6.84	6.48	7.74	6.48	6.3

Table 5.4: Cylinder Configuration Pugh Chart

5.2 - Top End

5.2.1 - Cam Configuration

A DOHC cam configuration was chosen due to its good performance. The Pugh chart for this decision can be seen below.

Characteristic	Weight (0-1)	Pushrod	Freevalve	Desmodromic/Arms	SOHC	DOHC
Performance	0.4	5	7	7	8	9
Complexity	0.3	4	4	3	8	9
Weight	0.1	3	4	7	9	9
Space	0.1	6	5	7	6	7
Cost	0.1	7	2	3	9	7
Total	1	4.8	5.1	5.4	8	8.6

Table 5.5: Cam Configuration Pugh Chart

5.2.2 - Valves per Cylinder

We decided to use four valves per cylinder since this offers high power, while having a relatively low cost.

Characteristic	**Weight**	**2 Valves**	**3 Valves**	**4 Valves**	**5 Valves**	**6 Valves**
Complexity	0.4	8	3	7	2	1
RPM	0.25	1	5	6	7	8

Power	0.25	3	5	6	7	8
Cost	0.1	8	6	8	6	5
Total	1	1.8	3.1	6.6	4.9	4.9

Table 5.6: Valves per Cylinder Pugh Chart

5.2.3 - Valvetrain Technologies

We chose to use both DVVL and VVT technologies for our engine. These increase the efficiency of the engine and add to the uniqueness of the design.

Characteristics	Weight	Variable Intake	DVVL	CVVL	VVT
Performance	0.3	3	6	7	6
Complexity	0.2	8	7	4	6
Reliability	0.2	8	7	5	7
Weight	0.1	6	8	5	7
Size	0.1	3	6	3	7
Cost	0.1	8	5	2	6
Total	1	5.8	6.5	4.9	6.4

Table 5.7: Valvetrain Technologies Pugh Chart

6 - Thermodynamic Analysis

6.1 - Combustion Analysis for Stoichiometric Conditions

In order to begin the thermodynamic analysis for our engine, we first had to define the target fuel to aim for. Due to a derived requirement regarding "standard gasoline," BTN Performance decided to use 87 octane gasoline for combustion in our engine. This type of gasoline is composed of 87% octane and 13% heptane. After combusting this substance, we get products of mostly CO_2, H_2O, and N_2. Balancing this reaction stoichiometrically we are left with:

$$0.87C_8H_{18} + 0.13C_7H_{16} + 12.2(O_2 + 3.76N_2) \Rightarrow 7.8CO_2 + 8.86H_2O + 44.63N_2$$

To obtain the air-to-fuel ratio (AFR) from this equation, we must break up the reaction into moles and molar masses.

Molecule	Molecular Weight (g/mol)
C_8H_{18} (octane)	114.2
C_7H_{16} (heptane)	100.2
O_2+3.76N_2 (air)	29.0

Table 6.1: Air to Fuel Molecular Analysis

Then, to calculate the air-to-fuel ratio with respect to mass (AFR_{mass}) we must first calculate it with respect to the number of moles of each reactant in the system (AFR_{mole})

$$AFR_{mole} = \frac{12.2 * (1 + 3.76) mole\ air}{(0.87 + 0.13)\ \ mole\ fuel} = 58.07$$

Now, by using the molecule weights listed in the Table 6.1 we can calculate the AFR_{mass} for stoichiometric conditions.

$$AFR_{mass} = AFR_{mole} \frac{29.0\ g/mol\ air}{0.87 * (114.2\ g/mol\ octane) + \ 0.13 * (100.2\ g/mol\ heptane)} = 14.9$$

Once we have solved for the stoichiometric AFR, we are able to accurately solve the combustion portion of the Otto Cycle. This AFR can also be updated in the future by dividing it by an equivalence ratio factor, ϕ. The equivalence ratio corrects the AFR when the engine is running rich (ϕ>1) at high load conditions and when it is running lean (ϕ<1) at low load conditions.

6.2 - Ideal Otto Cycle

6.2.1 - Overview

In order to start the thermodynamic analysis with relative ease, we decided to first analyze the Four Stroke Otto Cycle [1], a simple 4-step cycle commonly used to analyze internal combustion engines. The terms top dead center (TDC) and bottom dead center (BDC) will be utilized to describe the piston position at the smallest and largest cylinder volumes respectively. The values for this section were determined using FourStrokeOttoBTN.m and the trade studies were carried out using OttoCycleTradeStudy.m, both available for reference in Appendix E. Since this cycle is simplified in order to start working out initial engine characteristics, there were a number of assumptions that had to be made.

First, throughout all of the cycle analysis we assumed that the ambient air was at a temperature of 294K (~70 ^oF) and a pressure of 101.3 kPa. For this specific analysis, there had to

be large assumptions about the Otto Cycle processes themselves. We first assumed that the intake phase took in enough air to fill each cylinder fully with fresh air on each cycle. Then we assumed that the air experiences the full compression of the cycle, such that no air is able to escape from an open intake or exhaust valve. Next, we assumed that combustion is a one-step process that happens instantaneously as all of the reactants go to products. We also assumed that the exhaust phase was able to eject all of the products of the reaction for each cycle. Finally, we assumed that the specific heat ratio, γ, is a constant throughout this process. Later on when we look into the real Otto Cycle, all of these assumptions will be proven inaccurate, but for the case of simplicity they will do for now. Table 6.2 details the variables that we had to determine or approximate in order to complete the cycle analysis.

Symbol	Property
T	Temperature (K)
P	Pressure (kPa)
ρ	Density (kg/m^3)
R	Specific Ideal Gas Constant for Air (J/(kg-K))
rc	Compression Ratio
ɣ	Specific heat ratio
η_{Comb}	Combustion Efficiency
Q_{lhv}	Lower heating value for gasoline (kJ/kg)
C_p	Specific heat at constant pressure (kJ/kg)
C_v	Specific heat at constant volume (kJ/kg)
AFR_{mass}	Air-to-fuel ration (mass)

Table 6.2: Ideal Otto Cycle Units

6.2.2 - Phase 1: Intake

The intake phase is modeled as if atmospheric air fills the cylinder unchanged. This allows us to calculate an initial density which will change significantly during the compression phase. This phase generally occurs from TDC to BDC.

$$T_1 = T_o$$

$$P_1 = P_o$$

$$□_1 = \frac{□_1}{□□_1}$$

6.2.3 - Phase 2: Compression

The compression phase is the phase after the intake and after the piston reaches BDC. At this point, the intake valve closes and the piston compresses to TDC. This is an isentropic process because it is assumed to be adiabatic and reversible, with work transfer to the system of air.

$$□_2 = □_1 * □□$$

$$□_2 = □_1 * \left(\frac{□_2}{□_1}\right)^{□}$$

$$□_2 = \frac{□_2}{□_2□}$$

6.2.4 - Phase 3: Combustion

For this simplified ideal Otto Cycle analysis, combustion is assumed to occur instantaneously at TDC after compression. This process is modeled as a constant volume heat addition. During this process, the combustion efficiency is assumed to be a constant 0.8, however this assumption changes later in the detailed analysis.

$$T_3 = T_2 + \frac{\eta_{□□□□} * □_{□h□}}{□_□ * □□□_{□□□□}}$$

$$□_3 = □_2$$

$$□_2 = □_3□_3□$$

6.2.5 - Phase 4: Expansion

The expansion phase occurs directly after combustion at TDC and continues until BDC at which point all of the gases are ejected through the exhaust. This is also known as the power

stroke of the engine because it is when the combustion's heat is transformed into work. This phase, like compression, is assumed to be isentropic.

$$□_4 = □_1$$

$$□_4 = □_3 * \left(\frac{□_4}{□_3}\right)^{□}$$

$$□_4 = \frac{□_4}{□_4□}$$

6.2.6 - Findings

After running through this idea Otto Cycle analysis we were left with the following state points.

State	Temperature (K)	Pressure (MPa)
Intake	294	0.101
Compression	739	2.544
Combustion	3007	10.36
Expansion	1197	0.412

Table 6.3: Ideal Otto Cycle States

Important to note is that our compression temperature is lower than 87 octane's auto ignition temperature of 886K, so our engine would not experience any knock [2]. Also important to note is that these temperatures and pressures are still rather high, but we will see that they start to fall once we take into account realistic phenomena.

6.3 - Ideal Work and Power

6.3.1 - Overview

After finding the state points in the cycle, we can use these points to calculate the ideal work created by the cycle, and therefore, the ideal power at a reference RPM [1]. Below is a table of new properties needed to complete the analysis.

Symbol	Property
m_{air}	Mass of air (kg)
D	Total cylinder displacement (m^3)
C	Number of cylinders
ρ	Air density (kg/m^3)
rc	Compression ratio
T	Cylinder Temperature during combustion cycle (K)
c_v	Specific heat with a constant volume (J/kg)
V_{cyl}	Volume of cylinder (m^3)
W_s	Specific Work (J/kg)
W_T	Total Work (J)
Pw_T	Total Power (W)
N	Revolutions per Minute of Crankshaft
τ	Torque (N-m)

Table 6.4: Ideal Otto Cycle Work and Power units

First the maximum mass of air in the cylinder must be calculated.

$$V_{cyl} = \frac{D}{C} * \frac{rc}{rc - 1}$$

$$m_{air} = V_{cyl} * \rho_1$$

From here, we calculated final work by looking at the temperature differences between the compression (work in) and expansion (work out) stages.

$$W_s = c_v * ((T_3 - T_2) - (T_4 - T_1))$$

$$W_T = m_{air} * W_s * C$$

After calculating work, we can transform this into power produced by the engine per cycle through utilizing the engine RPM.

$$Pw_T = \frac{W_T * N\frac{rev}{min}}{60\frac{sec}{min} * 2\frac{rev}{cycle}}$$

Then, if the desired output is to be in horsepower (hp) for clarity, the P_T answer can be multiplied by a factor of 0.00134 to take it from watts to horsepower.

Finally, torque can be calculated through the following relation.

$$\tau = \frac{Pw_T}{N\frac{rev}{min} * 2\pi\frac{rad}{rev}}$$

For the case of ideal Otto Cycle, the power curve will end up being linear with RPM, which means that the engine torque will be a constant. This same relationship is later used to construct a power-torque curve for an Otto Cycle analysis with inefficiencies.

6.3.2 - Ideal Cycle Results

Through completing this ideal Otto Cycle analysis, some very important trades were able to be made that helped with determining engine characteristics. For example, below in Figure 6.1, taken from OttoCycleTradeStudy.m there is a trade of engine power vs compression ratio and displacement. This graph shows that we would be able to get enough power out of the engine at low displacement while maximizing compression ratio for efficiency purposes. This follows our goal of designing an engine to be very powerful at high load conditions and very efficient at low load conditions.

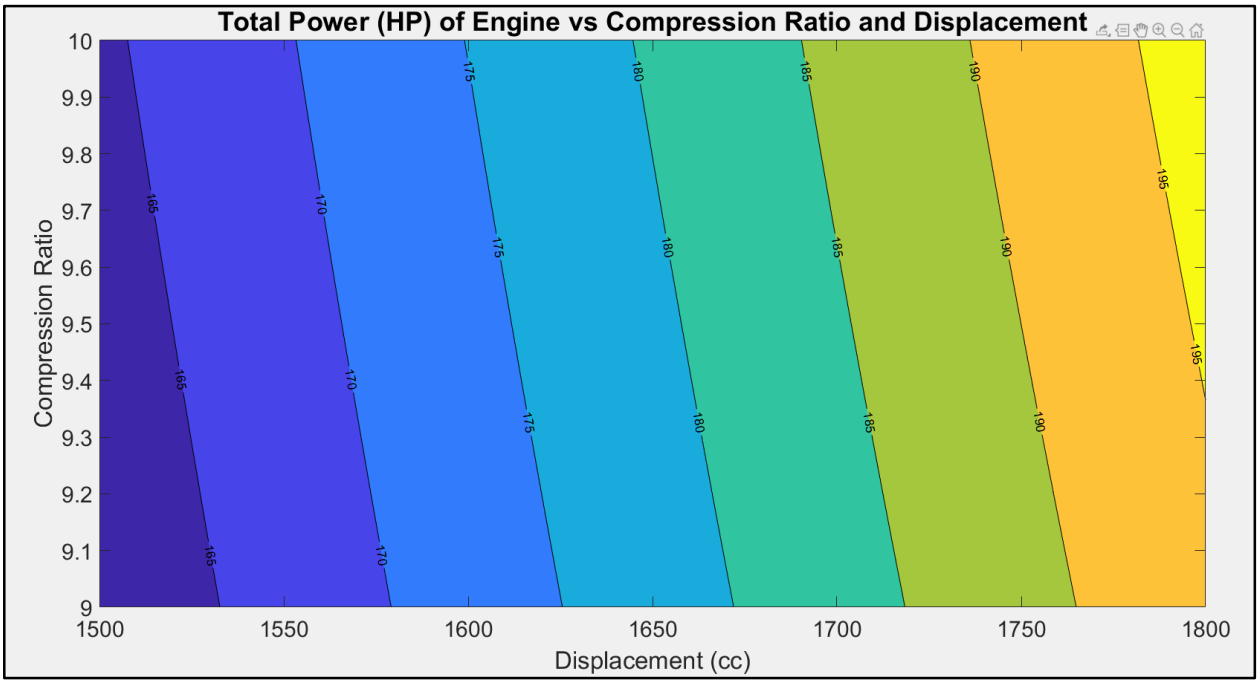

Figure 6.1: Compression Ratio and Displacement Trade Study

6.4 - Mechanical Redline Limit

6.4.1 - Overview

After completing the initial Otto Cycle and determining characteristics like compression ratio and displacement, we then focused on some trade studies that could help us determine other characteristics like bore, stroke, crank arm length, and other mechanical characteristics.

Symbol	Property
b	Cylinder Bore (mm)
bs	Bore to stroke ratio
s	Stroke
N	Engine RPM (rev/min)
Sp_{avg}	Mean piston speed (m/s)

Table 6.5: Mechanical Redline Units

Through use of the following equation, we were able to calculate the mean piston speed ratio for our engine assuming a bore to stroke ratio. According to Heywood, the mean piston speed should stay below 25 m/s in order to prevent catastrophic mechanical failure [1].

$$Sp_{avg} = \frac{s * 2 * N}{60}$$

6.4.2 - Trade Study and Selection

After getting this relation, we were able to trade bore to stroke ratio with mean piston speed in order to help determine the correct bore and stroke for our engine with the desired redline.

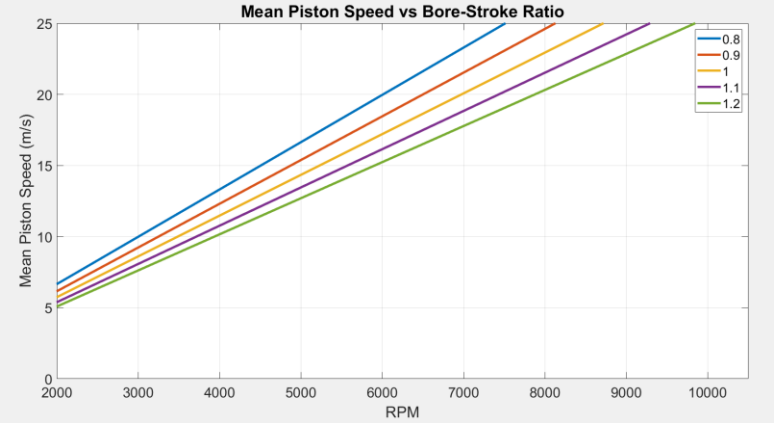

Figure 6.2: Bore - Stroke Ratio Trade Study

With our target redline being around 9000, we decided to go with a bore to stroke ratio of 1. This decision led our redline to be about 8800 RPM based on the graph below.

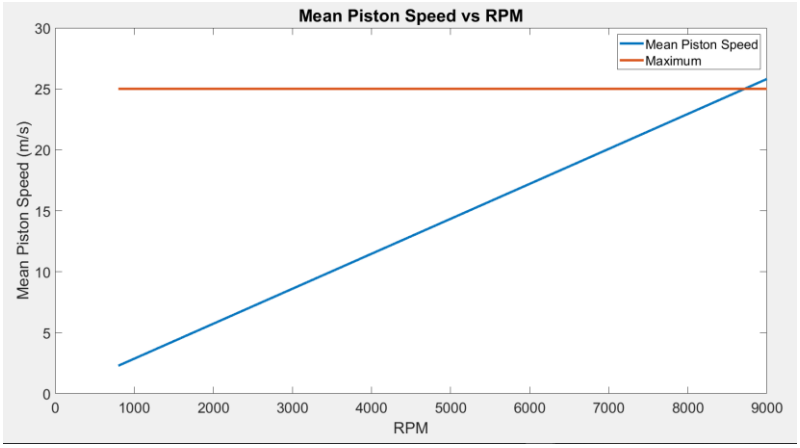

Figure 6.3: Plot Showing Mechanical Redline

6.5 - Properties Varying with Crank angle

6.5.1 - Overview

Now that a few engine parameters were determined through thermodynamic trade studies, we are then able to increase the fidelity of analysis by taking away the assumptions of instantaneous combustion and constant gammas. These changes allowed us to more accurately see the state values of our engine during the time of conceptual design, and we were able to use the functions again once we started to include inefficiencies.

Symbol	Property
θ	Crank Angle (radians)
θ_s	Start of fuel burn (radians)
θ_d	Duration of fuel burn (radians)
x_b	Cumulative Burn Fraction
a	Weibe efficiency factor
n	Weibe form factor
q	Dimensionless total heat release coefficient

Table 6.6: Crank angle units

6.5.2 - Volume

The first step to getting properties varying with the crank angle is to get a function for volume in order to determine other variables dependent on volume. This function for volume can be found in VolumeCalc.m which may be referenced in Appendix E. Below is a graph output using this function in order to visualize how volume and piston speed vary with crank angle.

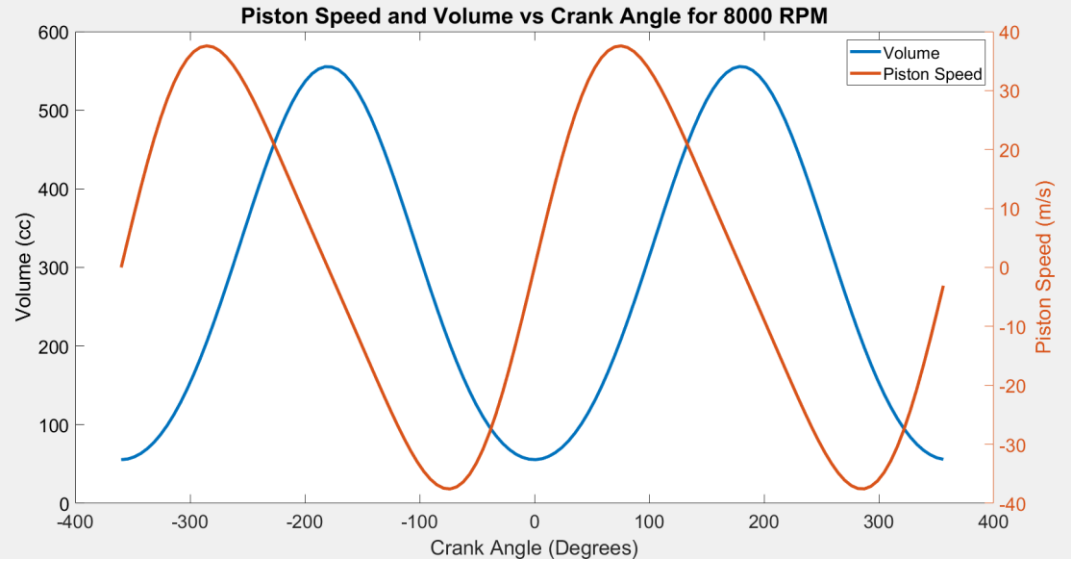

Figure 6.4: Plot of Cylinder Speed and Volume Functions

6.5.3 - Specific Heat Ratio (Gamma)

The next step in improving the accuracy of the analysis is to change the specific heat ratio, γ, with respect to temperature. To do this, we utilized Matlab code written in the Ferguson textbook [3]. Both functions are called in the program GammaCalc.m also shown in Appendix E. This γ calculation function calls two Ferguson functions that calculate γ at two different conditions. The first function, farg.m, calculates γ at low temperatures, or when the air gas mixture is unburnt. The other function, ecp.m, calculates γ at high temperature, or when the air-gas mixture is burnt. Since these two mixtures are composed of different gas compositions, it is important to make this distinction when calculating γ. Each γ calculation function from Ferguson includes tables of data for 87 octane gasoline at different temperature and pressure conditions as is represented in farg.m and ecp.m in Appendix E. The output of this code, shown below in Figure 6.5 is utilized in the weub function code to more accurately determine the ranges of temperatures and pressures that the engine experiences.

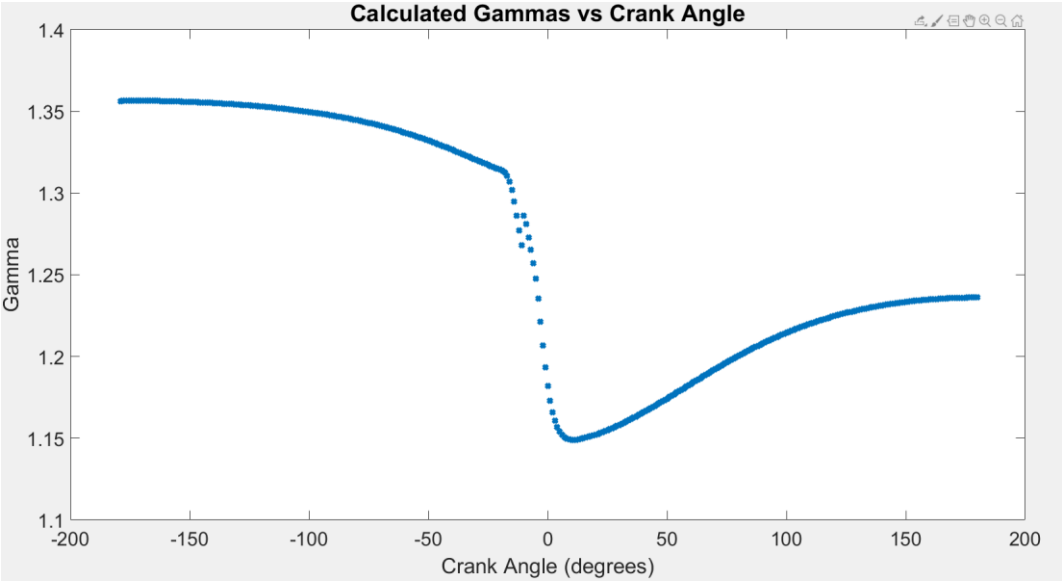

Figure 6.5: Specific Heat Ratio versus Crank Angle

6.5.4 - Weib Burn Function

In the ideal Otto Cycle, it is assumed that all of the chemical potential energy in fuel is instantly burned at a constant volume to produce work. Obviously, there must be some time for the combustion of the fuel-air mixture to completely propagate through the combustion chamber. The Weib Function accounts for this time by looking at temperature and pressure as differentials instead of instantaneous changes.

The first part of the Weib Function is the cumulative burn fraction. This function, shown below, allows us to understand how much of the fuel is burned by assuming a Wieb efficiency parameter, a, and Weib form factor parameter, n, given as 5 and 3 respectively in Ferguson as good estimates [3]. These assumptions allow us to relate burn fraction of fuel in regards to the crank angle, and also account for parts of the mixture that are unburnt. The Weib function is a much more efficient way of modeling flame propagation in the cylinder, since our alternative would be doing some type of simulation, which seemed out of scope for the project.

$$x_b = 1 - exp\left[-a * \left(\frac{\theta - \theta_s}{\theta_d}\right)^n\right]$$

After understanding the burn fraction equation, we could then combine this with our specific heat release coefficient. This will give us the amount of heat release corresponding to crank angle.

$$\frac{dq}{d\theta} = na\frac{q}{\theta_d} * (1 - x_b)\left(\frac{\theta - \theta_s}{\theta_d}\right)^{n-1}$$

Once we have the energy modeled, we can then relate the above two equations to physical properties of our system like temperature and pressure. These relations are outlined in detail in a modified Matlab script found in Ferguson, FiniteHeatReleaseBTN.m. Below are two outputs of the Matlab function which show how the temperature and pressure change with crank angle when you involve the mass burn fraction. Important to notice is how temperatures and pressures do not get as high as they previously did in the absolute ideal cycle. This is because not all of the combustion is happening at TDC, so we are not utilizing all of the compression work done by the system.

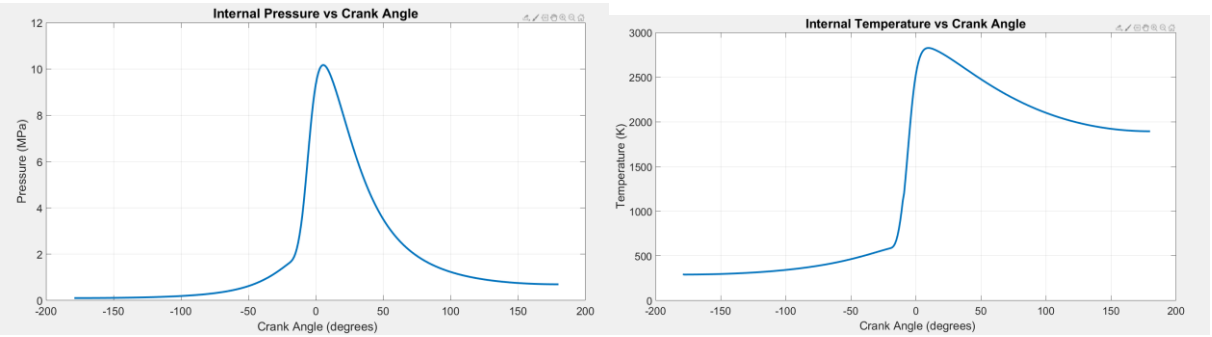

Figure 6.6: Pressure During Four-Stroke Engine Cycle (Left), Temperature During Four Engine Cycles (Right)

6.5.4.1 - Spark Timing

The spark timing above occurs at 30 degrees TDC, and while we did not do much optimization with this value we realize that the timing of this spark is very important. As outlined in Figure 6.7 below the spark timing can have effects on anything from the MBT (mean best torque) to the BSHC (brake-specific exhaust emissions for hydrocarbons).

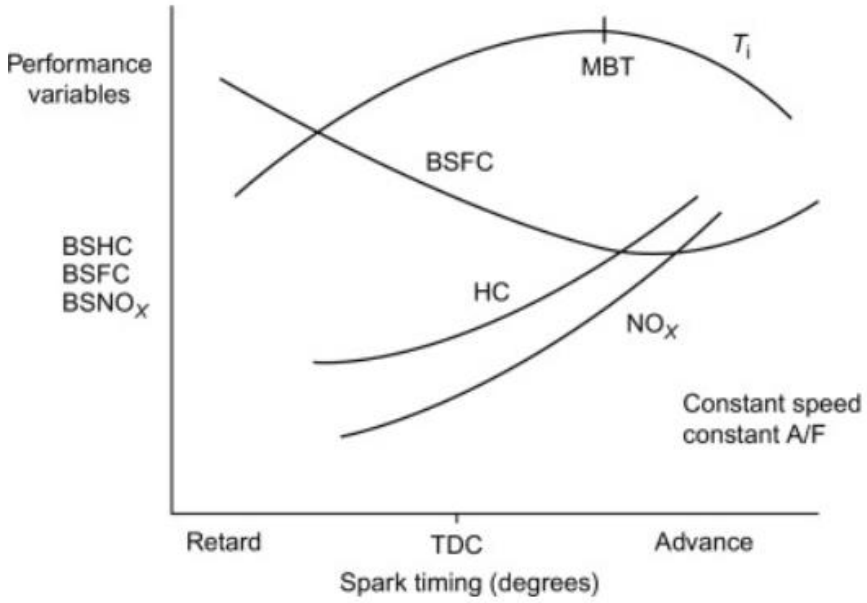

Figure 6.7: Spark Timing Diagram [4]

While the property of spark timing would have been useful to model, to do so is very complex. Usually, an experimental apparatus is necessary to fully understand the effects because of the complex flame speed in the cylinder. The spark-timing is almost completely based off of the flame speed which varies with the changing pressure of the cylinder [4]. Without combustion modeling tools, there was no accurate method for us to optimize the spark timing farther than it already is. In reality, both the spark timing and the equivalence ratio would be tuned, or calibrated, for all engine operating loads and conditions.

6.6 - Air Modeling

6.6.1 - Overview

This part of the thermodynamic analysis details the process of creating a model to predict how various designs of valves and cams affect the performance of our engine. To be brief, the goal of air modeling is to boil down all of the results to obtain a volumetric efficiency for a valve geometry at a specified engine RPM. As is shown, this process is anything but brief, and extensive care must be taken in the analysis to ensure the credibility of the results. Note that all of the calculations carried out below are done twice. Once for the intake valve and once for the exhaust valve.

Symbol	Property

θ	Crank angle (degrees)
θ_{op}	Valve lift open angle
θ_{cl}	Valve lift close angle
θ_{dur}	Valve lift duration
i	Properties that have to do with the intake valve
e	Properties that have to do with the exhaust valve
D	Valve diameter (m)
D_s	Valve stem diameter (m)
D_v	Valve head diameter (m)
w	Valve seat width (m)
D_m	Valve mean seat diameter (m)
□	Valve seat angle (degrees)
L_v	Valve lift (m)
A_m	Minimum flow area (m^2)
C_D	Flow Coefficient
T_{cyl}	Temperature in cylinder (K)
P_{cyl}	Pressure in cylinder (kPa)
P_o	Stagnation Pressure (kPa)
T_o	Stagnation Temperature (K)
ρ_o	Stagnation Density (kg/m^3)
c_o	Stagnation speed of sound (m/s)
R	Ideal Gas Constant (J/kg-K)
$\dot{m}$	Mass flow rate (kg/s)

Table 6.7: Air Flow Variables

6.6.2 - Valve Lift

The first step in air modeling is to determine a valve lift profile [1]. From a thermodynamic standpoint, a good starting point for a valve lift profile would be a second order polynomial with zeros at the points that your valve would open and close. This polynomial would be multiplied by the maximum lift, L_v (max), in order to achieve the correct lift function.

$$\theta_{cl} = \theta_{op} + \theta_{dur}$$

$$L_v(\theta) = -L_v(max) * (\theta - \theta_{op}) * (\theta - \theta_{cl})$$

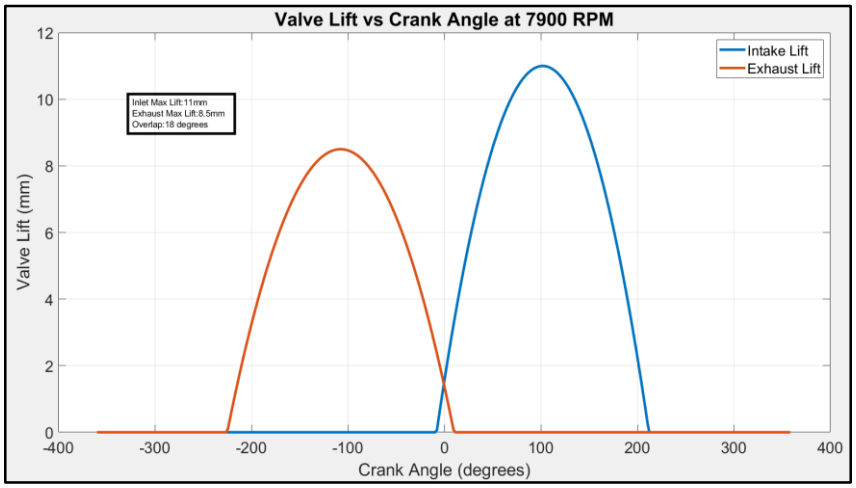

Figure 6.8: Initial Valve Lift Profile

After some feedback from the mechanical design team, this valve lift profile had to be edited in order to reduce unnecessary jerk and forces on the valves. While this change affects the thermodynamics minimally, a 6th order polynomial was decided on that caused the valve lift to change shape as shown below.

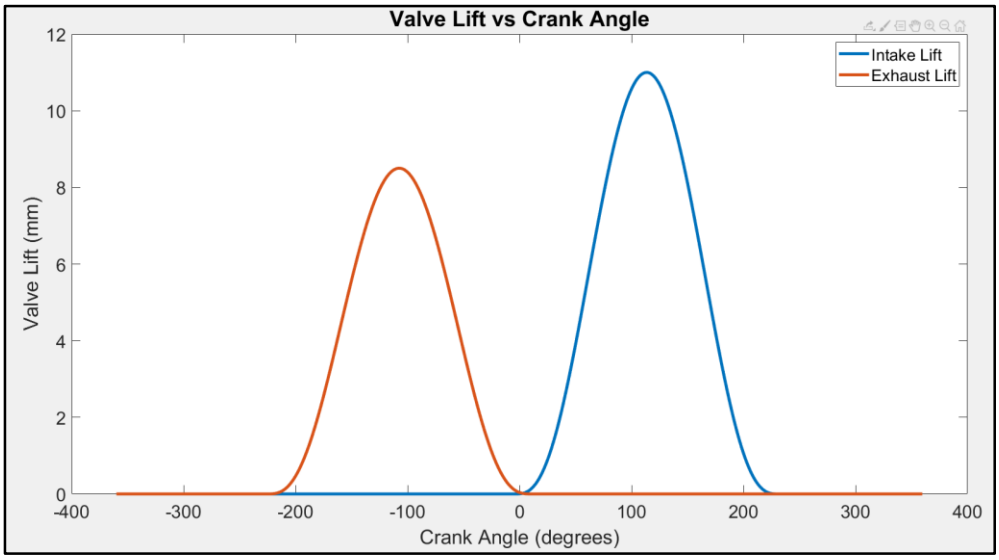

Figure 6.9: Final Valve Lift Profile

6.6.3 - Minimum Flow Area

After determining initial valve lift values based on a recommendation in Heywood, and receiving optimized valve diameters from the mechanical team, we could now begin defining new characteristics of the valves through relations provided in Heywood [1]. These valve characteristics are very important in determining how much air flow can get through the valves on any given cycle.

$$D_s = \frac{D}{4}$$
$$D_v = 1.1D$$
$$w = \frac{D_v - D}{2}$$
$$D_m = D_v - w$$

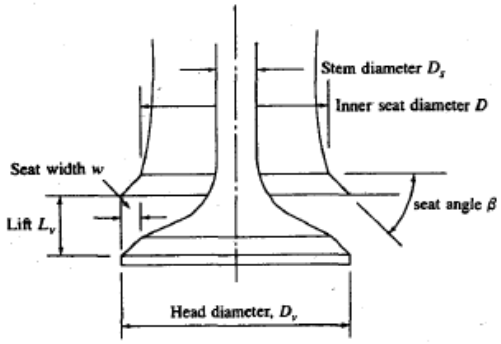

Figure 6.10: Basic Valve Shape [1]

Now that values are known for the valve geometry, we can start looking at the flow effect of these different geometries to see if we can maximize it in any way. To do this, we next looked at the minimum flow area versus the crank angle for our valve design. According to Heywood, the minimum flow area is broken up into three sections. The first two sections depend on the frustum of a right circular cone which touches the seat in two different ways, and the third area depends on the difference between the port area and stem area [1].

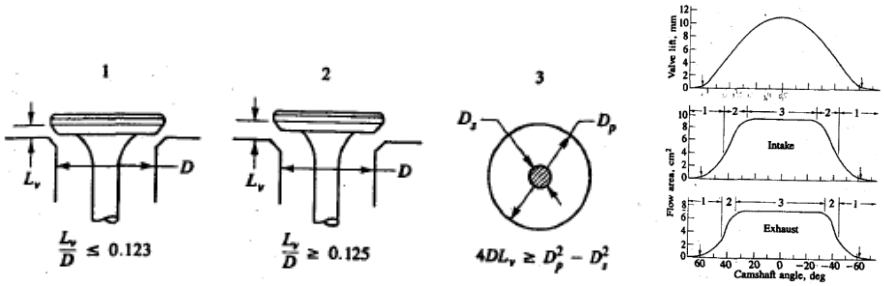

Figure 6.11: Additional Valve Properties [1]

$$A_{m1} = \pi L_v cos(\beta) * \left(D_v - 2w + \frac{L_v}{2} sin(2\beta)\right)$$

$$A_{m2} = \pi D_m * [(L_v - wtan(\beta))^2 + w^2]^{1/2}$$

$$A_{m3} = \frac{\pi}{4} * \left({D_p}^2 - {D_s}^2\right)$$

Using these equations during the right moments in the valve lift, as it is outlined in AirFlowModelBTNFinal.m in Appendix E, we acquired data for minimum flow area versus crank angle for a given cycle. Plotting the data we got the graph shown below.

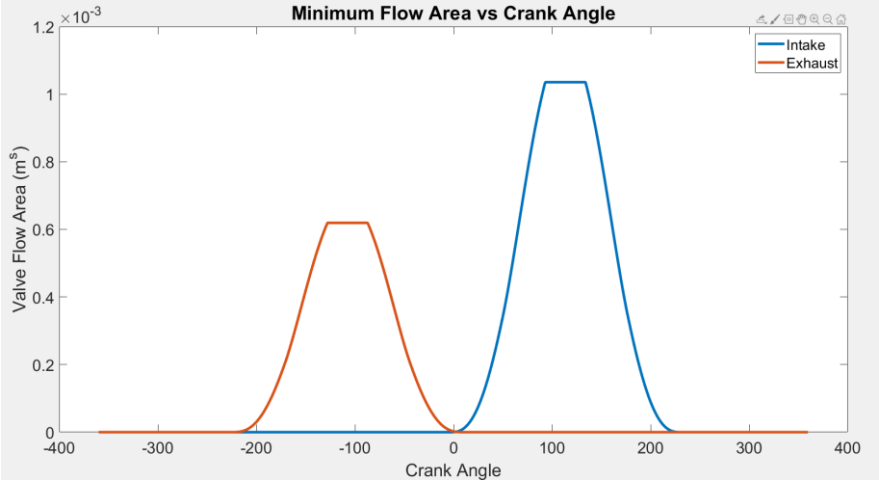

Figure 6.12: Inlet and Exhaust Minimum Area Profiles

6.6.4 - Flow Coefficient

The next necessary step in correctly modeling the air flow is to understand how flow coefficient through the valves changes with variables such as crank angle and valve lift [1]. These values are one of the main differentiating factors for intake and exhaust valves, because the flow behaves differently when flowing into or out of the cylinder. Both of these trends were taken directly from Heywood and were created using the Matlab polyfit feature.

For intake valves, the flow coefficient is controlled by how well the flow is jetting [1]. This correlation depends solely on the ratio between lift and valve head diameter. Much like the minimum flow area, there are three regions that correspond to this trend. At low lift, the flow remains attached to the valve head and the seat, which allows for a smooth jetting. This results in a rather high flow coefficient. Then, once the lift becomes too high, into the intermediate range, the flow becomes separated from the valve seat and is only attached to the valve head. There is still jetting that occurs here so the flow coefficient curve looks similar to how it did before. Finally, the flow becomes separated from the valve head and seat. At this point the flow area remains constant and jetting significantly reduces so the flow coefficient begins to drop.

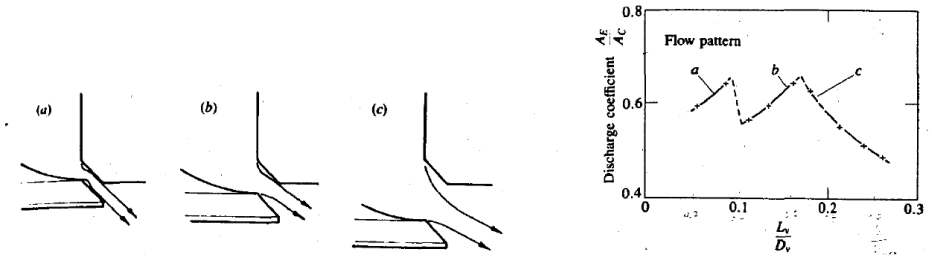

Figure 6.13: Effects of Jetting on Valve Airflow

For exhaust valves, the flow coefficient also depends on the ratio between lift and valve head, however, for slightly different reasons [1]. While the inlet valves have three discontinuous curves to model the discharge coefficient, the exhaust curve only has one, and it depends on the geometry in the exhaust manifold. At low lifts, the flow is able to swirl and be sucked out of the cylinder more, while at high lift, the flow again separates and the flow coefficient drops as a result. To maximize this flow coefficient over the entire lift range, we decided to go with the design associated with “d” in Figure 6.14.

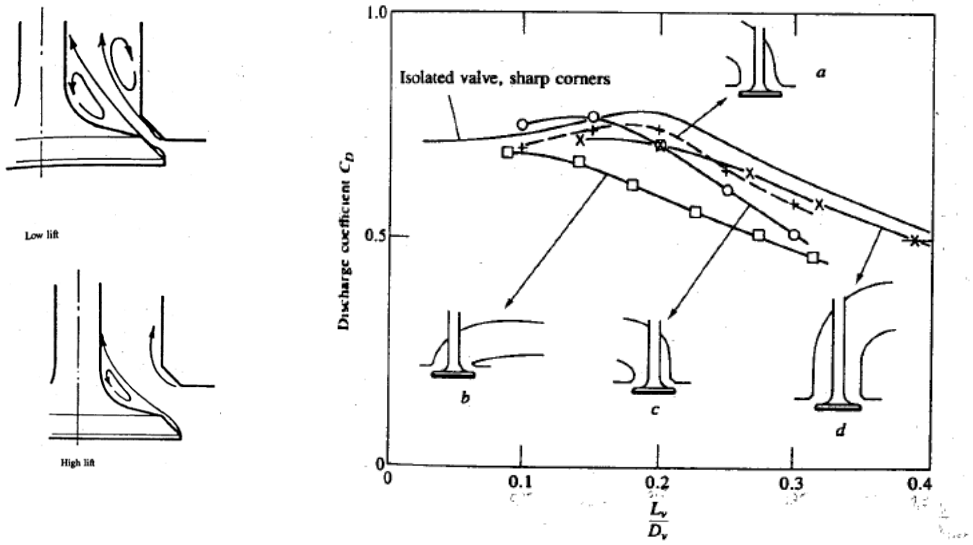

Figure 6.14: Effect of Swirling on Cylinder Airflow

Since lift changes with crank angle, we can then create a vector of flow coefficients that depends on crank angle. Plotting this data, we get the graphs shown below. Important to note is that the inlet C_d is full of discontinuities, much like the graph it is made from, whereas the exhaust graph is much more smooth.

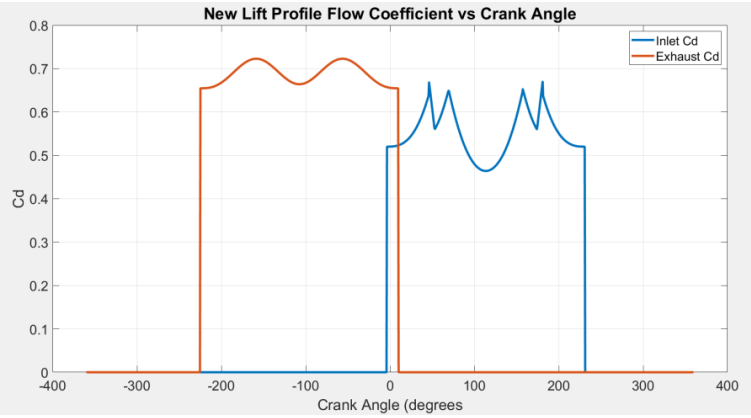

Figure 6.15: Lift Profile Accounting for Dynamic Airflow

6.6.5 - Mass Flow

Now that we have developed a model for the valve lift, minimum valve flow area, and flow coefficient, we can use all of these values, along with pressures values obtained from FiniteHeatReleaseBTN.m in order to calculate the total mass flow rate of air for a given cycle. During this process, ideal gas properties were assumed to relate pressure and density among other properties. While the equations for intake and exhaust are very similar, there are some key differences as to which pressure to use that are important to note.

6.6.5.1 - Exhaust

First, we modelled exhaust because it was the phase that we knew could start with known initial conditions of a cylinder initially full of burned products. Notice that we multiplied our mass flow by two in order to account for having two exhaust and two intake valves in each cylinder. When the exhaust valves are open, the flow will normally flow out as long as $P_{cyl}>P_{oe}$ [1].

$$\dot{m}_e = -\frac{2C_{De}A_{me}P_{cyl}}{\sqrt{RT_{oe}}} * \left(\frac{P_{oe}}{P_{cyl}}\right)^{1/\gamma} * \left[\frac{2\gamma}{\gamma-1} * \left(1-\left(\frac{P_{oe}}{P_{cyl}}\right)^{\frac{\gamma-1}{\gamma}}\right)\right]^{1/2}$$

If the pressure inside the cylinder became less than the stagnation pressure in the exhaust manifold, then the flow would reverse and the equation would change as it is shown here.

$$\dot{m}_e = \frac{2C_{De}A_{me}P_{oe}}{\sqrt{RT_{oe}}} * \left(\frac{P_{cyl}}{P_{oe}}\right)^{1/\gamma} * \left[\frac{2\gamma}{\gamma-1} * \left(1-\left(\frac{P_{cyl}}{P_{oe}}\right)^{\frac{\gamma-1}{\gamma}}\right)\right]^{1/2}$$

6.6.5.2 - Intake

Next, we modeled the intake flow into the cylinder. P_{cyl} is the same continuous vector as in the exhaust calculation. This means that in if $P_{oi}>P_{cyl}$ then the air will flow into the cylinder.

$$\dot{m}_i = \frac{2C_{Di}A_{mi}P_{oi}}{\sqrt{RT_{oi}}} * \left(\frac{P_{cyl}}{P_{oi}}\right)^{1/\gamma} * \left[\frac{2\gamma}{\gamma-1} * \left(1-\left(\frac{P_{cyl}}{P_{oi}}\right)^{\frac{\gamma-1}{\gamma}}\right)\right]^{1/2}$$

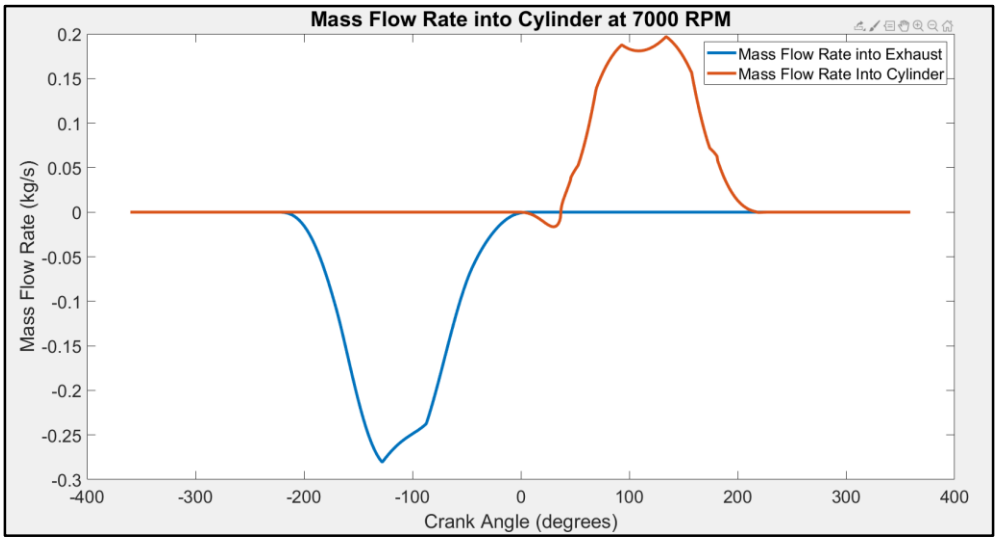

Figure 6.16: Mass Flow for Intake and Exhaust

If the pressure in the cylinder is too great, as it normally is at the initial inlet valve open, then there will be reverse flow.

$$\dot{m}_i = -\frac{2C_{Di}A_{mi}P_{cyl}}{\sqrt{RT_{oi}}} * \left(\frac{P_{oi}}{P_{cyl}}\right)^{1/\gamma} * \left[\frac{2\gamma}{\gamma-1} * \left(1 - \left(\frac{P_{oi}}{P_{cyl}}\right)^{\frac{\gamma-1}{\gamma}}\right)\right]^{1/2}$$

6.6.5.3 - Choked

For both the intake and exhaust cases (but mostly the exhaust), the pressure difference between the cylinder and stagnation condition can become so great that the air flow can not move fast enough. Once the flow into the cylinder reaches the speed of sound then the flow becomes choked. Choking the flow causes a significant mass flow drop as is represented in the equation below [1].

$$\dot{m}_{choked} = -\frac{2C_D A_m P_o}{\sqrt{RT_o}} \gamma^{1/2} * \left(\frac{2}{\gamma+1}\right)^{\frac{\gamma+1}{2(\gamma-1)}}$$

It was a design requirement to try to reduce choked flow as much as possible through valve design. Figure 6.17 shows that at 7000 RPM the pressure starts to rise very minimally in our current design. In order to choke, this pressure increase would have to be much more significant.

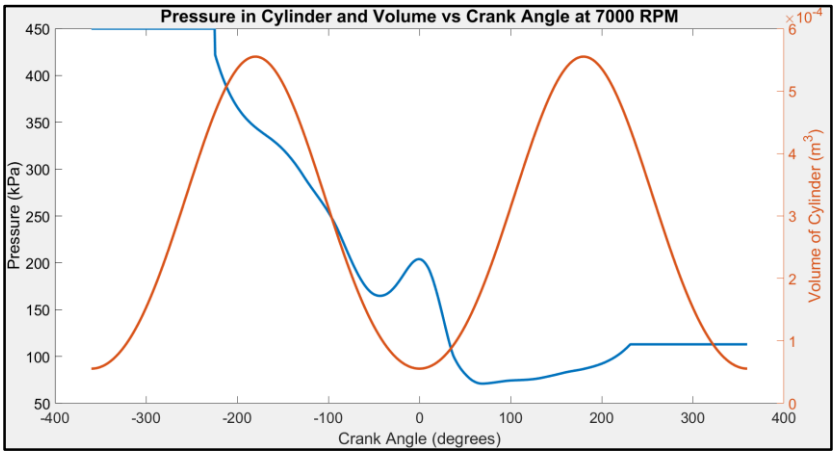

Figure 6.17: Plot of Relation of Pressure and Volume

6.6.6 - Mass in Cylinder

Once we have the total mass flow as a function of crank angle, we can determine how efficient our valves are at getting the mass of air into and out of the cylinder. This was done as a numeric integral, where we would take a small crank angle section, turn it into a small unit of time through relating it to the current engine RPM, and add or subtract small increments of mass for each time step. We would then use the ideal gas law to calculate the new density, pressure, and temperature in the cylinder for the incremental mass accounted for using conservation laws. This process can be clearly seen in AirModelBTNFinal.m in Appendix E.

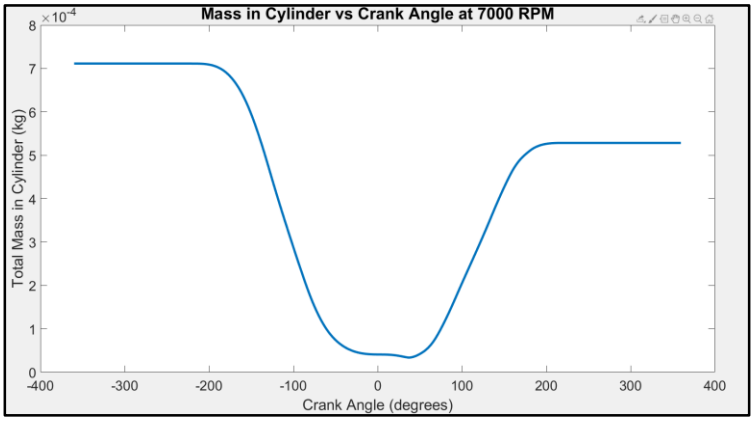

Figure 6.18: Mass Flow for Intake and Exhaust

6.7 - Variable Valve Technology

6.7.1 - Overview

Variable valve technology (Vtech) has countless opportunities to improve the thermodynamics of an engine. With the current thermodynamic engine model that we have developed so far, we are limited in the applications of Vtech, however there still are some very good prospects. Through completing trade studies of the current model we can see that there is some optimizing that can be done. We can look at low load, low rpm scenarios, like cruising. At these conditions, power is not as important because you would not be operating at full throttle. In this case you could sacrifice some of the power of the engine for better thermodynamic efficiency or fuel economy. Another option would be looking at the high load, high rpm conditions. At these conditions we would want to maximize torque and power to try to get the most out of our engine. There are many methods of doing this, but the one we explore using Vtech is to simply find ways to get more air into the engine.

6.7.2 - Variable Valve Timing (VVT)

Variable valve timing is the process of phasing the camshaft in some way so that either the exhaust or intake valve timings are differed. While this is very complex mechanically, this section will just discuss the thermodynamic benefit. Mechanical design will be specifically considered in a later section. Our plan is to utilize VVT at low load and low RPM conditions. Like discussed above, this would be done at cruising conditions in order to maximize fuel efficiency [8]. We accomplish this task thermodynamically by phasing the inlet cams 15^{o}. Through moving the inlet cam to a later starting time in the crankshaft, while keeping the lift profile identical, we operate more in the Atkinson Cycle. The Atkinson cycle is very similar to the Otto cycle, but it keeps the inlet valve open some time into the compression stage. While this reduces the overall power that the engine produces, it allows us to squeeze more work out of the gasoline that we are using to power the engine. Therefore, by phasing the inlet valve to start later, we are able to achieve a slight improvement in specific power. While the graph below shows only a marginal benefit, we believe that experimentally this benefit of using Atkinson Cycle at low load, low RPM conditions would be much more pronounced since our thermodynamic model ignores many phenomena including the flow in the intake manifold.

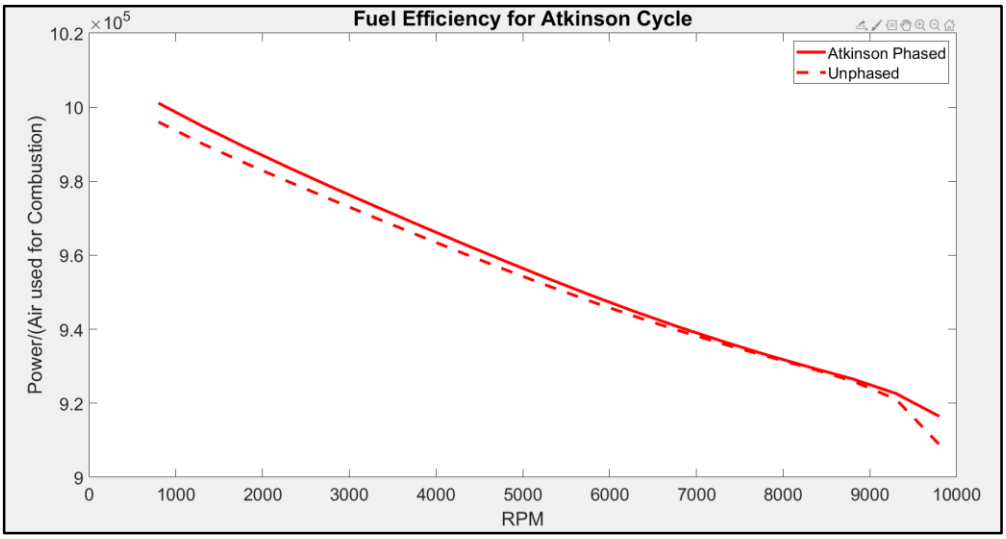

Figure 6.19: Benefits of Atkinson Cycle Phasing

6.7.3 - Variable Valve Lift (VVL)

Variable Valve Lift is the process of having a second set of cams on the cam shaft which the engine can switch to at specific conditions. Generally in VVL engines, there is a low RPM cam and a high RPM cam that can be switched between using complex mechanical features. Again, the thermodynamic impact will be discussed here while a later section will focus on mechanical implementation. In most cases of VVL, only the inlet cam is considered because it's valve curve properties have the largest outcome on overall engine efficiency. Since RPM is the major factor in determining which lift curves to use, VVL works very well with the thermodynamic model we have built. In order to maximize volumetric efficiency, discussed in more detail later in the analysis, across the entire RPM range, we can break up the RPM range into low and high sections, and analyze these sections separately. This way, we can determine the optimal lift curve for each condition and we can manufacture our cams in such a way to get the best performance out of the engine.

We completed these trade studies over high and low RPM ranges in order to maximize valve lift, duration, and timing for each cam configuration. Figure 6.20 below represents two trade studies completed to pick the duration for the small cam and the lift for the large cam respectively.

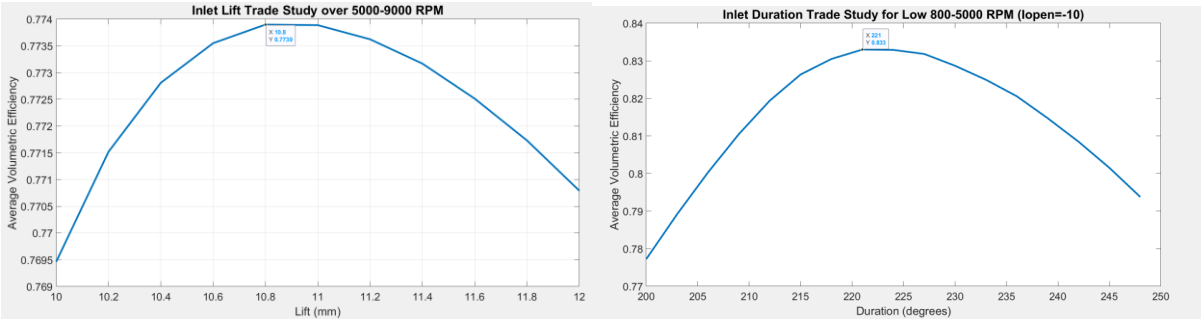

Figure 6.20: Thermo Trade Studies

As you can see, both of these decisions maximize the average volumetric efficiency. These trade studies were run through twice each in order to ensure accuracy, because a bad initial guess could have resulted in skewed results in another factor. These trade studies were also run for the exhaust valve over the entire RPM range in order to ensure that the exhaust valve's properties were maximized with respect to the inlet valve's properties.

In the end we determined the follow cam characteristics for the exhaust and both inlet cams as seen in Table 6.8.

	Large Inlet	Small Inlet	Exhaust
Lift (mm)	10.9	8.5	8.5
Duration (degrees)	235	220	235
Opening (degrees)	-4 before TDC	-8 before TDC	-45 before BDC

Table 6.8: Lift Angles Determined by Trade Studies

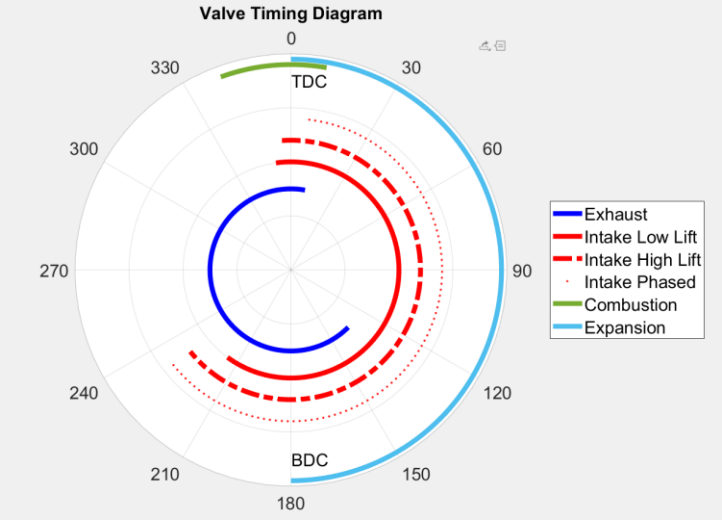

Figure 6.21: Visual Representation of Valve Timing

6.8 - Lubrication

In order to size the oil pump, the required oil flow rates through the engine were determined for startup, cruise, and redline. The most critical components for oil flow are the journal bearings and calculations for the main, rod, and cam journals were performed using the

method described in *Machine Component Design* [5]. An example of the properties and calculations for redline and maximum loading condition is shown in Table 6.9 below.

	Radius (mm)	Film Thickness (mm)	Clearance (mm)	Width (mm)	Max Load (N)	Temp (C)	Visc. (Pa)	Speed (rpm)	Sommerfeld	Flow Variable	Flow	Qs/Q	Flow to Replace
Main Journal	32.25	0.0015	0.02	23.7	34000	100	0.0119	9000	0.208147	5.9	13528.55	0.88	1623.42
Rod Journal	25.8	0.0012	0.02	27	34000	100	0.0119	9000	0.121410	5.8	12120.84	0.82	2181.75
Intake Cam Journal	30	0.0014	0.04	16	4154	100	0.0119	9000	0.231456	6.1	17568	0.9	1756.8
Exhaust Cam Journal	30	0.0014	0.04	16	3334.2	100	0.0119	9000	0.288369	6.1	17568	0.89	1932.48

Table 6.9: Oil Flow properties

The total head was estimated to be 1m. Overall head, flow rates for each bearing and headloss to them from path, and the additional effect of VVL were combined to calculate a required flow rate of 1.7 L/min and a required power of 223W.

6.8.1 - Oil Sump

When designing a system to pump oil around the engine there is a critical early design choice; wet vs. dry sump storage. Wet sump engines have a large oil pan directly below the crankshaft to collect oil which is then recirculated through the system by a pump. Dry sump systems take the oil and put it directly into a separate tank from which the oil pump draws oil. High performance bikes and cars typically use dry sump because as the vehicle turns at high velocities the oil doesn't slosh about in the pan as it would in wet sump systems. The system, however, is not without fault as it requires an additional pump and storage tank which take up space on the engine. Added components increase engine complexity, cost, and size all of which are limiting factors for our motorcycle engine. Also, for a sports touring market we don't expect sloshing of oil to be a major problem. Therefore a wet sump is sufficient.

6.8.2 - Oil type

Oil is essential to the function of any engine as it reduces the friction and wear on engine components, which increases efficiency and longevity. This means selecting the right oil is essential to the functio of an engine. Oils are named in accordance with an SAE (Society of Automotive Engineers) standard and are in the form __W-__. The two blanks correspond to

performance at different temperatures the first being low start up temperatures and the second being performance at operating temperature[16]. General rule of thumb follows that the lower the first number the better start up performance and the higher the second number the better operating performance. For this reason we selected a 10W-40 oil which has a good balance of start up and operating performance. Confirming our selection, many sports touring bikes on the market today use the same brand of oil.

Characteristic	Weight	15W-40	10W-40	20W-50	10W-30	5W-20
Bearing protection	0.2	8	9	6	8	5
High end viscosity	0.3	8	8	10	6	4
Low end viscosity	0.2	7	8	6	8	10
Corrosion resistance	0.1	10	8	7	8	6
Cost	0.1	5	7	7	9	10
Lifetime	0.1	9	8	6	10	5
SUM	1	7.8	8.1	7.4	7.7	6.3

Figure 6.22: Oil Specification

The next distinction between oil varieties is distinguishing mineral oil, semi-synthetic, and synthetic oils. Mineral oils are the cheapest and have minimal processing and are closest to natural petroleum that comes out of the ground. Synthetic oils are the opposite of mineral oils and only use compounds of petroleum to create a more efficient oil.They often include additives that improve performance and effectiveness of the oil but are more expensive. Semi-synthetic is somewhere in between, not providing all the benefits of synthetic but providing some additional longevity and a lower cost. Since our engine is designed to have as good performance as

possible, we recommend using a full synthetic oil, despite the cost, to improve mechanical efficiency.

Characteristic	Weight	Mineral Oil	Semi-synthetic	Full Synthetic
Lubrication	0.3	5	7	9
Thermal resistance	0.1	4	6	7
Lifespan	0.25	6	8	10
Cost	0.1	8	8	3
Hot vs cold performance	0.15	4	6	8
Evaporation	0.1	5	7	9
SUM	1	5.3	7.1	8.3

Figure 6.23: Oil Type

6.8.3 - Effect of VVT and VVL on oil requirements

One of the unique features of the BTN-1500E engine is its use of Variable Valve Lift and Variable Valve Timing to improve engine efficiency. These technologies adjust the camshaft and response of the intake and exhaust valves to change how the engine operates. These technologies rely upon shifting the camshaft horizontally using oil flow to activate the change in profile. This means that at a specified RPM (4000 for VVT and 6000 for VVL) additional oil must be injected into the system to replace the oil lost to activating these technologies. Oil is lost opening the channels for VVL and also in sliding the camshaft horizontally across the bearings shearing oil off their surfaces. We predict as much as 50% of the oil on the surface of the bearings could be lost and will need to be replaced by the pump system to accommodate for this change.

6.8.4 - Lubricant parts

While deciding on a specific pump and filter were determined out of scope as they would be very dependent on the rest of the motorcycle, the below properties are what would be required of a pump.

Flow rate (L/min)	1.7
Required Pressure (MPa)	0.4
Power (W)	223

Table 10: Pump Requirements

6.9 - Real Otto and Atkinson Cycle (Inefficiencies)

6.9.1 - Overview

There are a few main inefficiencies that can hinder an engine's performance versus RPM. The first inefficiency is how well the fuel injected into the cylinder can combust on each cycle, or combustion efficiency. This inefficiency is rather constant with RPM, unlike the others [1]. The second inefficiency takes into account the mechanical losses from parts of the engine moving through air and the losses due to lubricated parts causing friction, which we call mechanical efficiency. From Heywood, this inefficiency varies approximately linearly with RPM, but as we show in the following analysis, this is not completely accurate. The third inefficiency we analyzed is the inefficiency of the air going into the cylinders, or volumetric efficiency. This inefficiency varies significantly with RPM, especially with choking conditions, because of the shorter time step the valves are open at higher RPMs. Finally, we analyzed the basic pumping losses in the engine, which are the losses of work from pressure differentials during intake and exhaust.

Symbol	Property
θ	Crank angle (degrees)
θ_{op}	Valve lift open angle
θ_{cl}	Valve lift close angle
θ_{dur}	Valve lift duration
i	Properties that have to do with the intake valve
e	Properties that have to do with the exhaust valve
η_{comb}	Combustion Efficiency
η_{vol}	Volumetric Efficiency
η_{mech}	Mechanical Efficiency
q	Specific Weib Function Heat
Q_{lhv}	Lower heating value for gasoline (kJ/kg)

φ	Equivalence Ratio
m_{air}	Ideal mass of air in cylinder (kg)
P_1	Initial Cylinder Pressure (Pa)
V_1	Initial Cylinder Volume (m^3)
w_{cycle}	Specific Work per cycle
W_{cycle}	Work per cycle including mechanical inefficiencies (J)
W_{pump}	Pumping loss work (J)
$W_{netcycle}$	Work per cycle including all engine inefficiencies (J)

Table 6.11: Inefficiency Calculation Units

6.9.2 - Combustion Efficiency

While ideally all of the fuel that you inject can combust, due to some mixing and swirling characteristics, 100% combustion is virtually impossible. While modeling the turbulent swirling in a cylinder versus RPM is extremely complex, there are empirical relations that come close. Heywood states that combustion efficiency almost entirely depends on equivalence ratio, as is shown in the chart below [1]. To estimate combustion efficiency for our engine, we created a curve from the mean of the points shown below and calculated the combustion efficiency. In order to maximize fuel efficiency at cruise conditions and maximize power at max high load conditions we choose equivalence ratios of 0.974 and 1.190, respectively.

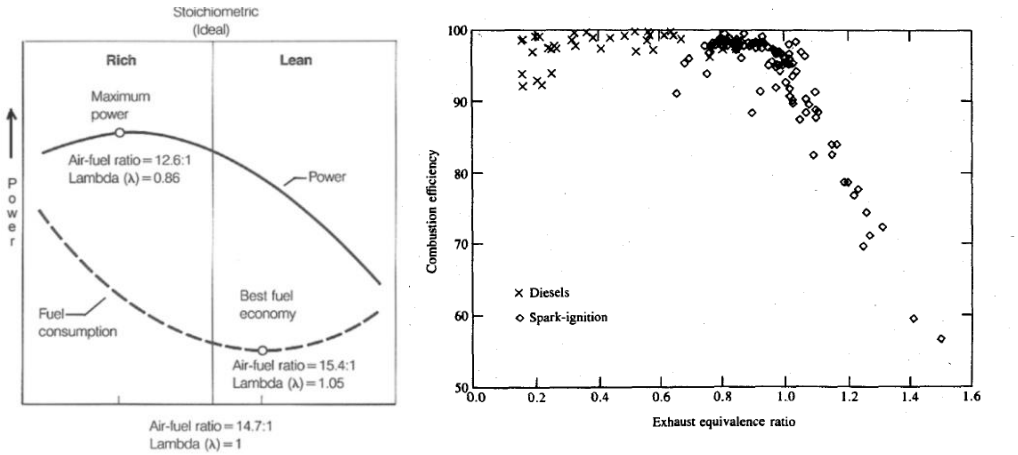

Figure 6.24: Rich versus Lean Fuel Analysis

Condition	Equivalence Ratio	Combustion Efficiency (η_{comb})

Fuel Efficient	0.974	0.93
High Power	1.190	0.81

Table 6.11: Efficiency of Fuel Ratios

6.9.3 - Mechanical Efficiency

Friction is a major source of energy loss for an engine. Depending upon the RPM, it can account for as much as 20% loss of the total power output. Unfortunately, without assembling the engine and testing it, calculating the friction on each surface is incredibly difficult. In Heywood there is a method for calculating piston friction which uses a graph that shows what portion of total friction is each component [1].

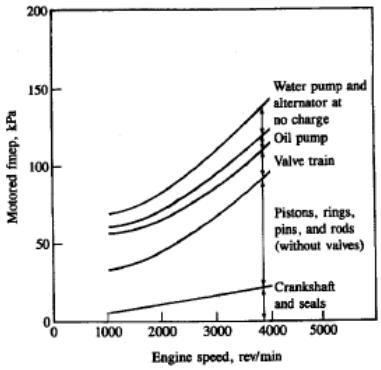

Figure 6.25: Mechanical inefficiencies

For each RPM, piston friction makes up approximately half the total friction. Therefore, by calculating the loss of the piston and doubling it we can estimate total mechanical losses. The work due to friction is calculated using the following equation.

$$W_f = F_f * Distance$$

The distance travelled is directly related to the RPM of the engine and the stroke of the cylinder. The force of friction is much harder to calculate as it varies based upon the pressure in the cylinder, the coefficient of friction on each piston ring, and the surface area of the piston rings. The coefficient of friction of the piston rings was found using the equation shown below which relates the oil friction and surface friction together to find the combined constant [1]. The constant α determines what percentage of friction is fluidic versus solid.

$$f = \alpha f_s + (1 - \alpha) f_L$$

To account for the uneven distribution of area and pressure, as well as the different materials of each piston ring, we used a weighted average to determine the friction of the solid. With a coefficient of friction established we could now find the normal force on the piston rings using another graph from Heywood which shows pressure on the piston rings at different motor conditions [1].

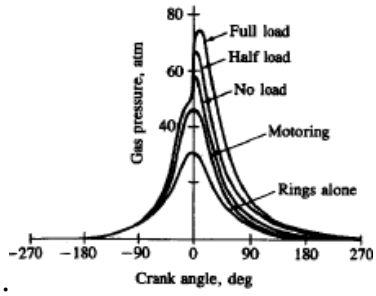

Figure 6.26: Pressure on piston ring versus crank angle

These motor conditions were equated to different RPMs, plotted using excel, and then a polynomial fit was performed on the data. This trendline provided a function of piston ring pressure versus RPM which could be used to find values at each RPM we tested. The surface area of the rings was provided by the mechanical teams, Using that value we were able to find the total work due to friction at each RPM.

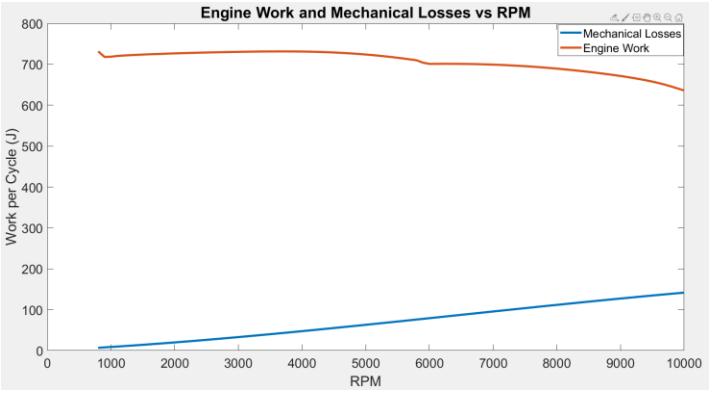

Figure 6.27: Loss Due to Mechanical Friction

The function has two modes: a linear portion due to the constant change in RPM and an exponential change due to the pressure within the system. At low RPM values mechanical friction accounts for 3% of total work but at redline, it is over 22% of the total work produced by the engine.

6.9.4 - Volumetric Efficiency

The volumetric efficiency is based off of the previous analysis for the air model in the engine. Simply stated, the volumetric efficiency is calculated from the percent of mass left in the cylinder after exhaust, multiplied by the percent of mass not able to completely fill up the cylinder during intake. This is because even if the valves are able to get 100% of the original mass in the cylinder at the end of each cycle, if the exhaust stroke is only able to get 50% of the burned fuel out then there will only be 50% of new fuel-air mixture to burn. These equations below represent how we calculated volumetric efficiency from the mass in cylinder, Figure 6.19, for each RPM.

$$\varepsilon_{vole} = 1 - \frac{m_{endex}}{m_o}$$

$$\varepsilon_{voli} = \frac{m_{end}}{m_o}$$

$$\varepsilon_{vol} = \varepsilon_{voli} * \varepsilon_{vole}$$

6.9.5 - Weib Function Work

After we determine all of the efficiencies above, we can start plugging them into the right sections in the analysis. Since an input to finite heat release is the specific heat transfer from burning the fuel, q, we can change it for the non ideal conditions. This number depends on the mass of fuel, which is related to the mass of air per cycle. This means that the mass of fuel directly correlates to the volumetric efficiency since we are trying to keep a constant air-fuel ratio. Also, q depends directly on combustion efficiency, because q says how much work we can get out of combusting the gas. Therefore we also multiply q by the combustion efficiency from Heywood. After that we can incorporate mechanical efficiency by taking a fraction of the work outputted by the algorithm in FiniteHeatReleaseBTN.m.

$$q = \frac{Q_{lhv}\varepsilon_{comb}m_{air} * \varepsilon_{vol} * \varphi}{AF_{mass}P_1V_1}$$

$$W_{cycle} = w_{cycle} * \varepsilon_{mech} * P_1 * V_1$$

From here we also get updated temperature and pressure in the cylinder during combustion as shown in Figure 6.28.

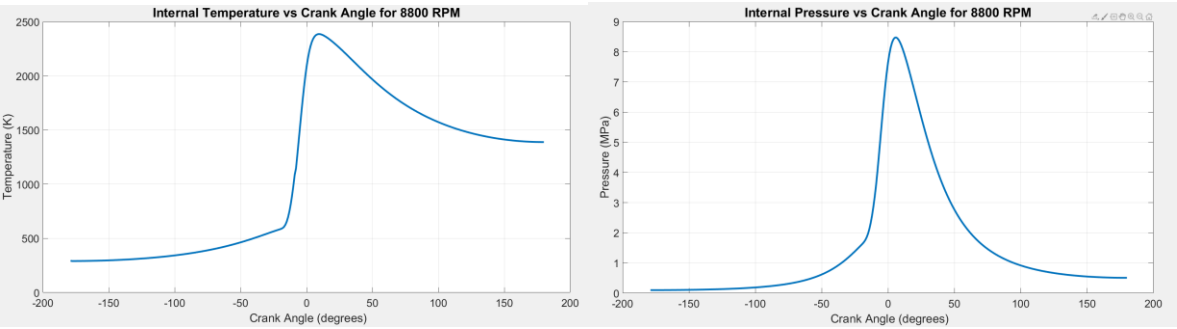

Figure 6.28: Cylinder Properties With Inefficiencies

6.9.6 - Pumping Losses (Simplified)

Much like it is difficult to get air into and out of a syringe, it is difficult to get air into and out of the engine. Significant work is done if the hole in the top of the syringe is small, due to the large pressure differences between the cylinder of the syringe and the environment during intake and exhaust. An engine can be modeled in the same way. Since we know that the work in a cylinder is directly related to the product of pressure and volume, we can calculate the work as an integral with small volume steps. With our current model, we have a constant pressure outside both the intake and exhaust valves, however this is inaccurate. While it is outside the scope of this project, if we were to model the intake and exhaust manifold, along with the pressure drop across the throttle and pressure build before the catalytic converter, we would be able to get a much better model of the pumping losses at less than ideal conditions [11]. However, if we ignore these phenomena for now we can model the pumping losses using the pressures in the cylinder determined from the volumetric efficiency and air model as shown below. For the exhaust, the pumping losses happen from BDC to TDC, since this is the time period where the cylinder is trying to push high pressure out of the cylinder. For the intake portion the pumping losses happen from valve open to BDC since the intake valve both pushes some high pressure air out of the valve, and causes a vacuum which sucks in lower pressure air.

$$W_{pump} = \int_{open}^{close} PdV$$

$$W_{netcycle} = W_{cycle} - W_{pump}$$

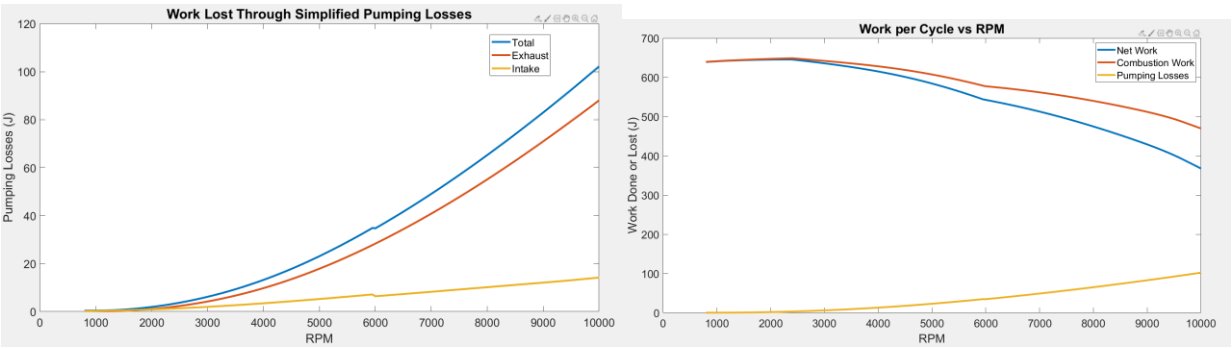

Figure 6.29: Effect of Pumping Losses on Total Work

6.10 - Final Power-Torque Curves

6.10.1 - Incorporating Inefficiencies

Power and torque are the main goal of this engine thermodynamic analysis. All of the other steps, from combustion modeling, air modeling, and everything in between act as inputs to this relatively simple calculation. From the processes outlined above, we now are able to determine the work produced per cycle for our engine model, and with a few equations we can turn these into our torque and power curves. First, below, in Figure 6.30 we summarize the efficiencies analyzed in the cycle that affected the power torque curves. Initially the torque curve is flat and the power curve is linear without any inefficiencies. However, the efficiencies outlined below show how the plots become curved.

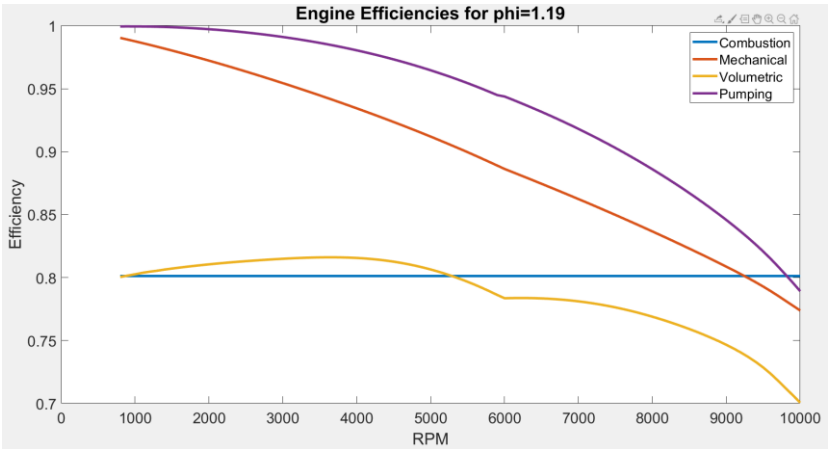

Figure 6.30: Four Primary Inefficiencies

6.10.2 - Torque and Power for Different Operating Conditions

Symbol	Property
Pw_{real}	Engine Power (kW)
τ_{real}	Engine Torque (ft-lb)
ξ	Unit Conversion (Metric-English Conversion)

Table 6.12: Torque and Power Units

$$Pw_{real} = \frac{W_{netcycle} * N * C}{2 * 60}$$

$$\tau_{real} = \frac{Pw\xi * 33000}{N * 2\pi}$$

Using these two equations, and changing the model to incorporate varying levels of variable valve lift and timing, we can get a few torque power curves that describe the engine well [1].

The first graph shown below is for constant valve lift (lower lift value), but variable valve timing in order to achieve a more Atkinson-phased cycle. This graph shows a lower torque and power for the Atkinson phase, at the benefit of fuel efficiency. Since this graph best represents fuel efficient driving, it is also created using our lean equivalence ratio. This torque power curve in real life would not mean much, because we would only be running Atkinson at low throttle and low RPM conditions. However, it is good to illustrate the drop in max power required in order to create better specific work from the engine.

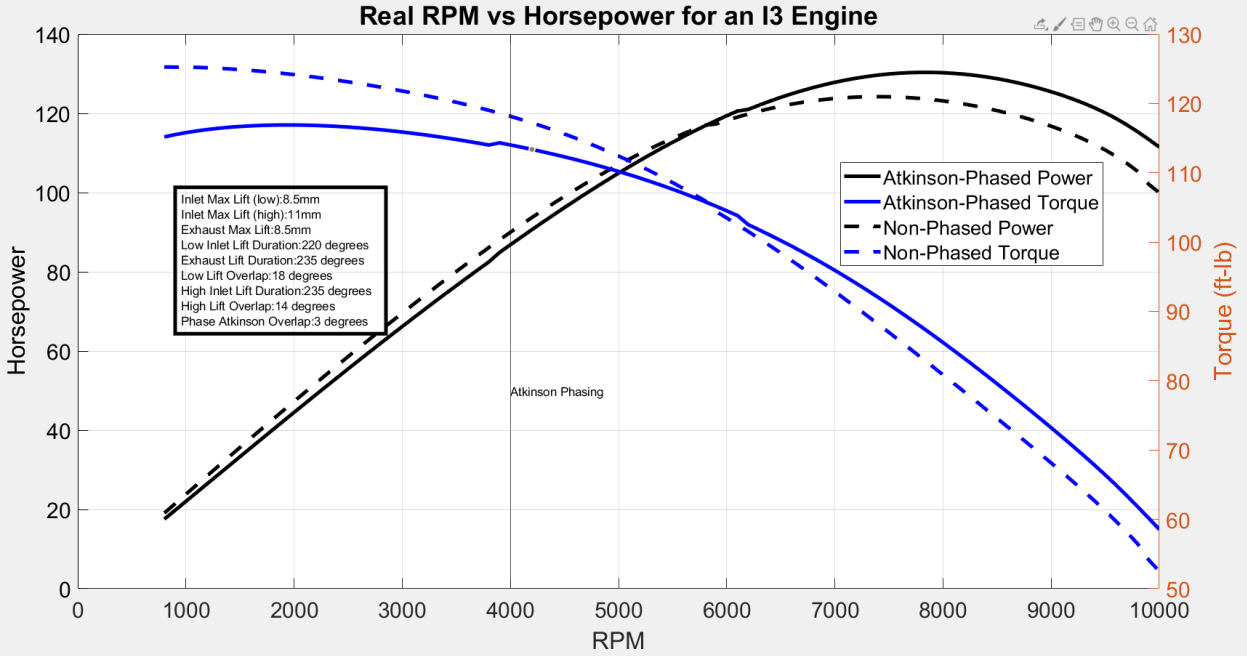

Figure 6.31: Initial Power and Torque Curves with Phasing

The next two graphs show more realistically how the engine would operate, using variable valve lift. The first graph shows both the low and high lift power torque curves in order to justify the switch between the two cam profiles. These curves are good for high load, or max throttle, and are both made using the rich equivalence ratio described in the sections above. They show that at low RPM it is beneficial to stay on the lower cam to achieve better volumetric efficiency and therefore better torque and power. Torque in particular is seen to be almost 10% higher at low RPMs for the low cam than the high cam. As the RPM starts to climb, the qualities of the two cams converge until they reach around 6000 RPM. At this speed, it is beneficial to switch to the high cams to improve volumetric efficiency. We can see that without this switch the power curve levels off a lot earlier, causing our redline to be closer to 7500 than 8800. Again, we also get around 20% better torque at very high RPMs for the high cam when compared to the low cam. Obviously, there are very large effects for max throttling conditions for variable valve lift technology.

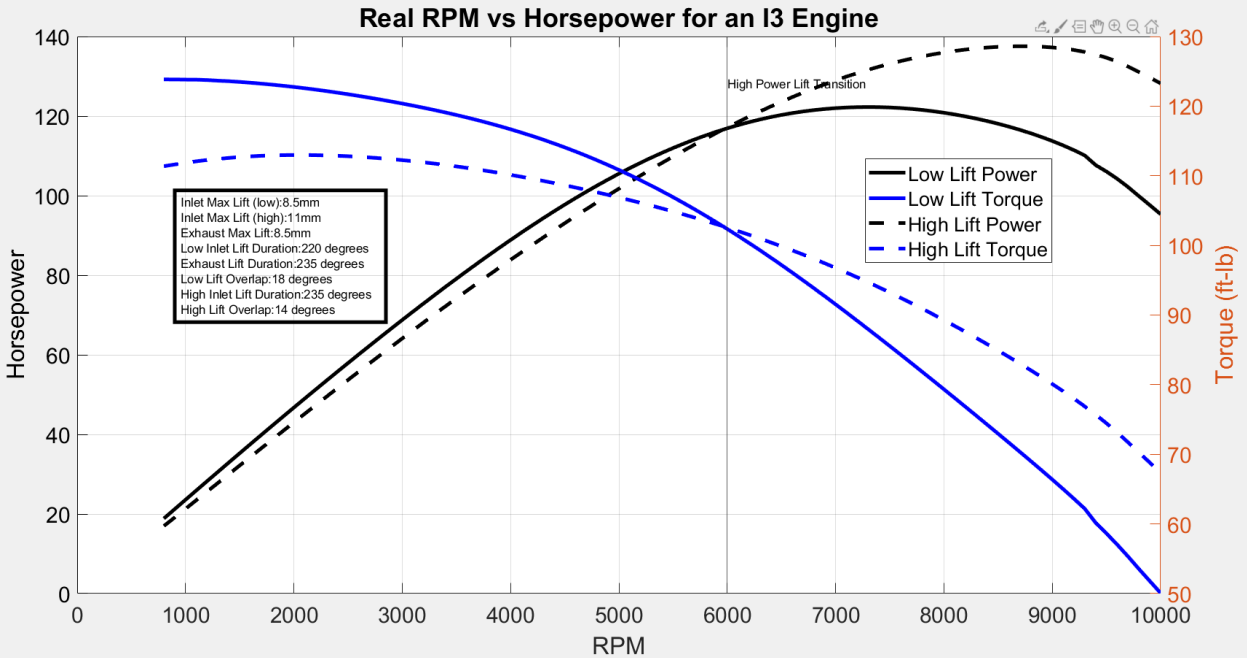

Figure 6.32: Final Torque and Power curves with High and Low Valves

Realizing the benefits of the variable valve lift technology, this graph below simply chooses the correct curve for the RPM that you are running at. Below 6000 RPM the camshaft is running the low cams, but after the engine is sensed to run above that speed the cams will shift to the high ones in order to get more air into the cylinder and improve redline performance.

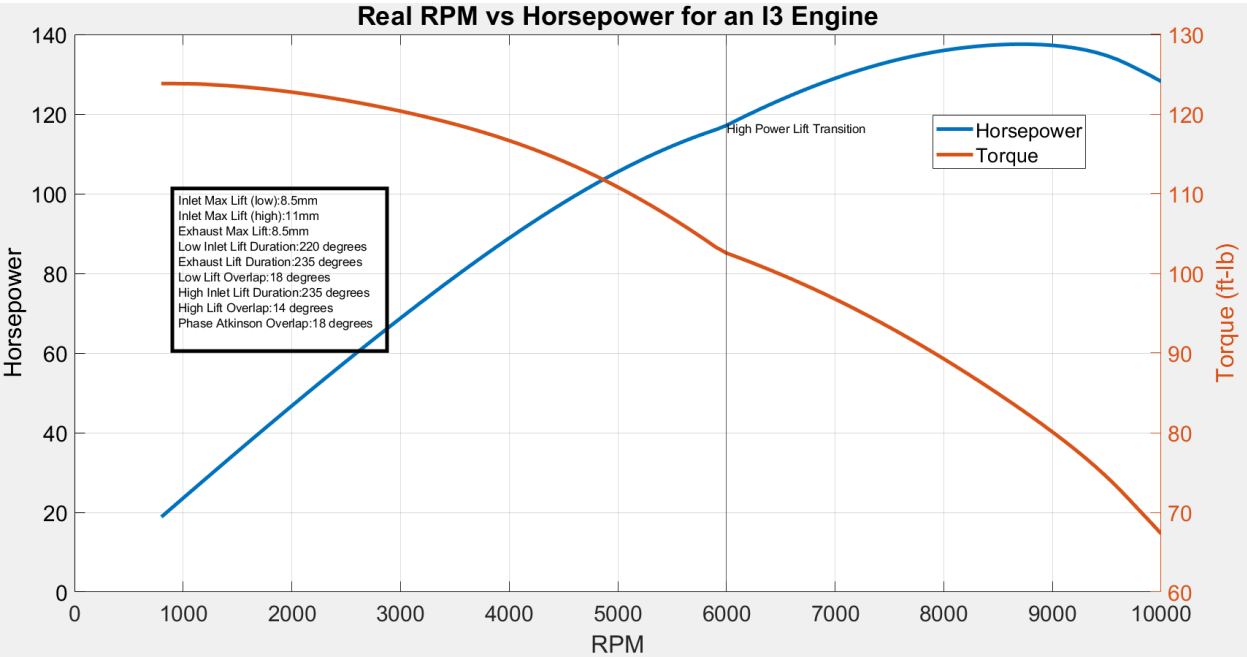

Figure 6.33: Final Torque and Power Curves

Overall, variable valve technology has significant impacts on engine performance and efficiency, and this thermodynamic analysis justified its use in our engine. Below is a table summarizing all of its benefits in our engine ranging from increased horsepower to better fuel efficiency.

Characteristic Improved	Variable Valve Lift (VVL)	Variable Valve Timing (VVT)
Idle Torque (%ft-lb)	13%	-8%
Redline Torque (%ft-lb)	22%	N/A
Redline Power (%hp)	20%	N/A
Redline Value (%RPM)	21%	N/A
Fuel Efficiency (%mpg)	N/A	4%

Table 6.13: Effect of Variable Valve Technologies on Power, Torque, and Fuel Efficiency

6.11 - Emissions Analysis

6.11.1 - Overview

A critical component of engine design is carefully considering if your engine will meet emissions standards laid out by the governing body you are using the engine in. This could be a time to consider redesign of the engine in order to make it use more or less fuel per cycle. Through using NASA's Chemical Equilibrium Applications (CEA) program, we are able to see how our engine operating conditions affect the emissions in the engine [17]. Below in Table 6.14 are the outputs of the CEA program for the two air-fuel ratios that we plan on operating at. Also, the percentages of the emissions that are controlled through strict standards are shown in Figure 6.34 across a wide range of air-fuel ratios.

6.11.2 - CEA Analysis

	Mass Fractions		
Air-Fuel Ratio	CO	NO_x	HC
15.4 (φ=0.954)	1.9663e-2	9.5619e-3	6.8031e-6
12.6 (φ=1.19)	6.4632e-2	2.5057e-3	6.0788e-6

Table 6.14: Air to Fuel Ratios

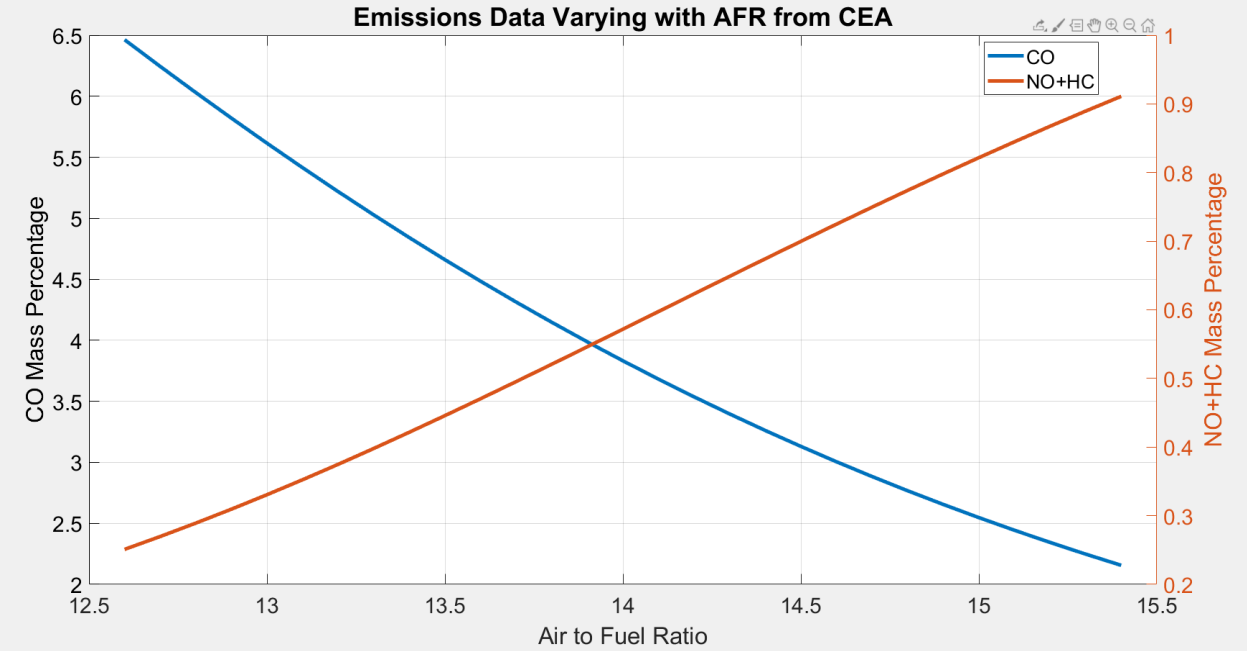

Figure 6.34: Emission of CO and NO+HC

6.11.3 - Standards and Emissions

Getting the data from CEA is the first part, now we need to see if our mass fractions are able to meet emissions at the testing speed designated for our class of motorcycle. For the United States government, the GPO standard § 86.501–78 states the below testing speeds for a motorcycle [6]. Since our thermodynamic engine model is most accurate at high load conditions, we will only be looking at the testing conditions for top gear. According to Figure 6.35 below this means that we want to look at the speed of 75 km/hr (46.6 mi/hr) for our engine. After completing some market research, and making our own estimates about the transmission designers at the Spartan Motorcycle company, we concluded that an RPM of 2500 would be sufficient estimate for this testing speed.

Shift	Speed
1st to 2d gear	30 km/h (18.6 mi/h).
2d to 3d gear	45 km/h (28.0 mi/h).
3d to 4th gear	60 km/h (37.3 mi/h).
4th to 5th gear	75 km/h (46.6 mi/h).

Figure 6.35: Speed Required for Emissions Test

Symbol	Property
X	CEA Mass Fraction
Sp	Vehicle Speed (km/s)
Em_X	Emissions of Component (g/km)

Table 6.15: Emissions Fractions

$$\dot{m}_{fuel} = \frac{\dot{m}_{air}\varphi}{AF_{mass}}$$

$$\dot{m}_{tot} = \dot{m}_{fuel} + \dot{m}_{air}$$

$$\dot{m}_X = X * \dot{m}_{tot}$$

Where X can be CO or $HC+NO_X$

$$Em_X = \frac{\dot{m}_X}{Sp}$$

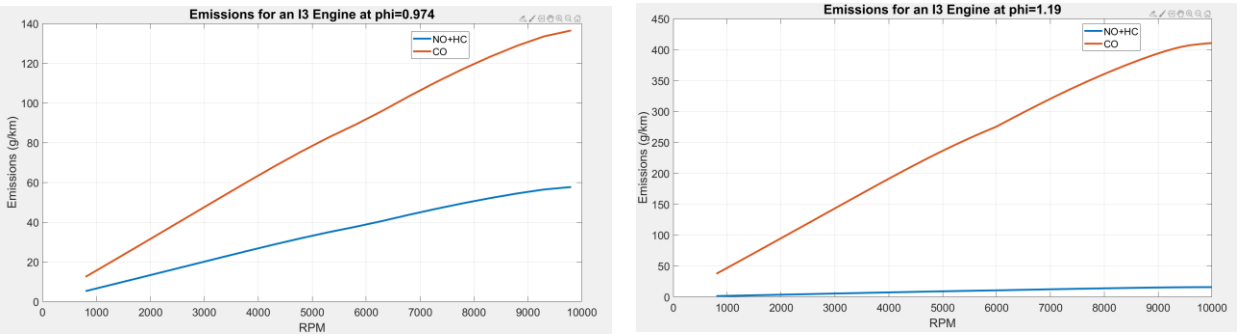

Figure 6.36: Emissions for Two Fuel Mixtures

Due to the size of our motorcycle engine, we fall under the class III motor vehicle specification. According to EPA regulation §86.410-2006 we must meet the emission standards laid out below [18].

TABLE E2006-2—CLASS III MOTORCYCLE EMISSION STANDARDS

Tier	Model year	Emission standards (g/km)	
		HC + NO_X	CO
Tier 1	2006-2009	1.4	12.0
Tier 2	2010 and later	0.8	12.0

Figure 6.37: Motorcycle Class

However, as shown in Table 6.16, our emissions at 2500 RPM are much too high to meet emissions standards. For this reason, BTN performance will utilize a catalytic converter in order to reduce emissions. While a catalytic converter is an expensive component, and has the potential to reduce performance, it is a necessity to make our engine legal. In order to reduce our emissions to an acceptable level as outlined in the standard above, we decided on the MagnaFlow California Grade CARB Compliant Universal Catalytic Converter, which can reduce CO emissions by 95% and NO_x+HC emissions by 95%.

Molecule(s)	Worst Case Equivalence Ratio	Untreated Emissions (g/km)	Catalytic Converter Efficiency	Treated Emissions (g/km)	Emissions Standards (g/km)
CO	1.190	120.5	95%	6.03	12.0
$HC+NO_X$	0.974	16.2	95%	0.81	0.8

Table 6.16: Effect of Catalytic Converter on Emissions

6.11.4 - Emission Benefits From VVT

Our NO_X emissions shown above are above the regulation and this is unacceptable for our design. Luckily there is a feature of our design that we have not taken into account in the analysis yet. Variable valve timing technology is able to reduce NO_X emissions by reducing the burn temperature of the fuel [7]. It does this by allowing some of the previous burned product into the intake manifold to mix with the incoming fuel-air mixture. This new mixture comes in

and is combusted. However, since it is not as fuel rich as the previous charge, it burns at a lower temperature. This lower burn temperature allows for a significant NO_X emissions reduction, at little to no change in other emissions. While we were not able to show this in our thermodynamic analysis due to the optimization and analysis of the intake manifold being out of scope we were able to find some sources to get some reasonable estimates. As shown below in Figure 6.38, from the journal of applied mechanical engineering, the NO_X emissions in one case were reduced by 7.5% [7].

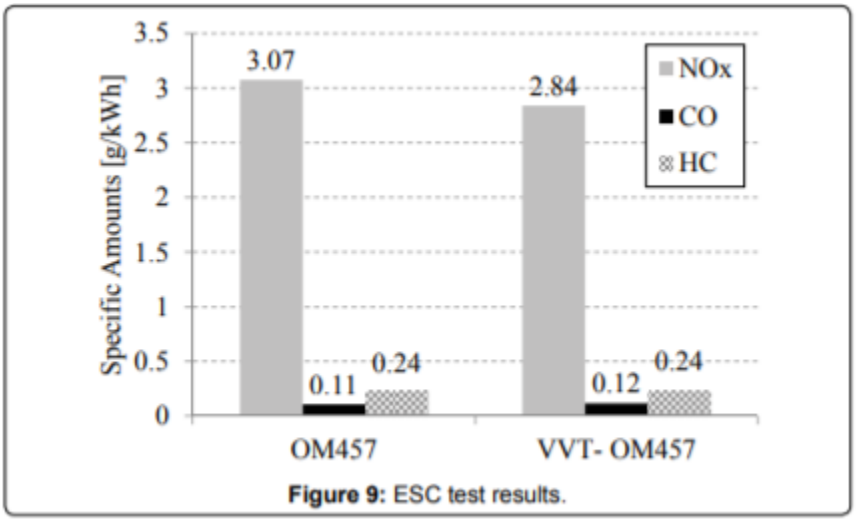

Figure 6.38: Emissions changes for Variable Valve Timing

In another study by Concordia university they showed that "... there was a 24 per cent reduction in NOx (Otto–Atkinson cycle) engine experiments [8]. The tests were emissions at mid-load with no change in hydrocarbons performed on a Ford 2.0 l, DOHC, 16-valve engine. (HC)." Using these two numbers in our design, and incorating the geometry of each engine used in the test, we determined a conservtive estimate for our engine would be to reduce NO_X emissions by 15%. Adding this into our analysis we get the results in the Table below.

	Worst Case Equivalence Ratio	**Untreated Emissions (g/km)**	**VVT Reduction of 15% (g/km)**	**Catalytic Converter Efficiency**	**Treated Emissions (g/km)**	**Emissions Standards (g/km)**
HC+NOx	0.974	16.2	13.79	95%	0.69	0.8

Table 6.17: Effect of Variable Valve Timing and Catalytic Converter on NOx+HC Emissions

Figure 6.39: MagnaFlow California Grade CARB Compliant Universal Catalytic Converter

The catalytic converter we elected to purchase is the MagnaFlow California Grade CARB Compliant Universal Catalytic Converter. Like traditional catalytic converters, it uses a chemical process to convert harmful emissions into less toxic molecules. As the chemicals within the catalytic converter saturate, it's efficiency will fall off from around 99% to 95% [19]. This threshold is still more than acceptable to ensure our emissions are below regulations. This model has a durable stainless steel structure and is fairly small, making it an ideal fit for a motorcycle. In addition, the model passes regulations for air quality in all 50 states ensuring we can sell our engine in valuable markets like California.

6.12 - Cooling Analysis

6.12.1 - Overview

Once the thermodynamic combustion analysis of our engine were completed, we needed to design a cooling system capable of keeping both rider and engine safe during operation. During combustion, each cylinder heats up to over 2000 ^{o}C briefly as the gasoline is ignited. This temperature, if allowed to heat up the engine block, will quickly scorch a rider. To ensure as much of this heat is dissipated as possible, we employed a liquid cooled engine. Liquid cooled engines circulate cooling fluid around the cylinders and cylinder head to dissipate a significant portion of the heat. The liquid is then passed through a radiator which transmits heat to the atmosphere which keeps the coolant from becoming too warm. Conduction through the metal engine must also be considered, however the radiation is small and can be neglected [1]. Using

these assumptions we began to analyze the heat loss from each cylinder individually using a thermal resistance approximation

Figure 6.40: Cooling Resistance Model

This model served as the basis for our cooling calculations R_{cyl}, R_{sleeve}, and R_{wall} are all constants found using the respective thermal conductivity of the metal. The convective resistance was found using the Woschni correlation. The correlation is based on a constant characteristic air velocity based on piston speed and pressure and is used to find an equivalent resistance. From there, we can approximate temperature of the outer surface without accounting for coolant flow. To calculate the heat transfer coefficient of the fluid we used properties of our coolant selection (50/50 mix of ethylene glycol and water) and dimensions of our cooling channels. Once these values were established we could iterate flow rate until the engine outer temperature was below our desired surface temperature of 40 ^{o}C. We were then able to do this iteration for each RPM value of the engine to find required flow at engine redline 9000 RPM.

6.12.2 - Convective Heat Transfer Analysis

One of the largest sources of thermal resistance in the model comes from the heat transfer between the air gas mixture and the cylinder wall. The heat transfer coefficient within the cylinder varies depending upon the flow velocity in the cylinder, the bore diameter, the temperature of the components, and pressure of the air as a function of crank angle. In order to find the flow velocity in the cylinder we used the Woschni Correlation from Heywood which suggests that the air speed is correlated to mean piston speed uses characteristic changes in pressure and temperature as compared to a reference state [1]. To calculate this for each RPM, a Matlab script was written to find airflow at each crank angle and then iterated to create a complete profile. After the velocity profile was calculated, through the use of the Hohenberg formula, we can approximate the heat transfer coefficient between the air-gas mixture and the steel cylinder walls.

6.12.3 - Conductive Heat Transfer

The conductive heat transfer coefficient between the various metal alloys in the engine was then calculated. Each of the values of thermal resistivity is found in CES Edupack and this is used to find the heat dissipated through each section. The thermal resistivity was multiplied by

the respective thickness of the metal determined by our mechanical teams to find an initial wall temperature. It is assumed that even as the cylinder heats up it dissipates the same amount of heat to simplify the thermodynamics model. From this point, we can set an acceptable outer surface temperature of the bike to figure out an appropriate resistivity for the coolant.

6.12.4 - Liquid Cooling

Liquid cooling involves flowing a cool liquid over and around the cylinders to carry away as much thermal energy as possible. The hotter the cylinder temperature the faster the coolant must travel to dissipate the heat. This is reflected in the increased thermal resistivity at higher fluid velocities. The coolant we selected for our engine was a 50% mix of Ethylene Glycol and 50% water to get a higher boiling point and a lower freezing point, both of which are advantageous for the system [9].

Ethylene Glycol / Water 50% Mix		
Freezing Point	-36.8	^{o}C
Boiling Point	107.2	^{o}C

Table 6.18: Freezing and Boiling Point of Coolant

The system also retains good thermal and fluid properties which we calculated using an average of the respective traits. To calculate the convective heat transfer coefficient of the coolant, we needed to find the Nusselt Number of the fluid, the thermal conductivity of the fluid, and the hydrodynamic diameter. The thermal conductivity and hydrodynamic diameter are determined by the coolant and coolant channel respectively, but the Nusselt number depends on the flow rate. As coolant flow increases, the Nusselt Number and thermal conductivity rise, decreasing surface temperature.

By iterating the flow rate for each RPM we could find the flow rate required to keep our surface temperature at a safe level. We found that for low RPM conditions, a low flow rate of less than 2 gallons per minute was required but at redline we needed over 15 gallons per minute to cool the outer surface. Due to our variable valve technologies, our cylinders get hotter than other comparable engines and thus require additional cooling. To enable this our system will require a slightly larger pump than a normal engine of this scale. Once fluid is pumped through the engine and heated it will pass over a thermometer which will restrict flow out of the cylinder making sure the engine doesn’t overcool before heading to the radiator to exchange heat with the environment.

6.12.5 - Cooling Channels

The engine cylinders are located centrally within the engine block and emit heat primarily through the cylinder walls and heads. This means that coolant must flow over these areas to ensure appropriate cooling for all parts of the engine. Our coolant was designed to have parallel flow around the Siamese bores as it was simpler to model and easier to implement than counterflow which provides more efficient cooling. Siamese bores provide additional strength to the engine since there is solid material between each of the cylinders. The Siamese bores also simplifies the heat flow model out of the cylinder. One challenge we encountered was an inability to cool the the top of the combustion chambers. The top of the cylinder experiences the same heat as the cylinder walls, but since there is less material less heat is dissipated. To limit some of this heat transfer we routed large coolant channels up and over the engine cylinders along the side of the cylinder head around the intake and exhaust ports. These channels are further illustrated in section 10.2

6.12.6 - Cooling results

Our cylinder air reaches an approximate temperature of 2025 ^{o}C which is higher than the standard melting point of iron. This extreme temperature must be diminished before the outer engine wall or it will burn the rider. We determined that 40 ^{o}C would be a safe wall temperature since the minimum temperature to sustain burns is 44 ^{o}C. We found that without any coolant in the engine whatsoever the outer engine temperature was 1200 ^{o}C. This shows important coolant is at high RPM. The graph below shows the flow rate of coolant in liters per second of fluid to dissipate the heat of the cylinder.

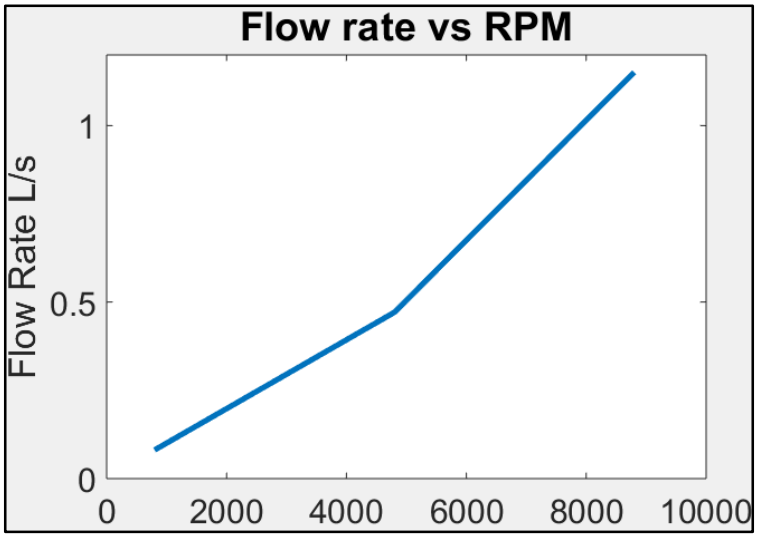

Figure 6.41: Plot of Coolant Flow Rate vs. RPM

In order to size a pump for the US market we converted our units to gallons per minute which are often used to size pumps for motorcycles. At the low end, our system needs to move

about 2 gallons per minute, and at the high end, 17 gallons per minute. This value is higher than traditional motorcycle engines but that makes sense as our engine temperature is higher than other motorcycles. It is important to note that that at specified RPMs the variable valve technology built into the engine activates causing a change in the ratio between flow rate and RPM. Once the valve technology is activated the engine heats up faster, requiring additional cooling to keep a safe wall temperature. Any pump selected must be able to force sufficient flow through the pipe network accounting for pipe flow losses, neglected during our initial calculation. The other essential component for the coolant is the radiator which must keep the coolant at the 90° threshold we want.

Figure 6.42: Meziere 100 Series Electric Water Pumps

Since the motorcycle requires a high flow rate we decided to specify a water pump that was capable of moving enough coolant. The pump needed a volumetric flow rate of at least 17 gallons per minute and the Meziere 100 Series Electric Water Pumps can move 30 gallons per minute [10]. The model is made of stainless steel with a number of gaskets to provide seals in and out of the pump. Power is supplied to the pump via the standard electric control unit and it runs using the twelve-volt electrical current of the engine.

6.13 - Fuel Efficiency Analysis

6.13.1 - Overview

The fuel efficiency of the engine might be the characteristic that we can most relate to. From our own everyday experiences we know the range of numbers we should be seeing, so it is easier to set and understand our own requirements. For our purposes, we utilized the specific fuel consumption along with the road load power method in order to evaluate how efficient our engine is. This method is appropriate for this analysis because it combines two simple methods in order to get a more accurate prediction for fuel efficiency.

Symbol	Property
SFC	Specific Fuel Consumption (kg/kJ)
m_{fuel}	Actual mass of fuel used per cycle (kg)
$\square_{trans}$	Transmission Efficiency
MPG	Fuel Efficiency (miles/gal)
Pw_R	Power required for cruise (kW)
C_R	Coefficient of Road Load Drag*
M	Mass of motorcycle (kg)*
g	Gravity (m/s^2)
C_d	Coefficient of Air Drag*
A_s	Surface Area of Motorcycle (m^2)*
Pw_{net}	Net Power for Vehicle (kW)
Pw_{ratio}	Ratio between power needed and power available
$W_{netcycle}$	Work per cycle with thermodynamic efficiencies (J)
$W_{totcycle}$	Work per cycle involving drag (J)
ε_{trans}	Transmission Efficiency*
Pw_{real}	Real Power produced by engine (kW)

Table 6.19: Fuel Efficiency Units

*Denotes an estimate was made for analysis

6.13.2 - Efficiency Analysis

The fuel efficiency equations below are a combination of the Heywood and Stone references. They attempt to capture a more realistic analysis of how fuel efficiency is for a real motorcycle [20].

$$Pw_R = (2.73C_R Mg + 0.126C_d A_s * Sp^2) * Sp * 10^{-3}$$

$$Pw_{ratio} = 1 - \frac{Pw_R}{Pw}$$

$$W_{totcycle} = W_{netcycle} * Pw_{ratio} * \varepsilon_{trans}$$

$$SFC = \frac{m_{air}\varepsilon_{vol}\varphi}{AF_{mass}W_{totcycle}} = \frac{m_{fuel}}{W_{totcycle}}$$

$$SFC(kg/kj) = SFC * 3.6x10^{6}\ (g/(kwh))$$

$$MPG = \frac{Sp * \rho_{fuel}}{Pw_{real} * SFC}$$

The fuel efficiency analysis already takes into account all of the previously discussed losses and efficiencies, but since we are now talking about the entire vehicle, we have to start looking at larger forces on the motorcycle itself. The P_R calculation above tries to estimate these losses by incorporating both a road drag and air drag that change with speed [1]. The constants that we used in this equation were determined through research of other similarly sized bikes and can be seen in FuelEfficiencyBTN.m. While incorporating road load losses on top of SFC (Specific Fuel Consumption) gives a pretty good estimate for fuel efficiency, there are still the phenomena of throttling unaccounted for. When the engine is throttled, there are complex pressure and density changes in the intake and exhaust manifold that can have significant effects on pumping losses. While we cannot account for this in the project, due to the design and analysis of the manifolds being out of scope, we would expect a fuel efficiency drop of anywhere from 10-20% when incorporating these losses. Also accounted for in this analysis is the benefit of variable valve timing on fuel efficiency. Due to VVT improving the specific work produced by the engine, we are able to go a little bit farther on the same fuel as is shown in Figure 6.20. While this difference is small shown in the graph, the improvement would be expected to be much more exaggerated once we take into account the other complex phenomena like throttling.

6.13.3 - Specific Fuel Consumption (SFC) Method

Figure 6.43 shows graphs of the fuel efficiency calculated with work per cycle, but not incorporating the drag from the air. Therefore, this method has a P_{ratio} equal to 0. A similar method was used in the Stone engine textbook to calculate fuel efficiency as well [20].

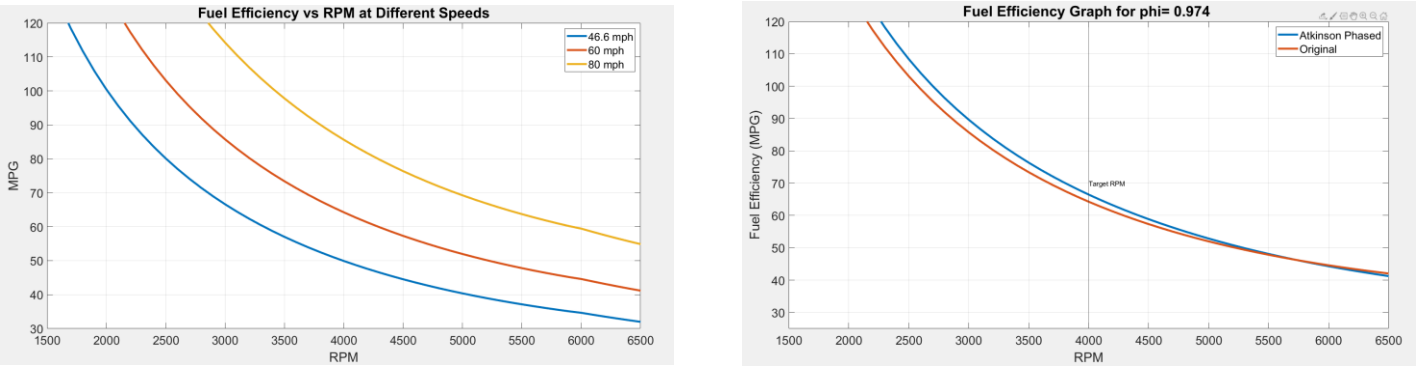

Figure 6.43: Calculated Fuel Efficiency for Cruising Conditions

6.13.4 - SFC and Road Load Combination

The graphs below in Figure 6.44 combine the SFC calculation with power losses due to air and friction drag. These graphs show a distinct maximum for fuel efficiency, with the condition that the transmission would have to be designed to operate at the designated RPM and speed. These plots better represent what we see everyday in our own car. If we increase RPM while keeping the speed constant, fuel efficiency will start to suffer. Also, if the engine is able to produce enough power at that RPM to travel at the speed, it becomes more efficient to go faster rather than slower at a target RPM.

Important to note is that in Figure 6.44 the fuel efficiency is only better for an Atkinson cycle in a range of RPMs for a certain speed. At too low of a speed, the engine is able to produce enough power to overcome drag, so it becomes more efficient to use the original. Also at high RPM the benefits of VVT are diminished as the volumetric efficiency decreases for the intake valve with more Atkinson phasing.

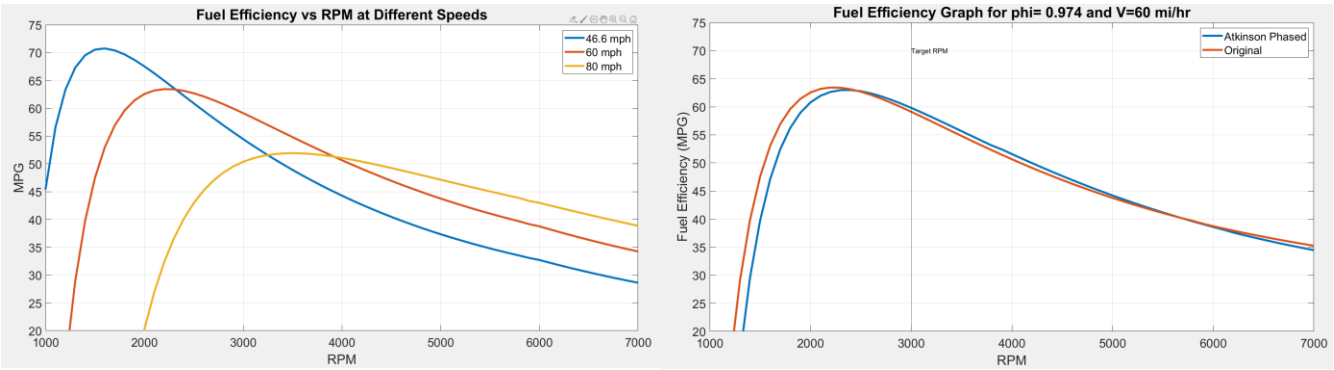

Figure 6.44: Fuel Efficiency with Road Friction

Mode	Fuel Efficiency at 3000 RPM

SFC Calculation (Pr=1)	90 mpg
Including Air/Road Drag	60 mpg
Expected with More Losses	50 mpg

Table 6.20: Difference in Cruising Fuel Efficiency

While these fuel efficiencies are still rather high for a motorcycle of our size, we do not expect these to be the final fuel efficiencies. If we were to do a more in depth analysis involving the greater pumping losses from throttling, including other losses in the intake and exhaust manifold, we would expect our fuel efficiency to drop anywhere from 15-40% more depending on the operating RPM [11]. In the end we would expect an actual maximum fuel efficiency of around 50 MPG

7 - Bottom End Component Design

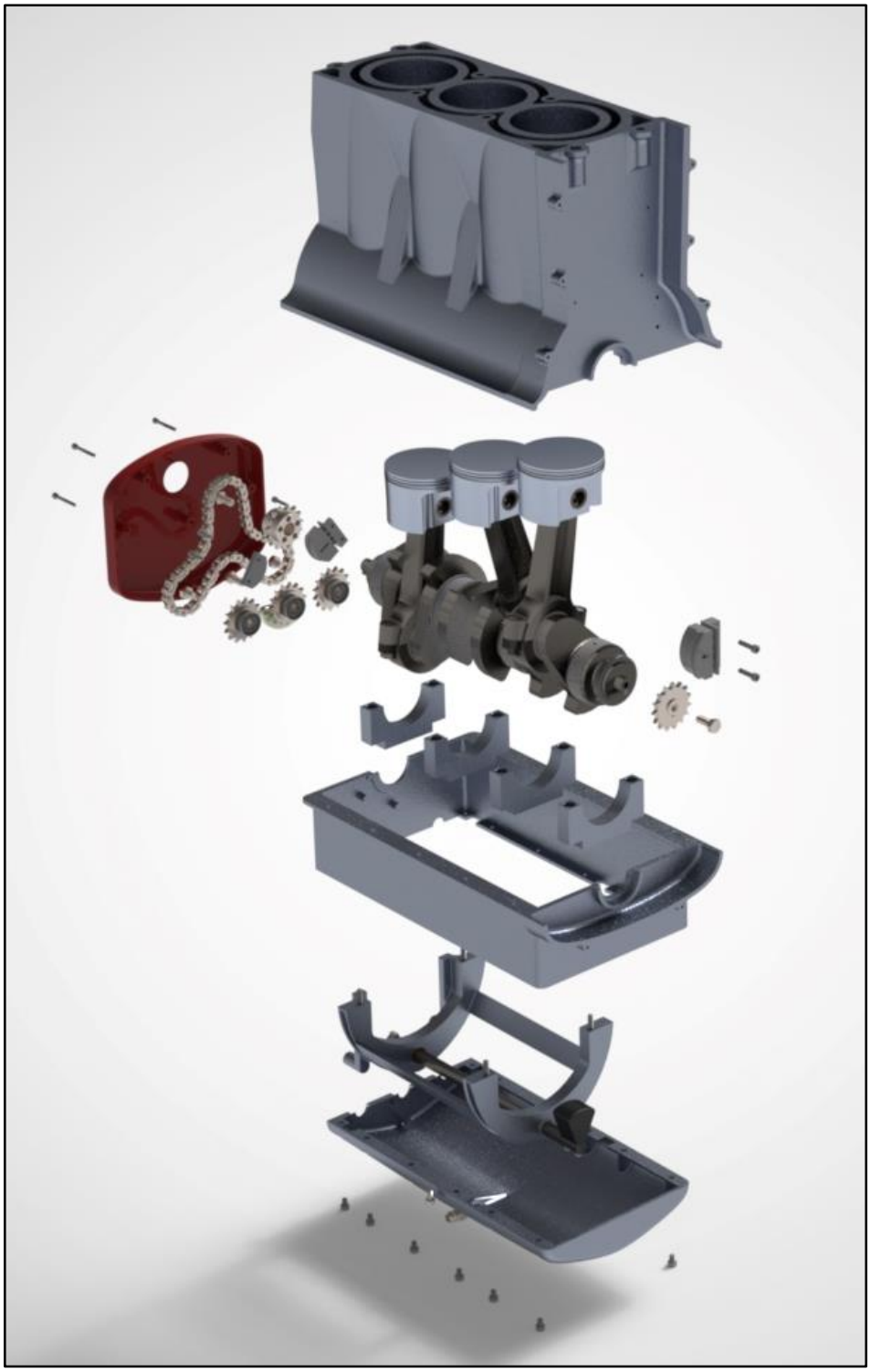

Figure 7.1: Exploded View Render of Bottom End

7.1 - Overview

The bottom end of our engine contains the engine block, rotating assembly, balance shaft system, and oil pan. For each component in this section, we will provide a description of the components purpose, an overview of the material choice and manufacturing method, a summary of the main qualitative design decisions, a walkthrough of the calculations used to drive our design, and a breakdown of the analysis that validates this design. Renders, section views, and FEA screenshots will be provided where applicable.

7.2 - Piston

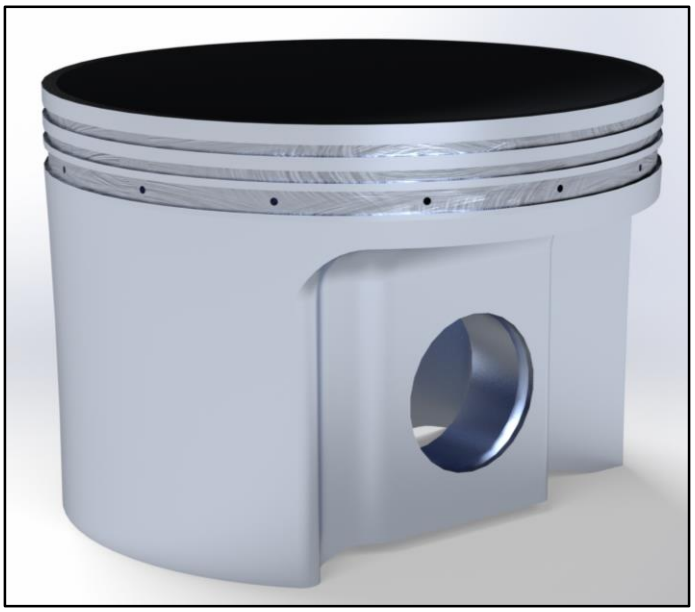

Figure 7.2: Render of the piston

7.2.1 - Overview

The piston is the means by which combustion forces are transmitted to mechanical components, namely through the wrist pin to the connecting rod and crankshaft. The largest force that it experiences is from the combustion itself, and the piston must be able to stand up to this and transmit the force without also damaging other components. Additionally, the piston is subjected to significant thermal loads due to the large thermal gradient present. Material choice and supporting calculations are used to ensure that the expansion of the piston and cylinder along with the piston rings allow proper sealing at the expected temperatures. As our design emphasizes fuel efficiency, we have also added a number of features to increase the efficiency and decrease the friction of the piston.

7.2.2 - Materials and Manufacturing:

For its improved heat dissipation capabilities, the piston will be made of forged 4032 aluminum. 4032 aluminum is a mid-tier strength aluminum that becomes stronger after a T6 temper. Forging was decided upon for its improved strength capabilities compared to casting. This decision was made using the following pugh chart.

Characteristic	Weight (0-1)	Forged Aluminum	4340 Steel	Cast Aluminum
Wear resistance	0.1	5	6	4
Strength	0.2	6	8	5
Cost	0.2	3	6	5
Thermal deformation resistance	0.2	5	6	4
Weight	0.3	8	2	8
SUM	1	5.7	5.2	5.6

Table 7.1: Piston Material Pugh Chart

After forging, the piston with undergo milling and turning operations. These are to cut the piston ring grooves, wrist pin hole, and clean the surfaces post forging. Then in order to further strengthen the surfaces of the piston, the piston will be mirco shot peened to improve it's fatigue life. The piston skirts are then plated with molybdenum disulfide, MoS_2, to improve the surface wear life and reduce the friction of the piston along the cylinder walls. The piston crown is plasma sprayed with a zirconia, titania, and yttria composite for strengthening as well as its reflective properties for improved thermal conditions.

7.2.3 - Design Considerations

BTN Performance initially considered square, undersquare, and oversquare bore to stroke ratios. Because we are pushing for a highly efficient engine, undersquare seems to have the most advantage. However, we decided that in order to keep good high end performance, a square configuration would give the best balance between efficiency and performance. This decision is covered in detail in section 5.4. This decision informs much of the design of the piston, the diameters necessary, piston ring design, and expected thermal loads. In addition to this, the required connecting rod design restricts the design of the piston skirt.

7.2.4 - Calculations

The largest force that the piston experiences is the force of combustion itself and much of the initial mathematical analysis to inform the design focused on this high stress state. The most important element is the thickness of the crown: designing it to stand up to both pressure and thermal loads. For pressure loads, the required thickness is based on the bore size B, maximum pressure of combustion, P_{ult}, and ultimate stress, σ_{ult}, of the material.

$$T_P = 0.43 * B\sqrt{\frac{P_{ult}}{\sigma_{ult}}} = 5.4mm$$

When thermal effects are taken into account, another equation for thickness from thermal stresses is added. For thermal loads, the required thickness is based on the heat power and change in temperature.

$$T_H = \frac{H}{12.56K\Delta T} * 10^3 \sim 10mm$$

In order to ensure the piston will fit properly with the effects of thermal expansion, the following equations were used to determine initial diameter such that in a hot, expanded state, the piston diameter will match the bore of width 86mm:

$$\frac{\Delta A}{A_0} = 2\alpha\Delta T$$

$$\frac{b^2 - d^2}{d^2} = 2\alpha\Delta T$$

$$d = 85.8mm$$

Piston ring dimensions were calculated considering the pressure on the rings. This pressure is estimated at 0.0042 MPa as recommended in *Design of Machine Elements* [13] and the factor of safety is set at 3. The ring thickness is calculated using the following equation:

$$T_r = B * \sqrt{\frac{3 * P * FOS}{\sigma_{ult}}} = 0.89mm$$

Also important to note is that the lands on the piston for the rings to seat into are 70% of their radial thickness. These general parameters were used to model the piston shape. Following the crown design, the skirt was then designed based on the load experienced from the thrust as well as the loads on the crown and wrist pin. To minimize the friction, ovality and barrel contouring were used in order to slightly decrease the surface area to which the force applies. The ovality and contouring are both on a scale of 1-3mm and therefore are difficult to see in the physical model, but the figures below show exaggerated versions of the concepts.

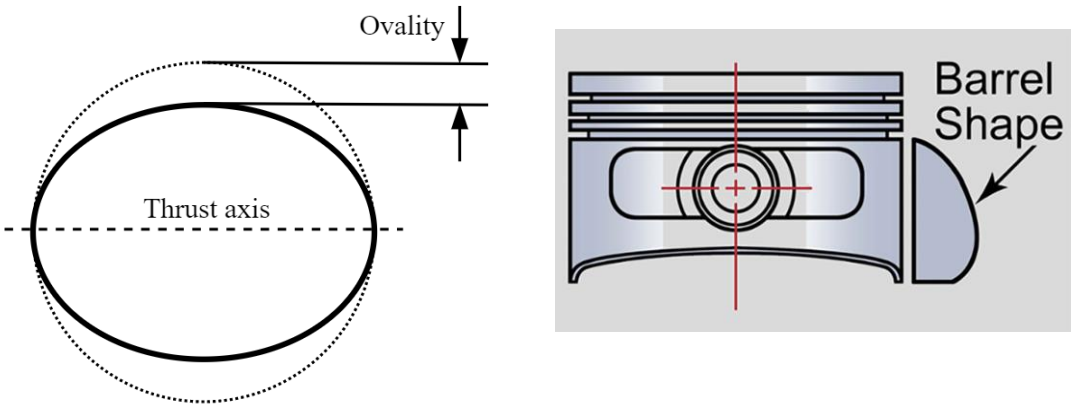

Figure 7.3: Exaggerated views of ovality, left, and barrel contouring, right [12]

In order to reduce weight, an asymmetric skirt was also iteratively designed considering thrusts on the major and minor sides. Finally, a small dishing of the piston crown was added to improve flow mixing and swirling and provide a slight benefit in terms of efficiency.

Lubrication holes were added between the interior portion of the skirt and the oil control ring land so that the splash lubrication of the connecting rod and wrist pin will provide lubrication of the piston.

7.2.5 - Analysis

Following the mathematical analysis and material decisions, FEA was performed on the piston model and changes were made to such parts as the thickness of material below the wrist pin, the thickness of the major and minor thrust sides, and the required fillets to avoid stress concentrations. Given the high temperature that the piston is expected to operate at, the analysis was done considering material properties at 200°C. The compressive load was calculated based off of the maximum pressure of combustion and the piston was fixed where the wrist pin touches the piston.

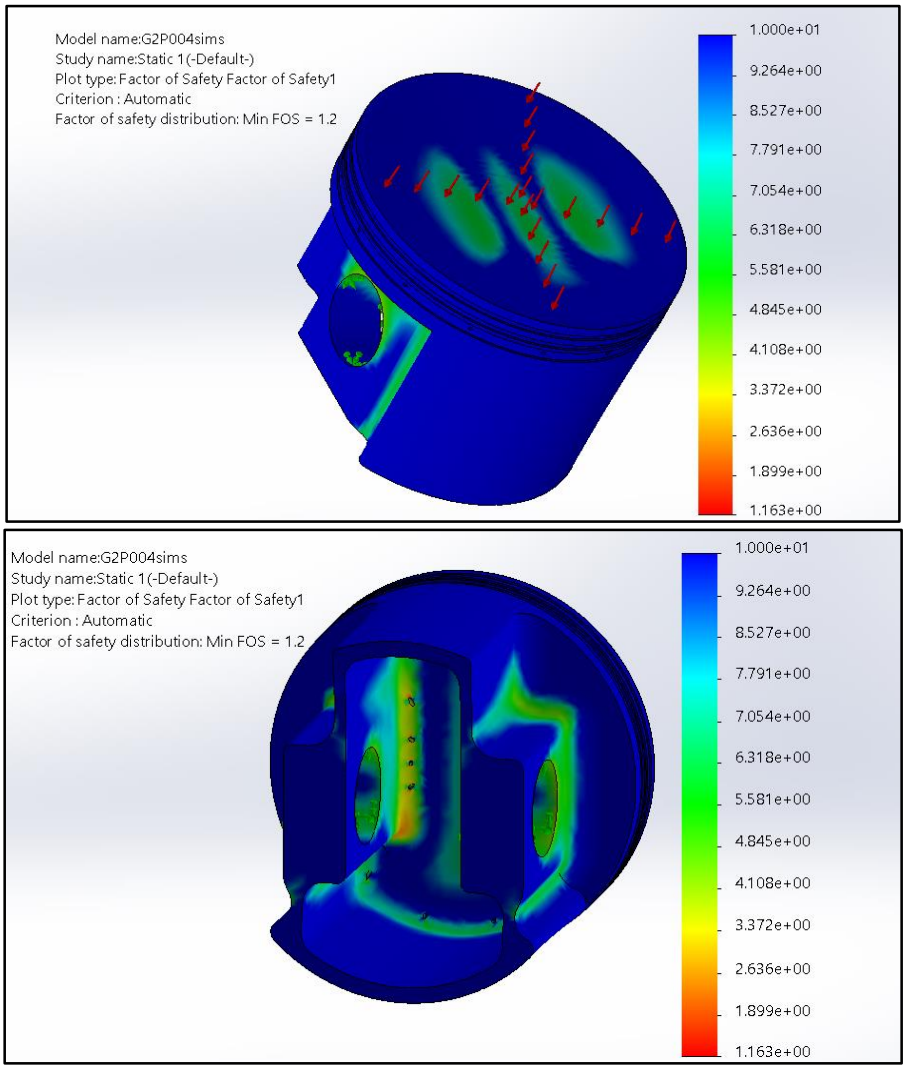

Figure 7.4: FEA FOS Plots for the Piston

As the piston is a critical component, a factor of safety in stress of greater than 3 was desired, however the Solidworks simulation finds a minimum factor of safety of only 1.2. As can be seen in the Figure below, the only place experiencing less than this is directly surrounding the lubrication holes, a noncritical component and location where work hardening is acceptable.

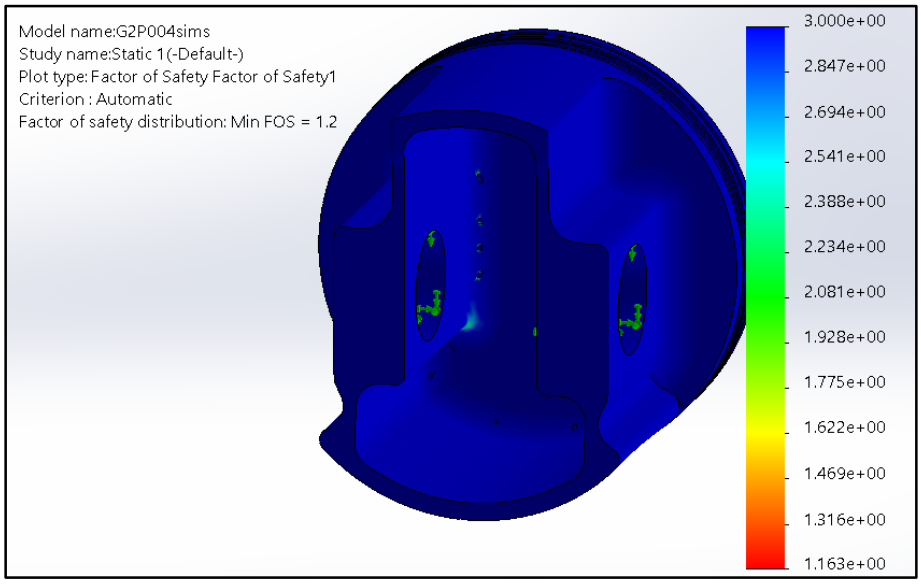

Figure 7.5: FEA FOS Plot for the Piston, Showing Areas with Lower Factors of Safety

7.3 - Piston Rings

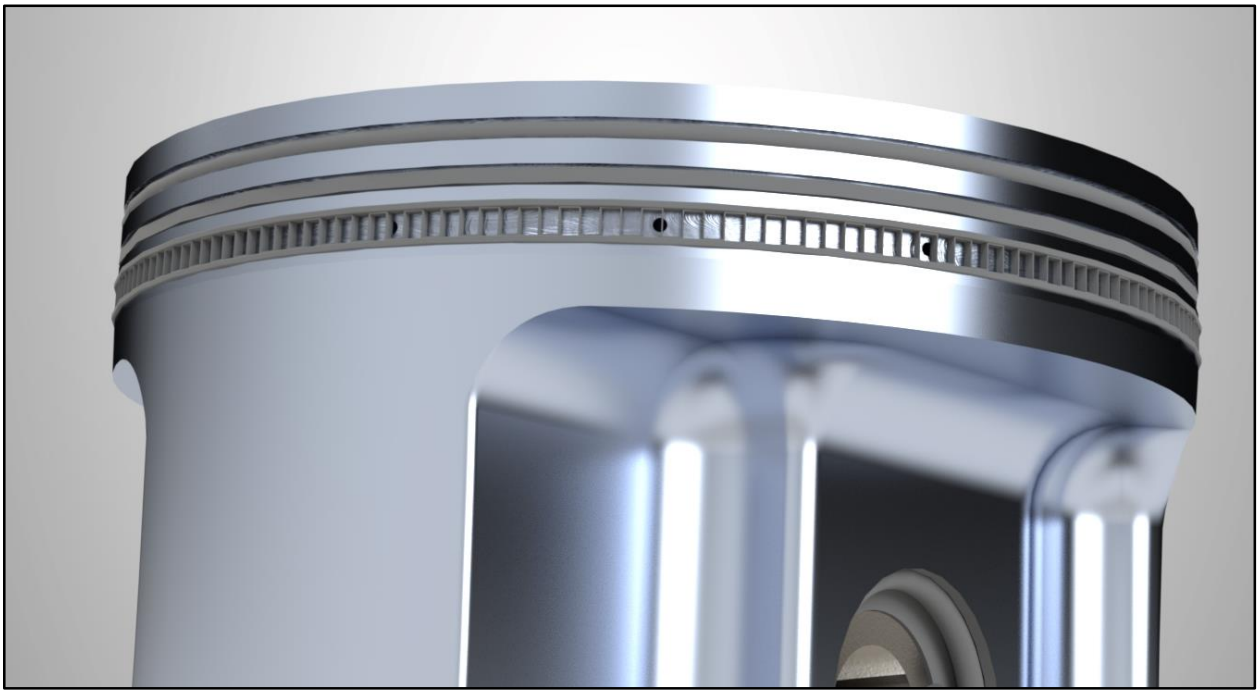

Figure 7.6: Render of Piston Rings

7.3.1 - Overview

The purpose of the piston rings is to separate the combustion chamber from the crankcase. They are located around the piston and move up and down with it. For our piston

rings, we decided upon two compression rings and an oil control ring. The compression rings act as moving seals between the piston and the cylinder walls. The oil control ring helps spread the oil released from the piston along the surface of the cylinders.

7.3.2 - Materials and Manufacturing

The two compression rings will be cast from nodular iron. Nodular cast iron was chosen over grey flake cast iron for its improved strength and ductility. The first compression ring will be chromium plated for reduced wear. The oil control ring will be a three part control ring made from a stamped low carbon steel. This means it will have two support rings and a spring ring. These rings will be nitrided to prevent corrosion.

7.3.3 - Design Considerations

For the ring cross-sectional profiles, we used variable profiles for different rings. We did a symmetrical barrel contour for the first compression ring. This was picked over the more common rectangular profile as it eliminates the run-in phase for rectangular rings. During the run-in phase, the rectangular profile is ground into the barrel contour. Eliminating this period reduces the friction in the system as well as the wear on the cylinder liner. The second compression ring will have a beveled leading shoulder for improved oil retention. The bevel works as a scraper to prevent excess oil from entering the combustion chamber. The oil control ring profile was picked from a standard style of oil control rings.

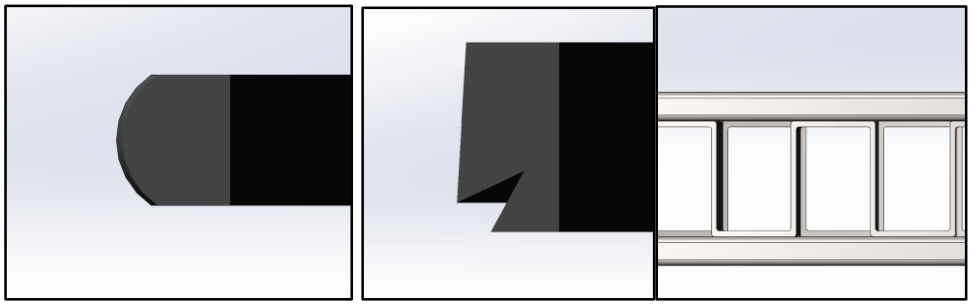

Figure 7.7: (From left to right) Cross Sections of 1st Compression Ring, 2nd Compression Ring, and Oil Control Ring

7.3.4 - Calculations

For the piston gap, we utilized the following table from SAE. This is in reference to the final gap for the piston ring. The recommended method of calculating the gap is the cylinder bore multiplied by 0.102 mm for the first compression ring and 0.127 for the second ring.

SAE RECOMMENDED AUTOMOTIVE COMPRESSION RING GAP CLEARANCE			
Ring Diameter		End Clearance Inspection Limit	
1.0000	2.3624	.006	.014
2.3625	2.9524	.008	.016
2.9525	3.5424	.010	.020
3.5425	4.3299	.012	.022
4.3300	5.1174	.014	.026
5.1175	5.9049	.016	.030
5.9050	6.8899	.020	.035
6.8900	8.9999	.024	.041
9.0000	10.9999	.029	.047

Table 7.2: SAE Piston Ring Gap

For piston ring thickness, refer to section 7.2.4.

7.4 - Wrist Pin

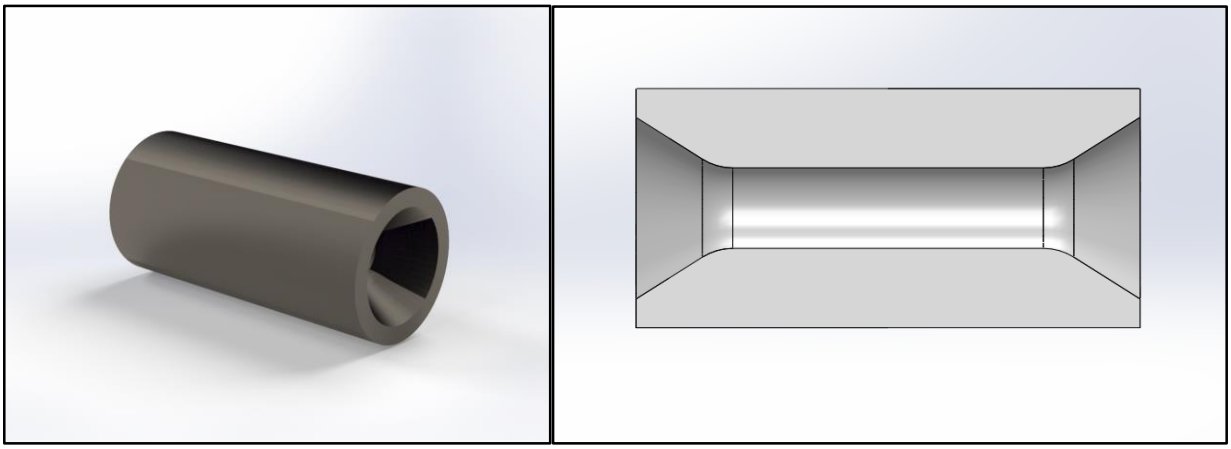

Figure 7.8: Renders of the wrist pin

7.4.1 - Overview

7.4.2 - Materials and Manufacturing

The wrist pin will be manufactured from extruded AISI 4340 steel. AISI 4340 was chosen for its high yield and fatigue strength as well as the strength it could gain through tempering. Following the extrusion, the wrist pins will be oil quenched and tempered to 205ºC. This temper temperature was chosen through CES Edupack after comparing the different heat treatments for this grade of steel. Following heat treating, the wrist pins will be turned and centerless ground with a taper.

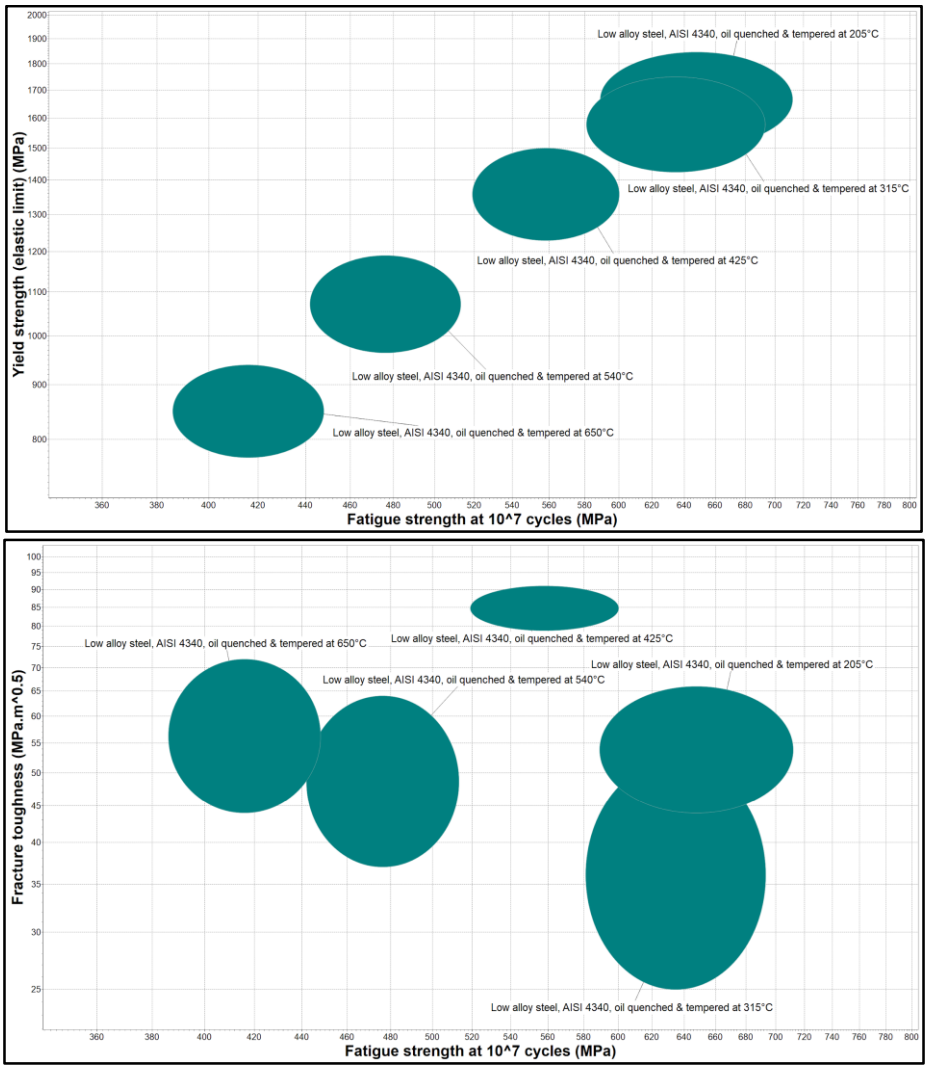

Figure 7.9: CES Edupack Plot of Yield Strength (Top) and Fracture Toughness (Bottom) vs Fatigue Strength for AISI 4340 at Different Heat Treatment Temperatures

7.4.3 - Design Considerations

We chose to use a full floating wrist pin due to the decrease in friction that it would provide. This is a costlier option as compared to a semi floating wrist pin but since our engine design emphasizes efficiency with increased cost as necessary we decided that fully floating made sense. A Pugh chart for this decision follows:

Characteristic	Weight (0-1)	Semi Floating	Fully Floating
Friction	0.7	3	7
Cost	0.3	7	3
SUM	1	4.2	5.8

Table 7.3: Wrist Pin Pugh Chart

7.4.4 - Calculations

Wrist pin calculations are relatively simple and depend only on being able to sustain the maximum stresses over a long life with neither fatigue nor abrupt failures. The maximum double shear stress of the wrist pin sets the required outer and inner diameters (OD and ID respectively) as in the following equation where the outer diameter itself is also chosen to make sense for the piston size. It is based on the maximum force, F, factor of safety, FOS, and yield stress, σ_y.

$$OD^2 - ID^2 = \frac{8 * F * FOS}{\pi \sigma_y} = 172mm$$

$$\text{Choose: } OD = 16mm \quad ID = 9mm$$

7.4.5 - Analysis

Once these required sizes were determined, internal taper geometry was iteratively designed with FEA to remove additional material and weight where it is unnecessary. Figure 7.10 below shows the results for stress and factor of safety.

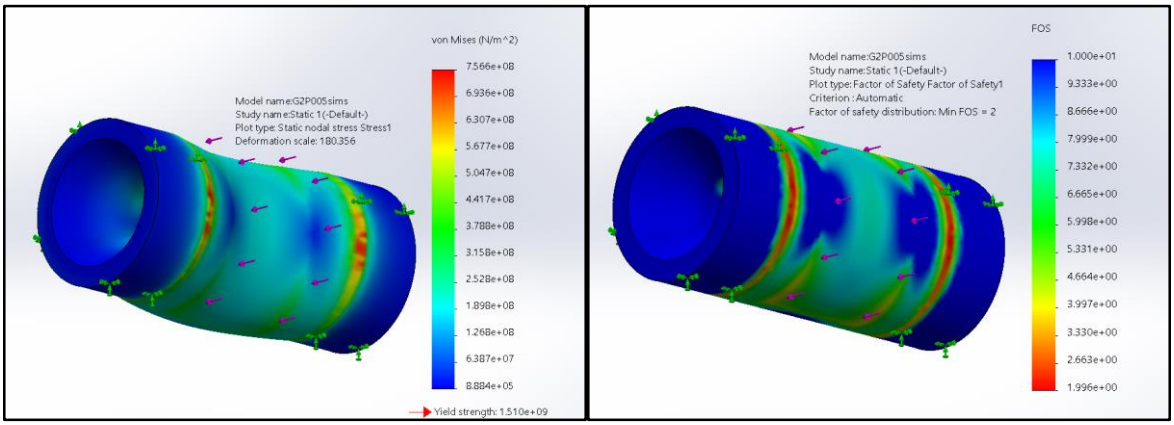

Figure 7.10: FEA Stress Plot (left) and Factor of Safety Plot (right) for Wrist Pin

Since the wrist pin was designed with a relatively low factor of safety of only 2, a fatigue study was conducted on this. Results are shown below in Figure 7.11. As the minimum everywhere is greater than 10^6, the infinite life threshold for steel, this means that infinite life is achieved.

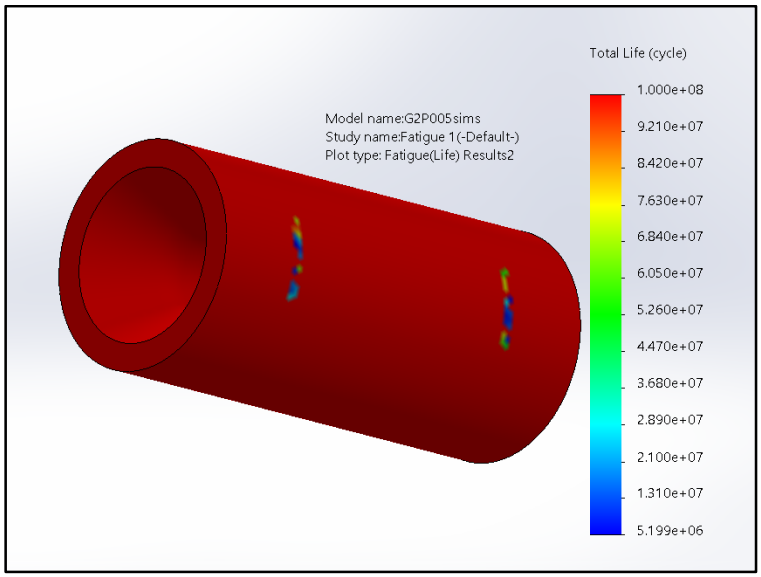

Figure 7.11: FEA Fatigue Plot for Wrist Pin

7.5 - Connecting Rod

Figure 7.12: Render of Connecting Rod

7.5.1 - Overview

The connecting rod is the means by which the force of combustion is transmitted from the piston to the crankshaft. As a result of this force, as well as the significant inertial forces that come with rotation at up to 8750 rpm, the connecting rod must be a very strong piece. The connecting rod is made of two pieces, the connecting rod cap and the connecting rod body, and is held together using M8 12.9 steel hex bolts and nuts, with an interfacing pocket machined for the heads.

7.5.2 - Materials and Manufacturing:

Similar to the wrist pin, the connecting rod will be made from AISI 4340 steel. However, for the connecting rod it will be forged.

Connecting Rod	Weight (0-1)	Titanium	Forged 4340 Steel	Forged Aluminum

Fatigue Life	0.25	6	8	5
Weight	0.35	8	5	7
Cost	0.2	1	8	5
Shock Absorbance	0.2	6	5	7
SUM	1	5.7	6.35	6.1

Table 7.4: Pugh Chart for Connecting Rod Material & Manufacturing

Following forging, the connecting rod will be oil quenched and tempered to 205°C. The end that connects to the crankshaft then needs to be split. To start the split, a laser etched line is drawn, then a wedge is pressed in using the etching as split line. The split face then would be milled to clean up the faces and will have holes drilled into them for fasteners. The bore will be bored and honed to ensure roundness. Oil passages will also need to be drilled.

7.5.2 - Design Considerations

In designing the connecting rod, the rod ratio is an important consideration. This is the ratio between the length of the rod, which in this case is the distance between the crank pin center and the wrist pin center, and the stroke length. In designing the BTN-1500E, it was decided to use a connecting rod ratio of 1.825. This would both improve efficiency and high end performance in order to better serve the market. (Table 7.4)

Characteristic	Weight (0-1)	1.5	1.6	1.7
Efficiency	0.35	3	5	7
High End Performance	0.3	3	5	7
Low End Performance	0.2	7	5	3
Height	0.15	6	5	4
SUM	1	4.25	5	5.75

Table 7.5: Pugh Chart for Connecting Rod Ratio

This longer rod means that there will be a slightly longer dwell at top dead center but the engine will be better able to deal with the forces of combustion in combination with a high red line. In accordance with these decisions and to provide a slight boost in high end performance, an I-beam design was chosen for the connecting rod.

Characteristic	Weight (0-1)	I	H
High End Performance	0.6	6	4
Low End Performance	0.4	4	6
SUM	1	5.2	4.8

Table 7.6: Pugh Chart for H vs. I Beam Connecting Rod Design

The cross section varies, slowly growing in width from the wrist pin to the crank pin. This ensures that the force is well distributed along the rod. In addition, in order to avoid the creation of stress concentrations, the connecting rod will not be threaded, and instead will be fastened together using a hex head bolt in a machined pocket, and a nut on the other end.

7.5.3 - Calculations

In determining the maximum forces acting upon the connecting rod, there were two considerations. First the vertical forces on the connecting rod were calculated, which rely on both the force of combustion and the inertial forces that are a result of the rotational speed of the crankshaft. The inertial forces were calculated using the rotational mass m_{τ} of the connecting rod and piston system, and calculated at redline, as that is when the forces would be at a maximum. Because the force of combustion varies with crank angle, θ, these values were taken at increments of 1 degree and added individually to create the plot below.

$$F_{Vert} = m_{\tau} \cdot redline^2 \cdot 0.043 \cdot \left(\cos(\theta) + \left(\frac{.043}{.146} \right) \cos(2\theta) \right) + F_{Combustion}$$

Next the horizontal forces were calculated, which were simply a product of the inertial forces mentioned previously.

$$F_{Hor} = m_2 \cdot redline^2 \cdot 0.043 \cdot \sin(\theta)$$

The calculations used can be found in the MATLAB file ConRodForcesBTN.m, and the results can be found in Figure 7.11 below.

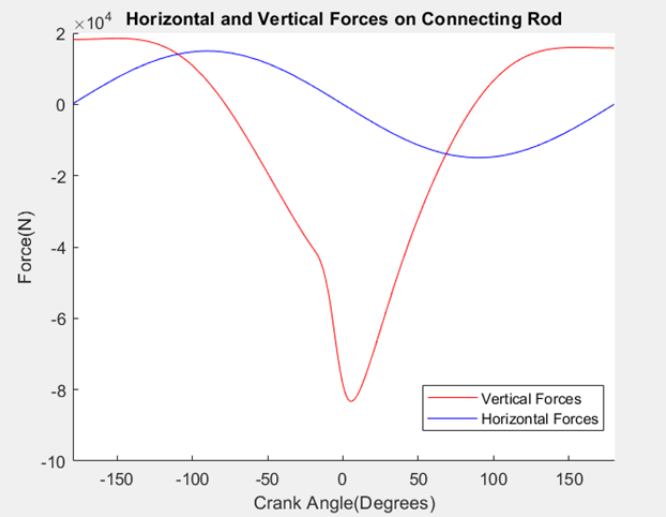

Figure 7.13: Plot of Forces on Connecting Rod

7.5.4 - Analysis

In determining whether the designed connecting rod would be strong enough to perform the necessary force transmissions, Solidworks finite element analysis was performed using both the maximum horizontal force, ~20kN, and the maximum vertical force on the connecting rod, ~79kN. In order to better show the distribution of the factor of safety to yield, the maximum factor of safety was set to 20. The minimum factor of safety for vertical forces is 5.3, and for horizontal it is 11. The location of this minimum is a result of the oil passage hole that passes from bore to bore. In determining the life of the connecting rod, a Solidworks fatigue analysis was conducted with S-n data from CES Edupack and the maximum compressive loading state from the earlier condition. As the force experienced is not fully reversed, this simulation was run using a minimum force of 0. This determined that the connecting rod would not fail under infinite life conditions.

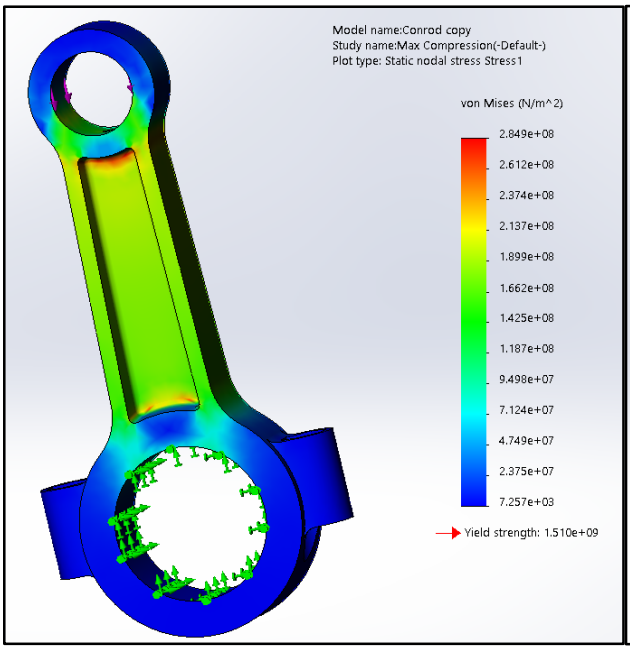

Figure 7.14: Vertical FEA for Connecting Rod

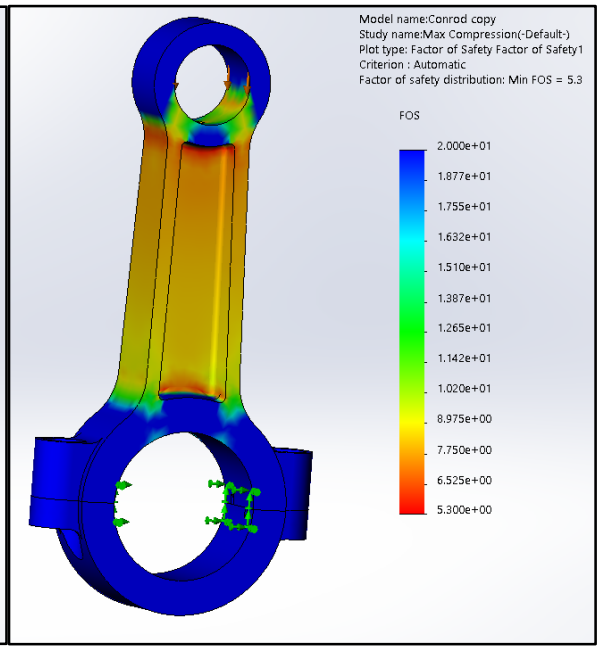

Figure 7.15: Vertical FOS Plot for Connecting Rod

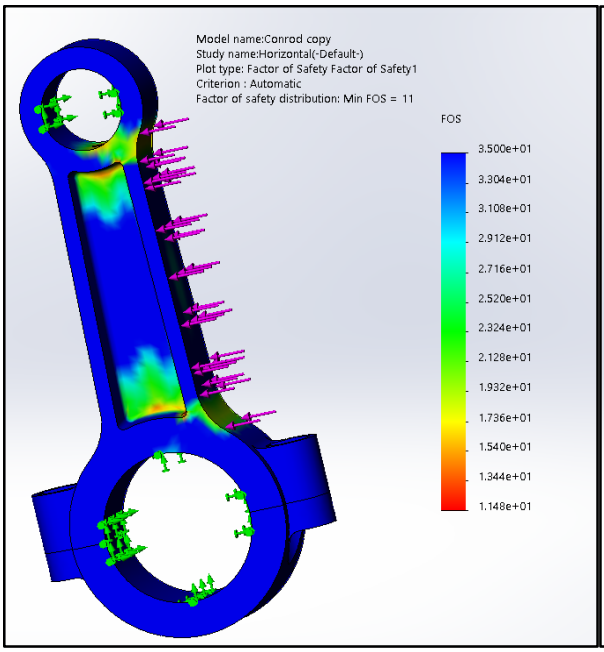

Figure 7.1: Horizontal (Inertial) FOS Plot for Connecting Rod

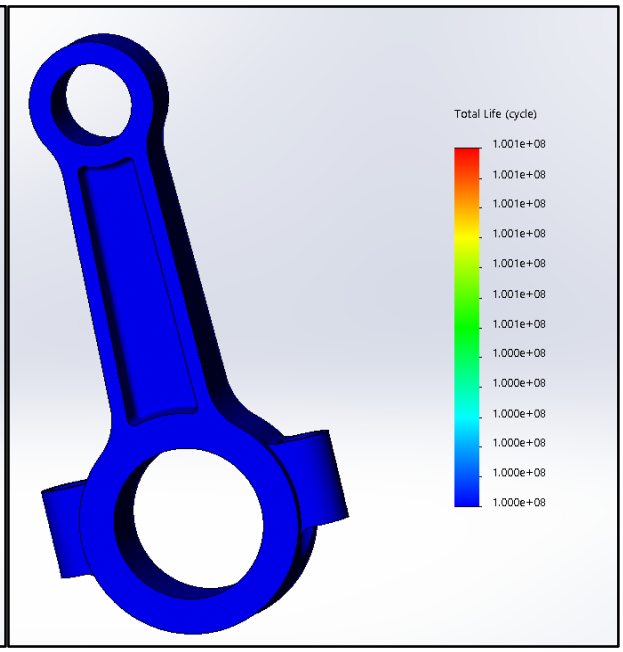

Figure 7.17: FEA Plot of Fatigue for Connecting Rod

7.6 - Crankshaft

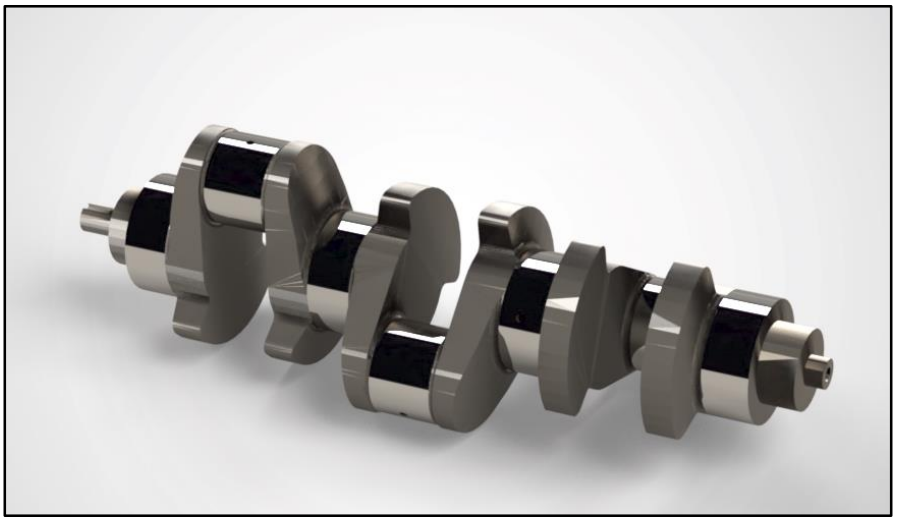

Figure 7.18: Render of Crankshaft

7.6.1 - Overview

The crankshaft is designed to create rotational motion from the linear motion created by the pistons. The shaft is supported by four journal bearings, two at each end, and two in between the connecting rod bearings. One of those two inner bearings is a thrust bearing, to deal with any axial forces. Each bearing is lubricated via pressurized oil channels that run through the crankshaft, from main journal to crank journal. Because the BTN-1500E is an inline 3 engine, each crankpin must be equally spaced around the crankshaft, at 120 degree increments. Finally, the crankshaft transmits power to the transmission.

7.6.2 - Materials and Manufacturing

The crankshaft will be forged from AISI 4340 steel. It is a strong steel commonly used for crankshafts. Following forging, the crankshaft will be oil quenched and tempered to 205ºC. It will then be turned and ground on critical points. Finally, oil passageways will be drilled.

Characteristics	Weight (0-1)	Cast Nodular Iron	Cast Mild Steel	Forged Mild Steel	Forged 4340	Billet Cromoly
Fatigue	0.35	3	5	5	7	7
Weight	0.45	3	4	5	6	7
Cost	0.2	10	9	8	7	1
SUM	1	4.4	5.35	5.6	6.55	5.8

Table 7.7: Pugh Chart for Crankshaft Material & Manufacturing

7.6.3 - Design Considerations

The crankshaft has two counterweights for each crankpin opposing the webs. These are designed to offset the mass of the crankpin and connecting rod. In addition, the oil passages run between the main journal to the crank pin, through the webs. These passages can be seen in the following Figures:

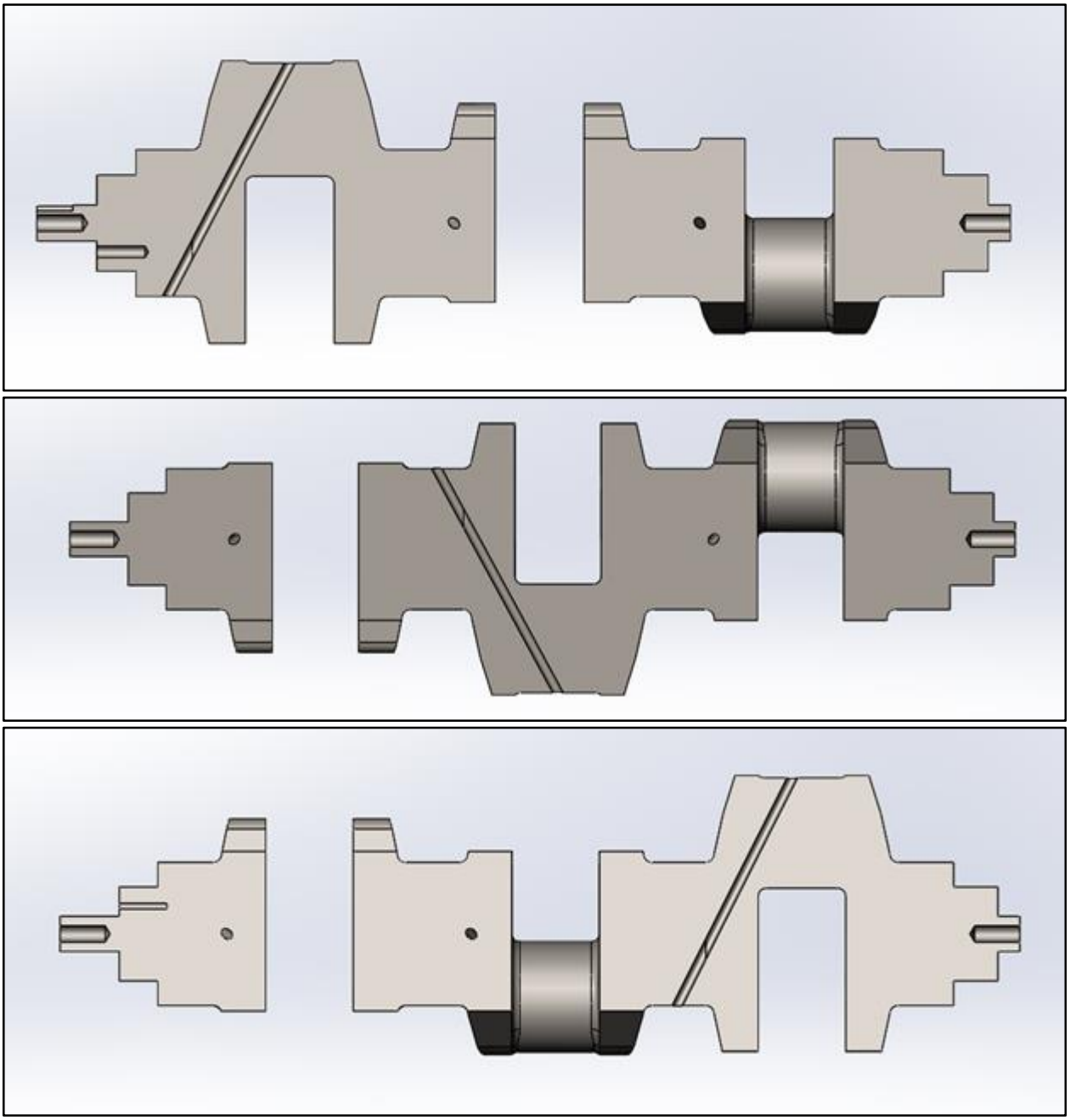

Figure 7.19: Oil Passages Through the Crankshaft

7.6.4 - Calculations

In order to determine the necessary strength of the crankshaft, the bending moment must be calculated using the rotational forces and the strength of the vertical forces on the connecting rod. Below is the equation for rotation force, with *F* being the rotational force, *R* the radius of rotation, *m* the rotation mass, and ωthe angular velocity.

$$F = mR\omega^2$$

As there are two counterweights per crankpin, each counterweight balances out half of the mass of the connecting rod and crankpin. The following equation ensures that the crankshaft is as close to balanced as possible.

$$m_{Counterweight} R_{COM\ Counterweight} = \frac{(m_{con\ rod} + m_{crankpin})}{2} \frac{Stroke}{2}$$

Calculating the bending moment itself is fairly simple. This calculation uses the reciprocating force from the connecting rod calculations, applied at top dead center. This is shown in the following equation.

$$M_{bending\ Max} = F_{TDC} * Stroke/2$$

Using the moment from the previous equation, it is possible to calculate the maximum bending stress the crankshaft should experience.

$$Bending\ Stress\ = MC/I$$

The maximum bending stress that results, however, is dominated by the vertical forces experienced by the connecting rod, and therefore those maximum forces as seen in Figure 7.13 above were used for our analyses.

7.6.5 - Analysis

To ensure that the designed crankshaft would be strong enough to hold up to the stresses it would be exposed to during its life, Solidworks FEA was performed. This took into account the forces that would be applied during the maximum loading period, top dead center for the first piston. In addition, at this same time the forces that the other two crank pins were experiencing were also included, although these are much less than the max force experienced by the first crank pin. The FEA shows a minimum safety factor to yielding of 11.3 which is fairly high, which is a result of the maximum stress of 134MPa. This analysis was then applied to a

Solidworks fatigue analysis, with a minimum force of 0. The results of that study determined that the crankshaft was well within infinite life.

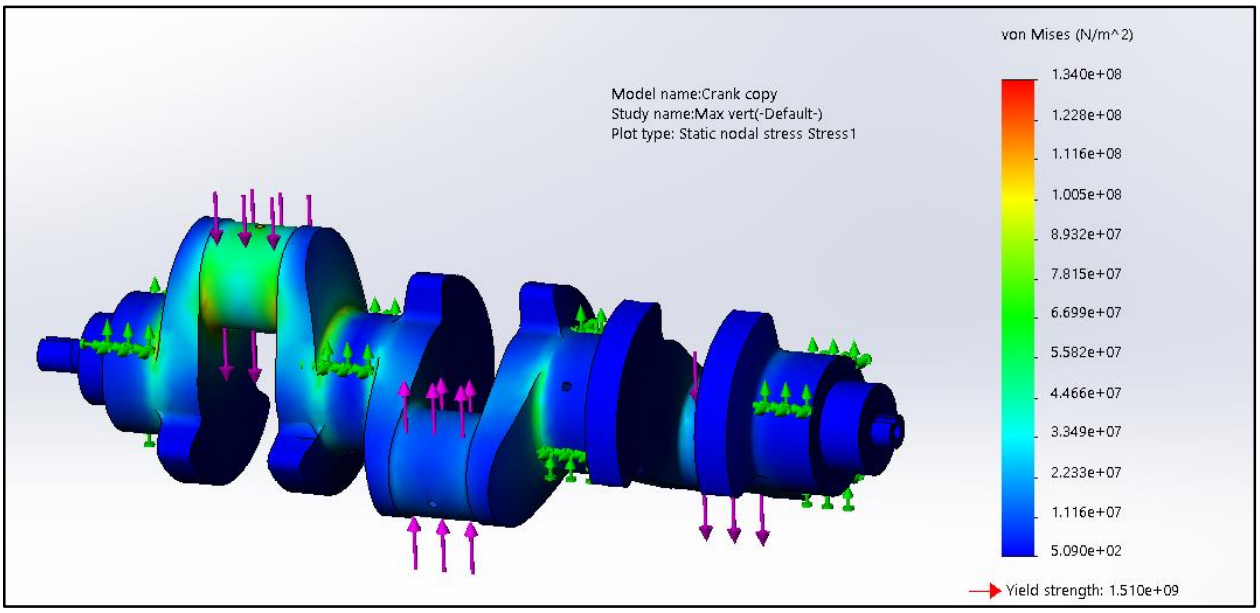

Figure 7.20: FEA Plot for Crankshaft

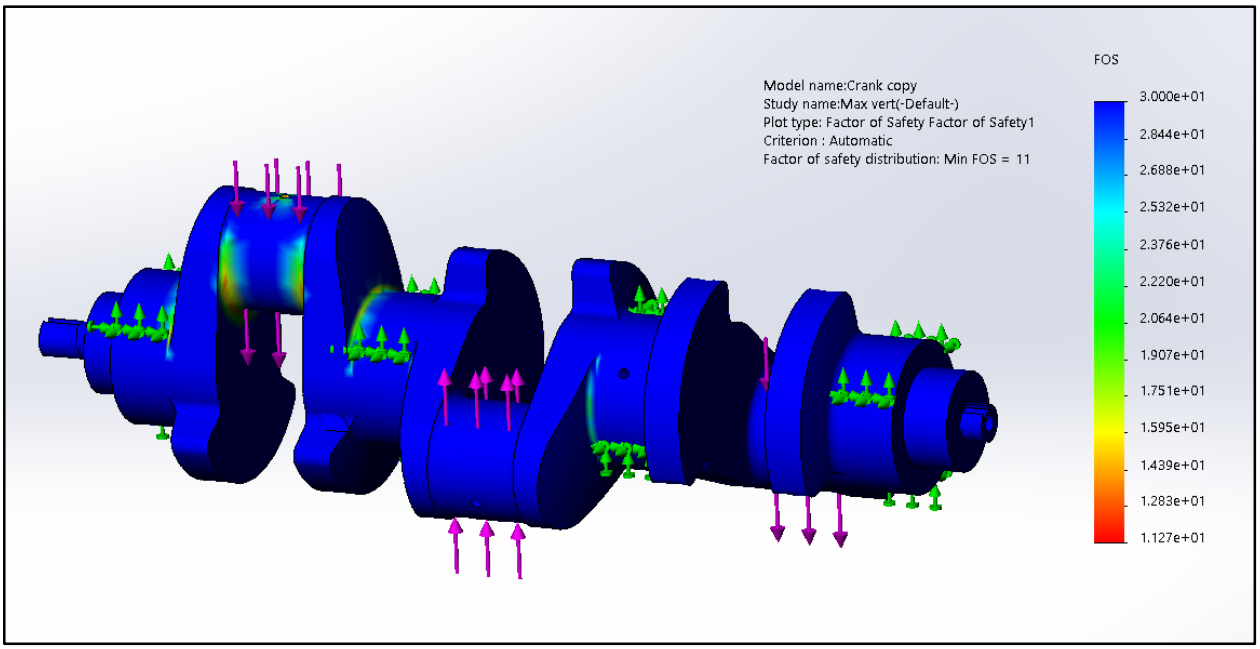

Figure 7.21: FOS Plot for Crankshaft

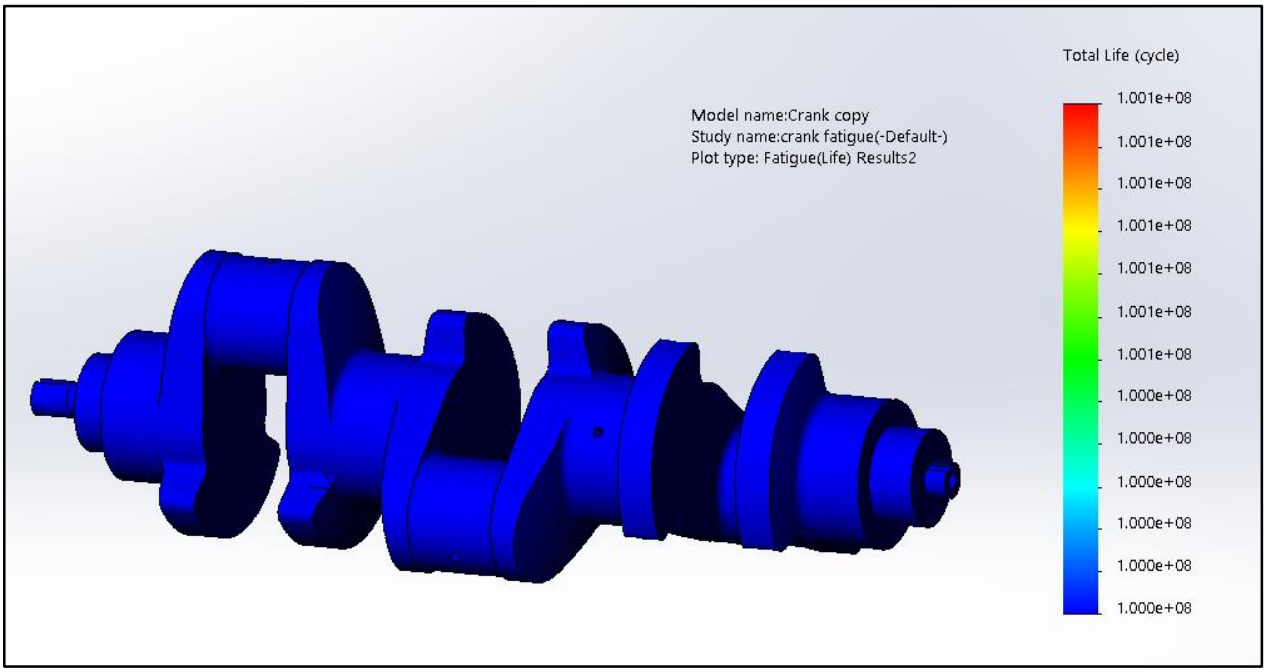

Figure 7.22: Fatigue FEA Plot for Crankshaft

7.7 - Engine Block

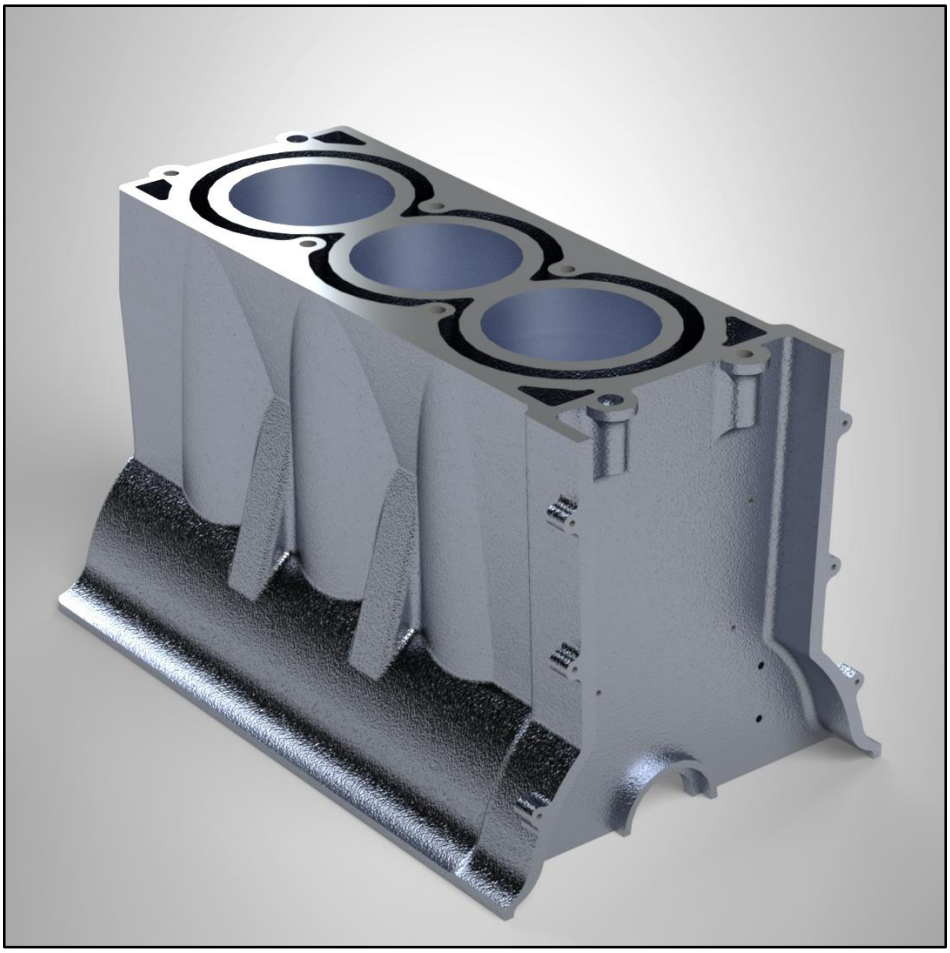

Figure 7.23: Render of Engine Block

7.7.1 - Overview

The engine block serves to tie together and contain all of the separate assemblies in the engine. It contains the cylinders, main journals, main seal bosses, oil pan sealing surface, and deck. It also contains the oil passages to the main journals and the lower cooling channels. As the inlet for oil and coolant, it also must interface with the cylinder head to carry both to the necessary locations, and must also provide a way for the cylinder head lubrication to return to the cylinder head.

7.7.2 - Materials and Manufacturing:

The engine block is made from A356 Aluminum, an aluminum alloy that is well suited for casting. Aluminum was chosen over cast iron for its higher coefficient of heat transfer, as

well as its superior weight savings. This alloy was chosen by comparing the most common alloys used to manufacture engine blocks through the use of CES EduPack.

Characteristic	Weight (0-1)	Aluminum	Cast Iron
Weight	0.25	7	4
Cost	0.1	5	8
Thermal Efficiency	0.3	7	4
Corrosion Resistance	0.15	8	1
Size	0.2	6	5
SUM	1	6.75	4.15

Table 7.8: Engine Block Material Pugh Chart

The engine block will be sand cast and then tempered to T6. Following casting, the block requires machining. The mating faces for the cylinder head and the oil pan will need to be milled flat, and the cylinders will need to be bored and honed. The main journals will also require boring and honing. Then the oil passages from the main oil rail to the main journals will need to be drilled. The coolant inlet needs to be drilled to the proper size.. Exterior mounting holes for chain guides, timing covers, and chain tensioners will also be drilled and tapped as needed. The holes for the main and head mounting holes need to be drilled and tapped with M10x1.25. Lastly the cylinders will be bored and plasma sprayed with a zirconia, titania, and yttria composite.

Plasma spray was chosen over cast iron cylinder liners because it is a lighter alternative. Plasma spray also allows for a more wear resistant surface and lower friction as well as allow greater heat dispersion to the aluminum block than cast iron sleeves. The zirconia, titania, and yttria composite was chosen from other plasma spray materials as it was rated for the high heat of the combustion.

Characteristic	Weight (0-1)	Cast Iron (Dry)	Nikasil	Plasma Spray
Wear resistance	0.3	7	7	9
Strength	0.25	6	7	8

Cost	0.1	8	4	6
Friction	0.35	6	9	9
SUM	1	6.5	7.4	8.45

Table 7.9: Cylinder Liner Pugh Chart

7.7.3 - Design Considerations

Our main decision we had to make for the design of the engine block was whether we wanted to incorporate an open, semi-open, or closed deck. An open deck has no material at the top of the cylinders connecting to the engine block, a semi-open deck has partial webs connecting the top of the cylinders to the engine block, and closed deck has no gaps between the cylinders and the top of the engine block. More open decks provide better cooling and are cheaper to manufacture, while more closed decks are stronger. In the end, our group decided to use an open deck style of engine block due to the relatively low compression ratio and corresponding maximum cylinder pressure.

7.7.4 - Calculations

The next major design consideration to determine to cylinder wall thickness, we treated the cylinder as pressure vessel. Utilizing the max pressure calculated during combustion along with the yield strength and bore radius to back solve for the vessel wall thickness, with the following equation. T is the thickness, P is the max pressure in the combustion chamber, r is the bore radius, and σ_o is the yield strength of the engine block material.

$$t = \frac{P * FOS * r}{\sigma_o}$$

With a factory of safety of four, we calculated the necessary wall thickness of the cylinder to be 10 mm.

7.8 - Balance Shaft

Figure 7.24: Render of Balance Shaft Assembly

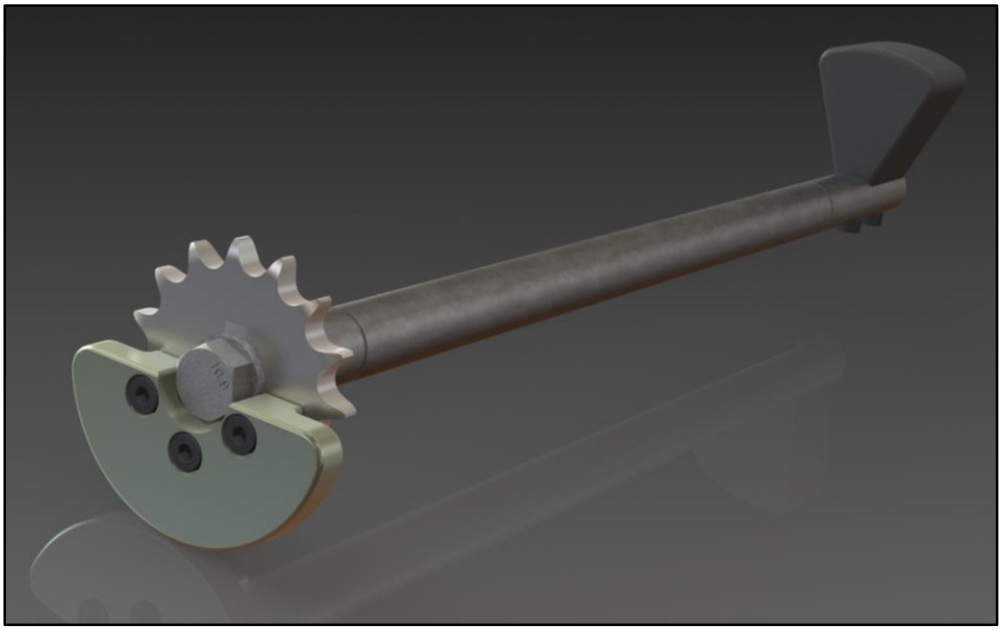

7.8.1 - Overview

The purpose of a balance shaft is to reduce the vibrations produced by an internal combustion engine. This is typically accomplished using a series of rotating shafts with eccentric weights, where the amount and location of these weights is dependent on the cylinder configuration. Our choice to use an inline-three cylinder configuration necessitated the design of a singular balance shaft due to a longitudinal rocking moment. This balance shaft will rotate in the opposite direction of the crankshaft but at the same RPM. With 120 degree firing interval, as our engine uses, the primary and secondary inertial forces are balanced. However, rocking moments are not inherently balanced in the inline 3-cylinder engine and so it needs a balance shaft module that produces moments with opposite phase.

7.8.2 - Materials and Manufacturing

Our balance shaft will be cold rolled out of 4340 steel, turned to the correct diameter and to add two grooves for retaining rings. 4340, while pricey, was necessary due to the small diameter and large forces being exerted on the shaft. One end will have a slot milled into it for the far weight while the other will be tapped for an M8 bolt and will also have a keyway milled in. The far weight will be cast out of white iron with two holes taped for M4 screws in the bottom, while the close weight will be made out of sintered tungsten. Cast iron was the preferred material for both weights, as it is cheap and relatively dense, but due to size constraints tungsten

was chosen for the close weight due to its much higher density. The relatively high material cost is offset by the significant performance gains due to the smaller size of the weight. The sprocket is purchased but will be broached for a key and will be tapped for three M4 holes to accept the close weight.

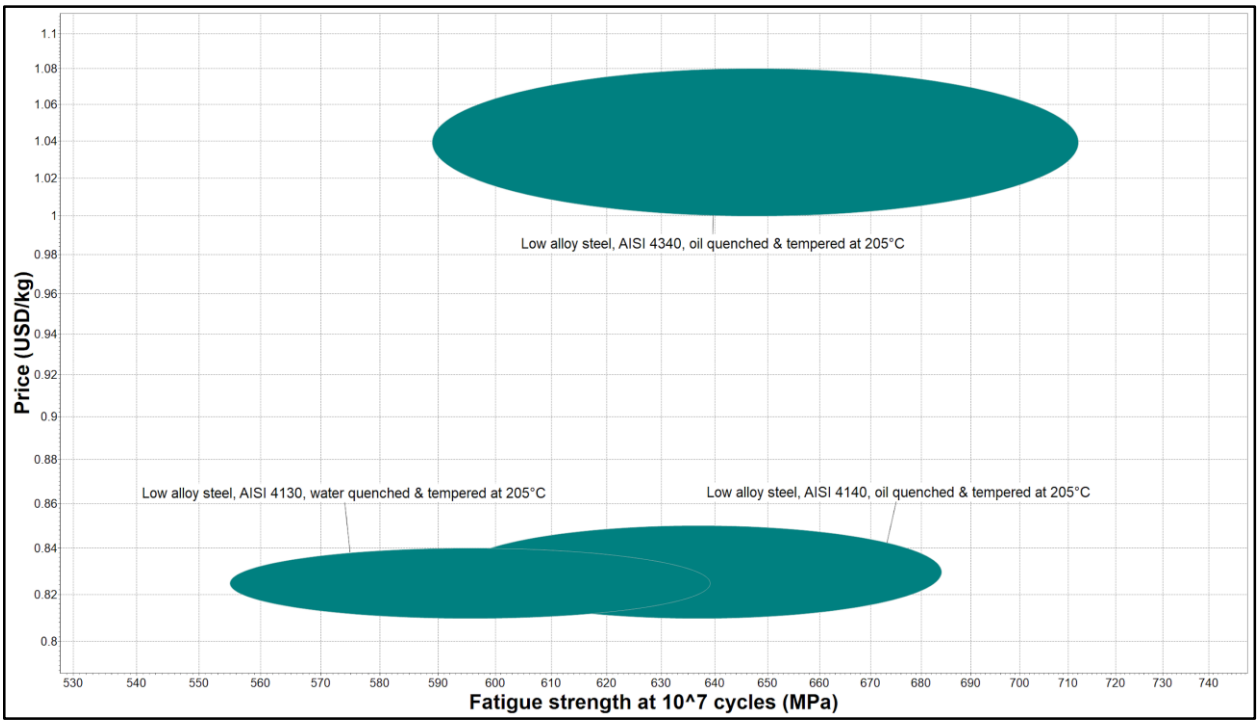

Figure 7.25: CES Edupack Plot of Price vs Fatigue Strength for AISI 4130, 4140, and 4340 for Balance Shaft Material Selection

7.8.3 - Calculations

Considering the No.1 cylinder as the reference cylinder, the balances of forces and moments due to the reciprocating masses of the piston and connecting rod, etc. are investigated. Since the No.1 cylinder is the reference cylinder, the No.2 cylinder lags 120 degrees behind and the No.3 cylinder 240 degrees behind. The total sums of the primary and secondary reciprocating forces at any crank angle α for the No.1 cylinder are in balance, however the primary and secondary reciprocating moments remains out-of-balance. The equations for both are given below, respectively, where $m_p$is the total reciprocating mass, r is the crank throw length, $\omega$is the rotational speed of the engine, l is the bore spacing, and α is the crank angle.

$$M_p = .5 * m_p * r * \omega^2 * [l * cos(\alpha - 120°) + 2 * l * cos(\alpha - 240°)]$$

$$M_s = .5 * m_p * r * \omega^2 * \frac{r}{L} * [l * cos(2 * \alpha - 240°) + 2 * l * cos(2 * \alpha - 480°)]$$

As can be seen by the equations, the primary moment is dominant, and so is the one addressed by the balance shaft. This means that the moment generated by the balance shaft should be the opposite of that of the primary moment (i.e. $M_p = M_b$). The next step was to calculate the necessary design parameters for the balance shaft itself, namely the spacing of the weights (l_b), the mass of the weights (m_b), and the distance from the center of the balance shafts to the center of mass of the weights (r_b). This was done using the equation below.

$$m_b * r_b = .433 * m_p * r * \frac{l}{l_b}$$

We then iterated across a range of different m_b and r_b values until we found a combination that fit with our geometry constraints. Additionally, as our weights are asymmetric, we needed to make sure that they had the same $m_b * r_b$.For reference, our analysis used an m_p of 1.44 kg, and we said that l_b was equal to .277 m to ensure that the far mass would rotate between the counterweights of cylinder 1. For our far mass, we calculated an m_b of .273 kg with an r_b of .043 m, and for our close mass we have an m_b of .470 with an r_b of .025 m.

7.8.4 - Analysis

Figure 7.26 shows the rocking moment of the engine before the balance shaft, the corresponding moment of the balance shaft, and the net moment after the balance shaft is installed. These graphs were generated using the MATLAB codes Unbalance.m and Balanceshaft.m, found in Appendix E. The max moment before the balance shaft is added is 5213 Nm, while the max moment after the balance shaft is only 794 Nm. This is a reduction of almost 85%, which well justifies the added cost and complexity of this component.

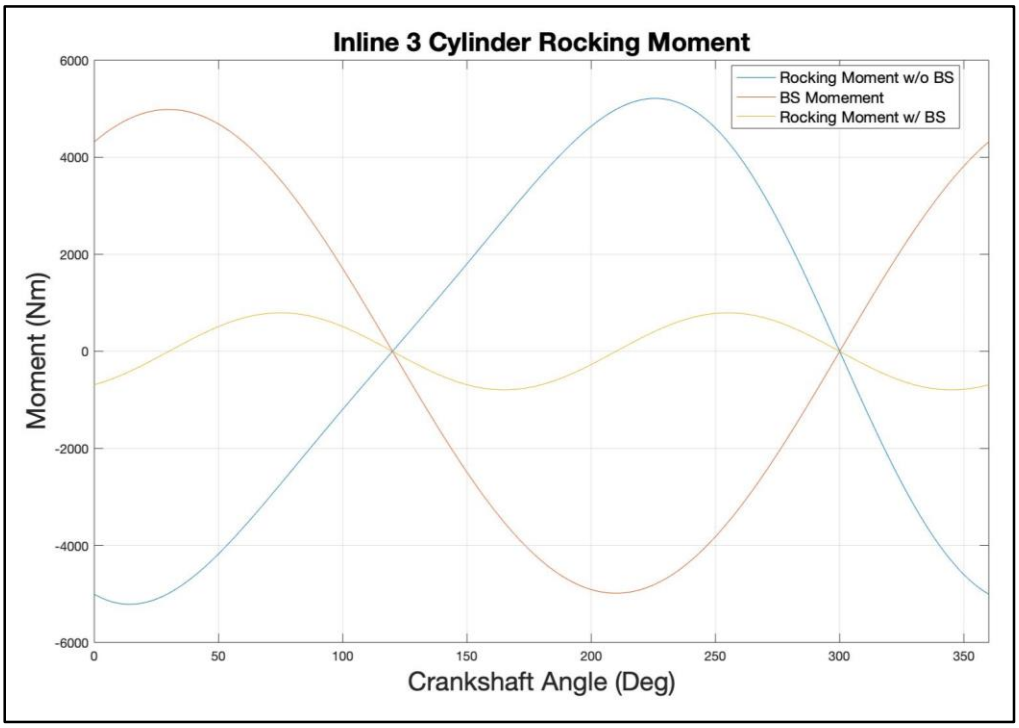

Figure 7.26: Plot of Engine and BS Rocking Moments

We also performed FEA on the far end of the balance shaft to ensure that, at redline, the centrifugal force of the weight would not cause balance shaft failure. We held the faces before the retaining ring fixed and placed our force on the mating face between the balance shaft and the far weight. Our force was derived from the equation for centripetal force, and came out to 504 N. Figure 7.27 is a FOS plot of this analysis, which shows that the minimum FOS for the balance shaft is above 2.

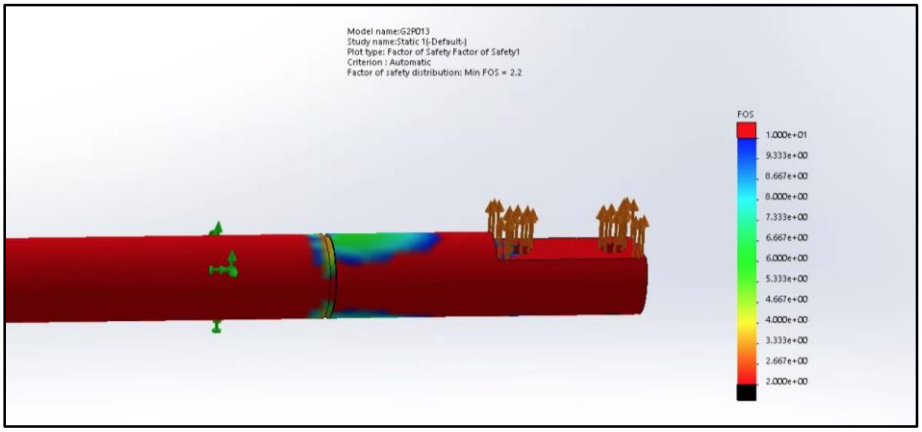

Figure 7.27: FOS Plot for Centrifugal Balance Shaft Loading

7.9 - Balance Shaft Girdle

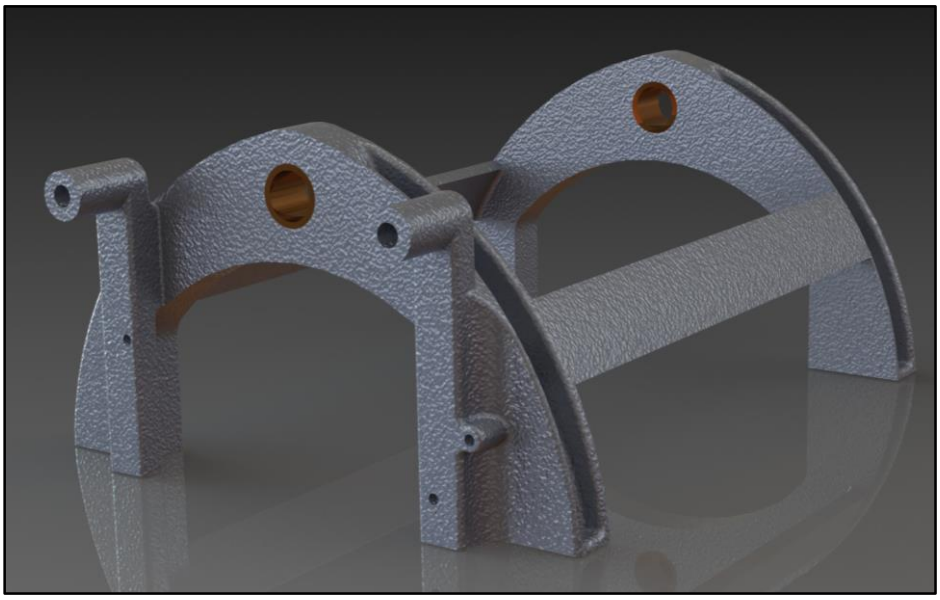

Figure 7.28: Render of Balance Shaft Girdle

7.9.1 - Overview

The balance shaft girdle exists to connect the balance shaft and balance shaft drive assemblies. It bolts directly to the bottom of the engine block and is installed after the upper half of the oil pan, but before the bottom half. It contains bronze bearings for the balance shaft, bosses for the idler sprockets, and also has mounting holes for the balance shaft chain guide and idler.

7.9.2 - Materials and Manufacturing

The balance shaft girdle will be sand cast out of A356 aluminum. This material was selected due to its excellent tensile properties and its abundance throughout the engine which should reduce manufacturing costs. After casting, the bores for the bronze bushings will be bored to final diameter and the bushings will be pressed into the bores. The mounting holes for the idler sprockets and chain guides will be drilled and tapped for M8 and M4 bolts, respectively, and the engine block mounting holes will be drilled for M10 clearance holes.

7.9.3 - Analysis

To ensure that the girdle could handle the centrifugal stresses from the balance shaft rotation, FEA was performed using SolidWorks. The results can be seen in Figure 7.29 below.

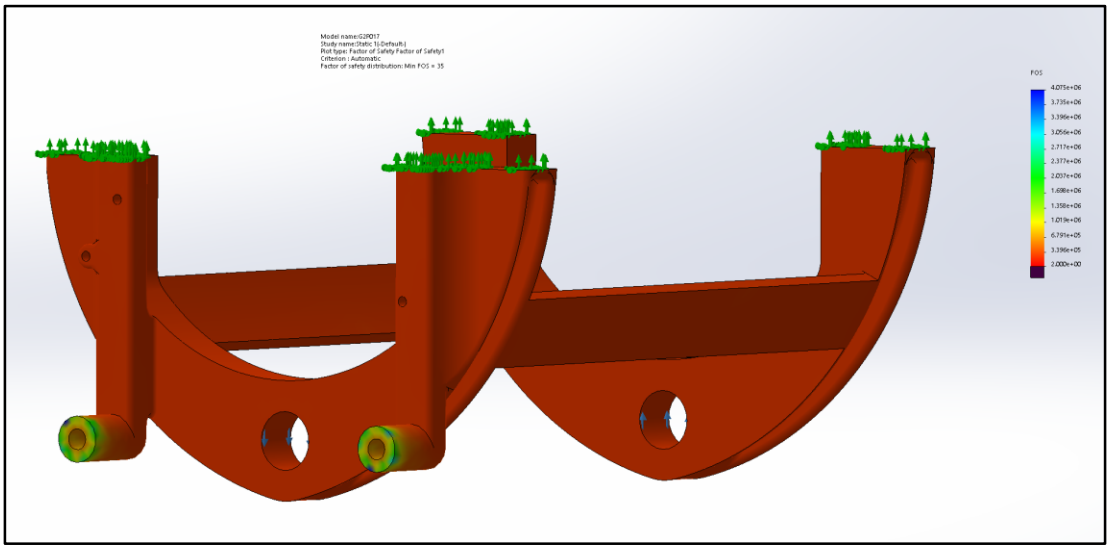

Figure 7.29: Balance Shaft Girdle FEA

As can be seen from the Figure, the balance shaft was constrained on the mating faces with the engine block and the bearing faces were each given a load of 500N in opposite directions (taken from section 7.8.4). With this loading, we have a minimum FOS of 35, which is well above what is required. This means that our girdle should hold up under any condition.

7.10 - Oil Pan

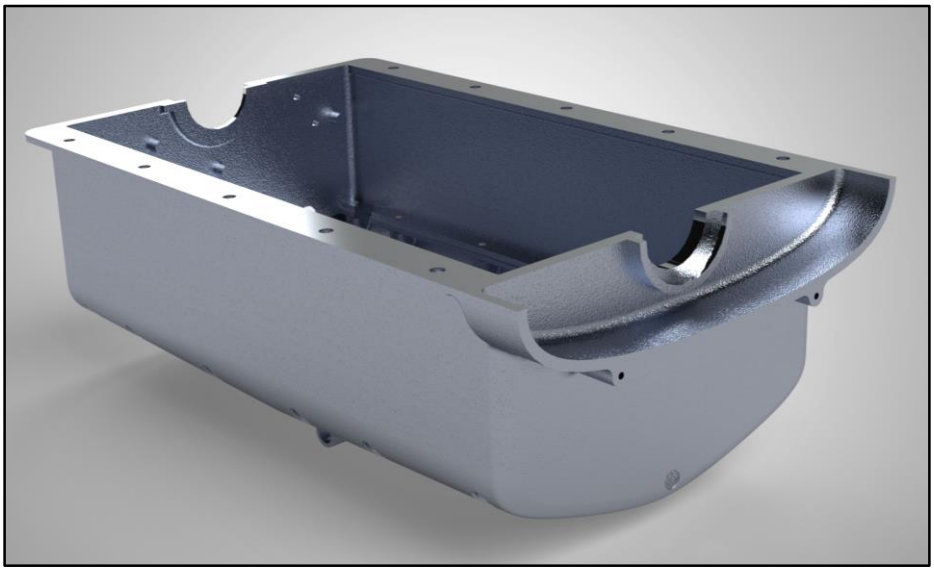

Figure 7.30: Render of Oil Pan Assembly

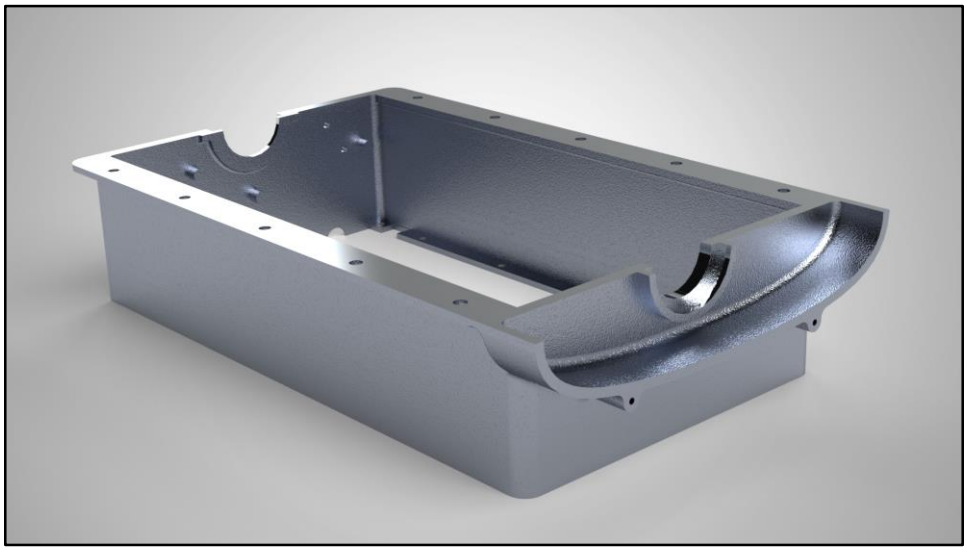

Figure 7.31: Render of Top Oil Pan

Figure 7.32: Render of Bottom Oil Pan

7.10.1 - Overview

The purpose of the oil pan is to contain and seal the engine oil used for lubrication. Our oil pan is split into two pieces to allow for the balance shaft girdle to be inserted. The upper oil pan seals against the bottom of the engine block with 10 M6 screws and silicone sealant, while the lower oil pan seals against the upper oil pan with 8 M4 screws and silicone sealant. The upper oil pan contains half of the bosses needed for the front main seal, rear main seal, both idler shaft seals, and the balance shaft seal. It also has mounting holes and bosses for the balance shaft timing chain tensioner, guide, and cover. The lower half contains bosses for both idler shaft seals and the balance shaft seal. It also has a ⅛” NPT threaded hole for an oil drain / pickup.

7.10.2 - Materials and Manufacturing:

The oil pan is made of Aluminum A360, a cheap die castable alloy. Die casting was chosen because it allows for higher detailed casting over sand casting. Die casting also becomes far cheaper the larger the batch size. Finally, casting was picked over stamping because it requires fewer operations. Engine box mating surface and mounting holes will be cleaned up by post machining. Additionally, a ⅛” NPT hole will be drilled in the bottom to allow an AN-8 fitting to be attached for draining and exterior oil pump pickup.

7.11 - Bearings

Figure 7.33: Image of King Trimetal XP Series, pMax Black

The bearings for the BTN1500-E will be purchased from King Bearings. In order to ensure that the bearings are able to perform in a similar manner to the rest of our engine, we will be using King Tri-metal XP bearings. These are high performance, high wear resistance bearings that use a proprietary coating for good performance. These bearings will be set into the engine block and the connecting rods, and the holes and grooves will ensure that each journal is well lubricated. Each bearing has one notch per half, which interface with the larger part of the two parts that the bearing will interact with.

The sizing calculations for the main, rod, intake cam, and exhaust cam journal bearings are shown in the lubrication section 6.8, above.

7.12 - Bolts

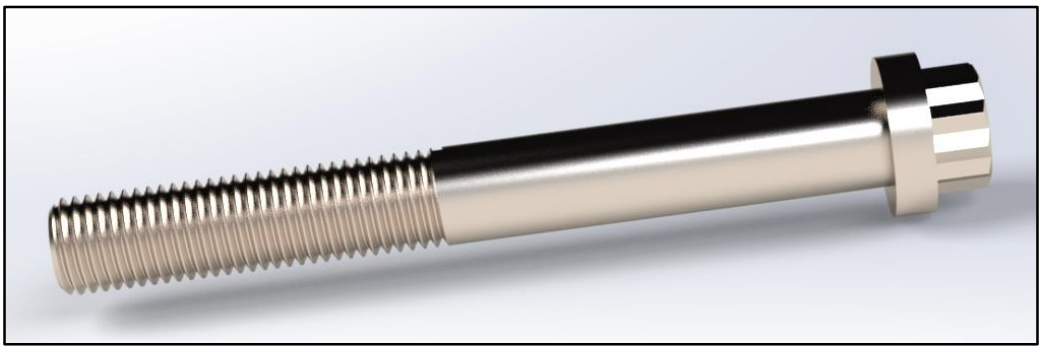

Figure 7.34: Render of Main Bolt

7.12.1 - Overview

For bolts, we determined the main bearing cap, connecting rod, and cylinder head to the engine block bolts are the most critical, and required proper sizings. These bolts were determined as the most critical as they deal with the direct loads from combustion.

7.12.2 - Materials and Manufacturing

For these bolts, we decided to use class 12.9 steel bolts. Class 12.9 steel stands for the yield and proof strength of the steel, with the 12 in reference to the 1220 MPa yield strength, and the 9 is in reference to the 970 MPa proof strength.

7.12.3 - Design Considerations

For the main and head bolts, we choose to use 12-point bolts heads for their improved load distributions compared to standard hex head bolts. While the connecting rod bolts are still hex head as they mate with connecting rod hex cut outs.

7.12.2 - Calculations

For the thread sizing we needed to define stress area, A_t. To calculate this area, the load, P, factor of safety, FOS, and proof strength, S_P.

$$A_t = \frac{P \times FOS}{S_p}$$

TABLE 10.2 Basic Dimensions of ISO Metric Screw Threads

	Coarse Threads			Fine Threads		
Nominal Diameter d (mm)	Pitch p (mm)	Minor Diameter d_r (mm)	Stress Area A_t (mm^2)	Pitch p (mm)	Minor Diameter d_r (mm)	Stress Area A_t (mm^2)
3	0.5	2.39	5.03			
3.5	0.6	2.76	6.78			
4	0.7	3.14	8.78			
5	0.8	4.02	14.2			
6	1	4.77	20.1			
7	1	5.77	28.9			
8	1.25	6.47	36.6	1	6.77	39.2
10	1.5	8.16	58.0	1.25	8.47	61.2
12	1.75	9.85	84.3	1.25	10.5	92.1
14	2	11.6	115	1.5	12.2	125
16	2	13.6	157	1.5	14.2	167
18	2.5	14.9	192	1.5	16.2	216
20	2.5	16.9	245	1.5	18.2	272
22	2.5	18.9	303	1.5	20.2	333
24	3	20.3	353	2	21.6	384
27	3	23.3	459	2	24.6	496
30	3.5	25.7	561	2	27.6	621
33	3.5	28.7	694	2	30.6	761
36	4	31.1	817	3	32.3	865
39	4	34.1	976	3	35.3	1030

Note: Metric threads are identified by diameter and pitch as "M8 × 1.25."

Table 7.10: Bolt Sizing Table [13]

After the area is calculated, the next larger area is picked from Figure 7.10 above. We went with fine thread for the improved resistance to vibrations compared to coarse threads.

Main Bolts	M10x1.25
Head Bolts	M10x1.25
Connecting Rod Bolts	M8x1

Table 7.11: Bolts Size

For preload we need to calculate the clamping force, F_i for the bolt and nut. From the following equation, A'_t is the new stress area, S_p is the proof strength and the 0.75 is a constant for fatigue loading.

$$F_i = 0.75 \times A'_t \times S_p$$

After the clamping force is calculated the preload is calculated by multiplying that force is by the constant 0.2 and the diameter of the bolt.

$$T = 0.2 \times D \times F_i$$

Main Bolts	89 N-m
Head Bolts	89 N-m
Connecting Rod Bolts	46 N-m

Table 7.12: Preload for Bolts

For thread engagement, t, the following equation is used. In this equation $\sigma_{ob}$and $\sigma_{on}$are the yield strength of the bolt and the nut. For the connecting rod, the nut and bolt are the same, while for the main and head bolt, the bolt is 12.9 steel while the nut is the A356 aluminum of the engine block.

$$t = \left(\frac{1}{0.75 \times 4}\right) \times (0.9)^2 \times D \times \sigma_{ob} \times \left(\frac{1}{0.58 \times \sigma_{on}}\right)$$

Main Bolts	31 mm
Head Bolts	31mm
Connecting Rod Bolts	4 mm

Table 7.13: Thread Engagement for Bolts

7.13 - Balance Shaft Timing

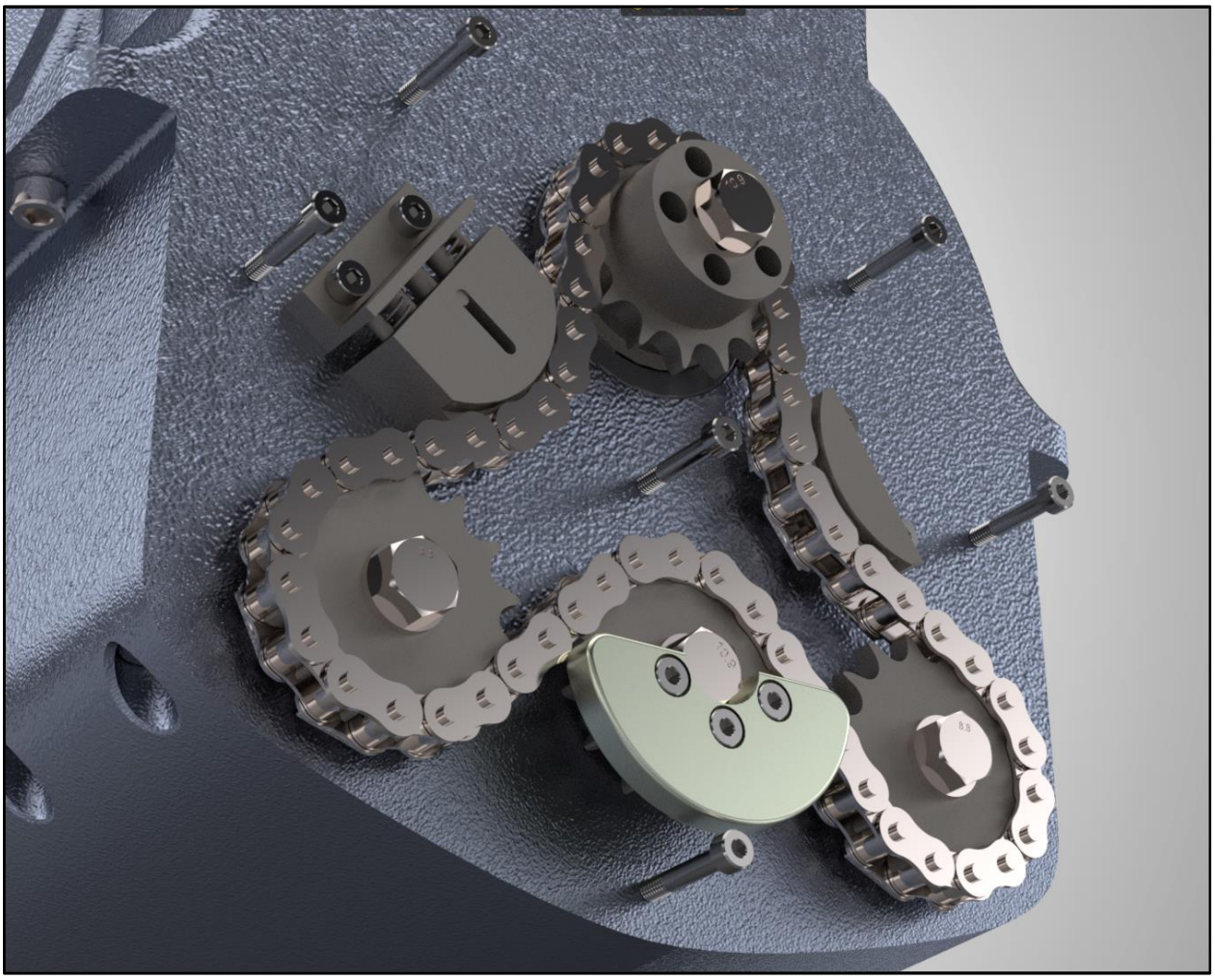

Figure 7.35: Render of Isometric View of Balance Shaft Timing System

7.13.1 - Overview

The timing system for the balance shaft serves to ensure that the balance shaft is at the correct phase with regard to the crankshaft. Without accurate timing, none of the vibration cancelling effects of the balance shaft would function.

7.13.2 - Design Considerations

The first and most major design decision for the balance shaft timing was whether we wanted a timing belt or chain. The justification for this is identical to the decision to use a chain in section 8.10.1.2; refer to that section for the justification. As we wanted to be consistent in our chain sizing, we decided to use the same chain size for the balance shaft and the cam timing:

06b. We also decided that, based on our design constraints, that the largest crank / balance shaft sprocket we could use was 50 mm in diameter.

7.13.3 - Component Selection

For the crankshaft and balance shaft sprockets of the balance shaft timing system, we decided to use the sprocket we were already using on the crankshaft for the camshaft timing system to reduce cost. However, the crankshaft sprocket for the balance shaft system will require the drilling of 5 clearance holes for transmission mounting. These holes are for M8 bolts and allow direct access to the crankshaft, allowing the mounting of whatever flywheel, gear, or transmission the Spartan Motorcycle Company chooses. These holes can be seen in Figure 7.36 below. Additionally, the balance shaft sprocket will require the drilling and tapping of three holes to mount the front balance shaft mass. We also used two idler sprockets of the same diameter as the driven sprockets to ensure that the balance shaft spins opposite to the crankshaft and has the proper amount of engagement. Additionally, we are using a purchased tensioner and chain guide to contain and correctly tension the chain. A render of this system can be found below in Figure 7.36.

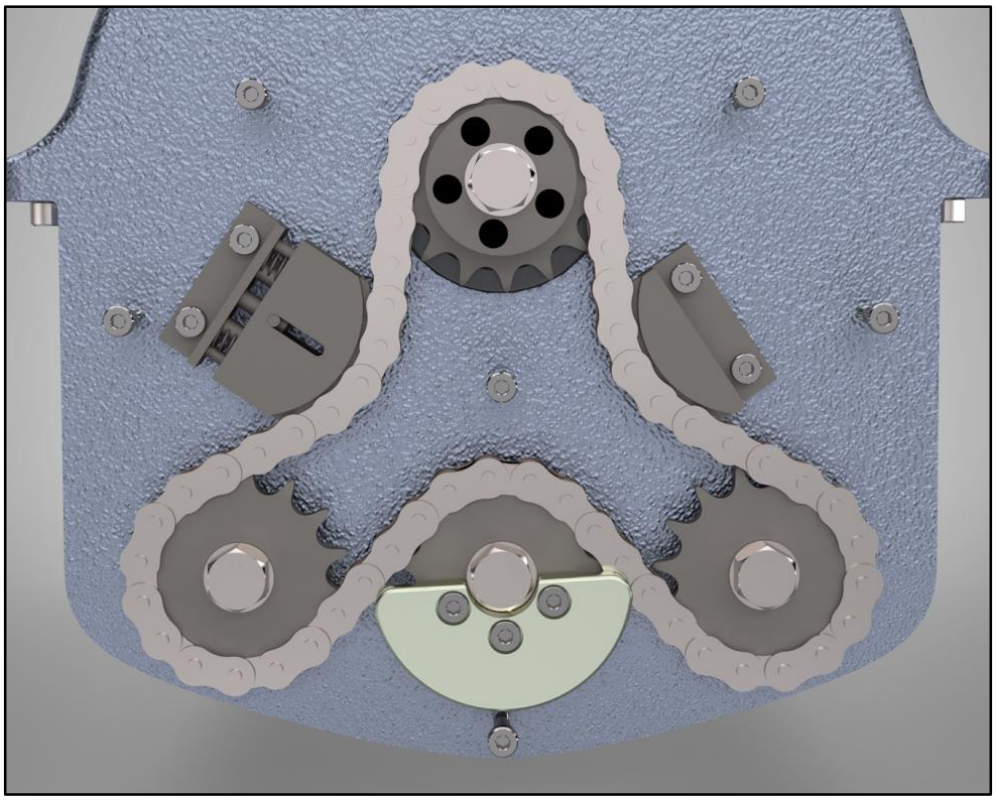

Figure 7.36: Render of Timing System for Balance Shaft

8 - Top End Design

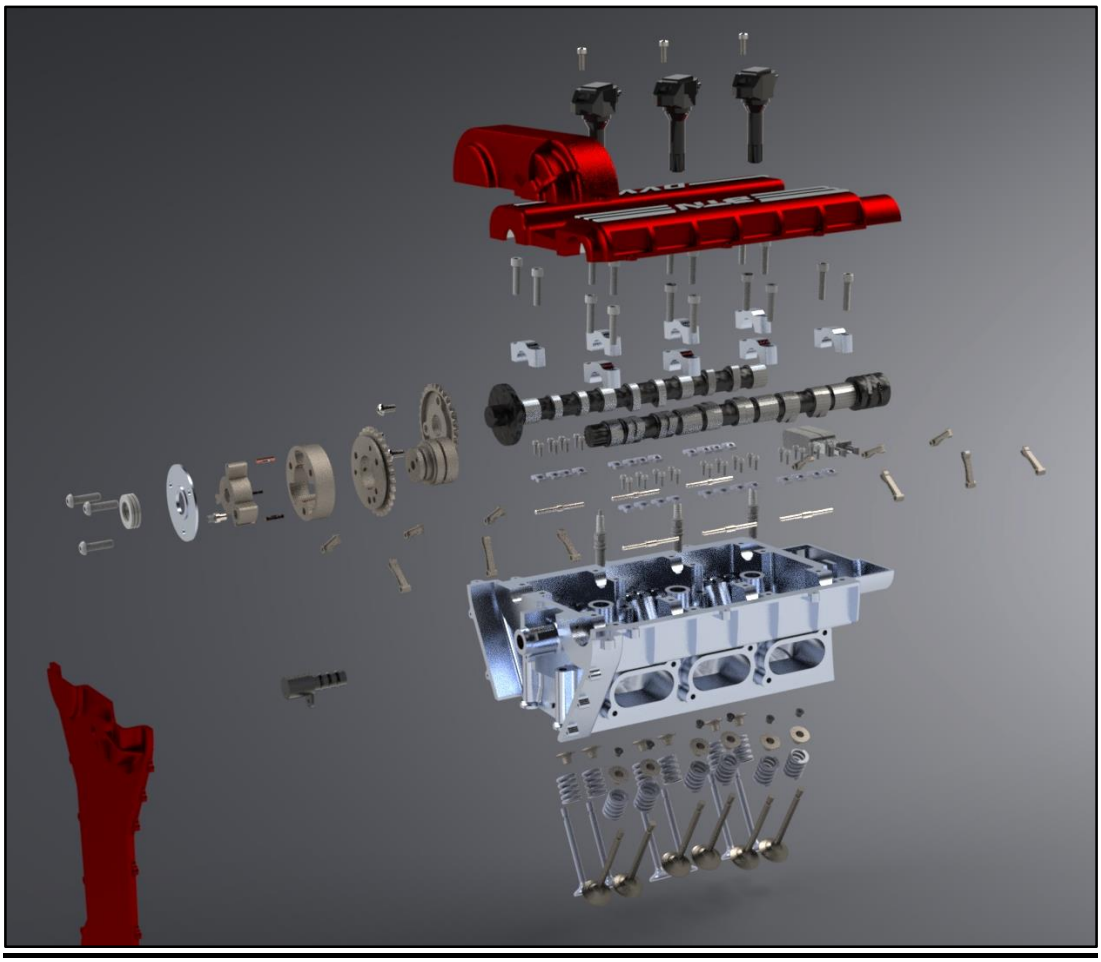

Figure 8.1: Exploded View Render of Top End

8.1 - Overview

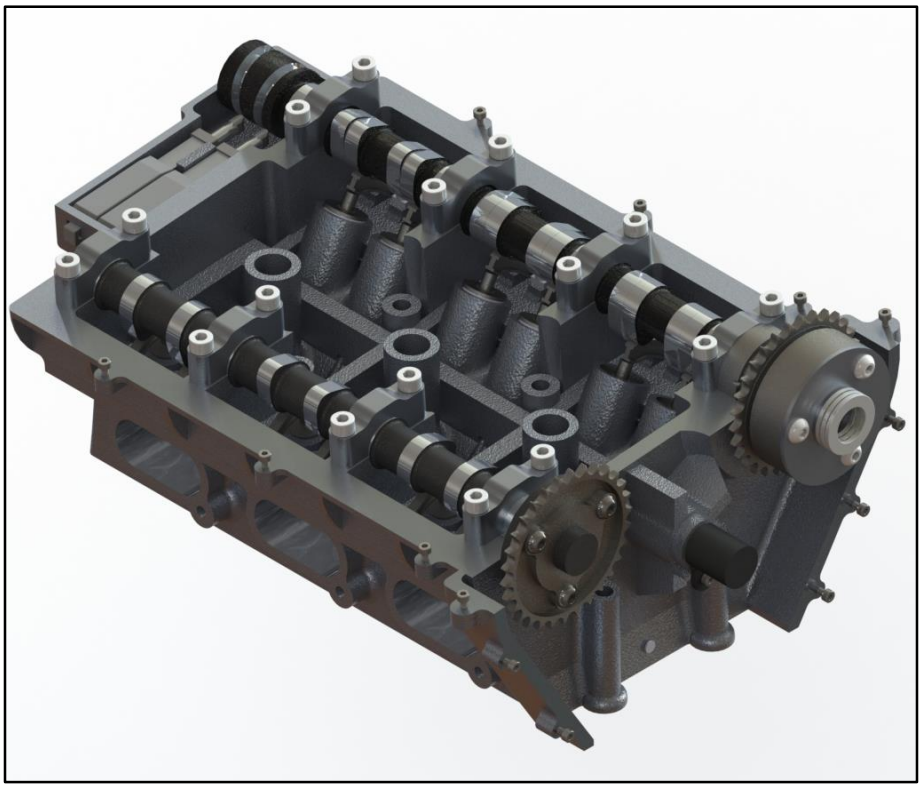

Figure 8.2: Render of Top End

Our top end is made up of the cylinder head, camshafts, valvetrain, DVVL system and VVT system. For each component in this section, we will provide a description of the components purpose, an overview of the material choice and manufacturing method, a summary of the main qualitative design decisions, a walkthrough of the calculations used to drive our design, and a breakdown of the analysis that validates this design. Renders, section views, and FEA screenshots will be provided where applicable.

8.2 - Camshafts

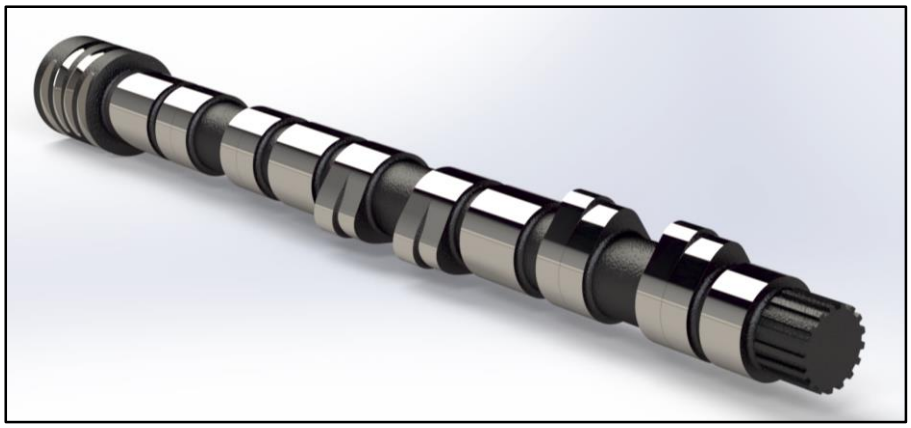

Figure 8.3: Render of Intake Camshaft

Figure 8.4: Render of Exhaust Camshaft

8.2.1 - Overview

The purpose of the camshafts are to accurately control the opening and closing of the intake and exhaust valves. The intake camshaft has two sets of lobes and a cylindrical cam on one end to apply our DDVL technology, while on the other end it is splined to allow for interaction without VVT sprocket. The exhaust cam is more traditionally designed.

8.2.2 - Materials and Manufacturing

To start our camshaft design, we first had to decide on material. After reviewing existing documentation on camshaft material selection and searching through CES EduPack for materials that fit our design criterion, we eventually decided on cryo treated grey iron. Cryo treated grey iron is a method of gaining the strength of white cast iron on just the surface while keeping the

toughness of the grey cast iron core. This is done by rapidly cooling the surface to white cast iron while allowing the core to slowly cool to grey cast iron.

8.2.3 - Design Considerations

The next step in our camshaft design was to make the major design decisions for this component. These decisions included how many camshafts, how many valves per cylinder, and what variable valvetrain technologies we wanted to use For each of these we utilized Pugh charts to ensure we empirically made the optimal decision. These pugh charts can be found in section 5.2. In summary, we decided to utilize a Dual OverHead Camshaft (DOHC) configuration with four valves per cylinder, using Variable Valve Timing (VVT) and Discrete Variable Valve Lift (DVVL) to achieve optimal combustion over various driving conditions. These last two technologies will be covered in a later section.

8.2.4 - Calculations

The most important part of the camshaft is the cam profile, and the creation of that profile will be covered in this section. Utilizing the values for lift, duration, and timing that were determined in the thermodynamics section, we first needed to decide whether we wanted to use a single or double dwell lift profile. The difference between the two is that the double dwell profile incorporates a dwell in between the rise and fall components of valve lift, while the single dwell profile does not. To determine which style was best for our engine, we plotted the flow coefficient (Cd) vs crank angle for both styles. These graphs are included below.

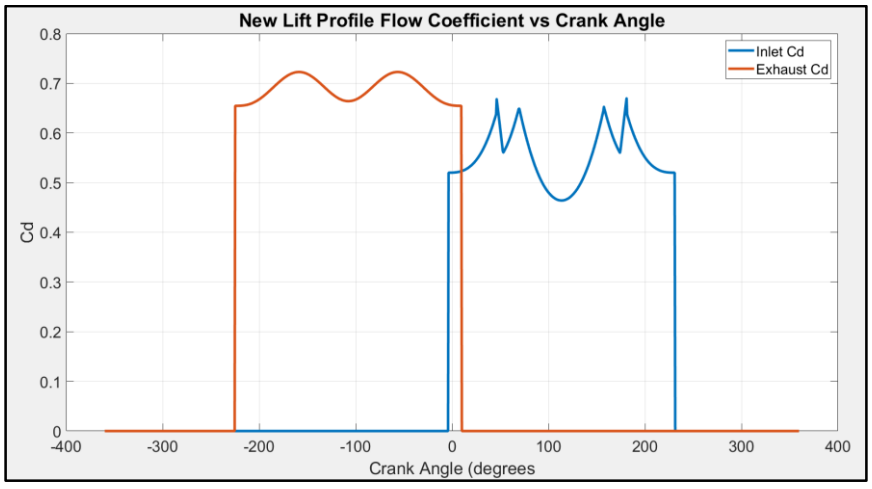

Figure 8.5: Flow Coefficient vs Crank Angle for a Single-Dwell Cam

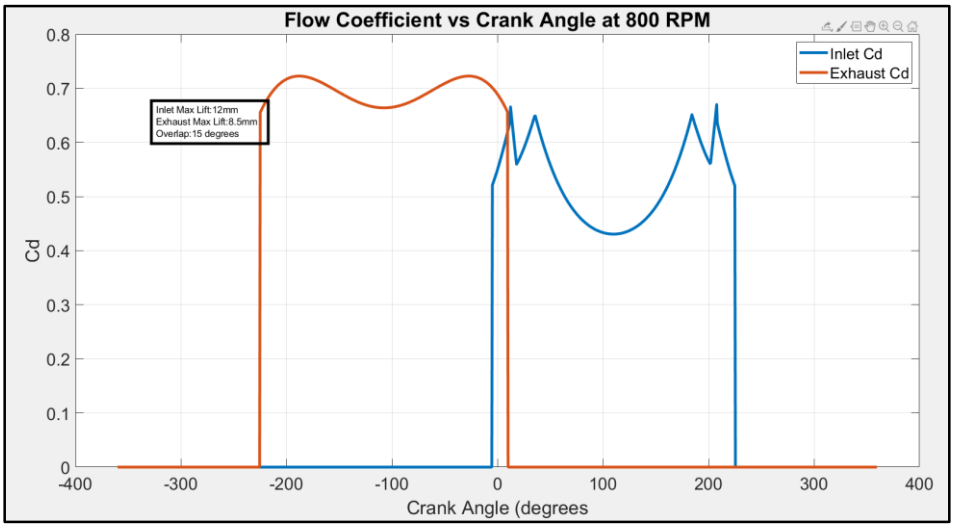

Figure 8.6: Flow Coefficient vs Crank Angle for Double-Dwell Cam

These graphs show that a single dwell profile has an average Cd value 10% higher than that of a double dwell cam profile due to vortex effects. This correlates with our search of IC camshaft design norms which show that nearly all IC cams are single dwell. Based off of this information, we decided to use a single dwell profile.

The next step was to determine which single dwell lift profile equation to choose. There were three choices: harmonic, cycloidal, or polynomial. Cycloidal was ruled out due it having discontinuous jerk and acceleration, and between harmonic and polynomial the latter has lower maximum acceleration. These factors led us to using a polynomial equation for our valve lift curve. Specifically, we chose to use a 3-4-5-6 polynomial as it has better jerk behaviour than a 3-4-5 polynomial and much lower max acceleration than a 4-5-6-7 polynomial [5]. This polynomial will take the form of $□(□) = □ * □^3 + □ * □^4 + □ * □^5 + □ * □^6$ where $□(□)$ is the amount of lift, x = $\theta/□$, $\theta$is the degree of cam rotation, and $\beta$is the total duration of the lift profile.

The next step in determining the valve lift curve is to determine the value of the coefficients in our valve lift equation. To do this we need to specify four boundary conditions, one for each unknown coefficient. These boundary conditions are as follows: $□'(□) = 0$ when$\theta = □$, $□''(□) = 0$ when$\theta = □$,$□'''(□) = 0$ when$\theta = □$, and $□(□) = h$ when$\theta = □$where h is the maximum lift of the lift profile. From this, we created a Matlab script where we setup a formula of the form A*y=b, where A was a 4x4 matrix of x values for each boundary condition, y was a 4x1 column vector of the coefficients we were looking for, and b was a 4x1 column vector of the values of $□(□)$for each boundary condition. We then used the LINSOLVE function to reduce the matrix, giving us values of a, b, c, and d for the given conditions. This process was done for the large inlet cam, small inlet cam, and exhaust cam to generate a cam profile for each. The Matlab code used for this process can be found in Appendix E under Cam_Profile.m. From these equations we are able to plot lift (S), velocity (V), acceleration (A),

and jerk (J). SVAJ graphs for each of the three profiles at 9000 rpm can be found below. Of interest is the maximum acceleration which will be used to design other valvetrain components such as the required valve spring forces.

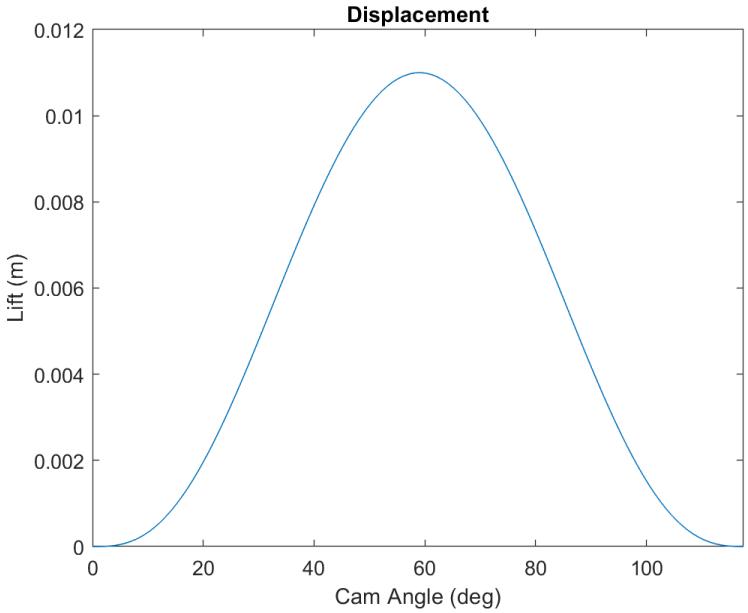

Figure 8.7: Plot of Large Intake Camshaft Displacement

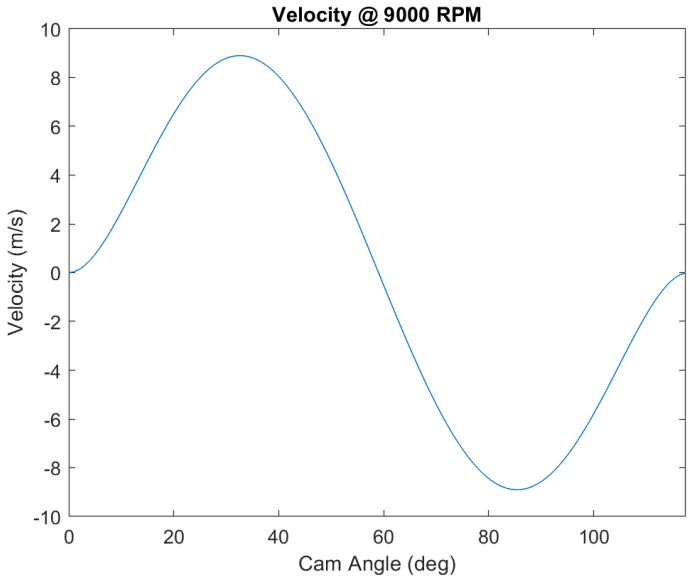

Figure 8.8: Plot of Large Intake Camshaft Velocity

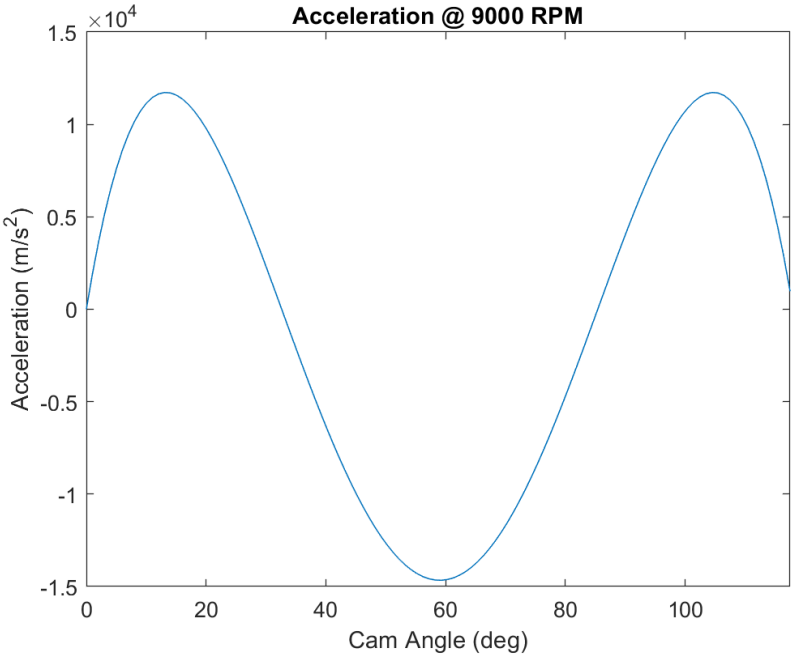

Figure 8.9: Plot of Large Intake Camshaft Acceleration

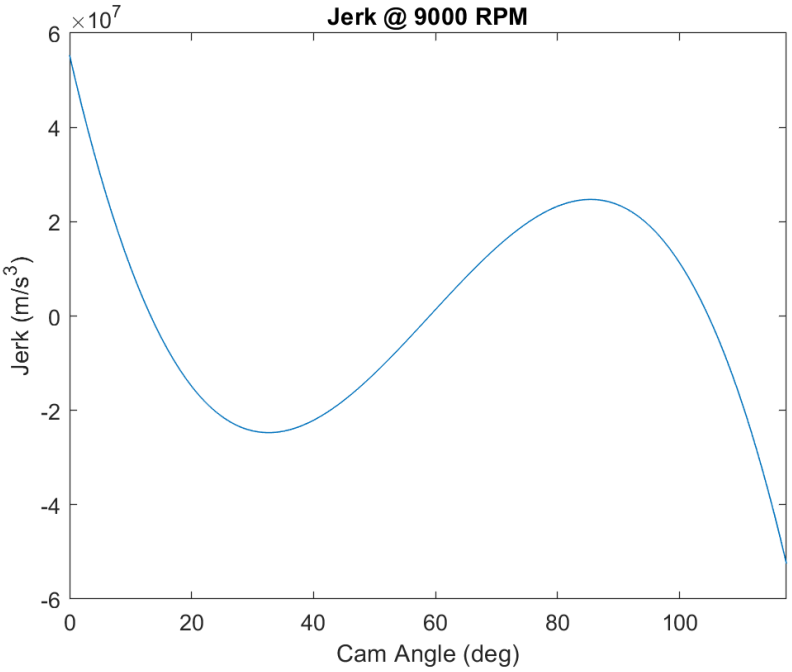

Figure 8.10: Plot of Large Intake Camshaft Jerk

The next step was to translate the valve lift profile into the camshaft profile. As we are using a curved rocker arm style of follower, the cam profile is extremely complex and asymmetric. To aid in our design we utilized a professional cam profile design software known

as Analytix Cams. This software allowed us to simply import our valve lift profile, specify certain values about our follower setup, and it would provide a vector file of the corresponding cam profile. It also enabled us to select a base circle diameter of 30mm which keeps our pressure angle below 30°. A screenshot of this process for our large inlet cam can be found in Appendix C. While this was incredibly useful in translating our valve lift profile into its corresponding cam profile, the ends of the cam profile generated by Analytix Cams were not tangential to the base circle. To remedy this, the vector file provided by Analytic Cams was imported into SolidWorks and manually modified to ensure tangentiality. An example of this for our large lift cam can be found in Appendix C. This geometry was then used to create our camshaft.

8.3 - Rocker arms

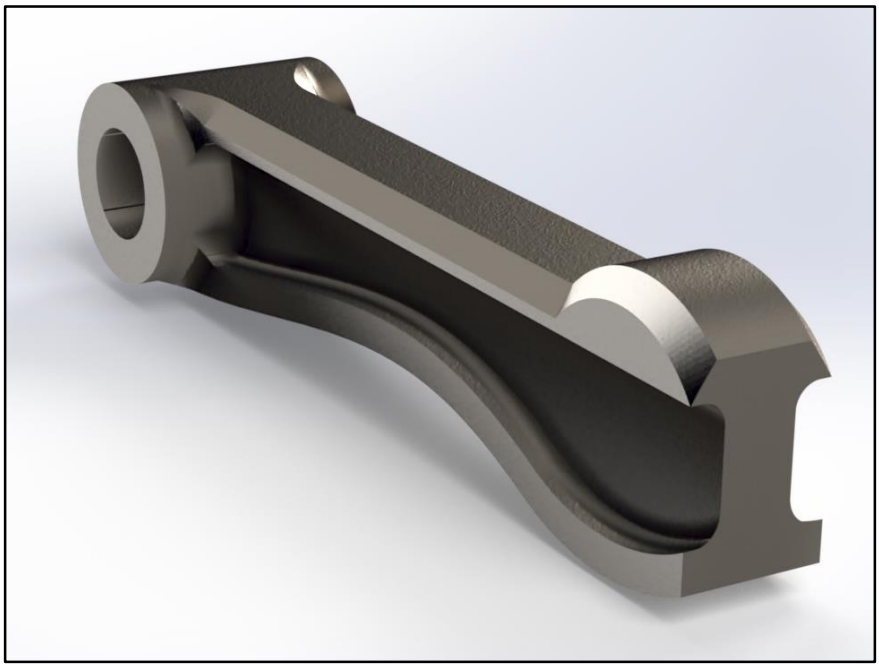

Figure 8.11: Render of Rocker Arm

8.3.1 - Overview

The rocker arm acts as an oscillating lever which conveys radial movement from the cam to linear movement at the valve to open and close it. One end is raised or lowered by the rotation of the cam while the other end acts directly on the valve stem. For our rocker arm, the fulcrum is at the end rather than in the middle. As a result, the cam pushes down on the middle of the arm which results in the opposite end opening valve. These types are commonly used in dual overhead cam motors.

8.3.2 - Materials and Manufacturing

In designing our rocker arm, one of the first considerations was material selection. After much research on typical materials used in the industry for rocker arms research through CES EduPack, we were able to determine our rocker arm material to be AISI 4140 Steel, oil quenched and tempered at 205^{o} C . The two types of materials commonly used for making rocker arms are aluminium and steel. However, AISI 4140 steel, which contains chromium and molybdenum as alloying elements have excellent strength to weight ratio and are significantly stronger than aluminum and standard steel and are used as a common material for high performance parts. The metal would be forged between 2200 and 1700^{o} F. The finishing temperature at which it is forged should be low in order to get as fine a grain size as possible. However, if it is forged at too low a temperature, it may result in unwanted formations. It is then tempered between 400 and 1200^{o} F depending on the desired hardness level. It is then finally hardened by heating and quenching. In this way, a structure suitable for machining may be obtained.

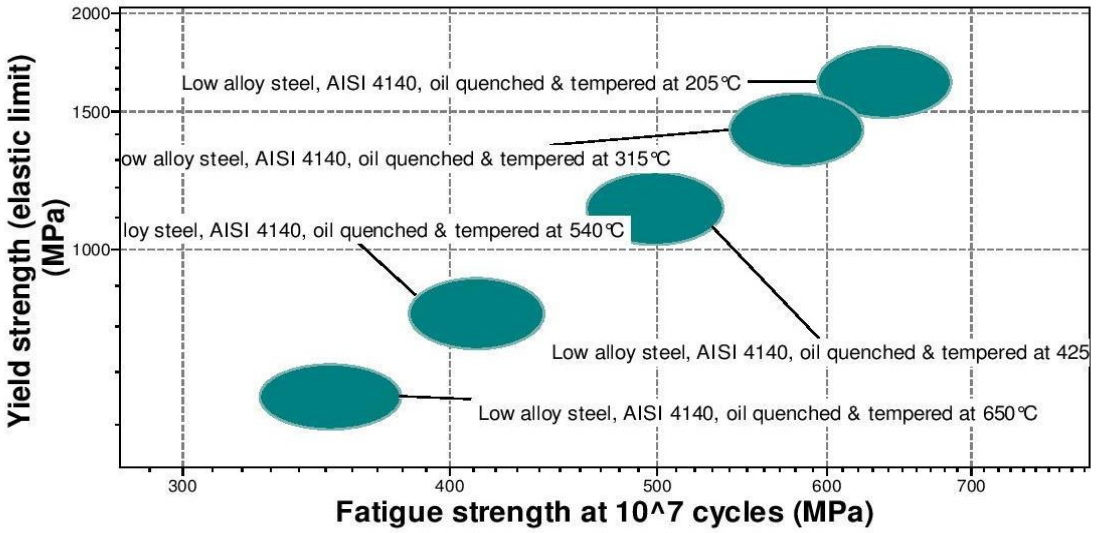

Figure 8.12: CES Edupack Plot of Yield Strength vs Fatigue Strength for AISI 4140 at Different Heat Temperatures

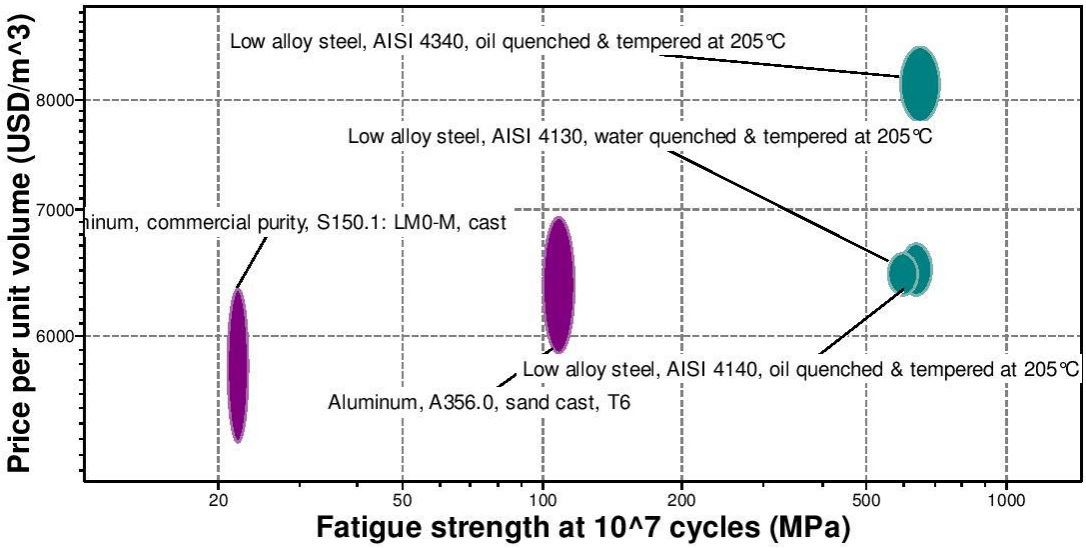

Figure 8.13 : CES Edupack Plot Comparing Price vs Fatigue Strength of Materials Commonly Used for Designing Rocker Arms.

8.3.3 - Design Considerations

There were several major design decisions made for this component. The major reason as to why we chose rocker for our cam-valve interface over buckets was its compatibility with Discrete Variable Valve Lift (DVVL). We had to decide at what angle the rocker arm would sit to have the best possible interface. After a visual inspection during modelling, it was determined that the rocker arm sitting perpendicular to the valve stem would provide optimal functioning. Another important consideration was the rocker arm ratio. We had initially settled on a ratio of 1.5:1 as that is the industry standard. However, after careful consideration, we realized that ratio would be problematic due to spacing concerns.Therefore, we decided to go with a neutral 1:1 ratio for compactness.

8.3.4 - Analysis

Finite element analysis was performed using Solidworks to determine the validity of the rocker arm design and determine the location and magnitude of the maximum stress. A static loading study was conducted and the load was determined by calculating the maximum force exerted by the cam lobe onto the rocker arm which was found to be 193.2 N. This was found by multiplying the acceleration of the valve spring (15000 m/s^2) by the mass of the rocker arm (12.88 g). Unsurprisingly, the region under the most stress is the top of the arm just after where it will be fixed and allowed to oscillate and the furthest from where the cam lobe will apply the force. The maximum stress that will be induced on the rocker arm is 121.3 MPa. This stress will

not induce yielding in the rocker arm as the yield strength of AISI 4140 steel is 415 MPa.The factor of safety for the component is 12 which is much higher than needed. This analysis was then applied to a Solidworks fatigue analysis. The results of that study determined that the rocker arm was well within infinite life.

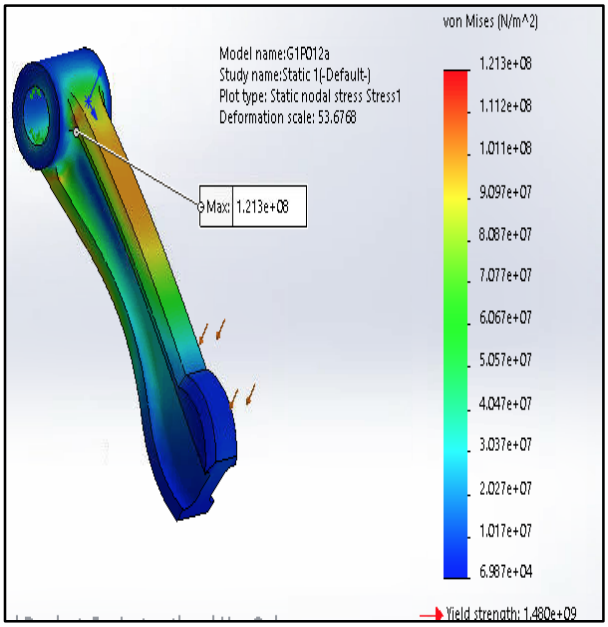

Figure 8.14: FEA Stress Plot for Rocker Arm

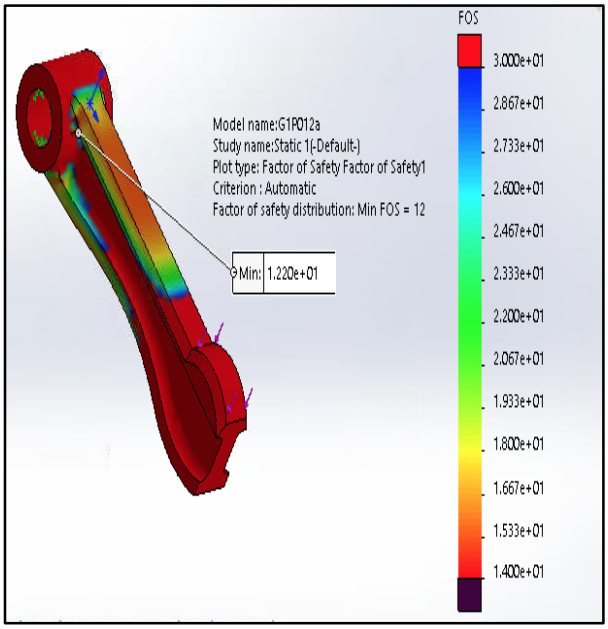

Figure 8.15: FEA FOS Plot for Rocker Arm

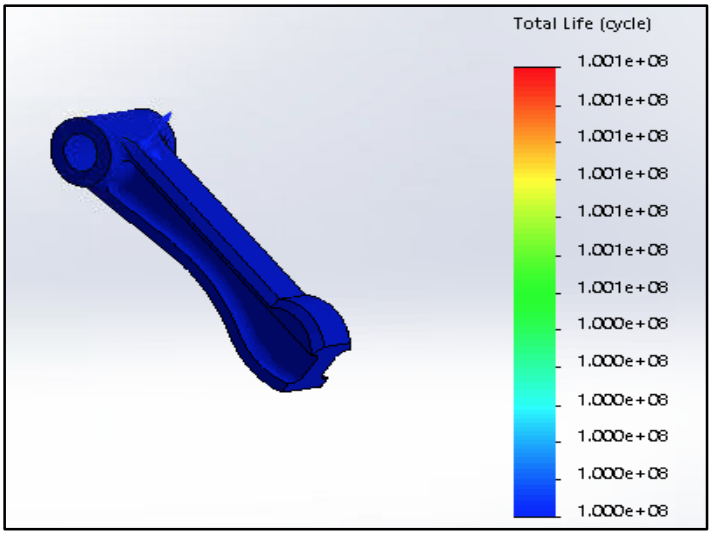

Figure 8.16: FEA Fatigue Analysis for Rocker Arm

8.4 - Valves

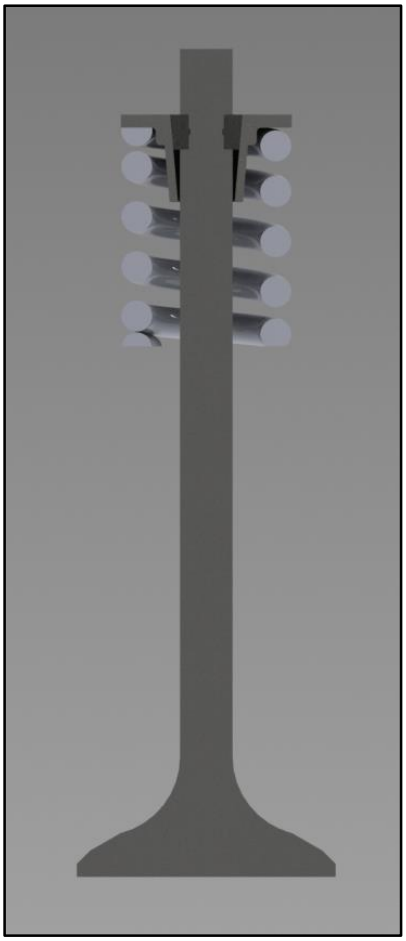

Figure 8.17: Render of Intake Valve Assembly (Section View)

8.4.1 - Overview

The use of proper valves in an internal combustion engine is vital to the proper function of the engine. The valves used in the application of internal combustion engines are called poppet valves, which control the flow of gas or combustion products into and out of the cylinder. The valves must also be able to completely seal the combustion chamber by properly mating with the valve seat so that gases cannot escape during the compression and power strokes. Valve guides are also used to ensure linear motion of the valves. There must be at least one intake and exhaust valve for each cylinder in the engine, to ensure that the combustion chamber in each cylinder is supplied with an adequate amount of the air fuel mixture prior to combustion and to provide an outlet for the exhaust gases and products of combustion to escape the cylinder during the exhaust stroke. In our three cylinder engine, we employ the use of two intake and exhaust valves per cylinder to take advantage of the full flow area available in the pentroof of our combustion chamber, so we will need to have a total of six intake and exhaust valves

manufactured. In this section, we will cover the materials and manufacturing methods of the intake and exhaust valves, as well as explain any major decisions that were considered in the design of these valves.

8.4.2 - Intake

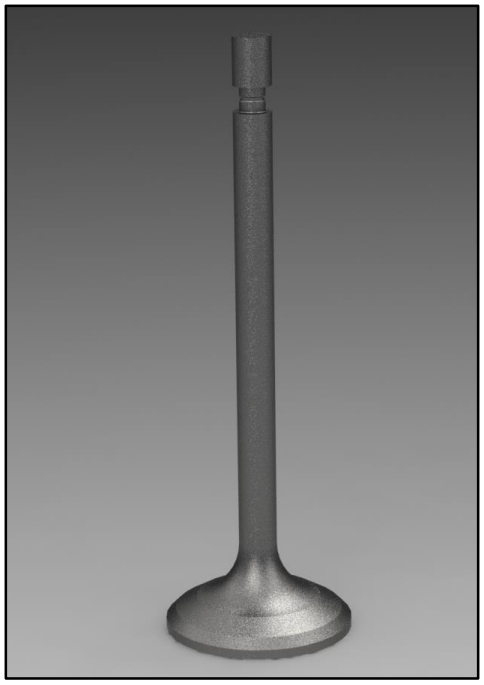

Figure 8.18: Render of Intake Valve

8.4.2.1 - Material and Manufacturing

In designing our intake valve, one of the first considerations was material selection. After much research on industry standards of intake valve materials and research through CES EduPack, we were able to determine our intake valve material to be Sil-1 stainless steel. This material exhibits mechanical properties that can endure countless combustion cycles while also being relatively lightweight and inexpensive. Because we use hollow valve stems in our design, the head of the valve and the stem will have to be manufactured separately and then friction welded together. We employ the use of upset forging with a custom die to manufacture the general shape of the valve stem and head. The blind hole on the valve stem will then be created via gun drilling. The valve will also have to be heat treated to increase wear resistance, fatigue strength, and hardness. After forging, the valve will be finished via turning and grinding. The valve will also have to undergo the post processing stage of polishing, which greatly improves gas flow around the surface. The tip of the valve will also have to be hardened, as this is the surface the rocker arm contacts in order to actuate the valve. Hardening this area would reduce the wear between the two contacting surfaces. To further reduce wear in this area, a chrome nitride coating (601 Bhn) will be applied to the valve tip.

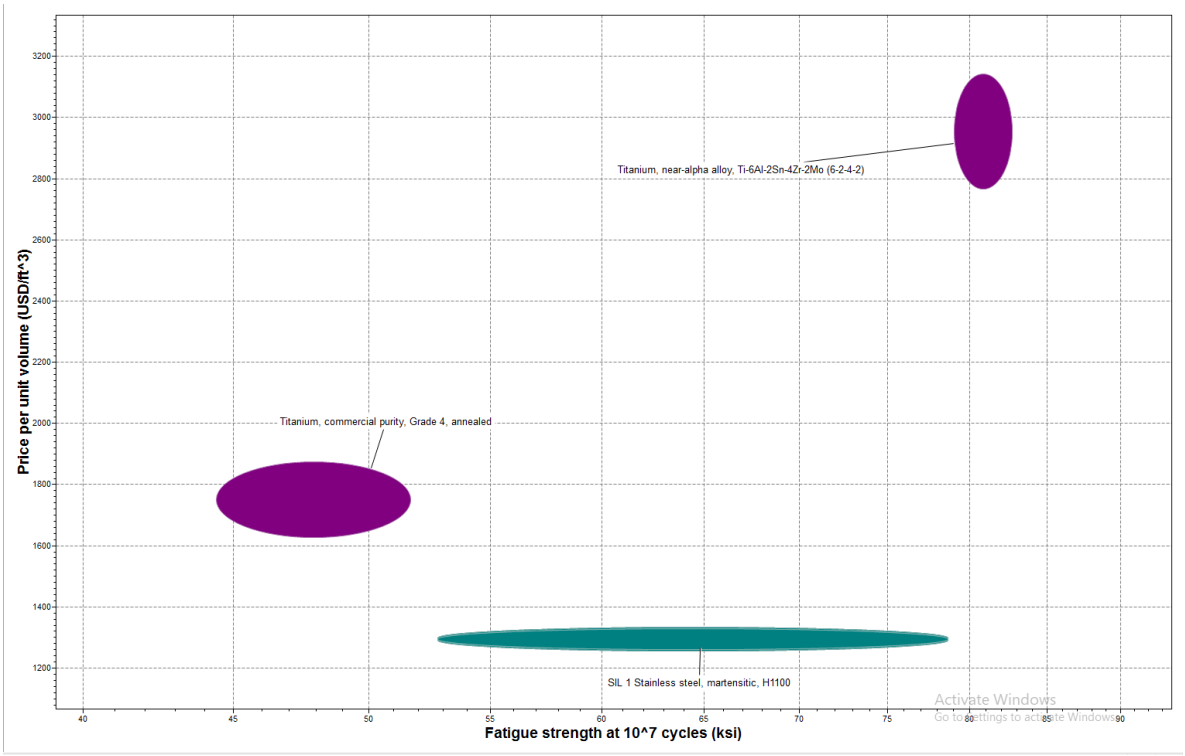

Figure 8.19: CES Edupack Graph Comparing Price vs. Fatigue Strength at 10^7 Cycles for Grade 4 Titanium, 6242 Ti Alloy, and SIL 1 Stainless

8.4.2.2 - Design Considerations

A major design consideration for intake and exhaust valves is weight. These valves make up a majority of the weight that must be moved by the valve springs, and as such have a large bearing on how much force the valve springs see. The reduction of the weight of the valve allows the spring to maintain a lower open pressure and therefore a lower spring rate for a given lift. Some methods of valve weight reduction include coring the valve stem and using materials such as titanium, which is lightweight but expensive. In our application, we choose to core the valve stem, with the hole extending from the start of the stem just above the valve head to just below the section of the stem where the keeper locks in position. This core on the valve stem will be filled with sodium to drastically improve heat dissipation through the valve. This will help reduce the risk of valve channeling, a failure mode that occurs due to the valve being exposed to excess temperatures. This can lead to a portion of the valve melting or warping, which can lead to a variety of problems including improper valve seating and the valve potentially being unable to adequately seal the combustion chamber.

For our intake valve, we settled on a diameter of 37.5 mm (1.48”), with a 0.060” margin, stem diameter of 0.25” and a seat width of 0.075”. Specifics on sizing the features on our intake valve can be found in the calculations section below. We make use of a relatively small seat

width on our valves, as the lower the seat width, the better the flow is into the cylinder under low lift conditions. For low RPM conditions when we make use of our low-lift cam profile, our intake valve will allow for more gas flow into the cylinder due to the reduction in seat width. The valve margin, including the sharp corner on the bottom face of the valve, contributes to improved flow as well as increased durability. Low lift flow is also improved by the addition of a 30 degree back angle cut after the valve seating surface. This smoothes the transition from the seat of the valve to the stem. In combination, these two features allow for the air fuel charge to more easily enter the cylinder. The seat angle for our valve is 45 degrees. A larger seat angle can generally improve flow into the cylinder, however can also lead to increased wear between the valve and its seat. Seat angles greater than 45 degrees can also result in the valve sticking in the closed position and requiring a greater force to be open. Aiming to maximize flow into the cylinder under the range of lift conditions, we employ the use of a 45 degree seat angle. This is also a seat angle commonly used in the industry.

We also make use of valve swirl polishing on the intake side. This superficial swirling on the head of the valve causes air to swirl into the cylinder rather than enter head on. This causes the inlet air to be more turbulent as it enters the cylinder, which encourages better mixing of the air fuel charge and more even combustion. This process also decreases boundary layer separation from the valve as air and fuel flow into the combustion chamber. Swirling of the air charge into the cylinder does not decay during compression, rather increasing in velocity late in compression as charge density increases.

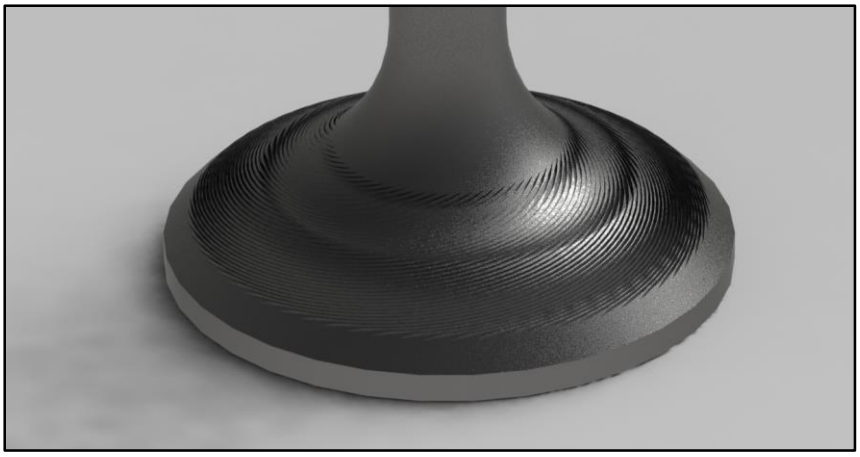

Figure 8.20: Render of Intake Valve Swirling

For our valves, we use separate seats that are installed into the port geometry of the cylinder head. These seats will be made from tungsten carbide with a pressed powdered metal matrix of H_{20} tool steel. This material has excellent wear properties while maintaining a low coefficient of friction with the valve and can ensure a full seal of the port over many cycles due to its wear resistance. Concentricity of the valve and its seat is essential for proper sealing of the combustion chamber. We account for this by specifying concentricity to 0.002” per 1.5” of valve

head diameter. Finally, for our overall valve system, we chose a valve included angle of 60 degrees, as this matches the angle of our pentroof combustion chamber and simplified the design of the ports as well.

8.4.2.4 - Calculations

Before sizing features on our intake valve, we first had to determine an appropriate valve head diameter and seat angle. For the intake valve, we chose a head diameter of 37.5 mm and a seat angle of 45°. We then were able to use equations given by Taylor and Heywood to size the remaining features on our valves. For the intake valve, the stem diameter was sized using the following equation given by *The Internal Combustion Engine in Theory and Practice* [24].

$$D_{stem} = 0.15 \times D_{head} = 0.22"$$

For added robustness we chose a slightly larger stem diameter of 0.25”. Next, we calculate our seat width based off of the ratio of the head diameter of the valve to the inner seat diameter given by *Internal Combustion Engine Fundamentals* [1]. The following equations were used to calculate our seat width.

$$D_{inner\ seat} = \frac{D_{head}}{1.1} = 1.342" \ (for\ 45°\ seat)$$
$$w_{seat} = \frac{D_{head} - D_{inner\ seat}}{2} = 0.67"$$

For better sealing capability, we make use of a slightly larger seat width of 0.075”. To calculate the height of the margin on our intake valve, we make use of another recommendation given by Heywood. Heywood suggests that the vertical distance from the bottom flat face of the valve to the inner seat diameter should be 0.095 times the inner seat diameter, as shown in the equation below.

$$h_{inner\ seat} = 0.095 \times D_{inner\ seat} = 0.127"$$

Using our previously calculated inner seat diameter, we find this value to be 0.127”. To find margin height from this, the vertical distance of the seat must be subtracted from this value. Because we make use of a 45 degree valve seat, the horizontal and vertical dimensions of this chamfer are the same. So we can make use of the following equation to size the margin on our intake valve.

$$h_{seat} = w_{seat} = 0.075"$$
$$h_{margin} = h_{inner\ seat} - h_{seat} = 0.53"$$

We increase this recommended margin height value to 0.060” in our intake valve design for added robustness.

8.4.2.3 - Analysis

Stress analysis was completed on the intake valve to determine the maximum stress and deflection in the valve under the working pressures in the combustion chamber. Using the maximum pressure inside the cylinder, which was determined to be 10.1 MPa, we applied a load to the bottom flat face of the intake valve. A fixture was applied along the seat chamfer of the valve, as this area is fixed by contact with the valve seat when the valve seals off the combustion chamber. An additional fixture was added to the valve tip, as this region is restricted in movement by the rocker arm and cam. The maximum stress in the valve was found to be 82.22 MPa, which occurred along the upper edge of the valve seat. This stress will not induce yielding in the valve, however, as the yield strength of Sil-1 steel is 686 MPa. A factor of safety plot was also generated, showing that the minimum factor of safety in our intake valve is 8.344, which is greater than our factor of safety of three for valvetrain components.

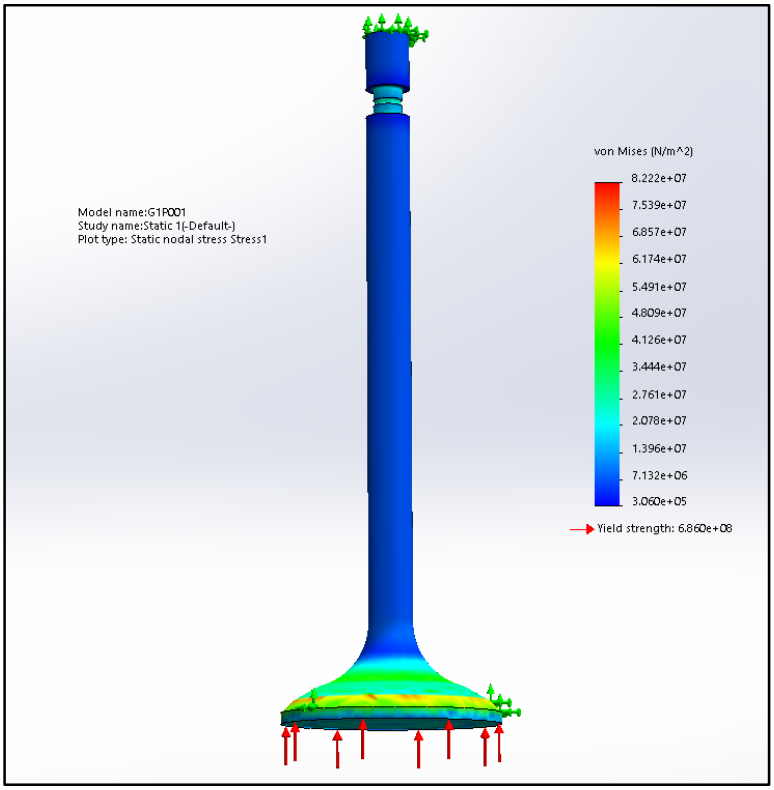

Figure 8.21: Stress Analysis of Intake Valve

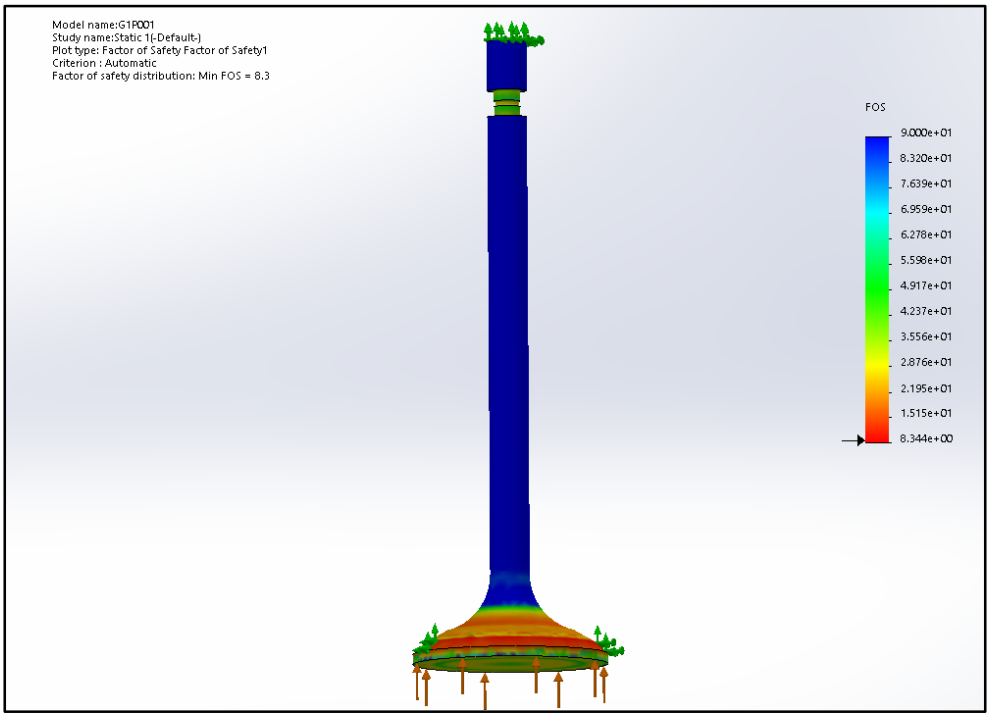

Figure 8.22: Factor of Safety Analysis for Intake Valve

8.4.3 - Exhaust

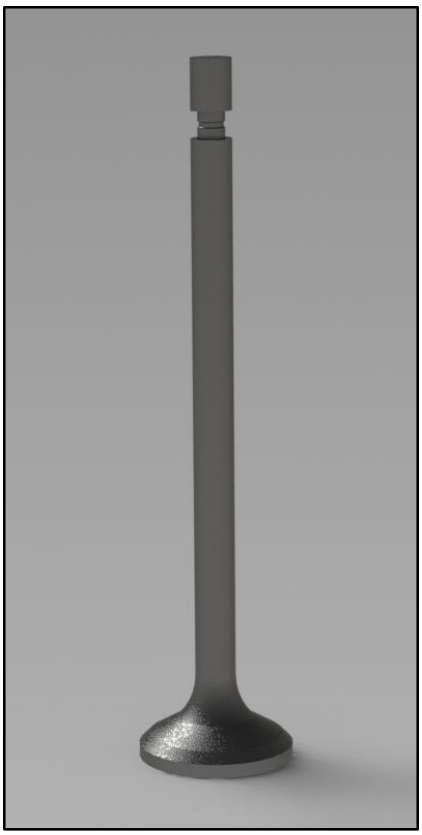

Figure 8.23: Render of Exhaust Valve

8.4.3.1 - Materials and manufacturing

In selecting materials for the exhaust valves, a similar process was conducted as the intake. Upon reviewing much literature and consulting with CES EduPack, we determined our exhaust valve material to be 21-4N stainless steel. This material has better thermal properties and a higher heat resistance than the steel grade chosen for the intake valve, as the exhaust valve is exposed to corrosive combustion products which are at a much higher temperature and pressure. This steel was also chosen due to its austenitic nature, which indicates a high chromium content and better corrosion resistance than martensitic grades. Because our exhaust valves will not be hollowed, the valves can be manufactured in one piece. The manufacturing methods for the exhaust valve are similar to the intake valves. We make use of upset forging for the general shape of the valve, finishing with turning and grinding operations to ensure dimensions are to spec. The exhaust valve will also be heat treated and polished to improve flow around the body of the valve. Much like the intake valves, the tips of the exhaust valves will also be hardened to reduce wear in the area of contact between the valve and rocker arm.

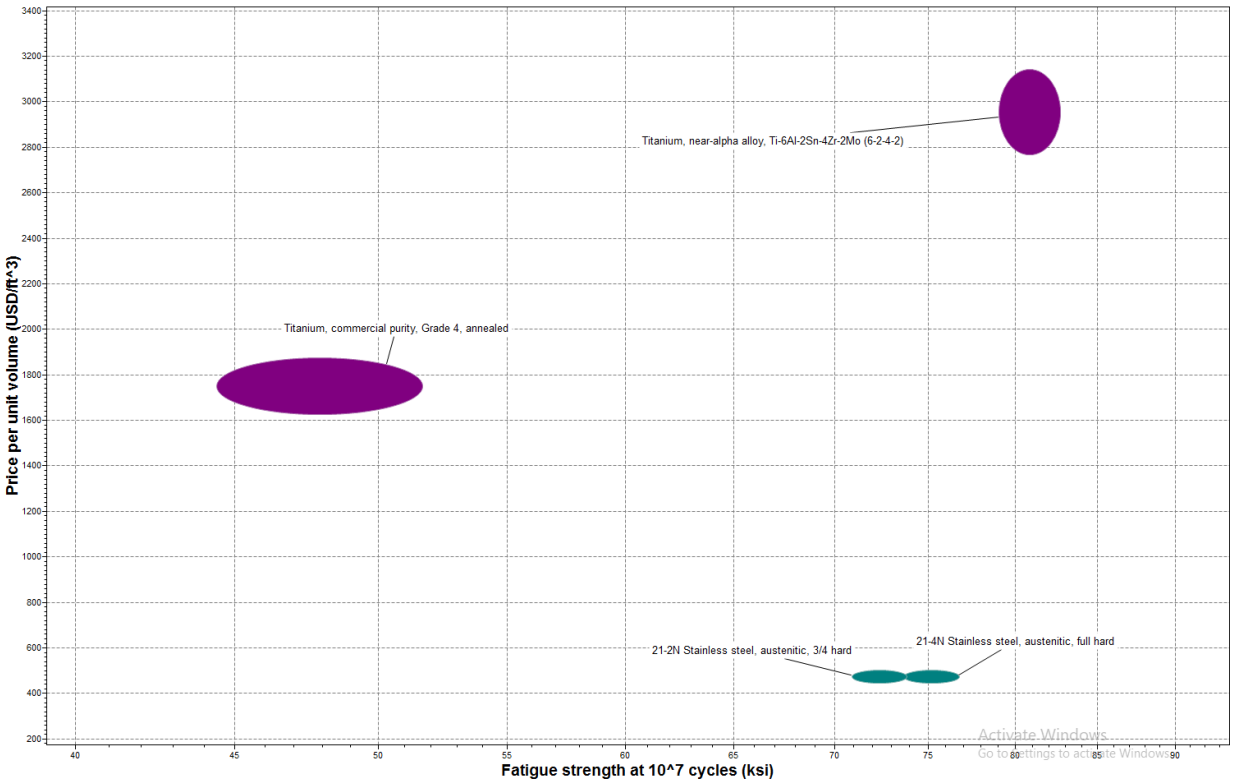

Figure 8.24: CES Edupack Graph Comparing Price vs. Fatigue Strength at 10^7 Cycles for Grade 4 Titanium, 6242 Ti Alloy, 21-2N Stainless, and 21-4N Stainless

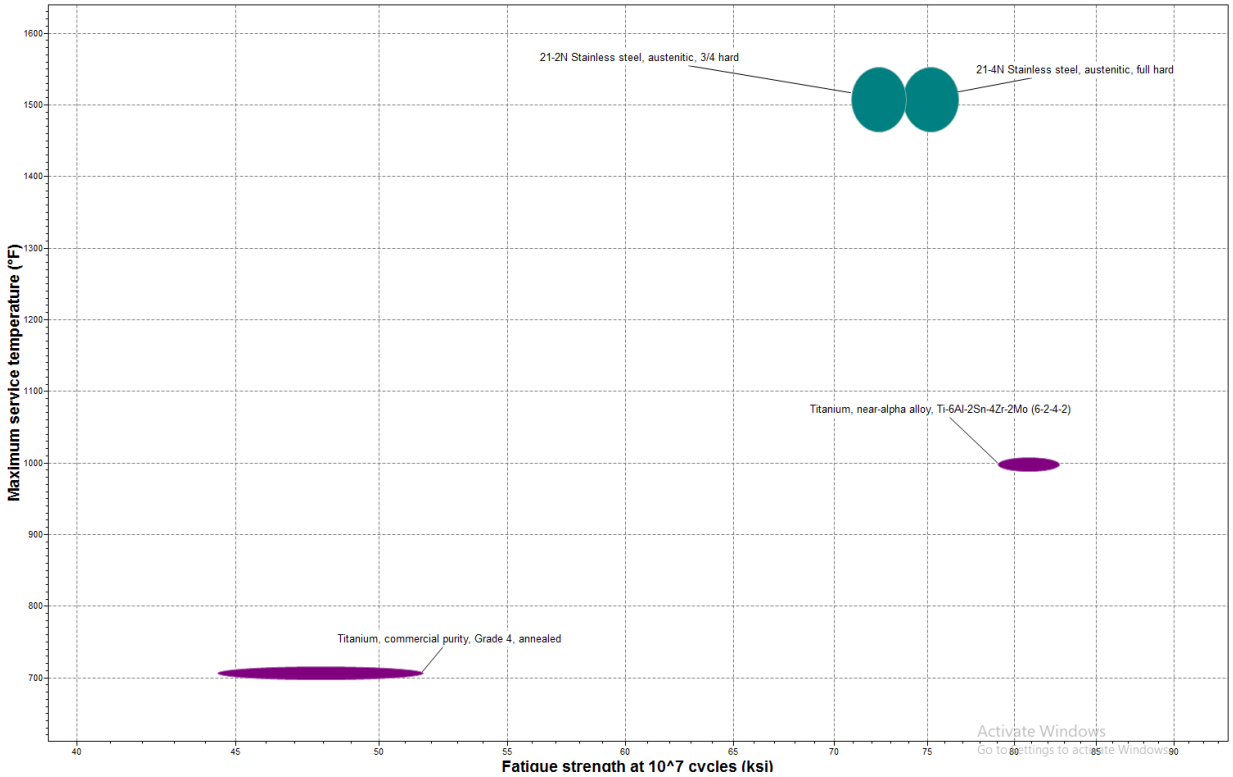

Figure 8.25: CES Edupack Graph Comparing Maximum Service Temperature vs. Fatigue Strength at 10^7 Cycles for Grade 4 Titanium, 6242 Ti Alloy, 21-2N Stainless, and 21-4N Stainless

8.4.3.2 - Design Considerations

For the exhaust valve, we chose a diameter of 29 mm, which is 23% smaller than our intake valve diameter. The exhaust valve does not have to be as large because it is not coaxing flow into the cylinder as the intake valve is, but rather just giving the air a pathway as the piston pushes up, emptying the cylinder. This is also a stoichiometric approximation from the composition of air, which is approximately 20% oxygen and 80% nitrogen. During combustion, if the oxygen is all expended while the nitrogen is not, to allow all of the gas to escape the exhaust valve diameter should be approximately 80% that of the intake valve. For the exhaust side, we increase our margin to 0.1”, reduce our seat width to 0.065”, increase our stem diameter to 0.3” and add more material to the bottom filleted region in the transition from the head to the stem of the valve. The specifics on how we sized features on our exhaust valve can be found below in the calculations section. The increased margin on the exhaust valve helps for greater heat dissipation. The exhaust valve sees much higher loads in comparison to the intake valve, so the valve itself needs to be more durable to withstand greater forces. The increased margin and the bulkier radius on the transition from the valve head to the stem increase the durability of the valve. The increase in the bottom fillet reduces the risk of flow recursion back into the cylinder during the exhaust stroke as well. While intake valves can be hollowed, this is generally not

advisable for exhaust valves as they need to be more robust in order to withstand the higher pressures of exhaust gases. For this reason, we elect to not use hollowed stems on our exhaust valves.

8.4.3.3 - Calculations

We made use of both the Taylor and Heywood equations to size features on our exhaust valves, using a similar process that was employed on the intake side. We had to once again determine our exhaust valve's head diameter and seating angle, and could then size the other features of the valve based off of these dimensions. For our exhaust valve, we chose a head diameter of 29 mm and a seat angle of 45°. We size our stem diameter for the exhaust valve using the following equation given by *The Internal Combustion Engine in Theory and Practice* [24].

$$D_{stem} = 0.25 \times D_{head} = 0.28"$$

For added robustness, we choose to use a stem diameter of 0.3" on the exhaust valves. To derive the value for our seat width, we make use of similar equations we used for the intake valve from *Internal Combustion Engine Fundamentals* [1], except for the exhaust side this time.

$$D_{inner\ seat} = \frac{D_{head}}{1.11} = 1.029"\ (for\ 45°\ seat)$$
$$w_{seat} = \frac{D_{head} - D_{inner\ seat}}{2} = 0.57"$$

We oversize the seat slightly to 0.065" to help in proper sealing of the combustion chamber while adding extra material to the sealing surface to improve the strength of the exhaust valve.

8.4.3.4 - Analysis

Stress and factor of safety analysis was completed for the exhaust valve as well. The same fixture and load conditions as the intake valve were applied to the exhaust valve. From stress analysis, the maximum stress seen in the exhaust valve under these conditions is 50.57 MPa. This stress occurred at the same location as the intake valve, just along the upper edge of the seat chamfer. This stress will not induce yielding of the material, as the yield strength of 21-4N steel is 560 MPa. The factor of safety plot showed that the minimum factor of safety of our exhaust valve is 11, which is greater than our determined factor of safety of three for valvetrain components.

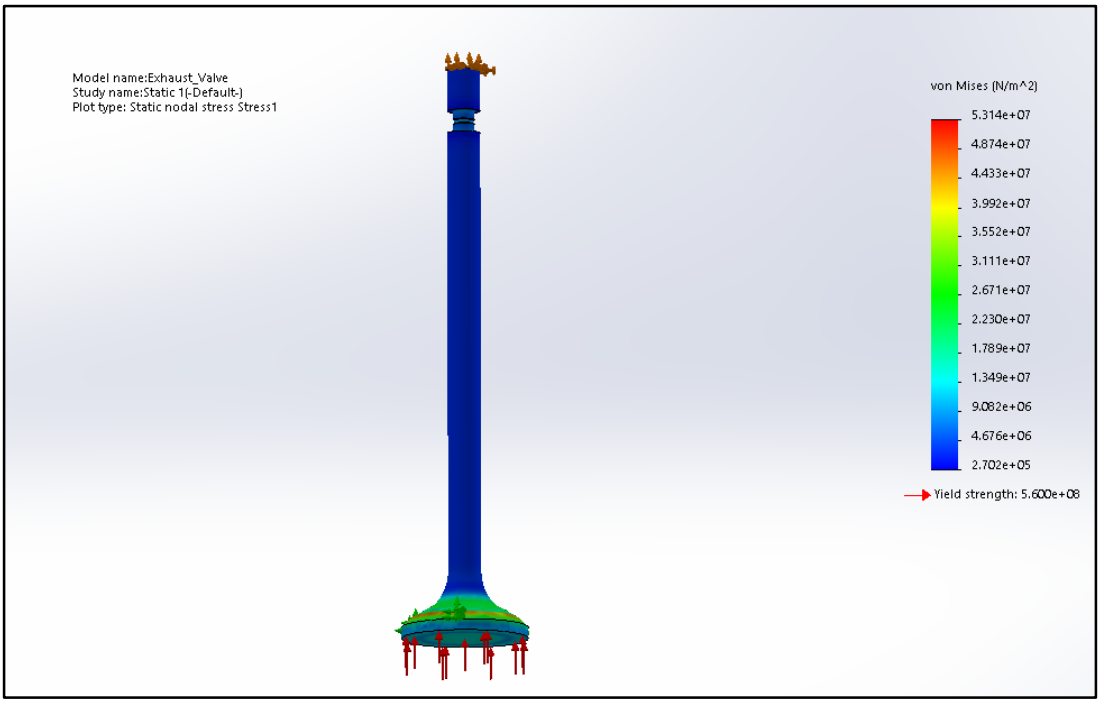

Figure 8.26: Stress Analysis of Exhaust Valve

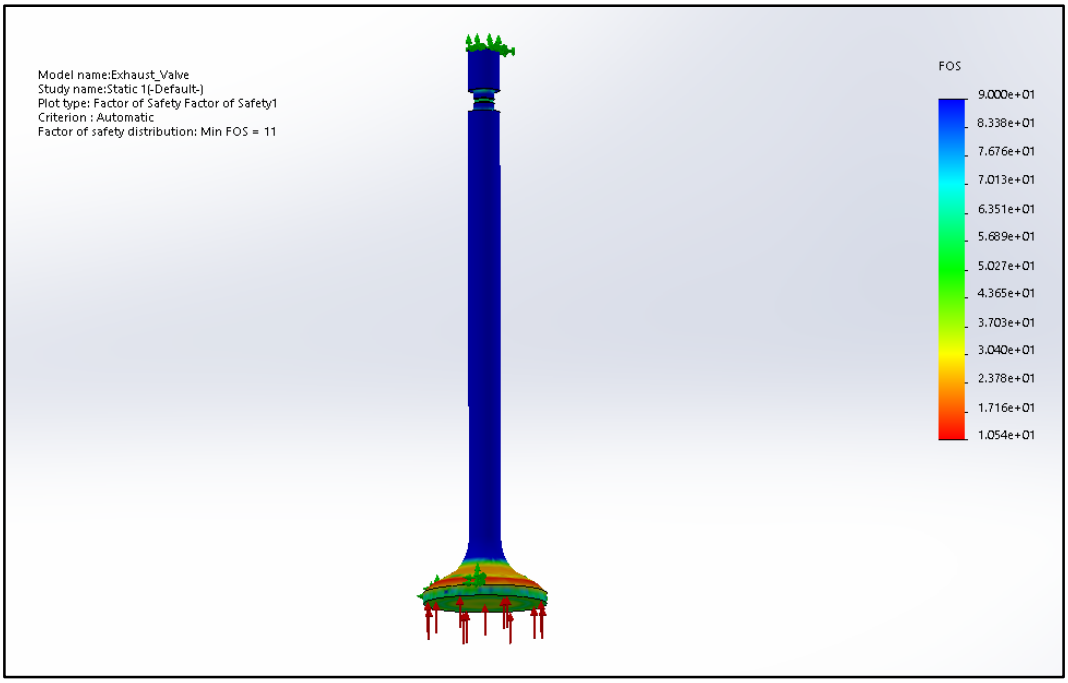

Figure 8.27: Factor of Safety Plot for Exhaust Valve

8.5 - Valve springs

Figure 8.28: Render of Valve Spring

8.5.1 - Overview

The poppet valve assemblies used in internal combustion engine applications require valve springs as well. These springs are fixed to the valve on one end via a retainer and keeper which lock into a groove on the tip of the valve. The other end of the spring sits flush with the cylinder head itself. When not being actuated by the camshaft, the valves of an engine need to be able to seal off the combustion chamber completely, and the valve springs are what provide the force necessary to keep the valve in contact with the seat throughout the sealing operation. Correct selection of valve springs is critical to the proper function of a valvetrain in an internal combustion engine, as they not only control how fast the valve closes and the amount of force the valve exerts on the seat when closing, but also determine how much force is required by the camshaft to actuate the valve during the opening procedure. In this section, we cover the materials used in the fabrication of our valve springs, major design decisions that were considered in the selection of springs, and accompanying calculations that allowed us to accurately define the valve springs for our specific application.

8.5.2 - Materials and Manufacturing

Valve spring material selection is critical in the functionality and longevity of the valvetrain over the life cycle of the engine. The material used in valve spring applications must exhibit superior fatigue life due to the enormous number of high frequency oscillations this component is subjected to under normal engine operation. The material must also be able to hold a consistent load value with minimal load loss over many cycles. Due to these strict considerations, many specific steel wire alloys have been formulated for the specific application

of valve springs. ASTM A877 is a standard that gives specifications for valve spring quality chromium silicon steel wire alloys. We select a chromium silicon steel wire alloy for our valve spring material as per the ASTM A877 recommendation. This material will also have to be hardened and tempered so that it maintains a high fatigue life and will experience minimal load loss over time. Once coiled, the ends of the spring must be closed and ground so that the spring has a surface that can sit flush with the flange on the spring retainer and the valve guide.

8.5.3 - Design Considerations

Many considerations go into selecting the correct valve springs for a given engine application. One major consideration is valve float at maximum RPM. Valve float can occur during the dwell phase of the cam. At max RPM, the cam actuates the valves to open at its highest frequency. This means that the valves have less time to close during the shorter dwell of the cam. The potential problem in this situation is that the valve springs may not be stiff enough to keep the tip of the valve in contact with the rocker arm and the rocker arm pushed against the cam during its dwell. This means that the valve is unable to fully close when it is supposed to, and this failure to close leads to the problem of an unsealed port when it should be sealed. For example, if the intake valve floats at redline RPM, the intake valve may still be open during the compression stroke of the engine, which would drastically reduce the amount of compression in the cylinder and have huge drawbacks in terms of both power and torque. For this reason, valve springs must exhibit a high enough stiffness to keep the valve tip in contact with the rocker arm and the rocker arm in contact with the cam in the most restrictive condition, which is redline RPM. Redline RPM was a factor that went into calculating the stiffness required for our valve springs.

While having too low of a stiffness can have drastic consequences near redline RPM, having too high of a stiffness can also be detrimental to engine performance. Having springs that are too stiff can actually cause the valve head to bounce off of its seat when closing. This can be detrimental because it causes increased wear between the valve and its seat, which can cause issues with sealing the port over thousands of repeated cycles. Valve bounce can also lead to decreased power output of the engine, as sealing the port becomes more difficult. Solidworks motion analysis will be employed in the future to ensure that valve bounce does not occur with the stiffnesses selected for our valve springs.

Another important factor in the selection of valve springs is coil bind. This is the condition when all of the spring’s coils are touching each other, i.e the spring is fully compressed. It is important to select a spring that will not experience coil bind prior to the valve achieving its max lift. For our application, our max valve lifts are 11 mm for the intake valve and 8.5 mm for the exhaust. We will have to select springs that can travel these distances without experiencing coil bind, otherwise we would be unable to achieve our max lift values. This would result in the cam trying to push further down on the valve, but the valve having no room to travel

any further. This can both cause increased wear between the cam and rocker arm and create very large stresses on the spring retainer, keeper, rocker arm, and the valve itself.

An often overlooked design consideration for valve springs is resonant frequency of the spring. The valve springs are actuated through a range of frequencies, depending on engine RPM. If resonance were to occur in the spring, a phenomena similar to valve bounce would occur. During the dwell of the cam, the valve would be allowed to undergo free oscillations if the spring is in resonance. This means that the port would not seal properly and would have the consequences of decreased engine power and lowered compression within the cylinder. To avoid this, generally springs with a resonant frequency of about 10 times max RPM are used. This ensures that the springs never undergo resonance throughout the range of valve actuation frequencies in the engine.

During the installation of the valve springs, it is essential that the installed height and seat pressure are within the given specification. If the seat pressure of the spring is too high, there is potential for failure in the spring retainer or keeper and increased wear between the valve and seat due to the working load exceeding the design loads on these components. For this reason, when installing the valvetrain assembly, we will make sure to diligently test the installed height of the springs and test the load of the springs once installed.

8.5.4 - Calculations

In calculating the necessary stiffness values for our intake and exhaust valve springs, first the masses moved by the springs had to be defined. This mass was defined as the mass of the valve, keeper, and retainer, and was calculated for both intake and exhaust.

$$m_i = \square_{\square\square\square\square\square} + \square_{\square\square\square\square\square\square} + \square_{\square\square\square\square\square\square\square\square} = 0.081\ \square\square$$
$$m_e = \square_{\square\square\square\square\square} + \square_{\square\square\square\square\square\square} + \square_{\square\square\square\square\square\square\square\square} = 0.085\ \square\square$$

The effect of coring our intake valve stem can be seen here, as it drastically reduces the weight of the intake valve and the mass being moved by the intake valve spring. Next, the maximum acceleration of this spring was found from our valve lift profile synthesized from cam design. Maximum RPM was used in the calculation of this acceleration value. Next, the max valve lifts for both the intake and exhaust side were defined.

$$a_i = 15000\ m/s^2 \quad L_i = 11\ mm\ (0.433")$$
$$a_e = 11000\ m/s^2 \quad L_e = 8.5\ mm\ (0.335")$$

Then, the maximum force in both the intake and exhaust spring could be calculated using the mass moved by each spring and the max acceleration of the spring.

$$F_i = \square_{\square}\square = 1215\ \square = 273.1\ \square\square\square$$

$$F_e = \square_{\square}\square = 935\,\square = 210.2\,\square\square\square$$

This maximum force value corresponds to when the valve is fully open, and is generally called the open pressure of the spring. In order to fully determine spring rate, a seat pressure had to first be defined. Seat pressure is the force in the valve spring when it is installed into the engine, at its installed length. The valve springs are pretensioned, meaning that even when the valve is fully closed, there is force in the spring. This initial force is called the seat pressure. Generally, it is recommended to not exceed 120 lbs of seat pressure. Using a recommendation from "Valve Springs" [25], we select a seat pressure of 100 lbs. Now the spring rate can be determined by subtracting the open pressure form the seat pressure, then dividing by the max lift.

$$F_0\ (seat\ pressure) = 444.8\ N\ (100\ lbs)$$

$$\square_{\square} = \frac{\square_{\square} - \square_0}{\square_{\square}} = 400\,\square\square/\square\square$$

$$\square_{\square} = \frac{\square_{\square} - \square_0}{\square_{\square}} = 329\,\square\square/\square\square$$

This was done for both intake and exhaust to give us k values of 400 lb/in and 329 lb/in, respectively. These values are quite high due to the high acceleration given from our valve lift profile, however we need stiffer springs to not float the valves at our redline RPM of 8700.

8.6 - Valve Keepers & Retainers

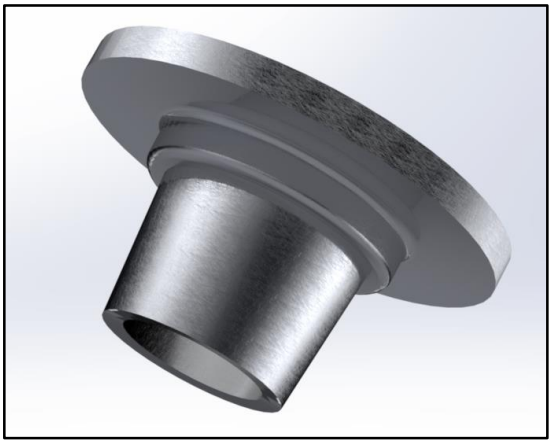

Figure 8.29: Render of Spring Retainer

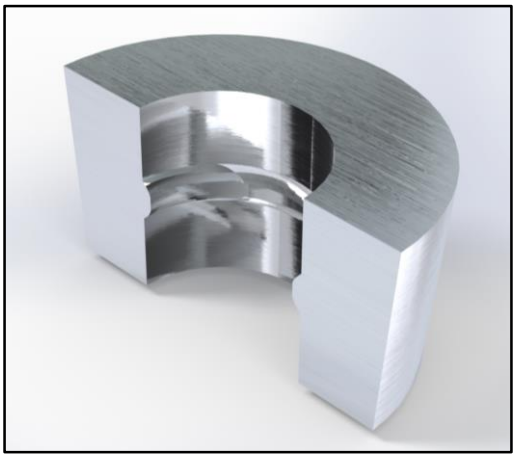

Figure 8.30: Render of Valve Keeper

8.6.1 - Overview

While the valve springs are essential in accurately controlling the opening and closing of the intake and exhaust valves while making sure that they have sufficient force to seal the combustion chamber, they must be adequately retained to the valve in order for the proper function of these opening and closing events. If the springs are not fixed to the valve on one end, the valve can drop into the cylinder and will no longer be able to seal the combustion chamber. To achieve this, valve keepers and spring retainers are used. The valve keeper is a component that is tapered on its outer diameter and has a groove on its inner diameter to lock with the mating groove on the valve stem. This groove holds the keeper in position relative to the valve. The spring retainer fits around the keeper and is tapered at the same angle as the keeper, but on its inner diameter, and has a flange that provides a seating surface for the end of the valve spring to rest on. This allows the end of the spring to move with the valve and gives the spring a surface to push up against in order to actuate the valve. In this section, we cover the materials and manufacturing methods for our valve keepers and spring retainers, explain some of the considerations that went into the design of these components, and complete analysis of stresses that these components see during normal engine operation.

8.6.2 - Materials and Manufacturing

For our spring retainer and keeper, the material we decided to use was heat treated 4140. The material choice for the retainer is important because it must be able to withstand many cycles of bending stresses applied to its outer flange from the spring force. The retainer must be able to withstand these stresses for many cycles without yielding, so selecting a material with high fatigue life was imperative. The grooves on the keeper and valve stem must be carefully finished and filleted and will be created by rolling as opposed to machining, as this improves the longevity of the keeper and reduces the risk of keeper groove failure [26]. Our spring retainers will be forged, then finished on a CNC lathe to ensure proper dimensionality.

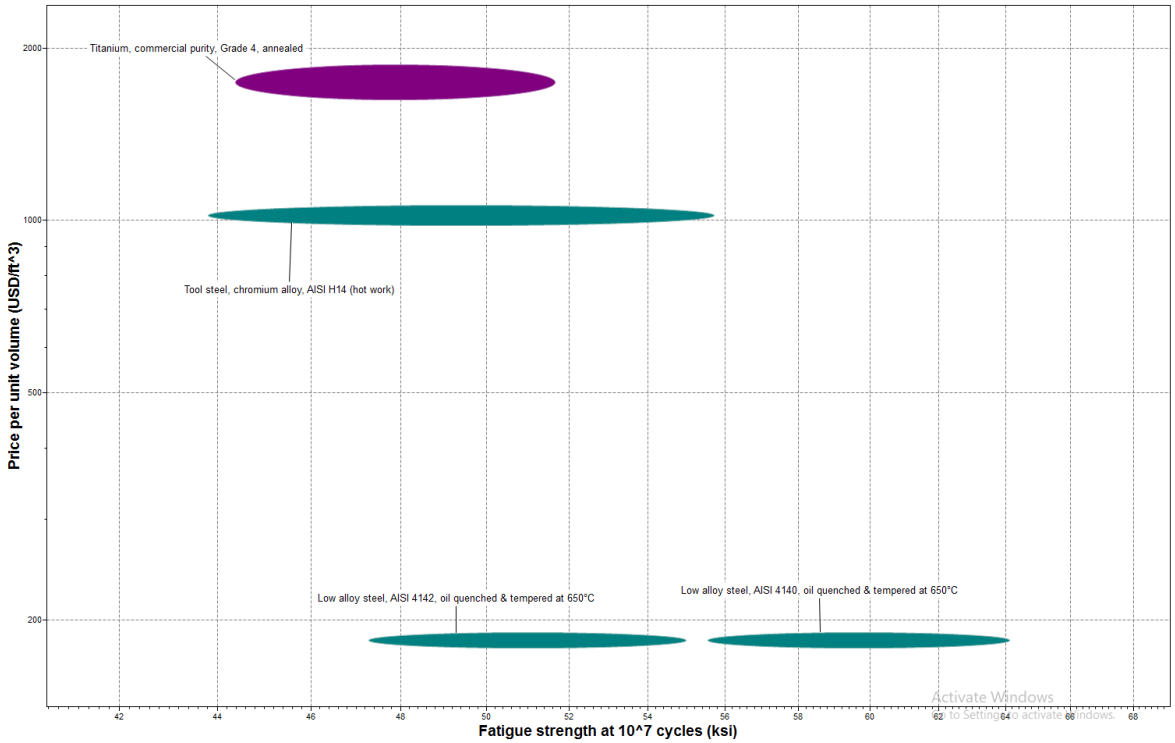

Figure 8.31: CES Edupack Graph Comparing Price vs. Fatigue Strength at 10^7 Cycles for Grade 4 Titanium, AISI H14 Tool Steel, 4142 Stainless, and 4140 Stainless

8.6.3 - Design Considerations

For our keeper, we decided to use a single radial groove locking mechanism with the valve stem. Using a radial locking mechanism instead of a square cut groove allows us to remove stress concentrations present in the locking interface on the keeper when sharp corners are used. On the outer diameter of the keeper, a 10° lock angle was used. This surface is in contact with the inner surface of the retainer, which is tapered at the same angle. Oftentimes a 7° lock angle is used, however the 10° angle provides more surface area for the spring load to be distributed, optimizing load spreading across the surface. This angle locks the retainer in position and ensures it can not slide out past the keeper, which would have drastic consequences for the valvetrain. The retainer's flange thickness is critical because this region is heavily stressed under a cyclic bending load. Further FEA analysis was completed on both the keeper and retainer to validate the initial design and ensure that parts will hold up to repeated loading cycles.

8.6.4 - Analysis

8.6.4.1 - Spring Retainer Force Analysis

Finite element analysis was used to determine the maximum stresses in the spring retainer during normal operating conditions of the engine. The inner tapered face of the retainer was fixed, as this is the surface in contact with the keeper. The keeper keeps this face in position and prevents the retainer from sliding relative to the valve. A load of 273.1 lbs was applied to the outer flange of the retainer, as this is the maximum force the valve spring exerts on this seating area. The maximum force was found from the maximum force in the intake spring, as the same retainer is used the inlet and exhaust valves but the intake spring sees a higher maximum force. The maximum stress in the retainer was found to be 123.1 MPa, along the inner edge of the floange which experiences the maximum spring force. This stress will not cause the material to yield, however, because the yield strength of 4140 steel is 460 MPa. A factor of safety plot was also generated, showing the minimum factor of safety in the spring retainer to be 3.74, occurring in the same region as the maximum stress. This minimum factor of safety meets our criteria of a global minimum factor of safety of 3 for valvetrain components. Fatigue analysis was conducted on the spring retainer as well, and the minimum rated life cycle values on any area of the spring retainer was $2.5*10^6$, giving this component infinite life as it is made from steel.

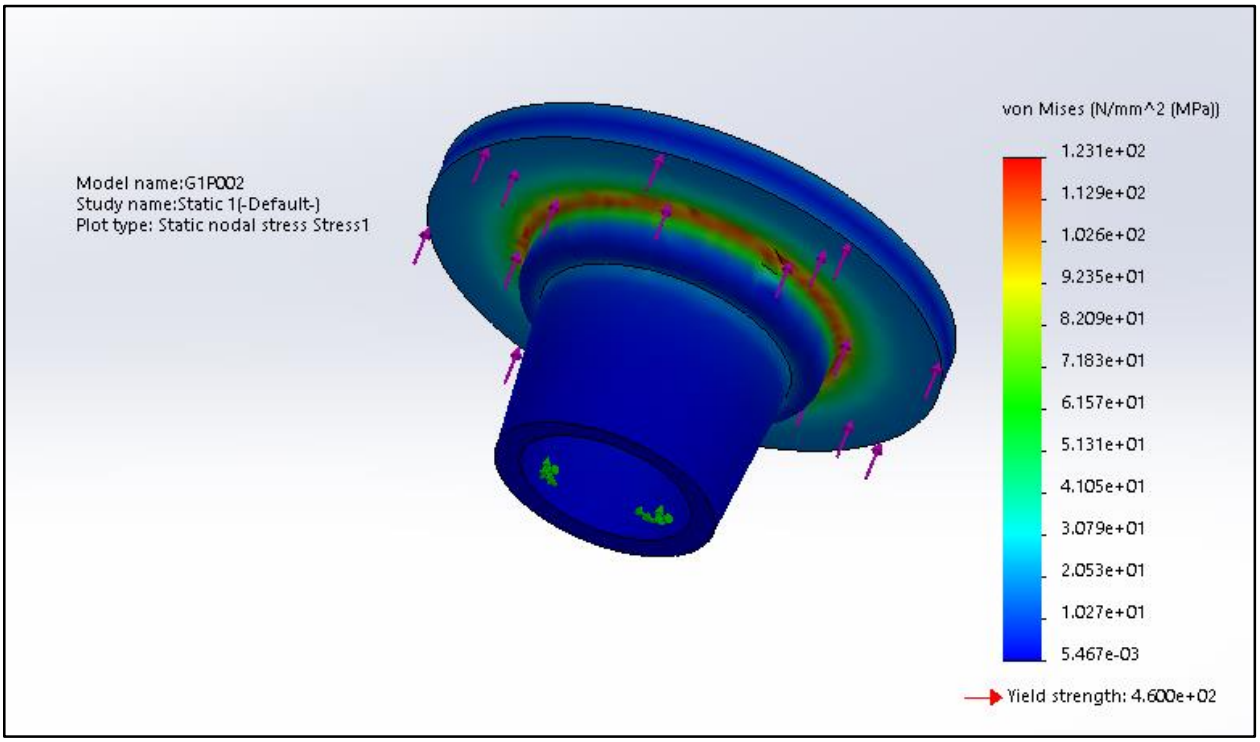

Figure 8.32: FEA Stress Analysis of Spring Retainer

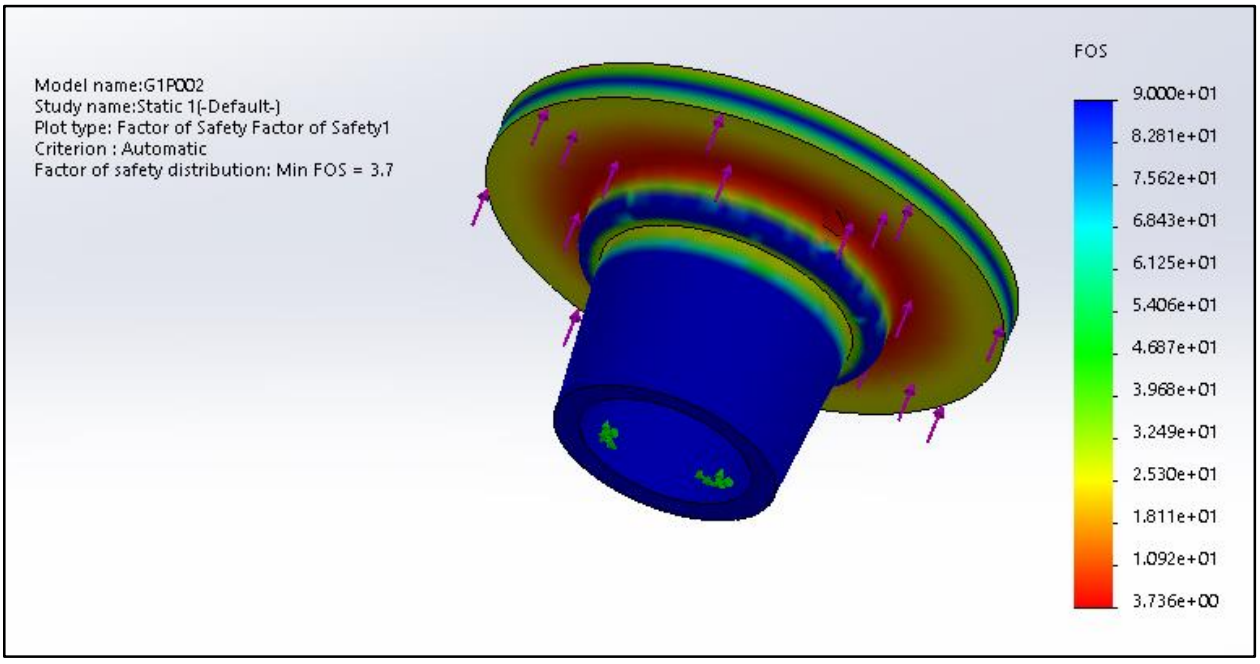

Figure 8.33: FEA Factor of Safety Plot for Spring Retainer

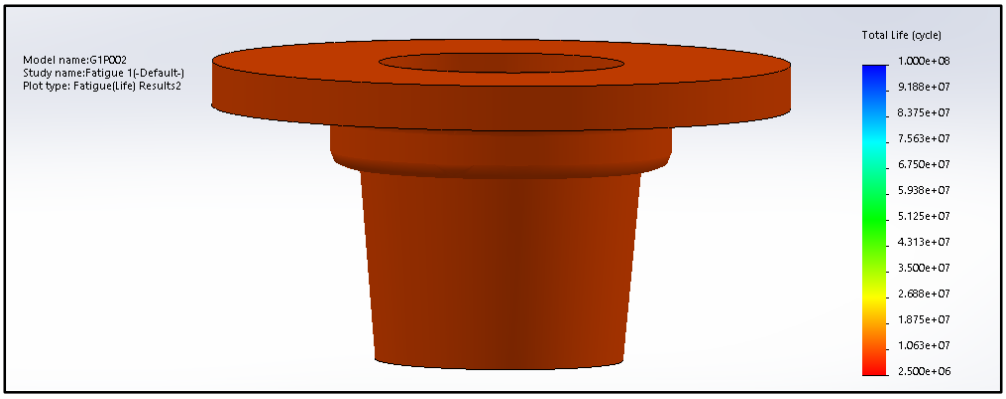

Figure 8.34: FEA Fatigue Analysis for Spring Retainer

8.6.4.2 - Keeper Force Analysis

Finite element analysis was also used in the analysis of the loads on the keeper. The keeper sees a load on its outer tapered surface from the action of the retainer pushing up against this surface via spring force. The keeper is fixed in a ring on its top surface and on the upper fillet of the locking groove, as these are the areas where it contacts the valve. The maximum stress in the keeper was found to be 20.5 MPa, which would not cause the keeper to yield, as 4140 steel has a yield strength of 460 MPa. A factor of safety plot was generated as well, showing that the minimum factor of safety in the keeper is 7.2. This is greater than the determined minimum factor of safety for valvetrain components of three. Fatigue analysis was

also conducted on the valve keeper, giving a minimum value for total life cycles of $1.25*10^7$. Because we make our keepers from 4140 steel, we can consider them to have infinite life as the minimum number of life cycles for the component is greater than 10^6 cycles.

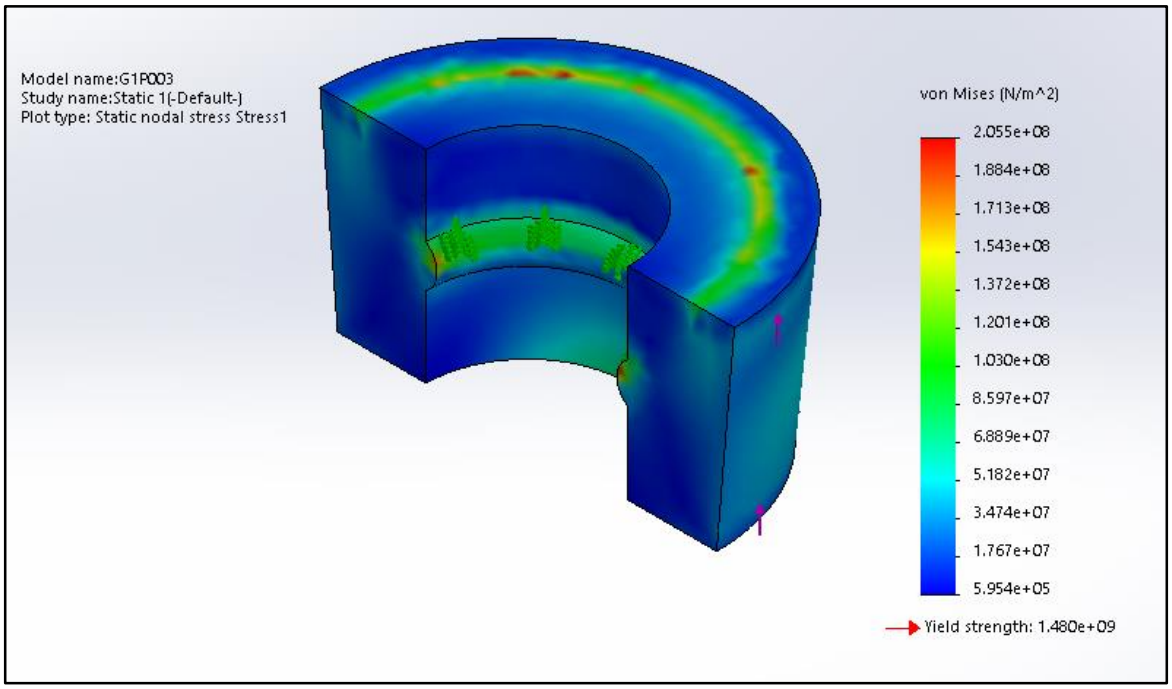

Figure 8.35: FEA Stress Analysis of Keeper

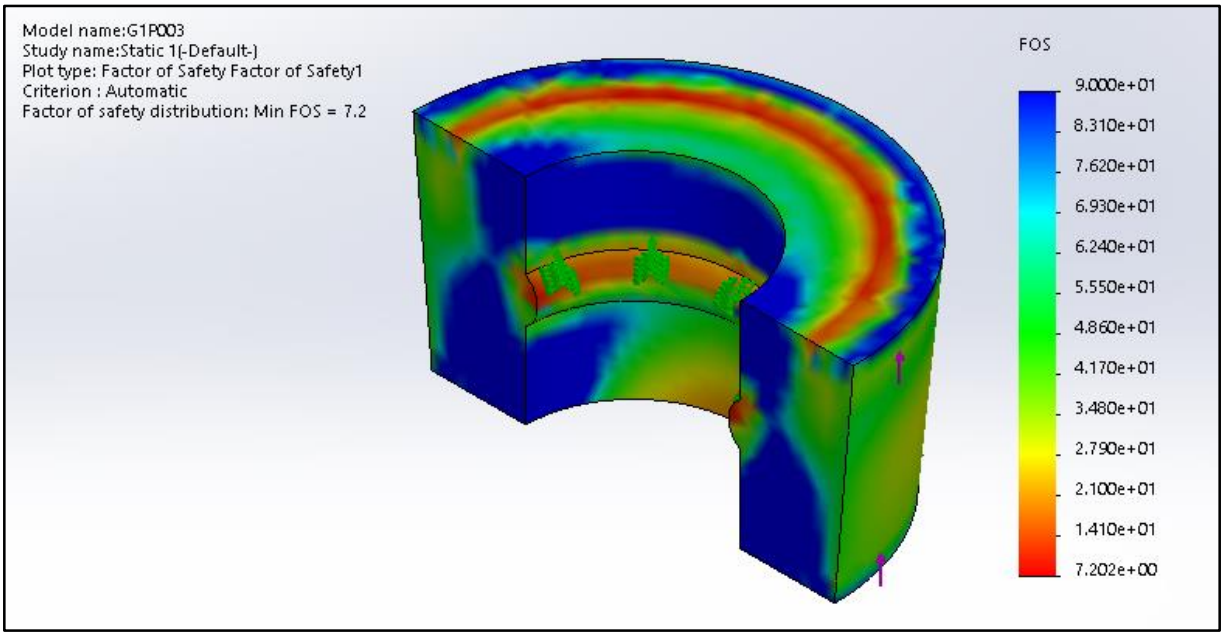

Figure 8.36: FEA Factor of Safety Plot for Keeper

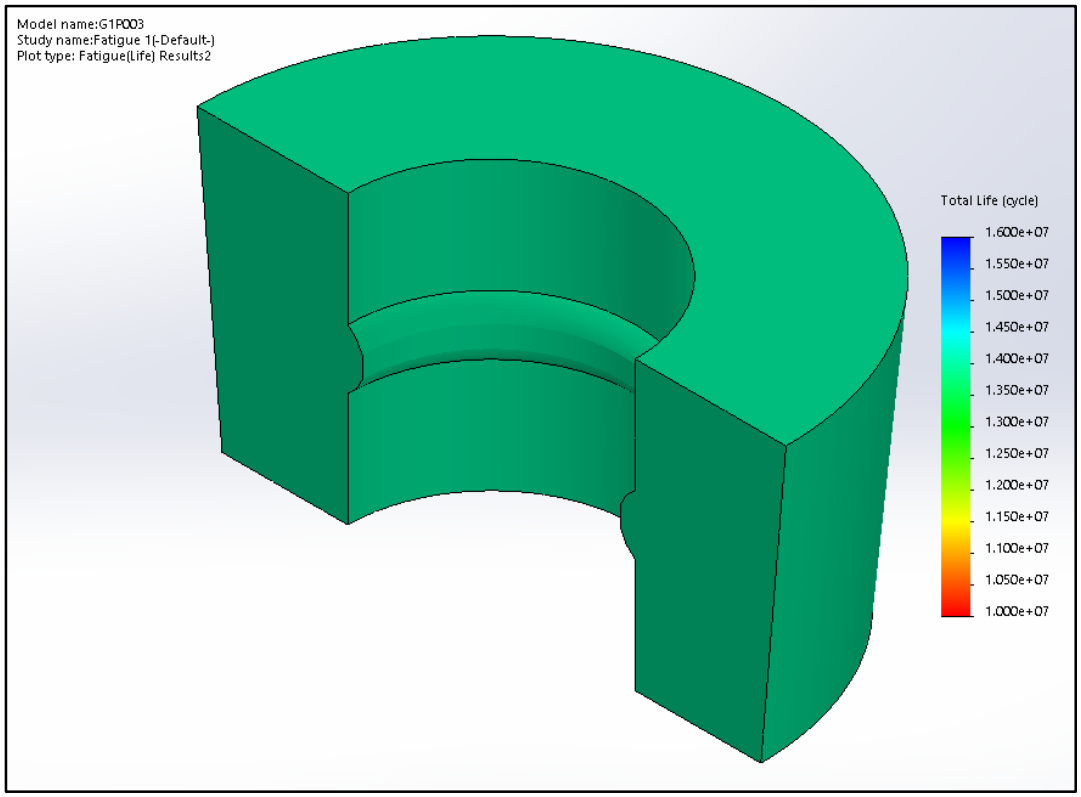

Figure 8.37: FEA Fatigue Analysis for Keeper

8.7 - Cylinder Head

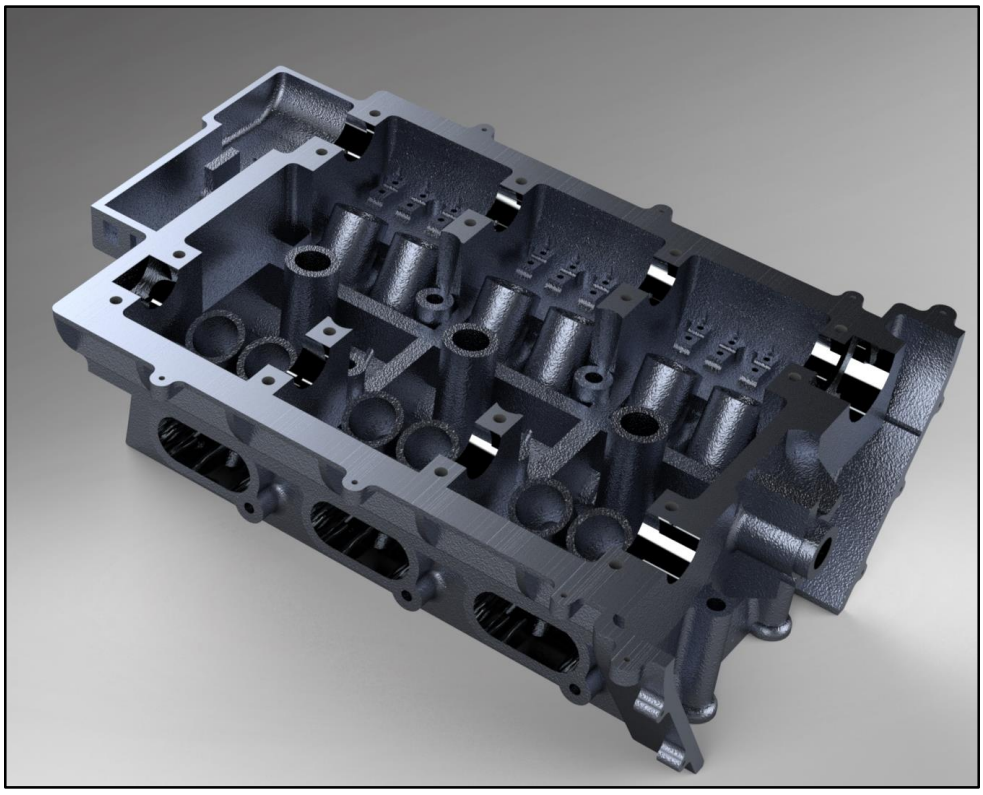

Figure 8.38: Render of Cylinder Head

8.7.1 - Overview

The cylinder head is located in the upper part of the engine, it primarily serves as the housing for valves, cam shafts, intakes, exhaust, rocker arms and spark plugs. It interfaces with the engine block and is sealed by the head gasket. Also, there are three main fluid passages for bearing lubrication, oil drain, and VVT oil channels.

8.7.2 - Materials and Manufacturing

The cylinder head is sand casted out of aluminum A356, the same material as the engine block. A356 was selected for its excellent castability, thermal conductivity, and lightness. It is tempered to T6 to improve hardness and wear resistance and post machined for critical surfaces such as the cam bearings, deck, intake and exhaust channels, and all threaded holes

8.7.3 - Design Considerations

The design of the cylinder head was heavily constrained by other design requirements such as the block, desired combustion chamber pent roof angles, and the size of the intake and exhaust valves. In addition, the cylinder head has to be able to fit both the DVVL and VVT system as well.

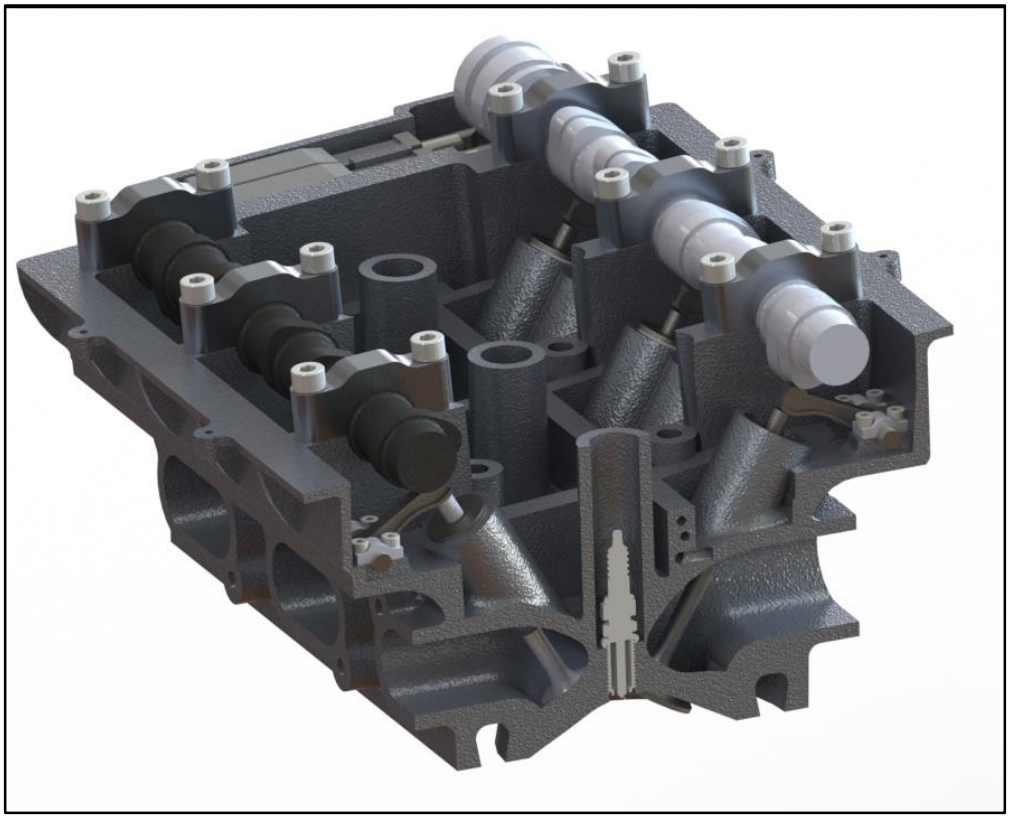

Figure 8.39: Render of Cylinder Head

8.7.3.1 - Intake and Exhaust Runners

The designs of intake and exhaust channels are the first part of the cylinder head design. The size of these channels is mainly dependent on the diameters of the intake and exhaust valves, which have been determined in sections 8.4.2.4 and 8.4.3.3. In line with this, and given that we are using four valves per cylinder, the intake and exhaust channels are designed to be ellipses with end diameters that corresponds to the diameters of the corresponding valves. This ensures smooth air flow and tight packaging. Each channel starts out as one ellipse and then separates into two circular channels closer to the valves.

8.7.3.2 - Combustion Chamber

The most important decision we had to make for our combustion chamber was what shape we wanted it to be. A pugh chart for this decision can be found below in Table 8.1.

Characteristics	Weight	Hemi/Pent	Wedge	Flat	In Piston
Efficiency	0.4	8	4	6	7
Emission	0.3	9	5	7	5
Cost	0.3	7	7	9	6
Total	1	8	5.2	7.2	6.1

Table 8.1: Pugh Chart for Combustion Chamber Shape

As can be seen from our pugh chart, we decided to use a pent roof / hemispherical chamber shape due to its higher efficiency and lower emissions. Between the two, the only difference is how many valves per cylinder an engine has, with hemispherical being for two and pent roof being for four. As we have four valves per cylinder, this led us to using a pent roof design.

The next important design decision was the angle of our pent roof. This angle is defined as the angle between both sides of the combustion chamber, as illustrated in Figure 8.40 below.

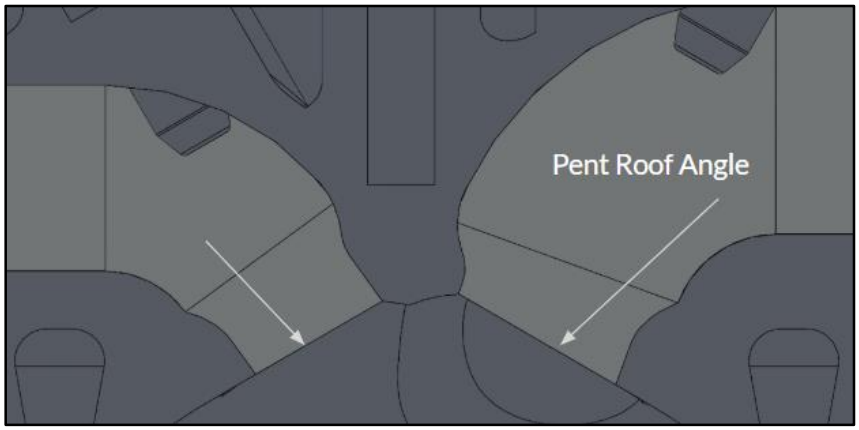

Figure 8.40: Illustration of Pent Roof Angle

A larger pent roof angle is recognized by industries to have a great combustion efficiency. However, the design of the pent roof is also constrained by the lift of the valves. As DVVL and VVT allows the intake valves to have a longer valve lifts and a longer period of time when both intake and exhaust valves are moving, the possibility of collision between intake valves and exhaust valves drastically increases in large pent roof angle. From extensive motion studies in Solidworks to ensure the valves won't collide with each other during DVVL and VVT process. A pent roof angle of 30 degrees was selected, so that the valves won't collide and still ensure efficient engine.

8.8 - Valvetrain Technologies

8.8.1 - Overview

One of the most unique features of BTN's motorcycle engine is its incorporation of valvetrain technologies that can vary our camshaft profiles. These systems allow the engine to gain both performance and efficiency. The DVVL is the cam shifting mechanism, which swaps between a high lift and low lift intake cam profile, allowing the engine to have optimal volumetric efficiency over a wide range of riding conditions. The VVT system is the oil-actuated phasing intake cam sprocket, which alters the timing of the intake cam to gain better fuel efficiency at low-load, low-rpm conditions. These valvetrain technologies allow the bike to be both a fuel-sipping cruiser and a powerful performance machine simultaneously. It is a design that has never been incorporated into a motorcycle engine before, and is what truly makes the BTN 1500-E so unique.

8.8.2 - VVT

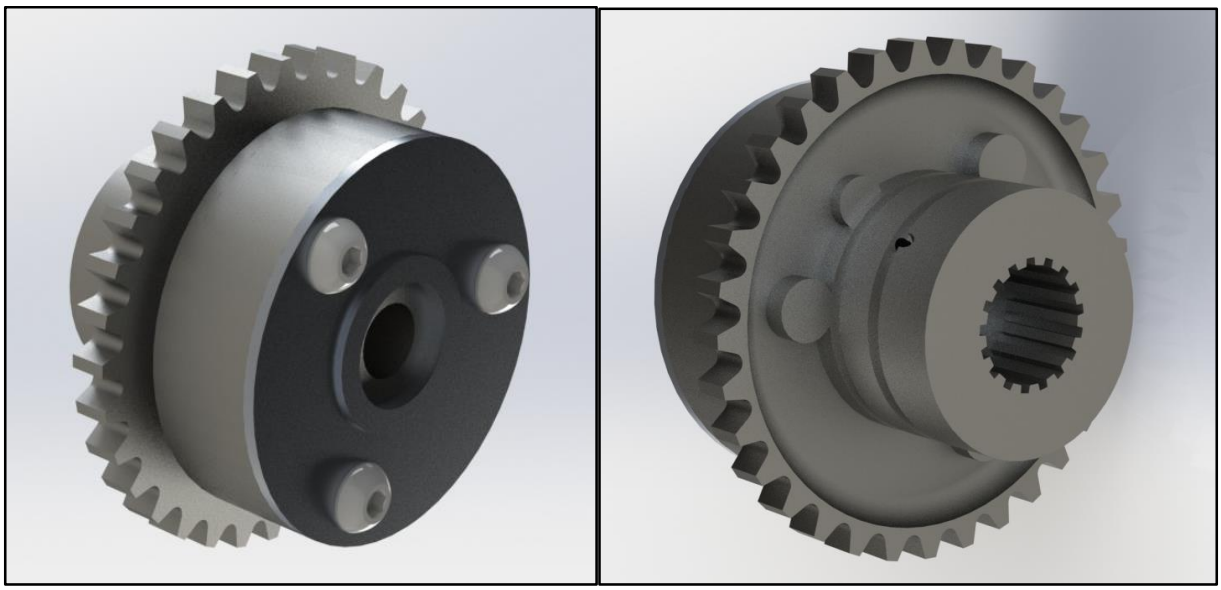

Figure 8.41: Renders of the Front (left) and Back (right) of the VVT Sprocket

8.8.2.1 - Materials and Manufacturing

After careful consideration of the material selection for the VVT sprocket assembly, we selected the material of main sprocket, housing, and shifting mechanism to be 4140 steel for its exceptional strength and wear resistance. Since the cover of the sprocket doesn't need to provide too much structural support, it is die cast out of aluminum A356 and post machined for surfaces that contact the sprocket housing. The plunger is machined out of 4130 steel so that it can move smoothly within the VVT housing.

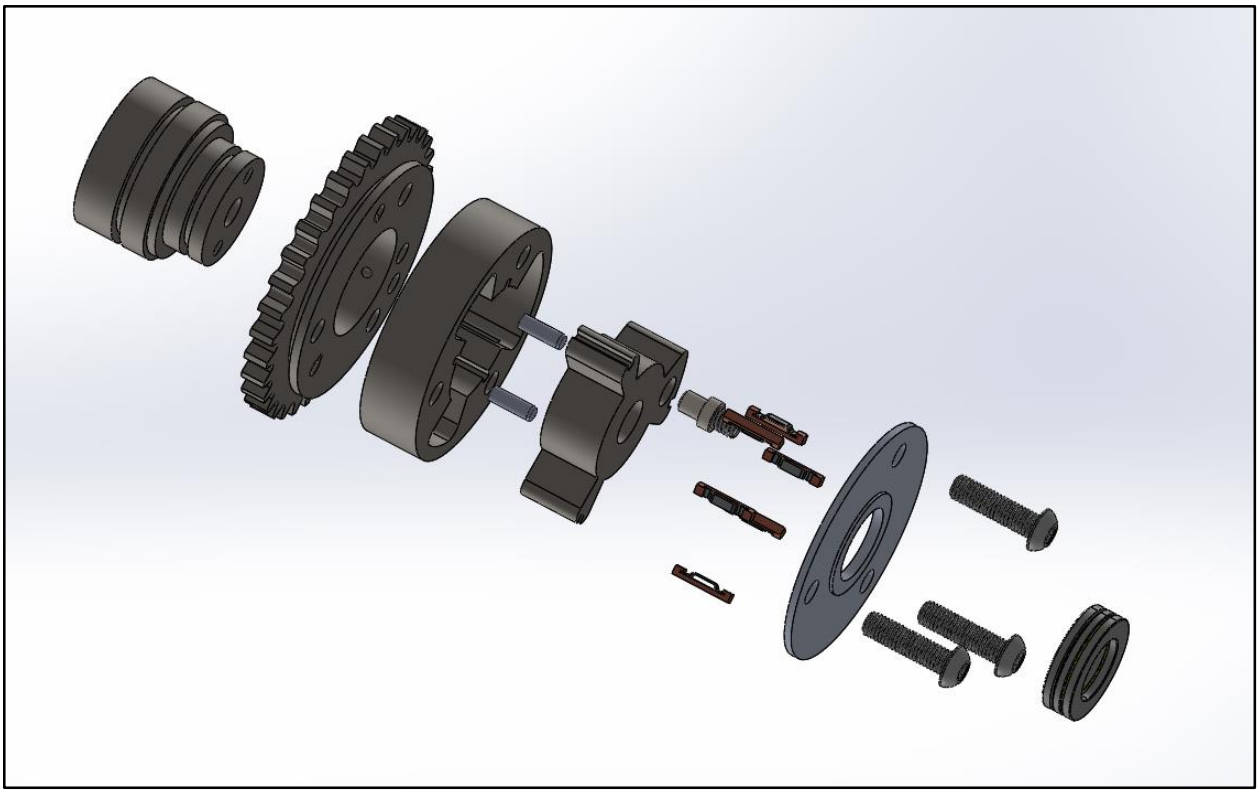

Figure 8.42: Exploded View of VVT Sprocket

Since the sprocket assembly has to precisely control the phasing of the intake and exhaust valve lift, prevent oil leakage, and withstand the high rpm loads of the engine, a majority of components of the VVT sprocket have to be post machined by CNC to obtain the tight tolerances necessary. The sprocket will be case hardened for improved durability. The seals that separate the oil channels in the sprocket are made out of plastic to reduce friction between the moving rotor and the outer housing. A sheet metal spring is placed in the back of the seal to ensure constant contact and make sure that there is no loss of pressure during the shifting process.

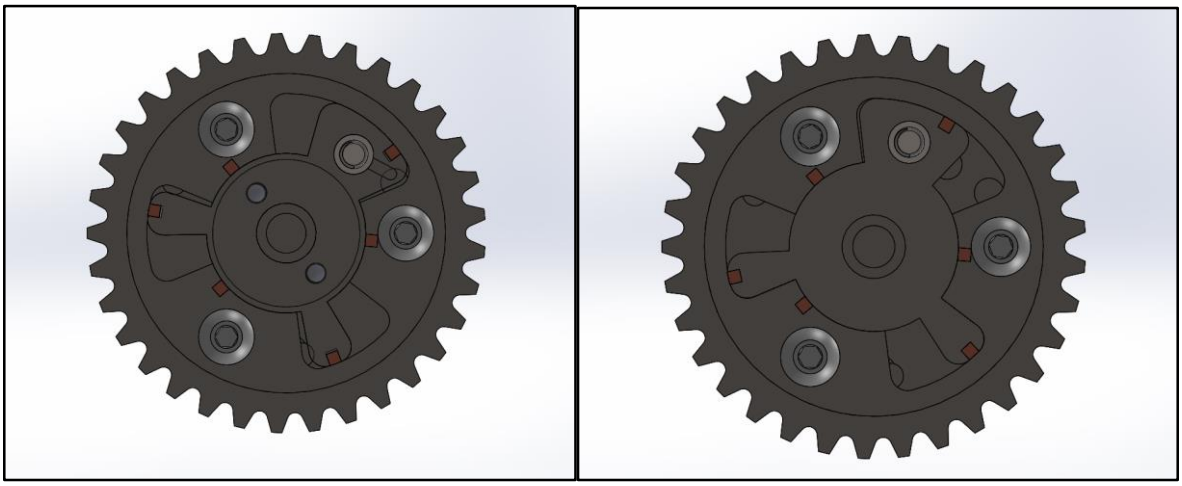

Figure 8.43: Normal Condition

Figure 8.44: VVT Rotor Shifted

8.8.2.2 - Design Considerations

Although many cars today feature VVT, it is still fairly uncommon for motorcycle engines to do so. There are currently several designs that allow the intake and exhaust valves to change phasing, however none of these designs also incorporate DVVL. To be able to have both, an oil actuated shifting sprocket is the only feasible option. The oil actuated VVT sprocket is controlled by a solenoid that is mounted on the cylinder head. This solenoid acts as a switch for the oil pressure within the VVT sprocket. Under normal riding conditions, the solenoid will be closed and there will be no oil pressure running through the system, leaving the sprocket in its non-shifted state. Additionally, a plunger on the shifting rotor is engaged by a spring into a hole on the face of the sprocket, locking the sprocket in place to reduce the chance of failure. When VVT is activated by the ECU, the oil solenoid will open and allow oil pressure to reach the system. This oil pressure will first disengage the locking plunger, which unlocks the shifting rotor from the face of the sprocket and enables the rotor to rotate. As the oil pressure increases between the rotor and the housing, the oil pushes the rotor counter clockwise, which allows the camshaft to shift.

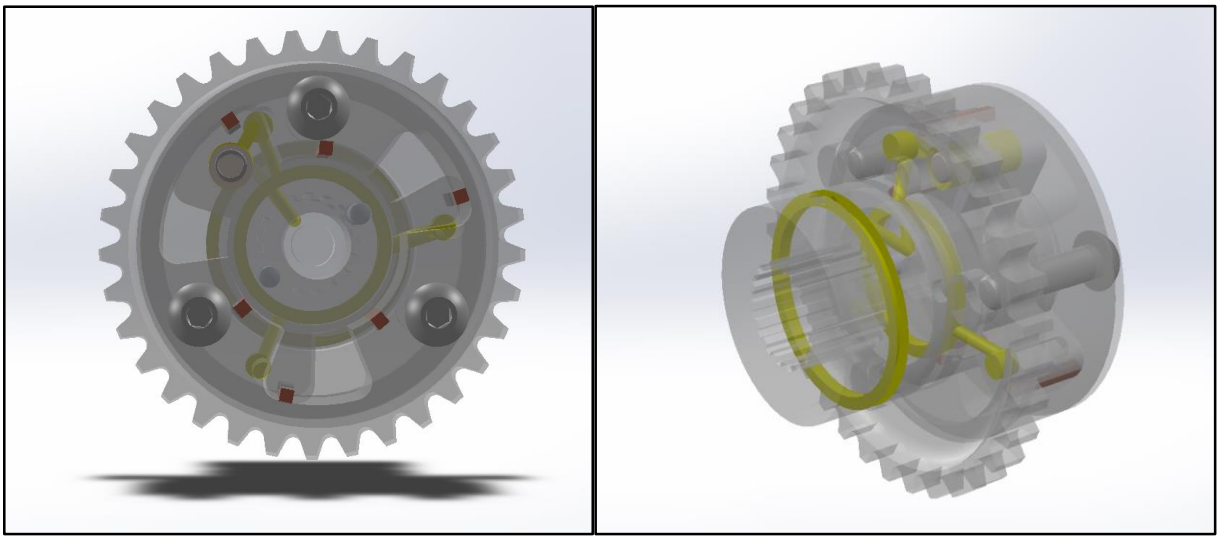

Figure 8.45: Illustration of the Front (left) and Isometric (right) Views of the Oil Passages in the VVT Sprocket

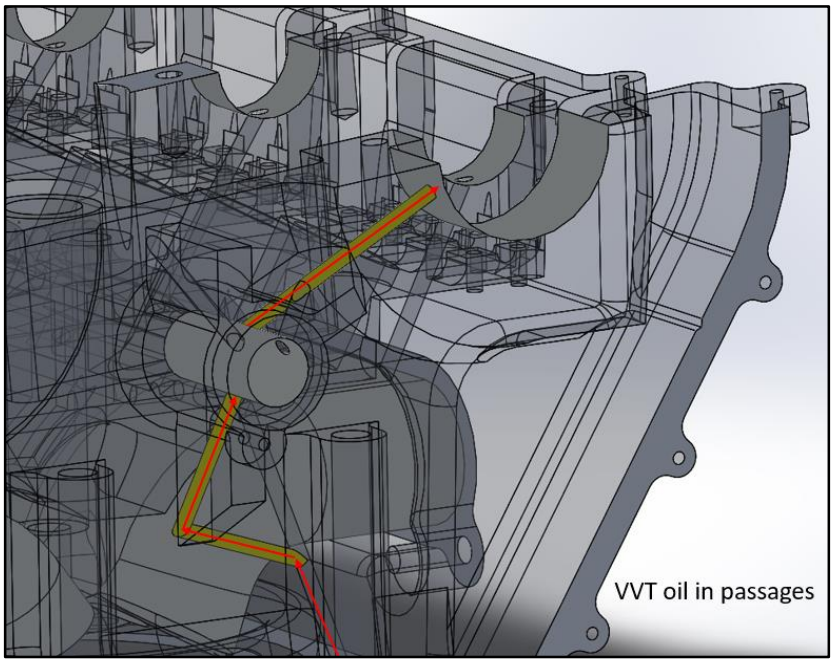

Figure 8.46: Illustration of the Oil Passages for the VVT Sprocket in the Cylinder Head

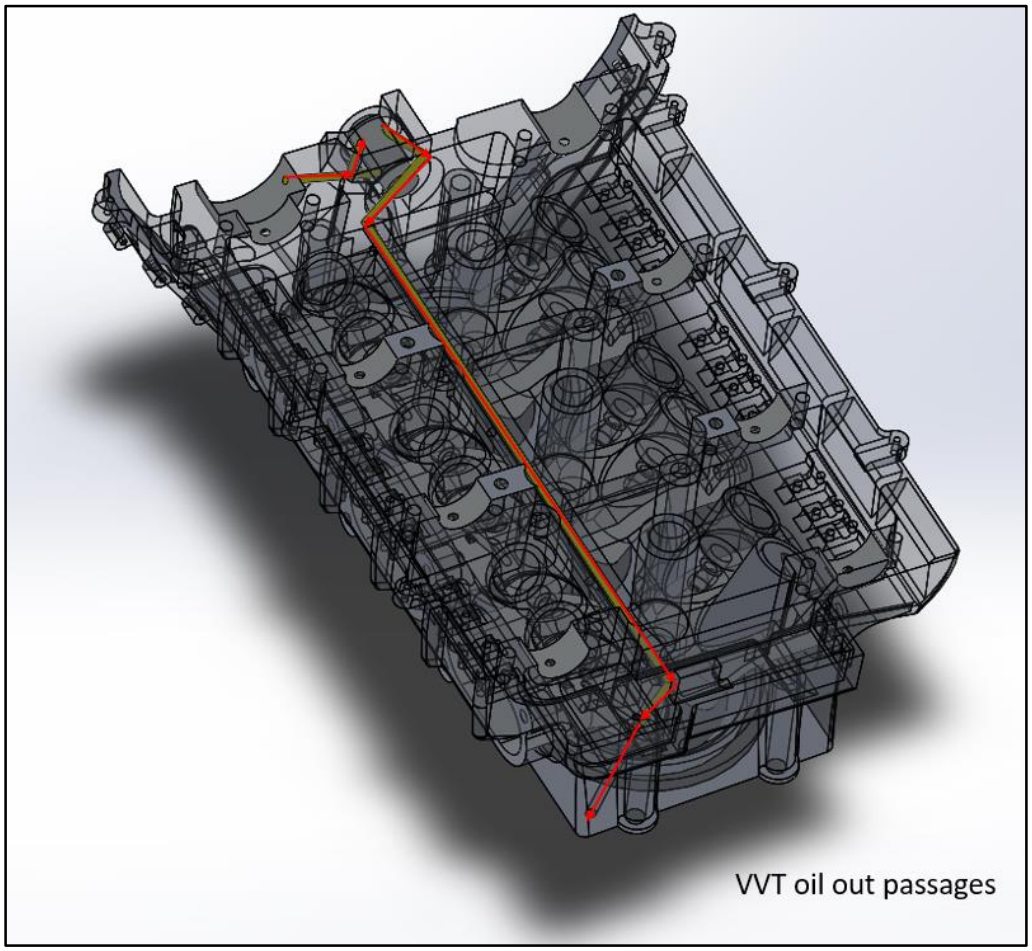

Figure 8.47: Illustration of the Drainage Oil Passages for the VVT Sprocket

8.8.2.3 - Calculations

The main calculation for the VVT system is how much oil pressure is needed to actuate it. Looking at the locking plunger first, the spring behind it has a spring rate of .9 lbs/mm and the plunger needs 5 mm to disengage from its locked position. This means that the plunger needs greater than 4.5 lbs of force to disengage, which translates to 29 kPa (4.2 psi) However, the most significant pressure requirement is driven by the oil pressure needed to shift the rotor in the VVT sprocket by 15 degrees. The force for this is equivalent to the force needed to compress the intake valves into fully open position, and are given in section 8.5.4. The torque needed to rotate the cam can be calculated from geometry and formula below.

$$\tau = r \times F$$

This comes out to 47 nm. Multiplying this To shift the VVT sprocket, the oil pressure in the sprocket needs to exceed the maximum torque to rotate the intake cam.

$$\tau = 3 \int \quad \int \quad P\mathrm{dAdr}$$

Assuming that the head loss from the oil in channel is negligible, given the length of the oil in channel is less than ten cm, the pressure required to activate the VVT sprocket is at least 58 kPa (8.4 psi)

8.8.2.4 - Analysis

FEA was run on both the rotor and the housing based on the maximum oil pressure the oil pump can output. As can be seen from Figure 8.x below, both of minimum factors of safety for both parts were above 50 for maximum oil pressure.

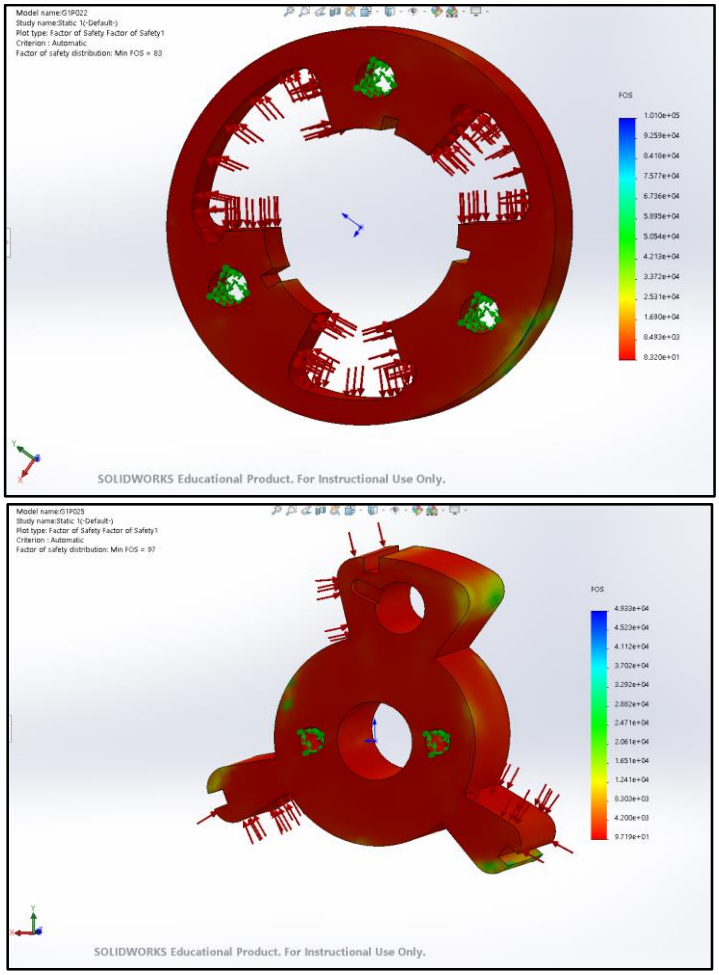

Figure 8.48: FEA Factor of Safety Plots for VVT Housing (top) and Plunger (bottom)

8.8.2.5 - Component Selection

We also had to choose what oil solenoid to use for our shifting. After an exhaustive search, we decided on the Dorman 45040023A due to its compact size. The Dorman 45040023A is a three gate oil solenoid that includes two oil outlets and one oil inlet. The oil inlet is used to

allow pressurized oil to enter the VVT sprocket. The oil outlets are to allow oil to escape from the sprocket and to drain out to the cylinder head.

8.8.3 - DVVL

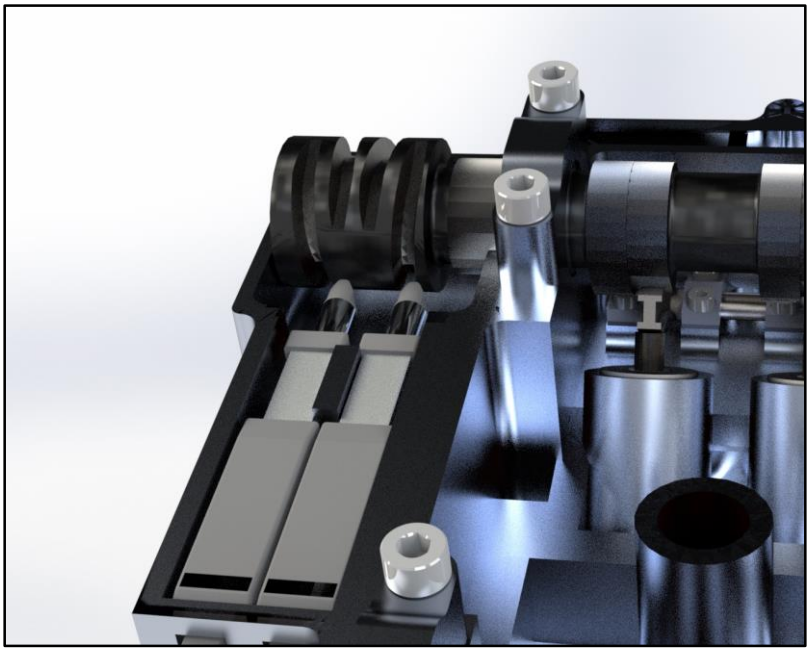

Figure 8.49: Render of DVVL Components

8.8.3.1 - Materials and Manufacturing

The discrete variable valve lift is a feature of the input camshaft. Therefore, the cylindrical cam would similarly made out of cryotreated cast iron. The tip of the linear actuator is swapped with one made of 4340 steel, heat treated and nitrided to improve wear resistance.

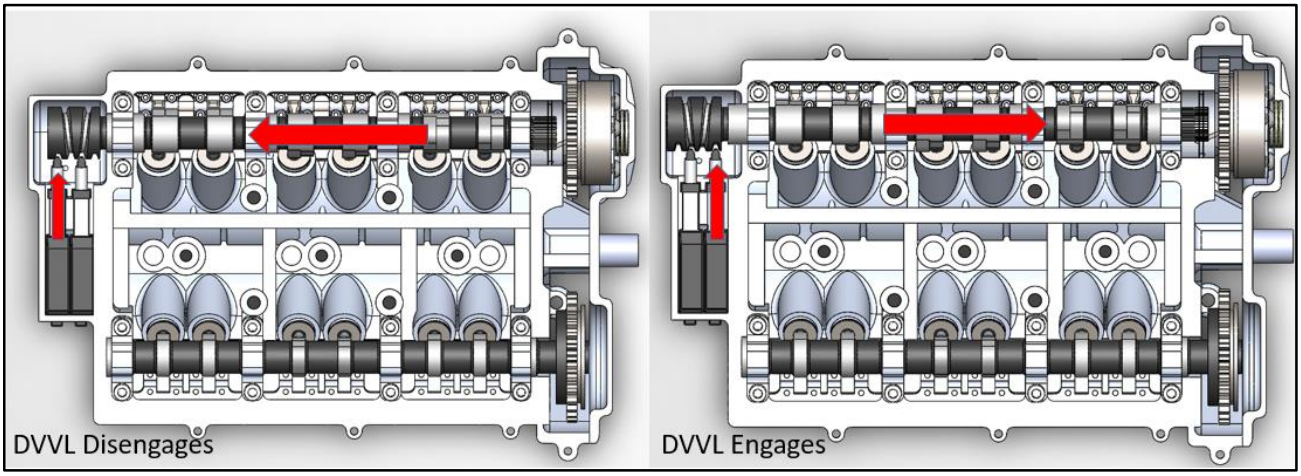

Figure 8.50: Image of DVVL Disengaging (left) and Engaging (right)

8.8.3.2 - Design Considerations

Many high performance cars on the market today have discrete variable valve lift, however, many designs drastically increase the complexity and the cost of the engine. In addition, many discrete variable valve lift designs do not work harmoniously with variable valve phasing. To enable the engine to have both DVVL and VVT at the same time for better performance and lower fuel consumption, we designed a camshaft that would shift to different cam profiles under different throttle condition. CamShift would first engage the small cam profiles in normal riding condition for better fuel consumption. When the rider applies sudden throttle, a linear actuator on the side of the intake camshaft would engage the groove on the camshaft and push the camshaft to the right such that the large cam profile would be engaged to give the rider a sudden increase in power. The camshaft can also shift back to its original location with the second linear actuator, when more power is not needed. The shifting distance of the camshaft is largely dependent on the thickness of the intake cam lobe. The cam lobe is 10 mm wide. So to shift the center of the lower cam lobe to the center of the higher cam lobe, the distance needed for the intake camshaft to travel is 10 mm.

8.8.3.3 Analysis

In performing FEA for the DVVL system, the worst case scenarios are considered for each component. Therefore, maximum load cases are used for FEAs on critical components. Since the normal force on the cam bearing are calculated, normal force can be calculated from the SVAJ curve in the to find the maximum load. In addition, the spring load on the rocker arms are known, the friction coefficient for the journal bearings can be calculated from the equations.

$$\mu_k = \frac{-I\alpha}{rN}$$

The maximum coefficient of friction can be found as .03, and after rearranging the formula to find the force that was needed to shift the cam, equation below is needed.

$$Fc = N \times \mu_k$$

Solving this, we find that the force needed to surpass the force of friction is 1221.84 newtons at 9000 rpm. The shaft of the linear actuator needs to be able to withstand the side force from the camshaft. The thread which the linear actuator engages to has an angle of 14.96 degrees. The force from actuation on the linear actuator is calculated from:

$$F = Fc/cos(14.96\ degrees)$$

The maximum force is calculated to be 1636N at the contacting tip of the linear actuator.

Additionally the shifting window can be found by taking the rotational speed of the cam at redline and finding how long it takes for the cam to rotate 30 degrees (the window in which the shaft needs to engage). This comes out to .5 ms. Knowing the necessary travel for the shifter is 1 mm, dividing the distance by the time gets us a necessary shaft speed of 1.8 m/s

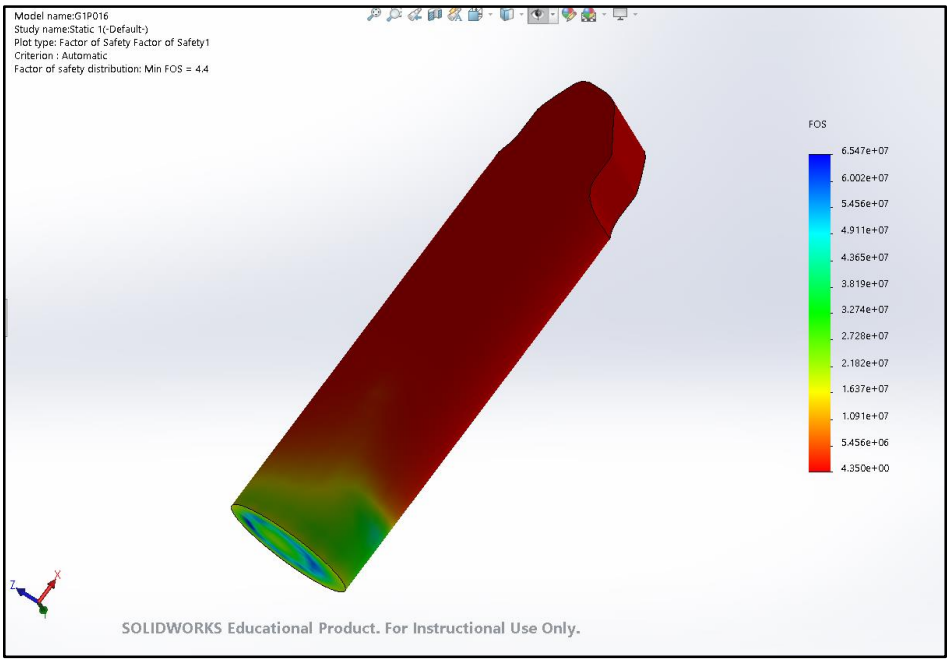

Figure 8.51: FEA FOS Plot for DVVL Shaft

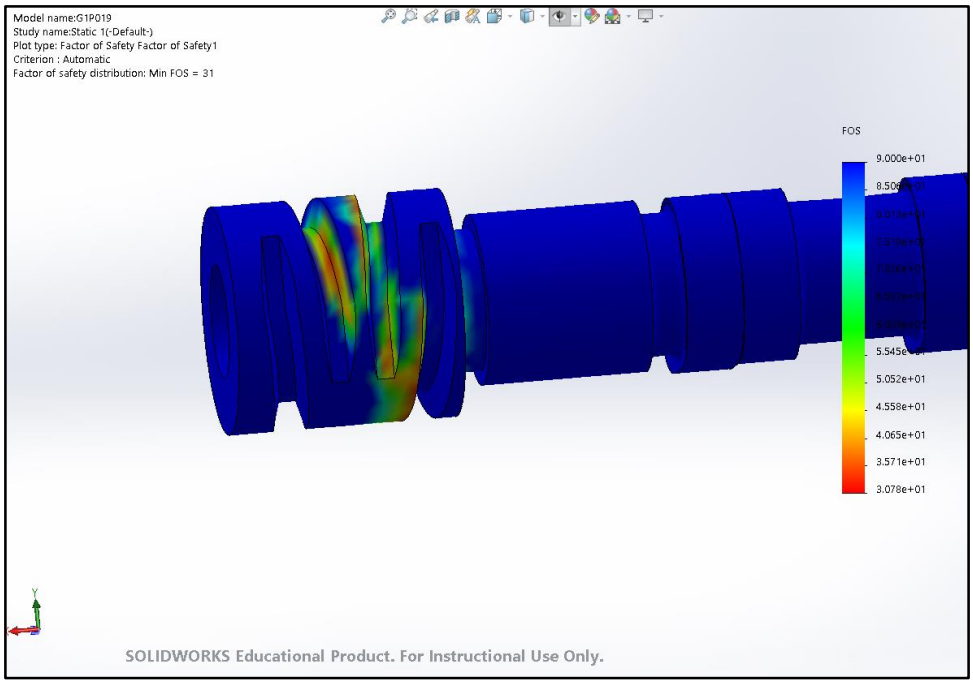

Figure 8.52: FEA FOS Plot for DVVL Cylindrical CAM

The minimum factor of safety on the DVVL components is 4.4 under maximum load. The load applied is on the tip of the linear actuator shaft, with the fixed geometry partially on where the shaft is still held in the housing of the linear actuator.

8.8.3.3 - Component Selection

For our linear actuator, we selected a compact 12V Morai Nexus with one centimeter of shaft travel. it can exert 25 N of axial force and has a travel speed of 2 m/sec, greater than is necessary.

8.9 - Covers

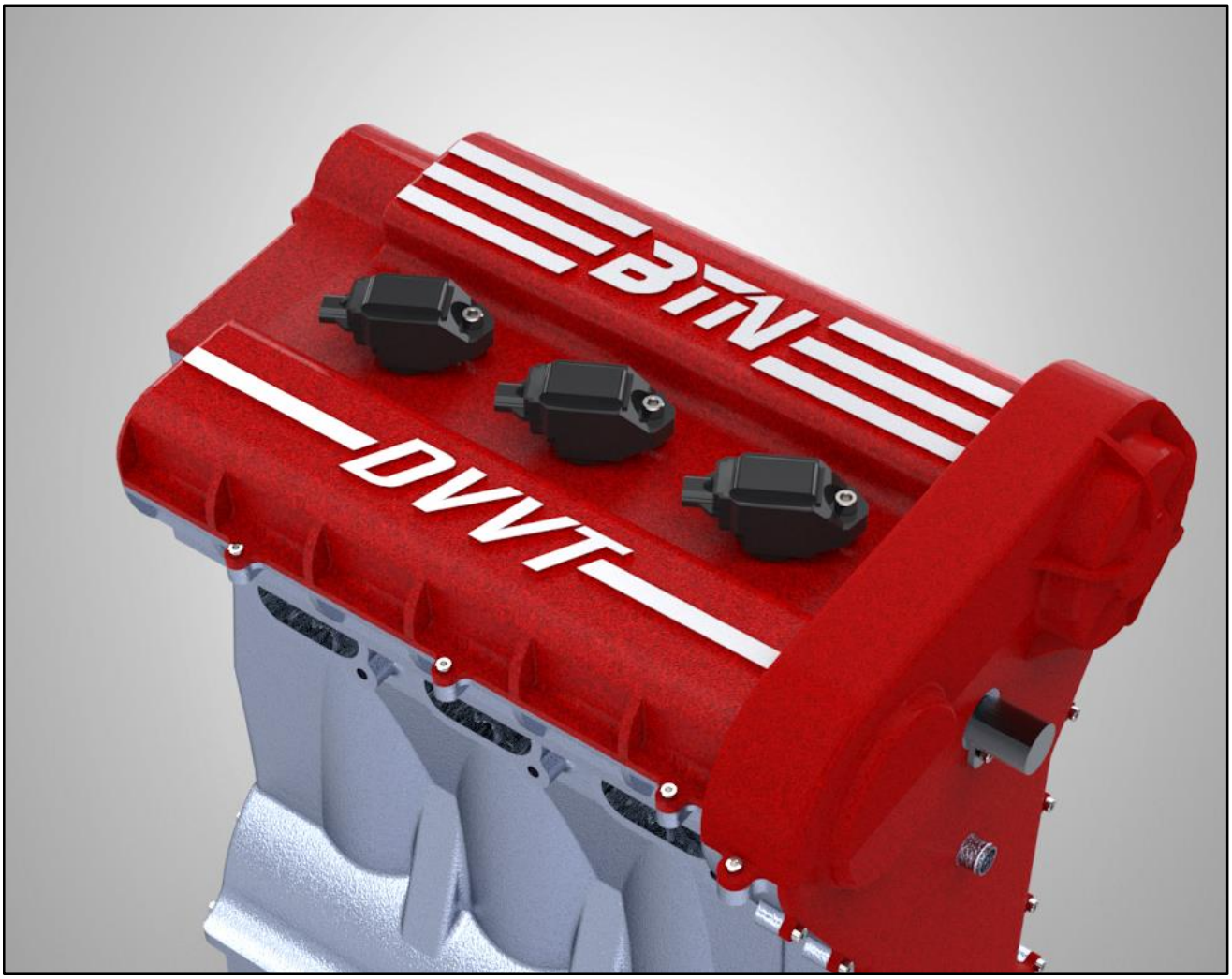

Figure 8.53: Render of Assembled Covers

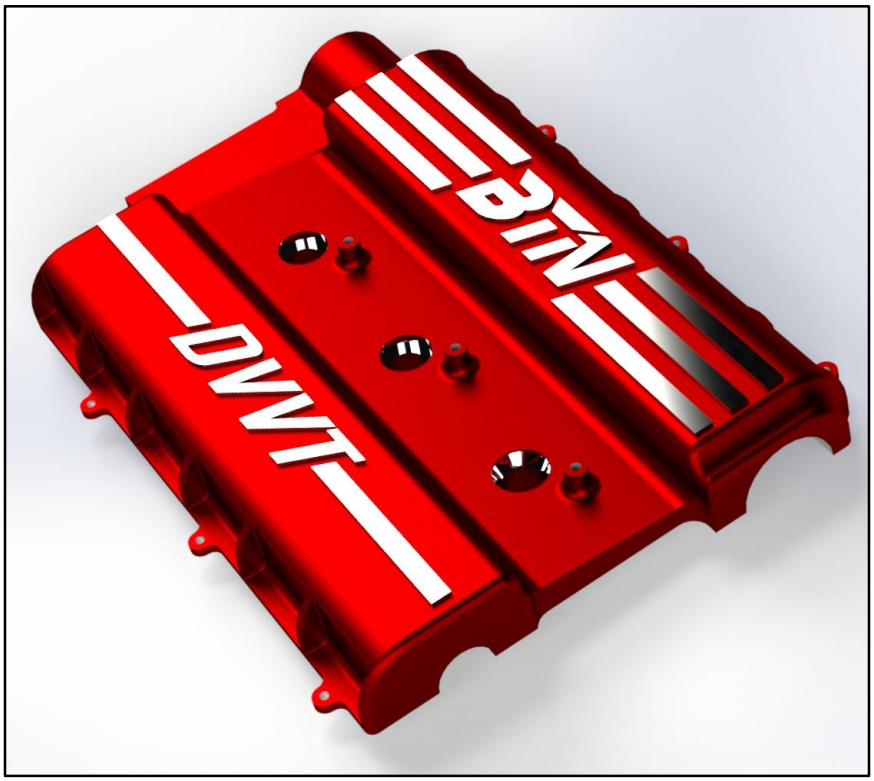

Figure 8.54: Valve Cover Top View Render

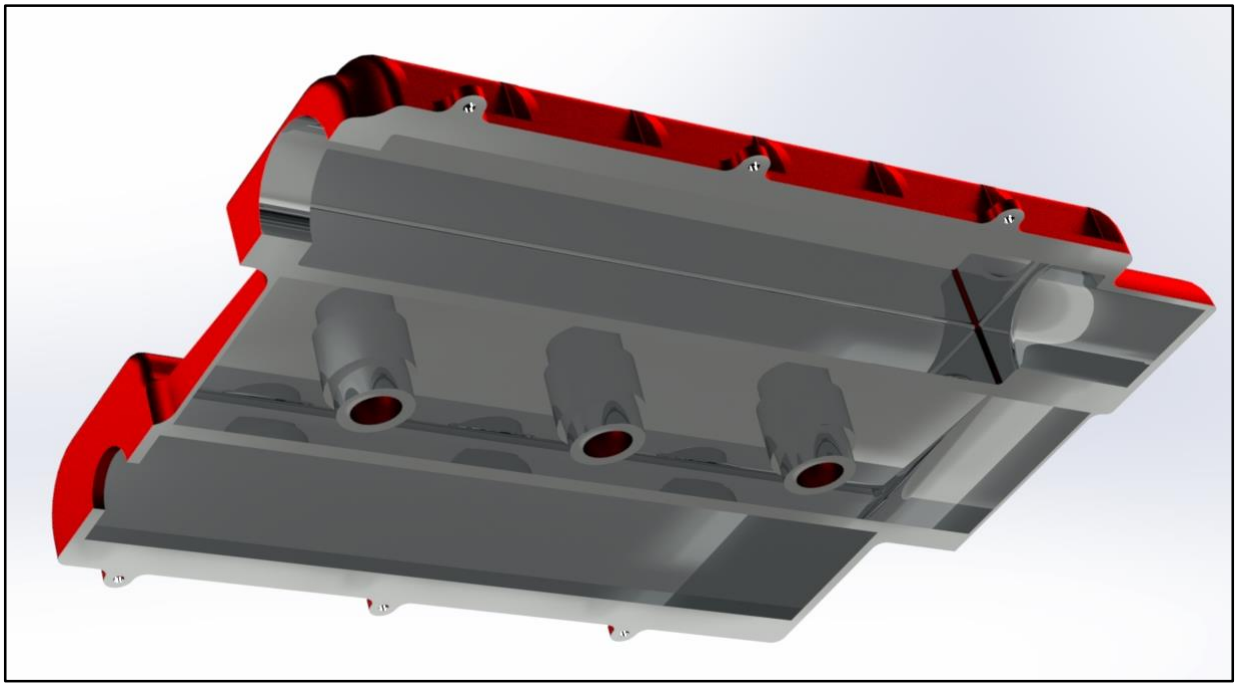

Figure 8.55: Valve Cover Bottom View Render

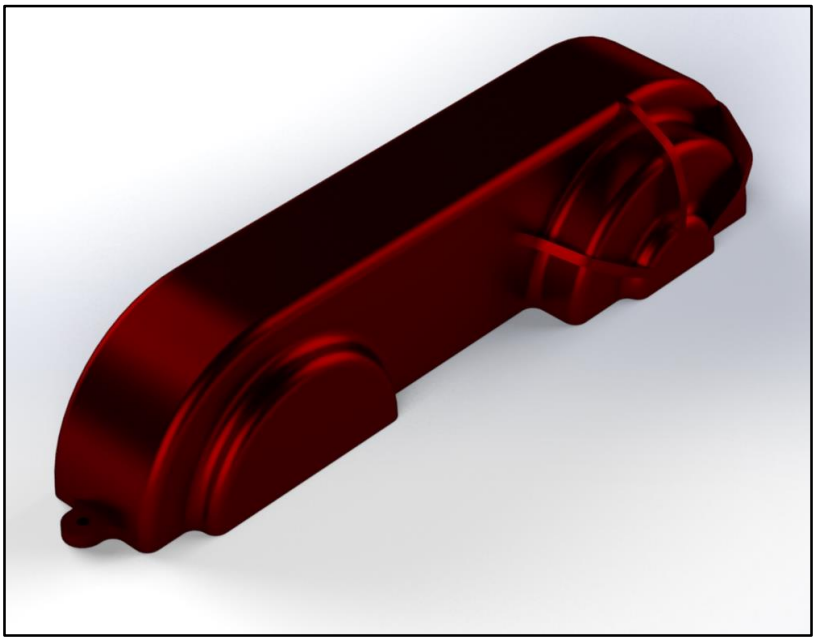

Figure 8.56: Sprocket Cover Render

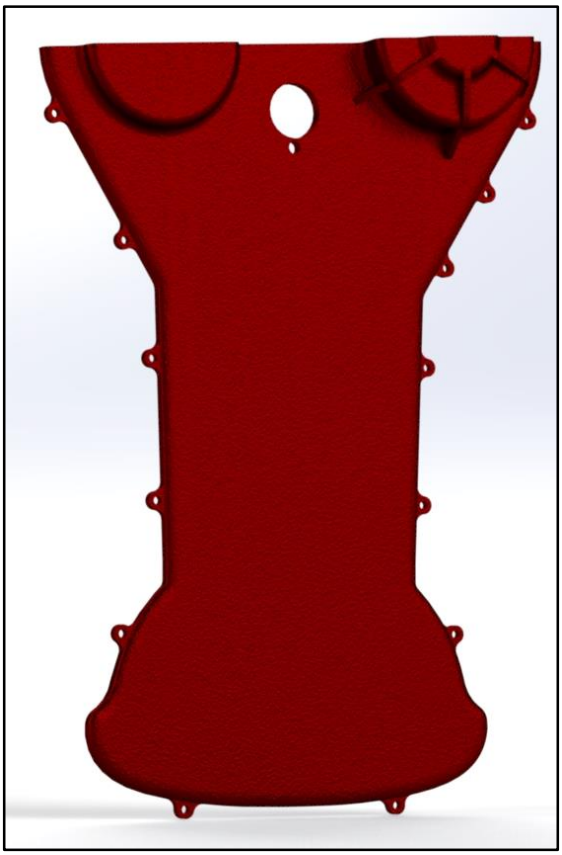

Figure 8.57: Timing Cover Render

8.9.1 - Overview

The covers serve to protect the cylinder head sub assembly and timing system. Also, they serve to make the engine more aesthetically pleasing. The valve cover protects the camshafts and valvetrain from outside debris while also retaining oil splashed out from the cam bearing. The sprocket cover protects the tops of the timing sprockets from debris, while the timing cover protects the timing chain and crank sprocket.

8.9.2 - Materials and Manufacturing

The covers are die cast out of aluminum A356 and post machined for critical surfaces. A356 was selected for its excellent castability and thermal conductivity. All the covers are powder coated in red to give the engine a unique sporty look. The racing stripes on the top of the valve cover are machined and polished to make the engine stand out.

8.9.3 - Design Considerations

The design of the covers are focused around their aesthetic, accessibility, and compatibility. Performance is a priority for BTN, and the scarlet red colored covers perfectly demonstrate BTN’s passion for motorsports. The covers are inspired by italian motorsports legend MV Agusta, who has been engineering motorcycle art since 1945. The beauty of the engine evokes powerful emotions and shows our passion for riding. The logo on the cover always remind the owners that the BTN 1500-E is something truly special. The three covers give the owners and the mechanics easy access to every part of the cylinder head from cam to sprockets. Finally, the covers have to be able to provide the structural support for the DVVL bearings. Therefore, a thrust bearing contacting surface was post machined for the DVVL thrust bearings. Overall, the valve covers make the engine aesthetically pleasing and functional at the same time.

8.10.1 - Camshaft Timing

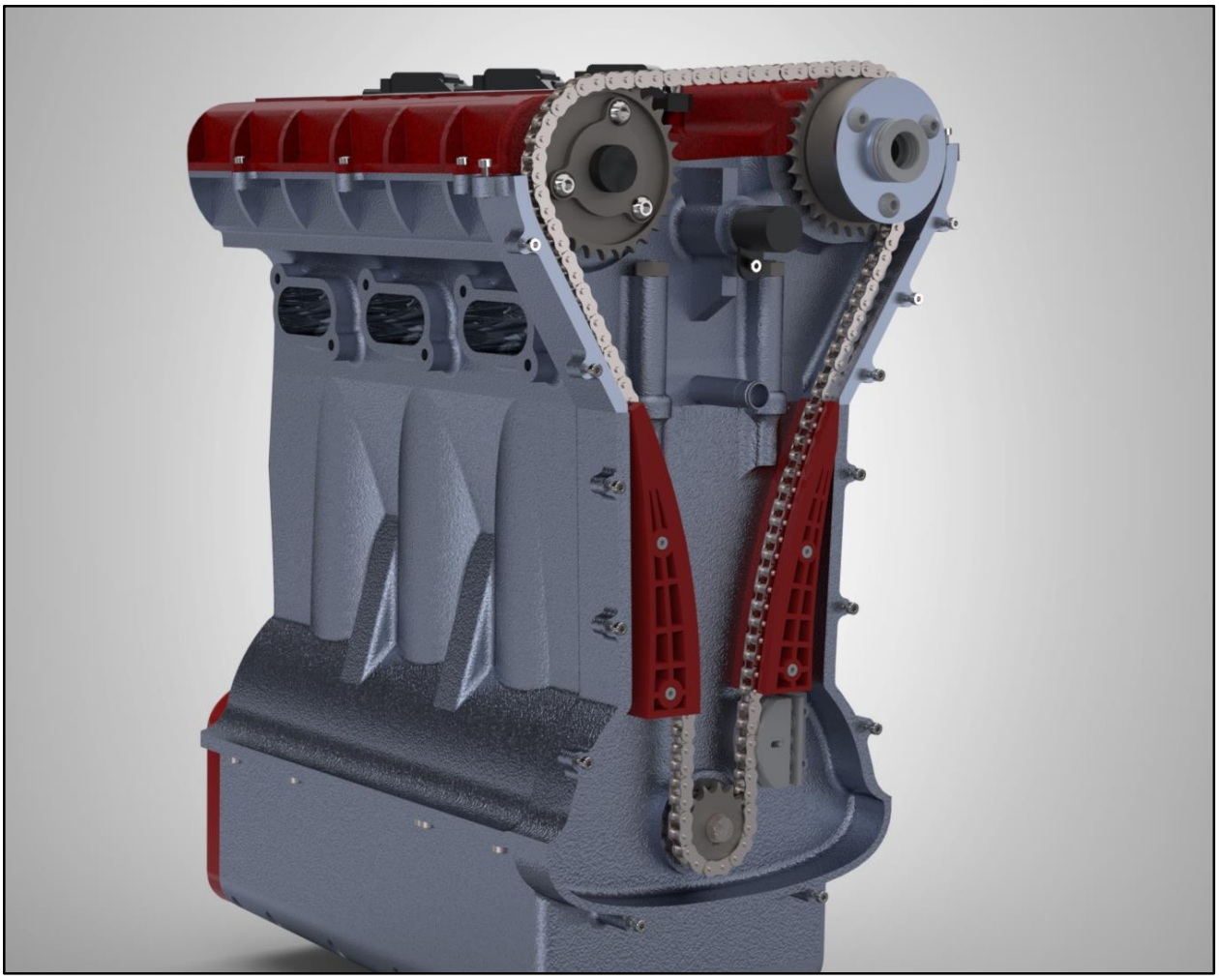

Figure 8.58: Render of Camshaft Timing system

8.10.1.1 - Overview

The timing system for the camshafts serves to ensure that the cams start at the correct phase with regard to the crankshaft. Without accurate timing, the combustion cycle of our engine would not function correctly.

8.10.1.2 - Design Considerations

The first and most major design decision for the balance shaft timing was whether we wanted a timing belt or chain. The pugh chart for this decision can be found below in Table 8.59.

Characteristic	Weight	Belt Driven	Chain Driven	Gear Driven

Maintenance	0.25	5	9	7
Cost	0.25	8	7	4
Service Interval	0.25	4	7	8
Performance	0.25	5	8	7
Total	1	5.5	7.75	6.5

Table 8.59: Pugh Chart for Cam Driving Method

As can be seen from our pugh chart, we decided to use a chain given its high strength and low maintenance interval and cost. The next design decision was what the pitch diameter our sprockets needed to be. Wanting this to be the greatest to reduce the force on the chain, the biggest our design would allow was 100 mm on the cam (D_1) and 50 mm (D_2) on the crank

8.10.1.3 - Calculations

To determine what size chain and sprocket we needed, it was first necessary to find the power required to drive the camshafts. From section 8.5.4, we have that the maximum force (F) needed to drive the intake and exhaust springs are 1215 N and 935 N, respectively. Knowing that their respective lifts (D) are 11 mm and 8.5 mm and that the maximum rotational speed of the camshaft (N) is 4500 rpm, we can use the equation below to find the maximum power (P).

$$P = F * D * N * (\pi/30)$$

For the intake cam this comes out to 6.30 kW, while the exhaust cam comes out to 3.74 Kw. This comes out to a total of 10.4 kW at redline (P_t). To calculate the corresponding force on the chain at the crank sprocket, where it would be a maximum, we then needed to convert that power to a force (F_c) using the equation below

$$F_c = P_t/(N * (\pi/30) * (D_2/2))$$

This came out to 852.5 N for the chain at the crank sprocket.

8.10.1.4 - Component Selection

The first step in this process was to select our chain, aiming to minimize mass and size. The smallest commercially viable chain we could find was metric 06B chain, rated for a maximum working load of 1757.05 N [21]. This gives us a FOS of 2.06, which, while low, assumes that all of the force is concentrated on one link. In practice, where multiple links share the load at the same time, this would be much higher. But it is reassuring to know that, however unlikely, one link could handle all of the load without failing. This chain size corresponds to a crankshaft

sprocket of 15 teeth and camshaft sprockets of 30 teeth. These sprockets and the required tensioner will be bought from external suppliers. We also designed chain guides to keep the chain centered and to provide the maximum engagement possible for the sprockets.

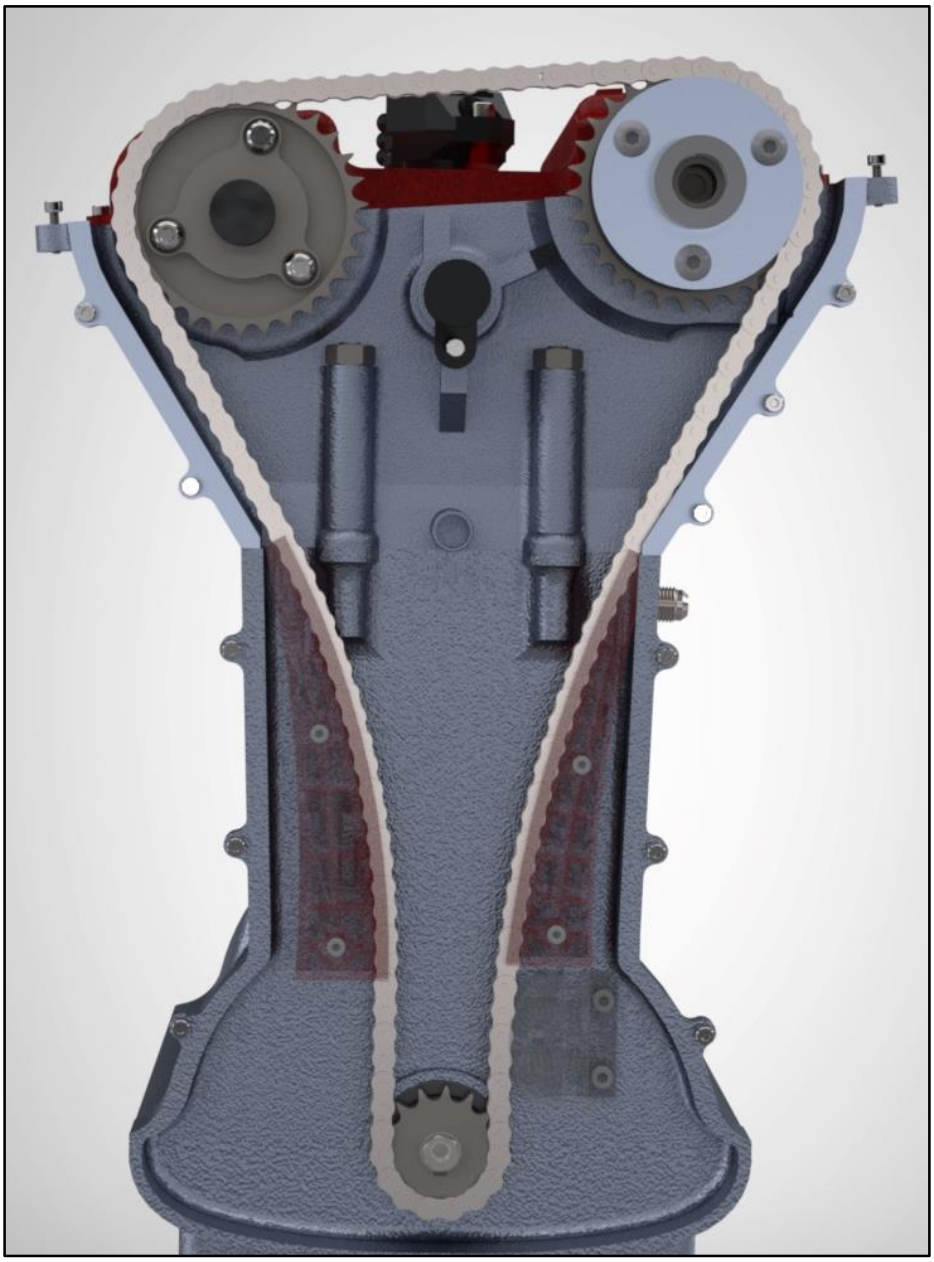

Figure 8.60: Render of Chain Path

8.11 - Other Purchased Parts

8.11.1 - Spark Plugs

8.11.1.1 - Overview

Spark plugs serve to allow the engine to create power. When high-voltage electricity is applied to the spark plug, an electric arc jumps over a specified gap between the two electrodes. This arc ignites the fuel-air mixture in the combustion chamber at the end of the compression stroke, starting the power stroke.

8.11.1.2 - Design Considerations

The major decision decisions for our spark plugs involved the material and construction. For the material, there are a wide variety of electrode materials out there which trade-off combustion efficiency for cost and reliability. As our engine is designed to be highly efficient and reliable at the expense of cost, the only logical choice was a double-iridium electrode construction, which has excellent efficiency and reliability. The other choice we had to make was whether we wanted a “cold” or “hot” spark plug. Spark plug temperature is a measure of how well the spark plug retains heat, and is based on the amount of thermal insulation present. “Hot” spark plugs are best for lower combustion pressure engines which generate less heat per cycle, while “cold” spark plugs are best for high combustion pressure engines which generate more heat per cycle [14]. As our engine has no forced induction and a relatively low compression ratio, we decided to use a “hot” spark plug.

8.11.1.3 - Component selection

Based on our previously stated design criteria, we decided to use the NGK MAR10A-J spark plug. This is a double-iridium “hot” spark plug made by a very reputable manufacturer and has shown previous success in motorcycle applications. At an estimated $5/each in bulk, this a reliable and cost effective choice for our engine [22].

Figure 8.61: Image of NGK MAR10A-J

8.11.2 - Injectors

8.11.2.1 - Overview

As our engine utilizes port fuel injection, we require fuel injectors to enable fuel to be inserted into the cylinders. These injectors are electrically actuated and disperse a specific volumetric flow rate of gasoline into the intake runners..

8.11.2.2 - Design Considerations

Our main design decision was whether we wanted to use port or direct injection. The pugh chart for this decision can be found below in Table 8.2.

Characteristics	Weight (0-1)	Direct	Port
Complexity	0.5	2	7
Cost	0.3	3	6
Performance	0.1	8	6
Efficiency	0.1	8	6
Total	1	3.5	6.5

Table 8.2: Injection Style Pugh Chart

As can be seen, we decided to go with port injection over direct injection due to its significantly smaller cost and complexity.

8.11.2.3 - Calculations

To size our injectors, we needed to know at what volumetric flow rate they needed to function at. From our thermodynamic analysis, we determined that the max mass flow of gasoline into our engine was 2.95e-3 ks/s ($\dot{m}$). Using the equation below, we were able to find the corresponding volumetric flow rate (Q), where $\rho = 748.9\ kg/m^3$ is the density of gasoline.

$$Q = \dot{m} * \rho$$

This equation gives Q to be $3.9x10^{-6}\ m^3/s$. Metric injectors are sized by cc/min, so converting gives us Q = 235.4 cc/min. However, this would mean that our injectors would have to run at 100% duty cycle, which isn't recommended for most engines. You typically want to have your injectors run at a predicted max duty cycle of 80% to allow for unexpected richer conditions [15]. Knowing this, we divide Q by .8 to get a final injector sizing of at least 294.25 cc/min

8.11.2.4 - Component Selection

For component selection our goal was to find a reputable, widely available component that met our previously determined specifications. In line with this, we have decided on the Bosch 0280158130 fuel injector for our engine. This injector is rated for 296.2 cc/min, above our performance specifications, and features a 10 hole nozzle for improved fuel dispersion. Available at an estimated $10/each in bulk, this a reliable, cost effective choice for our engine [23].

Figure 8.62: Image of Bosch 0280158130 Fuel Injector

9 - Assembly and Test

9.1 - Overview

The engine is assembled first in multiple subassemblies which may be worked on simultaneously. Following these assemblies, the main portions of the engine may be joined together at which point testing of the full engine will be performed.

9.2 - Quality Assurance

For our scale of production, quality assurance will mean testing the first few parts after each individual machining process has been performed. Once the process has been determined to give acceptable tolerances, tests will only be performed on between .5% and .1% of parts. Hardness tests will be performed on 1 in 500 each of the connection rod and crankshaft. As the balance shaft is less critical, such testing will only be performed on 1 in 1000 of these parts. X-raying to identify problematic cracks will also be conducted on a number of critically parts: 1 in 500 of each of the block, piston, and cylinder head, and a slightly lower ratio of 1 in 1000 for the less critical oil pan and balance shaft girdle.

Certain components will require more unique testing. The clearances in the main and rod journal bearings are critical for the proper lubrication and operation of the engine. One in 500 of each of these will be tested with a process-specific bearing clearance go/no-go gauge. Piston rings also require a unique process. Each compression ring will be placed into the bore without the piston and squared with a ring-squaring tool. A feeler gauge will then be used to check the ring gap. Due to their importance, this will be performed on 1 in 200 rings.

Finally, a simple visual inspection will be performed on every part before installation.

9.3 - Piston Assembly

The first subassembly that can be worked on is the piston subassembly. There are three of these that can be done in parallel in order to speed up assembly with an adequate number of workers. For each, the steps are as follows:

1. Mark the locations at which the ring gaps should fall on the piston using a marker in order to ensure that proper orientation is achieved
2. Get the oil control ring and split it into its three component rings: the expander ring and the two side rail rings
3. Lightly coat the expander ring in engine oil and work it past the compression ring grooves into the bottommost, larger ring land groove
4. Ensure that the ends of the expander ring are touching but not overlapping and adjust as necessary to reach this state
5. Put oil on the first side rail ring and work it over the compression ring grooves and onto the step of the expander ring
6. Be sure the end gap lines up appropriately with the mark on the piston
7. Repeat with the other side rail ring
8. Ensure that the oil control ring can move freely in its groove. If it cannot, take it out, wipe it off and try again
9. Next, the second compression ring will be installed. Get it out, ensure it is clean, and lightly coat it in engine oil
10. Use a piston ring expander to expand the ring enough to work it over the first ring land and into the second one
11. Ensure that the ring gap lines up with the marking made on the piston
12. Repeat this for the primary compression ring
13. Insert feeler gauges between the top each ring and its corresponding land surface in order to verify the clearance
14. If clearance is inadequate, remove piston rings and carefully measure the ring and the land. If the land is not of appropriate size, the piston must be remachined. If the ring is the problem, try a different ring

15. At this point, the rest of the piston-rod assembly can be performed so gather a connecting rod, wrist pin, two wrist pin-piston bushings, one wrist pin-connecting rod bushing, and two retaining rings
16. Press the bushings into the piston
17. Press the bushing into the rod
18. Put the first retaining ring onto the wrist pin using retaining ring pliers and slide it into the first bushing
19. Line the connecting rod and bushing up with the wrist pin and continue to push the wrist pin through that and the bushing on the opposite side of the piston
20. Use retaining ring pliers to place the second retaining ring on the second groove
21. Press the rod bearing into the top of the connecting rod and coat with oil

9.4 - Bottom End Assembly

Following the build of three of these piston-rod subassemblies, the assembly into the engine block may be completed as follows:

1. Place the main bearings into the engine block
2. Lightly coat the faces of the bearing in engine oil
3. Line the cylinders with engine oil
4. Drop the piston assemblies down into the cylinders through the top of the engine block
5. Place the crankshaft on top of the bearings
6. Press the bearings into the main caps and coat with oil
7. Press the dowels into the block and put the main caps on
8. Put the bolts in and torque to the required specification of 89 N-m
9. Check the bearing clearances
10. Rotate the crankshaft around and line it up with the first connecting rod
11. Press the bearing into the bottom of the connecting rod and coat with oil
12. Press dowels into bottom of connecting rod
13. Put the bottom of the connecting rod on
14. Put in bolts and nuts and torque to the required specification of 46 N-m
15. Repeat to attach the other two connecting rods to the crankshaft
16. Coat the upper oil pan with silicone sealant on its upper mating face and fasten to the engine block

At this point balance shaft assembly is needed:

1. Attach the rear mass to the balance shaft with screws
2. Push the balance shaft with one retaining ring through the girdle and put on the second retaining ring when it is fully inserted
3. Put the key into the balance shaft

4. Slide the shaft seals on to the balance shaft and idler shafts
5. Line the balance shaft up with the balance shaft sprocket and bolt down to a torque specification of 70 Nm
6. Screw down the idler pulleys

Continuing with bottom end assembly:

17. Attach the balance shaft assembly to the engine block
18. Coat the bottom mating surface of the top oil pan in silicone sealant
19. Attach the top section of the oil pan on
20. Attach the balance shaft timing sprocket to the crankshaft
21. Put the bolt in it and torque down to 70 Nm
22. Time it correctly as per Figure 9.1 below, lining up the yellow marks
23. Put the chain
24. Attach the guide and the tensioner
25. Release the tensioner to apply tension to the belt
26. Attach the front weight to the balance shaft with screws
27. Put on cover

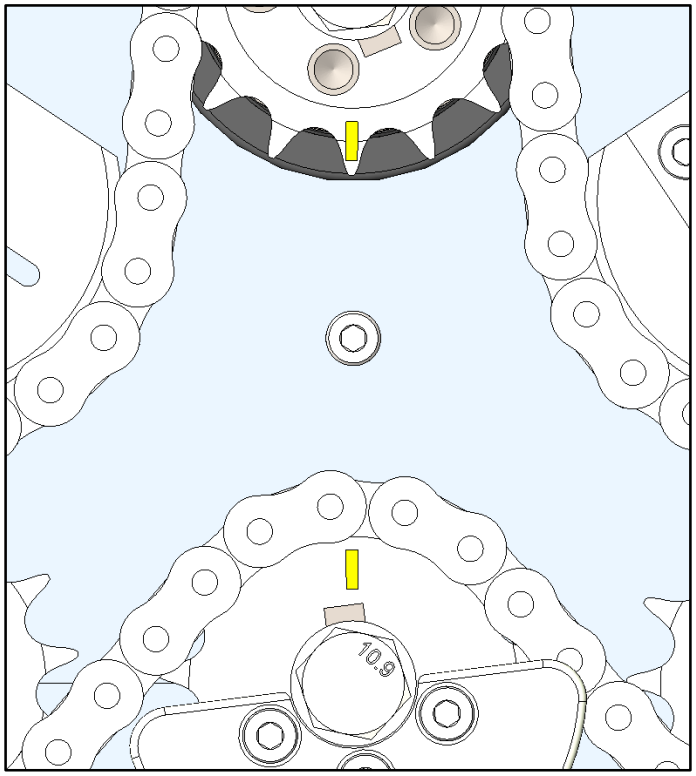

Figure 9.1: Illustration of Proper Balance Shaft timing

9.5 - Top End Assembly

At the same time as the bottom end assembly is taking place, the cylinder head can also be assembled. It is expected that the variable valve timing sprockets would be pre-assembled by their vendor. While this assembly will only involve one worker, another can help with support processes including assembly of the cams with the variable valve timing mechanisms. The steps in this assembly are as follows:

1. Put all seals inside and all the shifting mechanisms
2. Press in valve seats
3. Press in valve guides
4. Measure spring and use spring tensioner to get right installed length
5. Drop in valves
6. Check spring installed length
7. Put valves in
8. Locate where valve sits
9. Install valve stem seals
10. Install retainers
11. Use spring compressor to compress the springs
12. Put keepers in at correct height
13. Remove the spring compressor
14. Repeat for all intake and exhaust valves
15. Slip rocker arms onto shaft
16. Put shaft down onto lands
17. Put caps on
18. Put in bolts and torque to 25 Nm
19. Assemble sprocket and exhaust cam (can happen concurrently with previous steps)
20. Drop in camshafts
21. Put the shaft seals on
22. Put on the caps for the camshafts
23. Put in bolts and torque to required specification of 30 Nm
24. Screw sprockets on
25. Put linear actuators in
26. Put the side cover on
27. Put on valve cover after coating with RTV
28. Put chain on
29. Time it correctly as per Figure 9.2 below, aligning the yellow marks with the main axis of the oil solenoid
30. Put on the lower cylinder head timing cover
31. Put on the upper timing cover

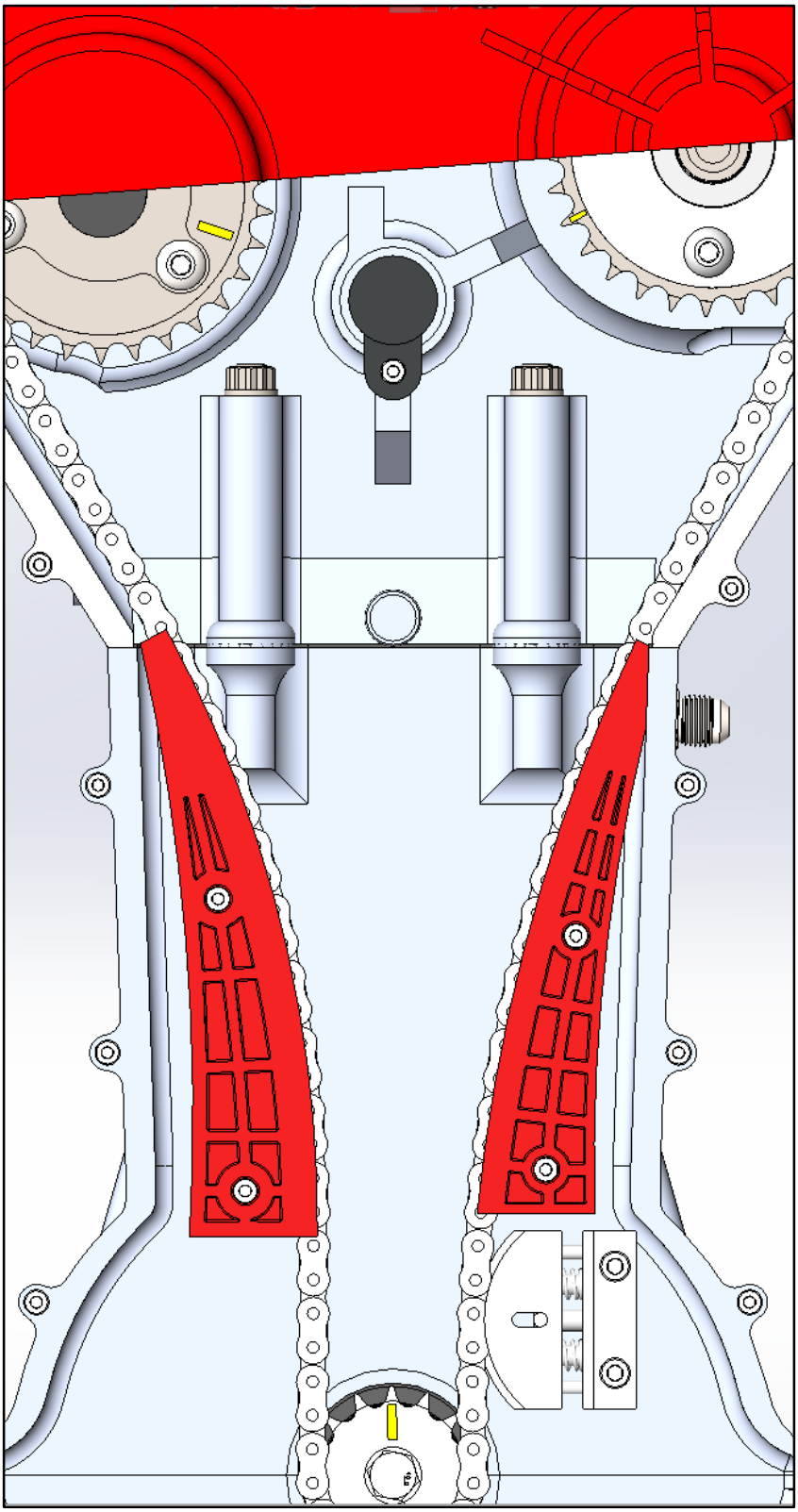

Figure 9.2: Illustration of Proper Camshaft Timing

9.6 - Final Assembly

At this point, the short block and cylinder head can then be assembled together in line with the following steps:

1. Put the tensioning and timing cover on the shortblock
2. Put the head gasket on
3. Put the cylinder head on top
4. Line it all up with the alignment dowels
5. Put the 4 head bolts and 4 studs into their positions
6. Torque the bolts to a specification of 89 N-m
7. Torque the studs to a specification of 89 N-m
8. Torque the nuts to the studs to a specification of 89 N-m
9. Drop the spark plugs in
10. Put the intake manifold gasket on
11. Put the intake manifold on
12. Put the exhaust manifold gasket on
13. Put the exhaust manifold on
14. Fill with oil
15. Fill with coolant
16. Put fuel rail in
17. Connect to fuel tank
18. Connect to cooling system
19. Connect to lubrication system
20. Bleed the coolant
21. Turn it on

9.7 - Test

Once our engine is assembled, every engine will then run at 5000 rpm for 1 hour. This test will verify that our engine works correctly and all components are correctly aligned. Additionally, we will perform destructive testing on every 5 out of 1000 of our engines to verify the long term integrity of our engine. These include:

- Running at redline until failure - needs to run at least 96 hours
- Starting up in an extremely cold and extremely hot environment - will be tested at -20 °C and 60 °C
- Running at 5000 rpm while continuously removing oil - should run with at least .5 quarts of oil in the pan

- Run with an increasing amount of vibration - entire engine will be put on a shaker table and a vibration sweep will be conducted from 20Hz to 1600Hz or until expected failure around 120Hz
- Running with continuous water ingress - needs to run with at least 20 ml/s of continuous water ingress

10 - Theory of Operations

10.1 - Combustion Cycle

The 4-stroke cycle of our combustion engine is depicted in the Figure below. The cycle consists of four phases: intake stroke, compression stroke, power stroke and exhaust stroke.

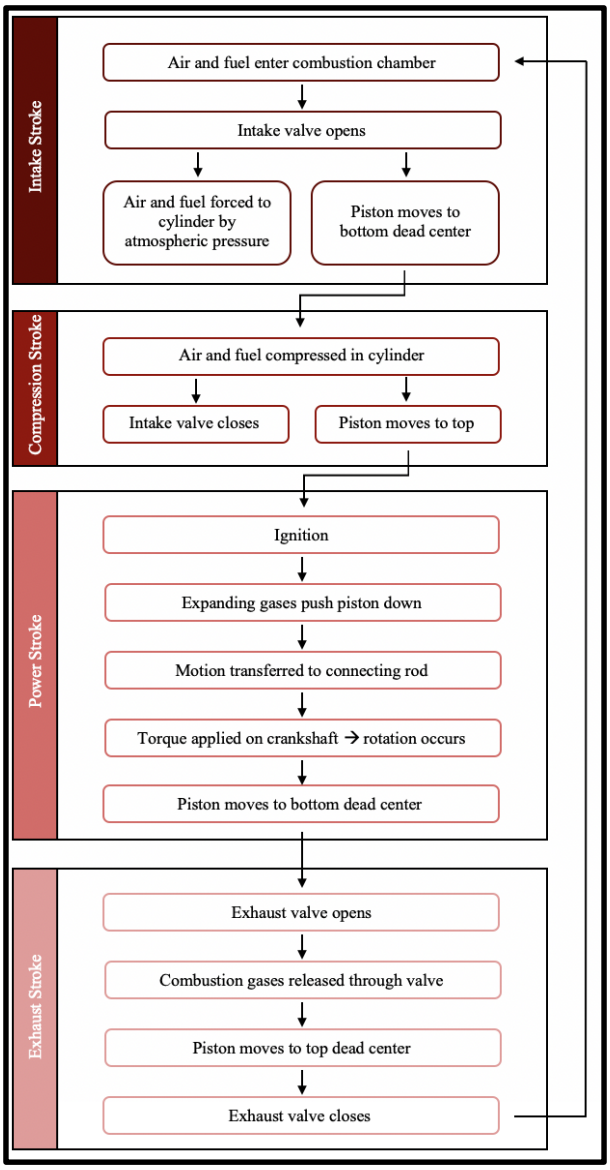

Figure 10.1: Combustion Cycle Diagram

10.1.1 - Intake Stroke

The cycle begins with a mixture of air and fuel entering the combustion chamber. At this point the intake valve opens, allowing atmospheric pressure to push the air and fuel into the cylinder. Meanwhile, the piston moves downward to the bottom dead center.

10.1.2 - Compression Stroke

During the compression stroke, air and fuel are compressed in the cylinder by the upward motion of the piston. The air and fuel are compressed to our desired compression ratio of 10:1.

10.1.3 - Power Stroke

Next, the spark plug ignites the air and fuel mixture. The hot, expanding gases push the piston down, transferring motion to the connecting rod, which exerts a torque on the crankshaft and causes rotation.

10.1.4 - Exhaust Stroke

Finally, the exhaust valve opens and expels the combustion gases. The piston moves back to top dead center and the exhaust valve closes. From here, the intake valve opens and the cycle begins again.

10.2 - Cooling

The engine block has cooling channels through which coolant can flow and reduce the temperature of the engine, as shown below.

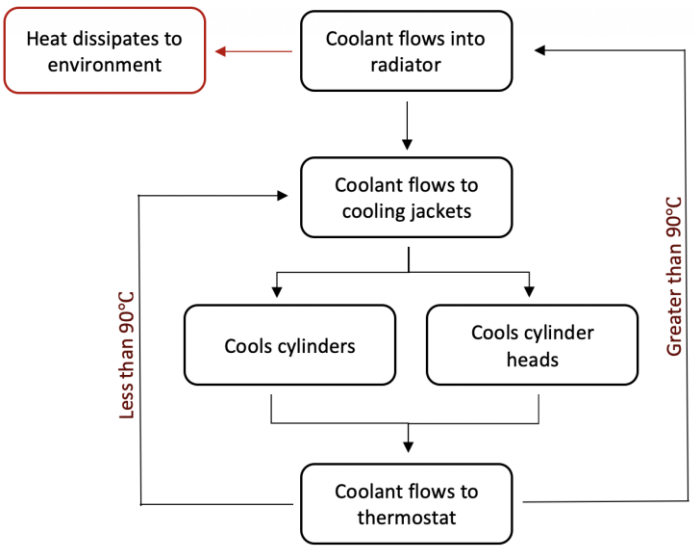

Figure 10.2: Cooling System Diagram

During the combustion process the engine heats up so cooling needs to be considered in order to keep the engine at a temperature at which it can operate. The goal was to keep the outside of the engine below 40 °C in order to avoid burning the rider. There is a thermostat inside the cooling channels in order to regulate the temperature of the engine. The coolant we chose is a 50/50 mix of Ethylene Glycol and water since it has a low freezing point and high boiling point. The coolant is pushed through the cooling channels by use of a pump.

10.3 - Lubrication

The engine utilizes wet sump storage, meaning there is a large oil pan underneath the crankshaft which collects oil. Lubrication channels are incorporated throughout the engine in order to keep all components well lubricated and running smoothly. The oil is circulated through the channels using a pump. The lubricant being used is 10W-40 due to its good performance during both start-up and operation. The lubricant circulates through the engine as depicted below:

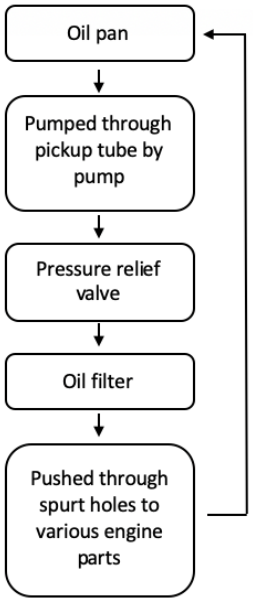

Figure 10.3: Lubrication Diagram

The lubrication channels throughout the block and head are shown in the following renderings:

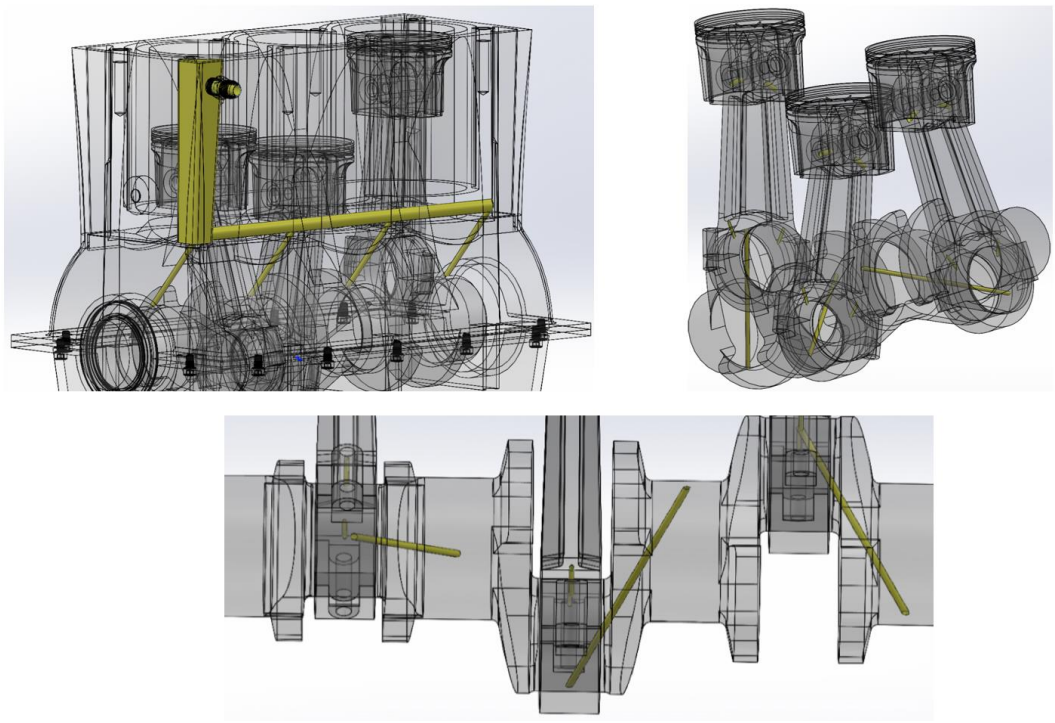

Figure 10.4: Illustration of Lubrication Channels

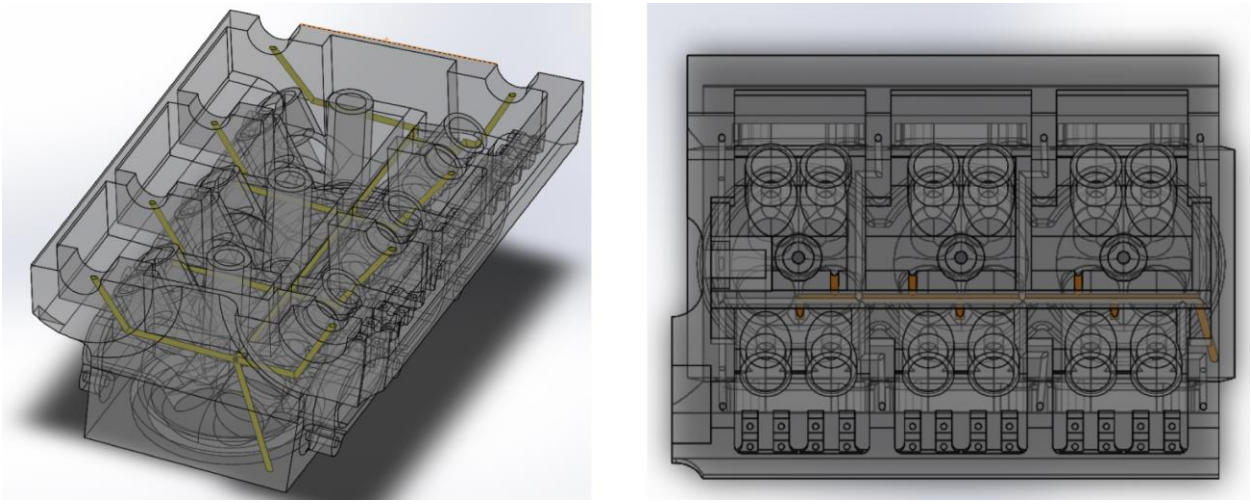

Figure 10.5: Lubrication Channels

10.4 - Noise

While the design as it stands does not give the full picture of noise, initial calculations and estimations were made based on what we have. Some vibrations are determinate with the extent of design that we have, but the main acoustic propagators will be based on the engine mounting as well as intake and exhaust manifolds which were determined out of scope. The

likely largest propagators for the surface vibrations are 41, 124, and 165Hz based on the RPMs at cruise and natural frequencies of the engine block and cylinder head while the likely largest propagators through intake and exhaust manifolds sized similarly to market vehicles (~1200mm) are 191, 382, and 1528 Hz considering simple modal analysis. The actual sound pressure level is difficult to calculate due to the lack of information about engine mounting and the intake and exhaust systems, but using the Lighthill and Mohring analogies an estimated SPL of ~72dB at 50ft was calculated. This is not particularly helpful for determining the noise propagation of the entire motorcycle, or even the engine with its final positioning and mounting, and further analysis with known components or a physical engine prototype will be required to determine if a muffler is required. That said, considering that the noise limit we are aiming for is 78 dB, we should be able to meet the standard.

10.5 - Electronics

Although electronics and sensors are not within the scope of this project, a few considerations were made about how these components would work with the engine design. Below is a list of the sensors that will be required for the function of the engine:

Sensor	Location/Subsystem
Coolant sensor/Thermometer	Cooling system
Oxygen sensor	Exhaust
Manifold absolute pressure sensor	Intake
Throttle position sensor	Intake
Mass airflow sensor	Intake
Manifold air temperature sensor	Intake
Crankshaft position sensor	Crankshaft
Oil pressure sensor	Lubrication

Table 10.1: Electronics/Sensors

11 - FMEA

In order to anticipate any possible component failure, a Failure Mode and Effects Analysis was performed. The team considered each part and the ways in which it could fail. Based on this, the effects of failure, potential causes, and mode of detection were identified. We

rated the severity, occurrence, and ease of detection on a scale of one to five and then multiplied these numbers to get the RPN. Then recommended actions were considered and new RPNs were calculated based on these. Below are the top five failure modes. The full FMEA can be found in Appendix F.

Sub-system	Part Name	Failure Mode	Failure Effects	Potential Causes	Detection	S	O	D	RPN	Recom-mended Action	S	O	D	RPN
Crank-train	**Piston**	Cracking	Eventual failure	Fatigue	Undetect-able before failure	3	2	5	30	Use FEA	3	1	5	15
Engine Block	**Oil Pan**	Fractur-ing/ Cracking	Loss of Oil	Fatigue, thermal cycling	increased noise, engine seizure	4.5	2	3	27	Engine oil level sensor, thermal fea	4.5	1	1.5	6.75
Crank-train	**Crank-shaft**	Fracture	Engine Failure	Fatigue, Material Defects	Surface Inspection	5	2.5	2	25	Quality assurance in manufac-turing	5	1.5	1.5	11.25
Engine Block	**Coolant Channels**	Cracks	Engine over-heats	Thin walls, bad casting	Engine fails to operate	4	2	3	24	Use coolant temp & pressure sensors	2	2	1	4
Engine Block	**Oil Channels**	Lubri-cation leak	Loss of oil supply	Thin walls, bad casting	Loss of efficiency, more noise	4	1.5	3.5	21	Use oil pressure sensor	2	1.5	1.5	4.5

Table 11.1: Top Five FMEA Items

12 - Cost Estimates

12.1 - Overview

The costing of the engine was broken down into multiple sections. These sections were manufactured parts, purchased parts, part costing error, labor costs, defects, and profit. How each of these sections were calculated will be discussed. For each year after the first year, we reduced the part costing by 5% to account for larger batch sizes that reduce manufacturing and purchasing costs.

Cost	Year 1	Year 2	Year 3
Parts	$4,189.22	$3,979.76	$3,780.77
Estimate Error	$418.92	$397.98	$378.08
Labor	$293.33	$209.17	$197.33
Defects	$628.38	$596.96	$567.12
Estimated Cost	$5,529.86	$5,183.87	$4,923.30
Sale Price	$7,000.00	$7,000.00	$7,000.00
Profit per Engine	$1,470.14	$1,816.13	$2,076.70
% Profit	21.00%	25.94%	29.67%
Total Profit	$11,026,062.50	$21,793,615.00	$31,150,542.81

Table 12.1: Cost Estimate for the Engine

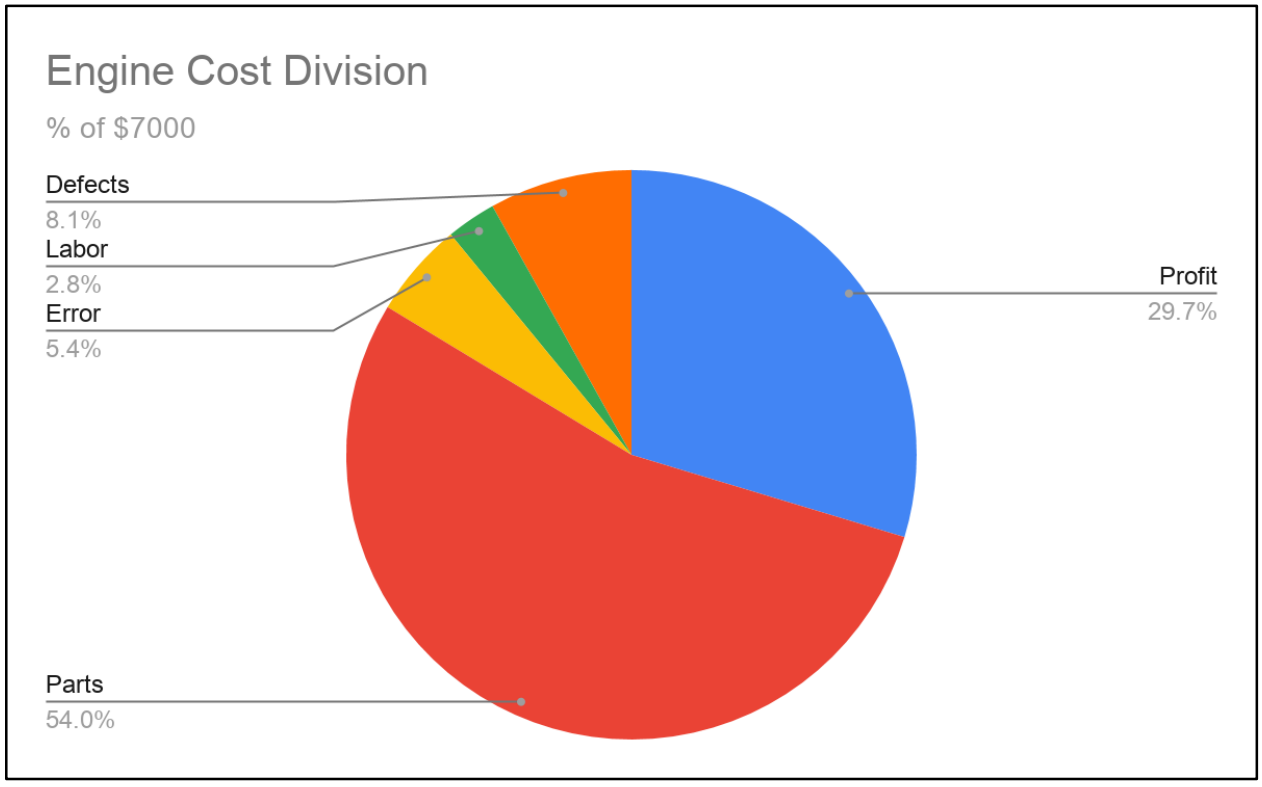

Figure 12.1: Cost Estimate Breakdown for Year 3

12.2 - Manufactured Parts

For manufactured parts, we utilized the part cost estimator built into CES EduPack. EduPack uses costing data gathered from a number of manufacturing sources to build its process costing library for the part cost estimator. The way the part cost estimator works is by selecting the material, primary, and optional secondary process, then by providing the mass, length, batch size, load factor, overhead rate, and capital pay off period, as well as what's needed for the secondary process. For most of the parts the secondary process was machining, so the needed variable was percent scrap, which was varied between 1-5% of the final mass. The final input that the part cost estimator needed was part complexity and for casting and forged part, whether the dies were standard or custom. Part complexity could be simple, standard, or complex. In order to keep things simple, complexity was kept at standard except for the engine block and cylinder head which were set to complex. Load factor is daily percage that the machines running the process are operating, this was kept at the preset amount.

Mass (kg)	Part-dependent
Length (m)	Part-dependent
Batch Size (units)	7500
Load Factor (%)	50
Overhead Rate (USD/hr)	600
Capital Write-off Time (yr)	3

Table 12.2: Input Variables for CES EduPack Part Cost Estimator

Below is an example of the costing results for engine block that are provided by the part cost estimator.

Source records
  Material = Aluminum, A356.0, sand cast, T6
  Primary Process = Green sand casting, automated
  Secondary Process = CNC machining

Component details
  Value of scrap material = 0 % of virgin price
  Part mass = 14 kg
  Part length = 0.4 m
Primary shaping process
  Load factor = 50 %
  Overhead rate = 600 USD/hr
  Capital write-off time = 3 years
  Availability = Custom form
  Part complexity = Complex
Secondary shaping process
  Amount of scrap = 5 % of material
  Part complexity = Standard
  Scrap recycled? = Yes
Additional attributes
  Tool life (units) - Primary process = 2.162e4
  Capital cost - Primary process = 5.499e4 USD
  Production rate (units) - Primary process = 49.52 /hr
  Material utilization fraction - Primary process = 0.8
  Tool life (units) - Secondary process = 180.1
  Capital cost - Secondary process = 7728 USD
  Production rate (units) - Secondary process = 9.007 /hr
  Material utilization fraction - Secondary process = 0.95
  Tooling cost per part - Primary process = 1.655 USD
  Tooling cost per part - Secondary process = 10.72 USD
  Overhead cost per part - Primary process = 12.2 USD
  Overhead cost per part - Secondary process = 66.68 USD

Figure 12.2: EduPack Part Cost Estimator Results

This process was repeated with all manufactured parts in the engine block and cylinder head. These costs are then adjusted by 10% to account for the errors in the inputs. A full breakdown of costing by part can be found in Appendix D.

Total Manufactured Parts Cost	$2,942.96
Total Engine Block Manufactured Parts Cost	$1,103.91
Total Cylinder Head Manufactured Parts Cost	$1,839.06

Table 12.3: Manufactured Parts Break Down

12.3 - Purchased Parts

Purchased parts costs were found through searching through OEMs for parts that would fit our specifications.

Total Purchased Parts Cost	$1290.58
Total Engine Block Purchased Parts Cost	$458.13
Total Cylinder Head Purchased Parts Cost	$210.68
Total Full Assembly Level Purchased Parts Cost	$621.77

Table 12.4: Purchase Parts Break Down

12.4 - Costing Error

We accounted for a 10% costing error on our purchased and manufacturing parts. This was to account for any cost in their costs that were overlooked. These costs could be changing taxes or fees on purchased parts or manufacturing process changes to manufactured parts.

12.5 - Labor Costing

For labor, we looked at the overarching categories of workers we would have to have as employees. We determined that we would need engineers, inspectors, machinists, and assembly floor workers. We did not account for support staff in our labor cost estimates. For each type of employee, we assumed 2000 hours of labor per year. That is based on the standard 40 hours a week and assuming they work and average 50 weeks in a year. For engineers, we went with a standard pay of $40/hr, for inspection $30/hr, machinist at $20/hr, and assembly at $25/hr. Over the three year period we are looking at, we reduce the number of engineers while increasing the number of inspection, machinist, and assembly. The increase in the employment of these types of employees are directly related to the increase in production size.

12.6 - Defects

Defects is for parts that are manufactured but fail to pass inspection or improper purchased parts. To account for this we added the cost of all parts multiplied by a factor of 15% factor. We assumed that this factor holds constant for each of the three years.

12.7 - Profit

For profit, we aimed for about 30% profit at the end of three three years. To reach this we set the final price at a value close to the 30% margin at year three. This final price is held constant across all three years. The final cost is at $7000 per engine.

13 - Project Review

At the start of the project the requirements for our engine design were carefully defined as described in the previous sections. Throughout the design process we have looked back to these requirements to ensure we were staying on track and within scope. Now that the project is completed, we have determined that all initial requirements have been met and the design should meet the customers approval.

In order to plan out the project, multiple project planning techniques were employed, including a task list, work breakdown structure, and Gantt chart. The task list provided an overview of all tasks that needed to be completed in order to finish the engine design. The list is shown in Table 13.1 below, broken into sections according to our design phases:

Project Planning	Team Charter, Task list / work breakdown structure, Responsibility Matrix, Gantt Chart, File storage scheme
Conceptual Design	Scope, Derived Requirements, Performance targets, Size, Weight, Market selection, Market research, High level design decisions, Product design specifications
Short Block Detailed Design	Piston rings, Piston skirt, Wrist pin, Lubrication, Connecting rod, Crankshaft, Block, Cylinder, Oil Pan, FEA
Cylinder Head Detailed Design	CFD, Intake valve, Exhaust valve, Combustion chamber shape, Head bolts, Head gasket, Camshaft, Belt vs chain drive, Valve Spring, Valve Retainer, Fuel injectors, Spark plug, Cam lobe interface, FEA
Final Analysis	Assembly Drawings, FMEA, CFD, Cost Estimate, Theory of operations, Thermodynamic analysis, Fuel efficiency, Emissions, DDR slide deck, Final Report

Table 13.1: Task List

The work breakdown structure ensured that all tasks were assigned to a person or subgroup. Dividing responsibility in this way helped to get all assignments done.

Task	Group
Project Planning	
Team Charter	All
Project Statement	TL / PM
Task List / Work Breakdown Structure	TL / PM
Responsibility Matrix	TL / PM
Gantt Chart	TL / PM
Scope	All
PPR Slide Deck	All
Conceptual Design	
Derived requirements	All
Market selection / research	Group 1
Social, Political, and Legal Requirements	Group 2
Trade Study	All
High level design decisions	All
Basic thermodynamic analysis	Thermo
CDR Slide Deck	TL / PM

Detailed Design	
Shortblock Design	Group 2
Cylinder Head Design	Group 1
Engine Block and Lubrication Design	Group 2
Thermodynamic Analysis	Thermo
Theory of operations	All
FMEA	Groups 1&2
Cost	Groups 1&2
Assembly Drawing	Groups 1&2
Slide Deck	All
Final product design specification	All
Final Report	All

Table 13.2: Work Breakdown Structure

The Gantt chart was aided in meeting all deadlines, both set by our group as well as the class. All tasks are listed as shown below, along with the weeks they needed to be completed by. The stars denote important deadlines or deliverables and float time was included for breaks.

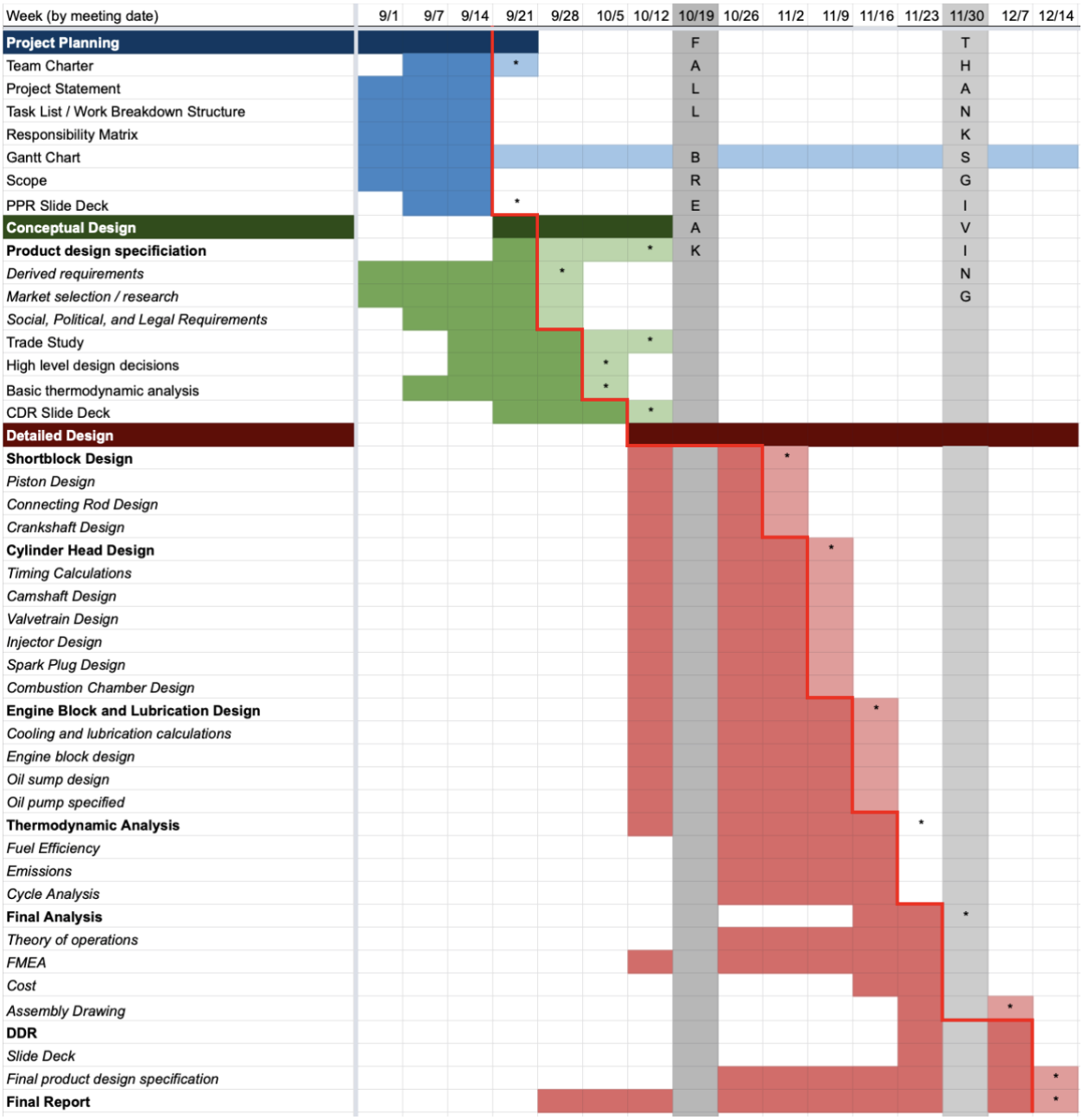

Table 13.3: Gantt Chart

14 - References

Use IEEE

[1] J. B. Heywood, *Internal Combustion Engine Fundamentals*. .

[2] “Fuels and Chemicals - Autoignition Temperatures,” Engineering ToolBox. [Online]. Available: https://www.engineeringtoolbox.com/fuels-ignition-temperatures-d_171.html. [Accessed: 11-Dec-2019].

[3]C. R. Ferguson and A. Kirkpatrick, *Internal Combustion Engines: Applied Thermosciences*, 3rd ed. Chichester, West Sussex, United Kingdom: John Wiley & Sons, Inc., 2016.

[4] Ribbens, William. *Understanding automotive electronics: an engineering perspective*. Butterworth-heinemann, 2017.

[5] R. Juvinall, *Machine Component Design.* Hoboken, NJ: John Wiley & Sons, 2017.

[6]Environmental Protection Agency (1977). *Subpart F—Emission Regulations for 1978 and Later New Motorcycles; Test Procedures*(40 CFR Ch. I (7–1–01 Edition)). Washington, D.C: U.S. G.P.O.

[7] A. D and A. A, “Effect of Variable Valve Timing to Reduce Specific Fuel Consumption in HD Diesel Engine,” *Journal of Applied Mechanical Engineering*, vol. 05, no. 06, 2016.

[8]Khudhur, Sabaa H., Adel M. Saleh, and Miqdam T. Chaichan. "The effect of variable valve timing on SIE performance and emissions." *International Journal of Scientific & Engineering Research* 6, no. 8 (2015): 173-179.

[9]“Ethylene Glycol Heat-Transfer Fluid,” *Engineering ToolBox*. [Online]. Available: https://www.engineeringtoolbox.com/ethylene-glycol-d_146.html. [Accessed: 11-Dec-2019].

[10]“Electric Pump Center Section - 100 Series,” Kentico E-commerce site. [Online]. Available: https://www.meziere.com/Products/Cooling-System-Products/Replacement-Parts/Center-Sections/Electric-Pump-Center-Section-100-Series.aspx. [Accessed: 11-Dec-2019].

[11]Schwaderlapp, Markus, Knut Habermann, and Kurt I. Yapici. *Variable compression ratio-A design solution for fuel economy concepts*. No. 2002-01-1103. SAE Technical paper, 2002.

[12] *Are Your Pistons Round?* The High Performance Engine Builder’s Technical Resource. *Hot Rod Engine Tech.*

[13] V. B. Bhandari, *Design of Machine Elements.* New Delhi: Tata McGraw Hill Publishing, 2008.

[14]“Spark Plug Heat Range,” *The Green Spark Plug Co*. [Online]. Available: https://www.gsparkplug.com/shop/spark-plug-heat-range. [Accessed: 03-Dec-2019].

[15]
Fuel Injector Pulsewidth Calculator. [Online]. Available: https://www.rbracing-rsr.com/calcinjpulse.html. [Accessed: 11-Dec-2019].

[16] “Electric Pump Center Section - 100 Series,” Kentico E-commerce site. [Online]. Available: https://www.meziere.com/Products/Cooling-System-Products/Replacement-Parts/Center-Sections/Electric-Pump-Center-Section-100-Series.aspx. [Accessed: 11-Dec-2019].

[17]Chemical Equilibrium with Applications (CEA). (2004). NASA.

[18] “eCFR - Code of Federal Regulations §86.410-2006,” *Electronic Code of Federal Regulations (eCFR)*, 09-Dec-2019. [Online]. Available: https://www.ecfr.gov/cgi-bin/text-idx?c=ecfr&sid=620bf9f924a835822fd4c718d18607cf&rgn=div8&view=text&node=40:19.0.1.1.2.5.1.13&idno=40. [Accessed: 11-Dec-2019].

[19]“MagnaFlow California Grade CARB Compliant Universal Catalytic Converte,” MagnaFlow. [Online]. Available: https://www.magnaflow.com/products/334104-catalytic-converter-magnaflow-california-grade-carb-compliant-universal-catalytic-converter. [Accessed: 11-Dec-2019].

[20]R. Stone, *Motor vehicle fuel economy*. Houndmills, Basingstoke, Hampshire, 1989.

[21]
“Short Lead Times on Cement Chains,” Renold. [Online]. Available: https://www.renoldjeffrey.com/media/2395952/british-standard-roller-chain-renold-jeffrey.pdf. [Accessed: 03-Dec-2019].

[22]
“NGK Laser Iridium Spark Plug 6994,” *Advance Auto Parts*. [Online]. Available: https://shop.advanceautoparts.com/p/ngk-laser-iridium-spark-plug-6994/15650459-p?product_channel=local&store=5862&adtype=pla&store_code=5862&gclid=EAIaIQobChMI6Z6osK2r5gIVCr3ACh37kwd4EAQYASABEgJ84vD_BwE&gclsrc=aw.ds. [Accessed: 04-Dec-2019].

[23]
INJECTOR PLANET CORP. [Online]. Available: https://www.injectorplanet.com/products/bosch-0280158130. [Accessed: 11-Dec-2019].

[24] “Electric Pump Center Section - 100 Series,” Kentico E-commerce site. [Online]. Available: https://www.meziere.com/Products/Cooling-System-Products/Replacement-Parts/Center-Sections/Electric-Pump-Center-Section-100-Series.aspx. [Accessed: 11-Dec-2019].

15 - Appendices

A - Team Charter

PURPOSE

The purpose of this project is to design a unique motorcycle engine that meets the criteria outlined in our design requirements. The team will strive to maximize fuel efficiency and performance while minimizing size, weight and cost. This team will create a complete CAD model of the engine and a final report detailing the design process and end result. This report will

include, among other things, technical specifications, a theory of operations, FMEA and a bill of materials in order to show the full details of our design.

BACKGROUND/REQUIREMENTS

BTN Performance, a subset of Spartan Motorcycle Company, has been assigned the task of designing an innovative engine for a motorcycle. Production is set to begin in 2021. This project will also serve to introduce the members of BTN Performance to large team design efforts as a part of the course EMAE 360: Design and Manufacturing II.

The motorcycle with our engine will be sold in the United States and, as such, will meet all relevant standards for noise, emissions, and safety. Projected demand is 7,500 in the first year, 12,000 units in the second year, and 15,000 units in the third year. Other teams in the Spartan Motorcycle Company will design other components of the motorcycle with our team concentrating on the design of the engine able to be integrated into the final product.

The key stakeholders for this project include our sponsor, Dr. Sunniva Collins, the Spartan Motorcycle Company, and our subteam BTN Performance. The users of this project are the Spartan Motorcycle Company and the purchasers of the Spartan Motorcycle Company product.

The following requirements have been assigned to our team by our stakeholders:

1. The system shall be suitable for installation in a motorcycle
2. The system shall power a six-speed transmission
3. The system shall have spark ignition
4. The system shall run on standard gasoline
5. The system shall have a compression ratio of 9:1 to 10:1
6. The system shall have a displacement of 1500 to 1800cc
7. The system shall have 2 or more cylinders
8. The system shall have a 4-stroke cycle
9. The system shall have fuel injection
10. The system shall be capable of 5000 rpm continuous service
11. The system shall idle at 800 rpm
12. The system design should maximize fuel efficiency
13. The system design should minimize cost
14. The system design should minimize overall dimensions
15. The system design should minimize weight

SCOPE

This semester, BTN Performance will develop an internal combustion engine for motorcycles using thermodynamics and mechanical principles to maximize efficiency and performance while minimizing weight, size and cost. In addition, this project will optimize design for manufacturing through conscientious part and drawing creation. All of the components of the engine will be designed or purchased by the team. External components such as transmission, fuel pump, chassis, ECU, and exhaust are designed/sourced by other teams within the Spartan Motorcycle Company and are considered out of scope. The scope of the project will include not only the CAD design files and drawings of all engine components, but also all the technical specifications, calculations, and design decision documentation. This will all be completed by December 13, 2019.

In below we listed a sample of what components we have considered to be in or out of our scope:

In scope:

1. **Design and manufacturing of engine components such as:** short block, cylinder head, lubrication system, and valvetrain.
2. **Selection of purchased engine components such as:** sparkplugs, water pump, starter motor, injectors, sensors, and bearings.

Out of scope:

1. **Auxiliary components such as:** transmission, fuel pump, gas tank, ECU, TCU, chassis, production intake and exhaust manifold, catalytic converter, and exhaust.

TEAM COMPOSITION

The BTN Performance is a motorcycle engine design team composed of ten undergraduate engineering students. The group is led by a Team Lead who is directly supported by a Project Manager. Each remaining member is assigned to one of three groups: Design Group 1, Design Group 2, or the Thermodynamic Analysis Group. Each design group is led by a Group Lead and has a Material Specialist and a CAD Specialist.

Both design groups will be responsible for mechanical analysis and CAD of engine components, but these responsibilities will be divided between the teams by engine zone (such as the short block and the cylinder head). The thermodynamic analysis group consists of a Thermodynamic

Team Lead and a Thermodynamic Specialist. This group takes first responsibility for all thermodynamic calculations and analysis, working closely with the design teams as needed.

Additionally, for work breakdown clarity, the Team Lead will be an honorary member of Group 1, while the project manager will be an honorary member of Group 2. Each team member has a part-time role in this design project, committing an average of three hours a week to their tasks. As the design process proceeds further, members are expected to commit more time into the project. The figure below illustrates the team structure.

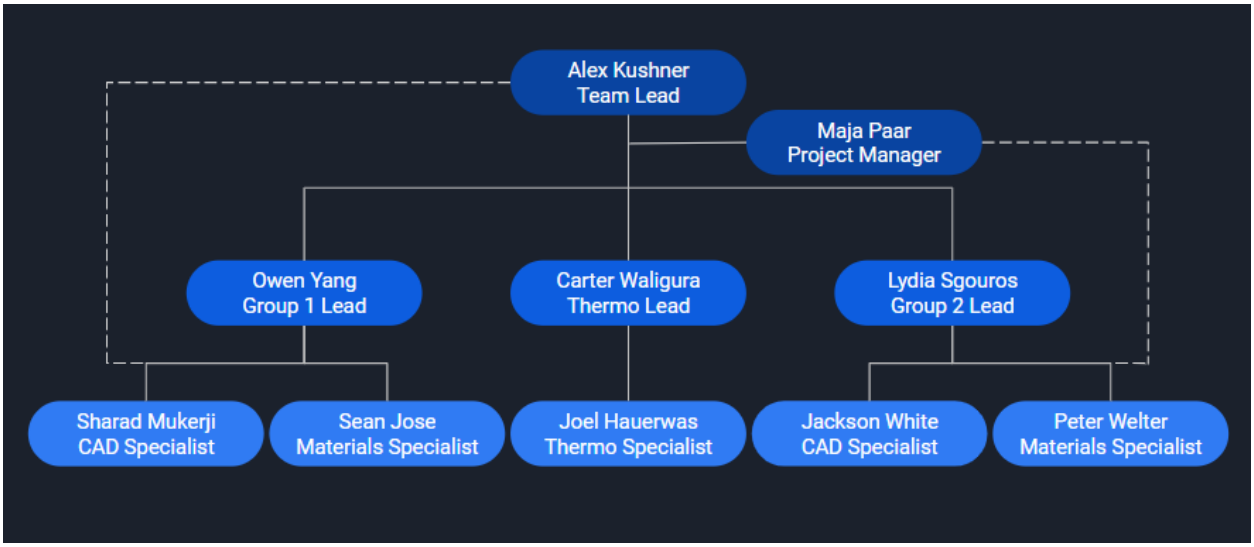

MEMBERSHIP ROLES

Team Member	Phone Number	Email	Team Role
Alex Kushner	608-628-1991	ark119@case.edu	Team Lead
Maja Paar	413-275-2532	mfp42@case.edu	Project Manager
Lydia Sgouros	401-219-2079	ljs140@case.edu	Group 2 Lead
Jackson White	314-954-2163	jsw112@case.edu	Group 2/CAD Specialist
Peter Welter	216-973-1582	paw62@case.edu	Group 2 /Material Specialist
Jinghao Yang	443-878-7284	jxy504@case.edu	Group 1 Lead

Sean Jose	301-260-5809	smj7@case.edu	Group 1/CAD Specialist
Sharad Mukerji	262-343-4992	sxm844@case.edu	Group 1/Material Specialist
Carter Waligura	724-366-8826	cjw123@case.edu	Thermodynamic Group Lead
Joel Hauserwas	508-494-2106	jah301@case.edu	Thermodynamic Analysis Group

TEAM EMPOWERMENT

As all team members are fourth year engineering students at a high-caliber engineering school like CWRU, all team members are assumed to have a deep understanding of mechanical design. Due to this, all team members are empowered to make minor design changes at will and at their best judgement. Further empowerment based on position is listed below:

The Team Lead is empowered to make any major decisions, typically after consultation with other group members. He has the power to lead discussions at meetings but will allow other members to take over if needed. He is also empowered to reassign tasks within or between groups in consultation with the respective group members.

The Project Manager is empowered to act as a liaison between groups or team members if the Team Lead is unavailable. In addition, the project manager has the authority to make any changes to documents in the google drive without altering their core contents in order to add clarity or make them more aesthetically pleasing.

Group Leads are empowered to delegate tasks between their respective group members in accordance with their strengths and weaknesses. They are also allowed to make any decisions regarding the tasks assigned to their respective groups without needing consent from the project manager or Team Lead.

TEAM OPERATIONS

Meetings:
The team meets as a whole once per week on Saturdays at 5:00 pm in the Kelvin Smith Library, with the understanding that additional meetings can be scheduled if needed (e.g. to prepare for design reviews or when key design decisions necessitate discussion). Group meetings will also take place once per week outside of the time scheduled for the whole team meeting. The time

and date of group meetings will be scheduled at the discretion of the respective Group Lead. The Team Lead will prepare agendas for each full team meeting while the project manager will take notes. For group meetings, the respective Group Lead will prepare an agenda and lead the meeting while a delegated group member will take notes. In each meeting the following topics are discussed: progress by individual groups, timeline tracking, decisions that need to be made, and action items for next week on a group or individual basis.

Action Item Tracking:
Between meetings, action items are tracked in multiple ways. All action items discussed in meetings are put in meeting minutes, and, following meetings, the project manager will create a card for each of these items on the team Trello board. The cards are automatically assigned to the Team Lead and the Group Lead of the responsible group, and then the Group Lead will delegate and assign further. Once the responsible member completes the task, they will move the card to the "Completed" category, and all assigned members will receive a notification. This ensures effective oversight and action item responsibility. On a less granular level, action items appear in the team Gantt chart and the responsibility matrix. Though these do not show every single item to be accomplished in the way the Trello board does, these tools allow us to make sure we are moving at an acceptable pace and that people are aware of what is expected of them in the upcoming weeks.

Decision Making:
In general, major decisions will be discussed among the full team at the next regularly scheduled team meeting or at a specially called session. If there are clear criteria to compare for a decision, then a Pugh Chart will be used for unbiased decision making. Otherwise, the decision will be put to a general team vote. In the event that the team cannot come to a majority decision, the Team Lead will have the final say.

RISK MITIGATION

Staying on Schedule:
We have created a Gantt chart in order to have an overview of all of our tasks and so that we can see all important dates at once. At each team meeting we will assess everyone's progress to ensure all assignments are on track.

Communication:
To avoid miscommunication or lack of communication we have made a Slack channel so that all team members can be contacted. This includes chats for each subteam so that subTeam Leads can easily communicate with each other.

Inaccurate Work:
To avoid incorrectly completed work, all tasks done by individual group members must be reviewed by their respective Group Lead before larger group viewing. This will be done through a Trello category called “To be Reviewed”, where group members will first move their tasks after completion. After the Group Lead reviews the work, they will then move that card to the “Completed” category.

Loss of Team Member/Member Not Attending Meetings:
To avoid catastrophic results in the case that a group member fails to complete their responsibilities, we have implemented a primary/secondary assignee system so that there is always a second team member who can take over responsibility if the primary fails to. If a team member fails to attend a meeting without 24 hour notice, the Team Lead will first discuss the issue with them and try to find a resolution, otherwise they will speak to Dr. Collins if the problem persists. In the event of the loss of the Team Lead or project manager, a special election will be held during the next meeting in order to move a team member into the new position.

Interpersonal Conflict:
In the event of interpersonal conflict within a group, the respective Group Lead will first have a discussion with the affected members. If they fail to find an amicable resolution, the group members will then meet with the Team Lead. If this fails, they will then meet with Dr. Collins as a last resort.

Failure to Complete Work or Not Enough Work Assigned:
To avoid incomplete work, we have made a Trello board in order to keep track of all assignments. This process is described in detail in previous sections.

Loss of Data:
To keep track of all files and data, we have made a shared Google Drive folder. All files and research used for the project will be stored there, organized in folders by topic. The exception to this is that all SOLIDWORKS design files will be stored using SOLIDWORKS PDM. Both of these systems are externally redundant and cloud driven, drastically reducing the chances of data loss.

PERFORMANCE ASSESSMENT

The team will track its progress against the Gantt chart in order to ensure that each task is being completed as per the schedule. This, in combination with the responsibility matrix, will allow the team to ensure that each member's performance is consistently at the level it needs to be.

Important Dates:
Project Plan Review: 9/18
Conceptual Design Review: 10/07
Design Review: 12/06
Final Report: 12/13

SIGNATURES:

Alex Kushner:

Carter Waligura:

Jackson White:

Joel Hauerwas:

Lydia Sgouros:

Maja Paar:

Owen Yang:

Peter Welter:

Sean Jose:

B - PDS

Product Identification

Our team has designed an engine for a motorcycle sold by the Spartan Motorcycle Company (SMC). There is only one model of engine, but the engine could be used in multiple different motorcycles as SPC seems fit. The engine will function as a standard internal combustion engine operating on four-stroke cycles, converting chemical potential energy of the fuel into kinetic energy that results in propulsion of the motorcycle.

Our engine vastly exceeds the efficiency of our competitors while maintaining similar performance. To accomplish this, the engine makes use of variable valve technology, including discrete variable valve lift and variable valve phasing. We will also use cutting-edge bearing and interface materials whenever possible to minimize friction and the subsequent reduction in inefficiency

The horsepower and torques for the engine are 138 horsepower (103 kW) and 124 lb•ft (168 Nm) of torque. The fuel consumption of the engine has been determined as 55 mpg. The engine meets all relevant emissions and noise standards.

The product is primarily intended to be used by SMC in their motorcycles, and will be configured to fit in the engine envelope of a variety of sport touring motorcycles to facilitate the integration of our engine with the rest of the SMC bike. The motorcycle manufacturers will have to interface our engine to their transmission and the remainder of the motorcycle powertrain. The product has some potential for misuse by enthusiasts who attempt to fit the engine into a motorcycle that has an incompatible engine envelope. This could lead to fitment issues between the engine and transmission and the engine being unable to be inserted into the engine envelope.

Our engine will use control interfaces identical to other motorcycle engines on the market, so specialised training will not be required. Generic basic motorcycle engine operation training may be required for novice users.

Market Identification

There are around 500,000 motorcycles sold every year, as well as over 13 million registered motorcycles in the United States. Our target market is the Sports Touring Bike segment which

takes up about 15% of the entire motorcycle market. Thus, our annual market demand would be about 75,000 bikes.

Our major competitors include Harley Davidson, Polaris' Indian Motorcycle and Honda. Harley Davidson dominates the industry with a market share of around 45%, followed by Honda at 14% and Indian Motorcycle at 10%. Some of their top products include the Honda Gold Wing and the Harley Davidson Road Glide.

Although the motorcycle industry has generally seen a downward trend in sales for the last couple of years, these are well established products with loyal customer bases. Therefore, there will be significant competition for our product when going up against these established companies. We set ourselves apart by having outstanding performance and efficiency and therefore expect a loyal customer base.

Our motorcycle engine brand name will be BTN Performance (a.k.a "Boom to Nyoom!") and we will use our logo (provided below) to distinguish ourselves from our competitors in the market.

Key Project Deadlines

Deliverable	**Due Date**
Deliverable	September 11
Progress Report	September 18
Project Plan Review	September 23
Progress Report	September 30
Conceptual Design Review	October 7
Progress Report	October 18
Progress Report	October 30
Progress Report	November 4
Progress Report	November 15
Progress Report	November 22
Detail Design Review	December 6

Physical Description

Motorcycles' abilities to maneuver through turns are important for most riders. Although sports touring motorcycles do not have the same agility and power delivery as sports motorcycles, they should still have low centers of gravity and be comfortable for riders to go on long distance ridings. In the current touring motorcycle market, the weight of the engine is about 35 percent of the dry weight of the motorcycle, which ranges from 90 kgs to 125 kgs. The BTN-1500E has a total weight of 59.4kg.

In addition, touring motorcycles generally have the largest physical dimensions among most types of motorcycles. Depending on the engine configurations, the width of the motorcycles are no larger than 900 mm. The final size is 0.583 x 0.466 x 0.332 m so it should easily fit into a variety of sports touring motorcycles.

Using advanced decision making tools (such as Pugh charts), we have also decided the overall configuration and displacement for our engine that will result in the maximum efficiency and performance. Our engine will have three cylinders in an in-line configuration. Each cylinder will have a swept volume of 500 cubic centimeters, leading to an overall engine displacement of 1500 cubic centimeters or 1.5 L.

Financial Requirements

BTN Performance will be offering a 5-year or 50,000 mi warranty, the estimated useful life of the product. This warranty will cover the replacement of parts that have
been deemed to have factory defects. Pricing over the life cycle will be detailed with the component cost in the Bill of Materials.

The design period requires no capital investment but once manufacturing begins, a large capital investment will be required for manufacturing equipment and labor.

Life Cycle Targets

The EPA states a useful lifetime exceeding 5 years or 30,000km (18,640 miles). Additionally, we aim to meet their High Mileage regulations with a lifetime exceeding 80,500 km (50,000 miles).

When not in use, the engine will have a reliable shelf life exceeding 10 years given proper storage. Installation is expected to take a team of 4 people 5 hours at an expected cost of $500 for installation fee plus cost of engine.

A maintenance schedule will be thoroughly documented in final product documentation and a summary of these tasks based on EPA regulations, NHTSA regulations, as well as industry standards is given below:

Monthly (User performed):

- Check oil with dipstick, “top off” as needed

Annually or every 4000-6000 mi (Certified mechanic performed):

- Change oil
- Inspect fuel lines
- Check oil filter and change as necessary

Biannually or every 8000-12,000 mi (Certified mechanic performed):

- Replace spark plugs
- Replace air filter

After 80,500 km, additional maintenance steps can be taken if the engine is still performing. It is suggested that at this point the timing belt be replaced. The reliability of individual components will be analyzed using finite element analysis and will be detailed in the Bill of Materials. Wear is expected and less reliable components will require more frequent checks and replacements. These components will be readily replaceable by a mechanic.

When the engine reaches the end of its useful life, the engine can be turned into either this company, a junkyard, or various mechanics. Useful components may be kept as replacement parts for other engines and otherwise the metal parts will be reclaimed and recycled.

Social, Political, and Legal Requirements

Safety and Environmental Standards

There are a number of standards that BTN Performance must comply with in order to ensure the safety of the customer, others on the road, company personnel, and the environment.

Company Safety

Regarding company personnel, BTN Performance will follow the safety standards of the Occupational Safety and Health Administration (OSHA).

Road Safety

Regulations for safety of the driver and other motor vehicles on the road are mostly given by the National Highway Transit Safety Administration (NHTSA) and outlined in the Federal Motor Vehicle Safety Standards (FMVSS). Besides these main standards, ISO TC 70 defines many standards for testing. Additional standards exist for flammable liquids (OSHA), lubrication (ASTM), oils (JASO), materials (ASTM), and many other things that will be used with our engine. While we do not have to directly follow these, we will ensure that purchased components meet the relevant standards.

Emissions

Emissions are regulated by the Environmental Protection Agency (EPA) in the 40 CFR regulations. 40 CFR subpart F outlines the emission test procedures while 40 CFR 86.410-2006 states the emissions standards for vehicles after the year 2006. Our product will be used in a class III vehicle which means that we are restricted to 12 g/km CO emissions and 0.8 g/km (or 1.4 g/km with different averaging) HC + NO emissions. X

Noise

Noise is also regulated by the EPA along with local and state regulations. Since we are aiming to market our engine throughout the United States, we chose the most restrictive regulations to design our product to. Connecticut has the lowest noise regulations in CGS 14-80a which states that the motorcycle can not emit more than 78 dB going below 35 mph in soft site conditions at a distance of 50 feet from the centerline of the vehicle. Additionally, we are aiming to meet the Low-Noise-Emission Product certification standards of 40 CFR 203 and 205 which permit only 71 dB in the same conditions.

Product Liability

The product shall be sold with a 5 years or 30 thousand kilometers warranty, consistent with the standards of EPA. However, unintended uses of the product shall void this warranty. These may include modification of the engine (and unauthorized maintenance that may result in modification) as well as using the engine outside of its intended use in a motorcycle. Proper labels about warranty, safety, and liability will be affixed to the product following the standards of 49 CFR Part 567.

While this engine will be unique in the way that elements are integrated together, the individual elements will be similar to those in other manufactured motorcycle engines. Therefore, it is unlikely that there will be the need to create patents for elements of our design. The more important part will be reviewing existing patents in order to avoid violation of intellectual property.

Manufacturing Specifications

While key parts of our engine will be manufactured in-house, many components will instead be sourced from a variety of suppliers. For purchased parts, the Bill of Materials will list specific suppliers, costs, and why the decision was made to buy the individual component as opposed to making it. Broadly, the decision to buy is pushed by a component's availability, cost, and ability to meet our requirements. This means items such as fasteners are purchased, but also things like spark plugs which are easily available and more cost-effective to purchase than to set up the additional manufacturing processes for. These make vs buy decisions are also detailed in the definition of our scope.

For in-house manufactured components, the Bill of Materials will list the specific materials and manufacturing processes for each individual part. Manufacturing specifications vary depending on the material, size, complexity, and necessary tolerances of each part. At this time, required in-house manufacturing processes are predicted to include CNC Milling and Turning, painting, and coating. Casting and heat treating will be outsourced in order to reduce costs.

C - Thermo Graphs

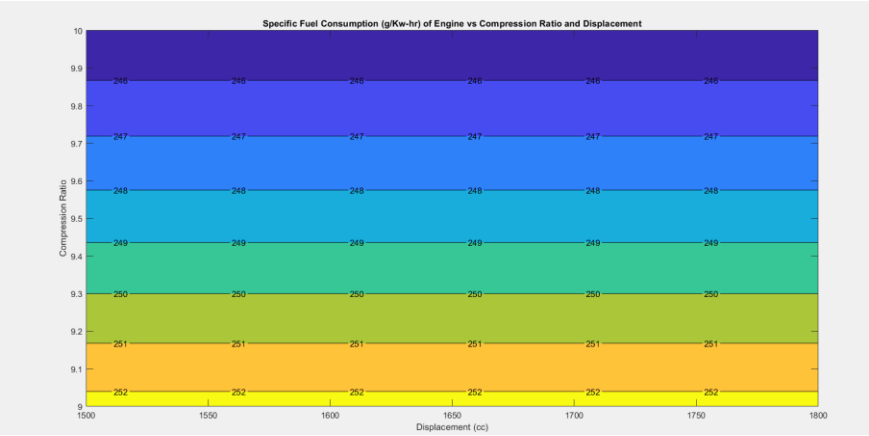

Figure C.1: Specific fuel consumption trade study

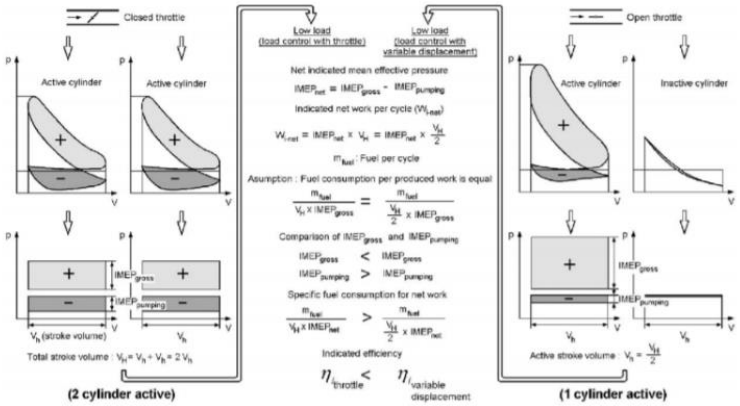

Figure C.2: Loss Trends due to throttling [16]

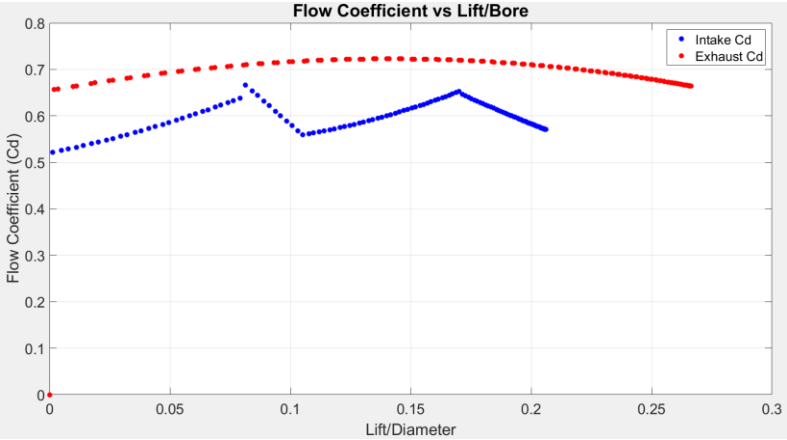

Figure C.3: Recreated Cd graphs [1]

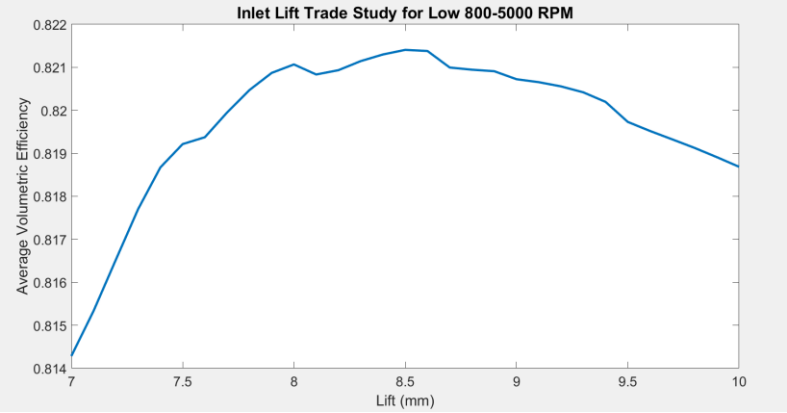

Figure C.4: Small cam lift trade study

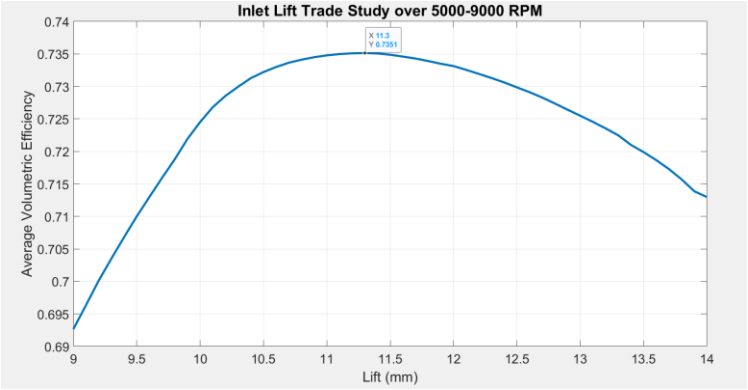

Figure C.5: Large cam lift trade study

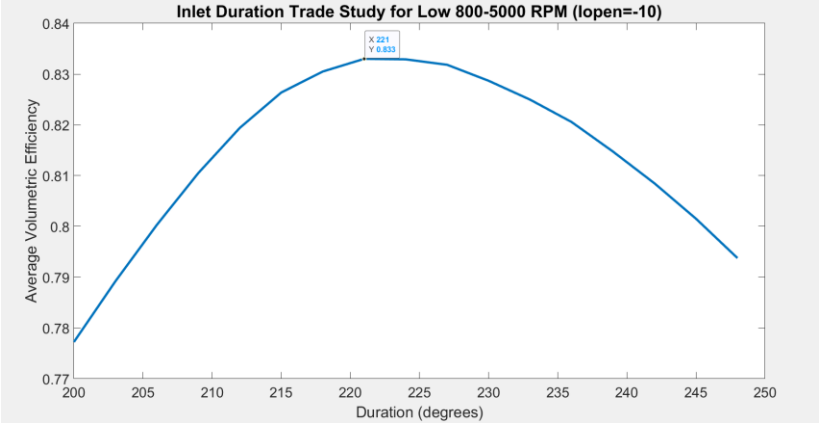

Figure C.6: Small cam duration trade study

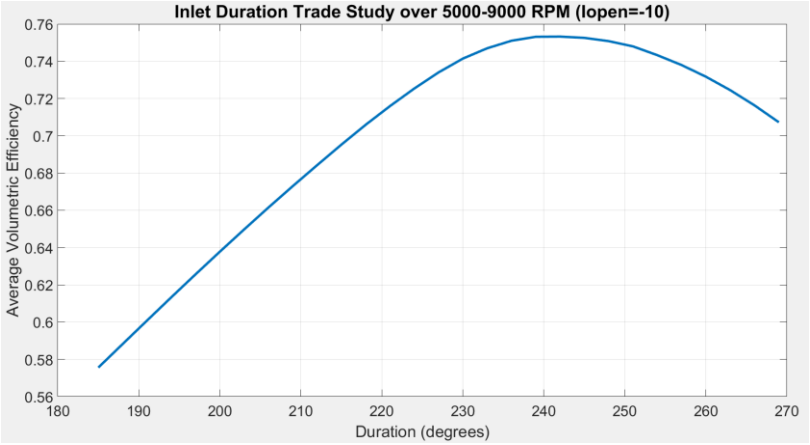

Figure C.7: Large cam duration trade study

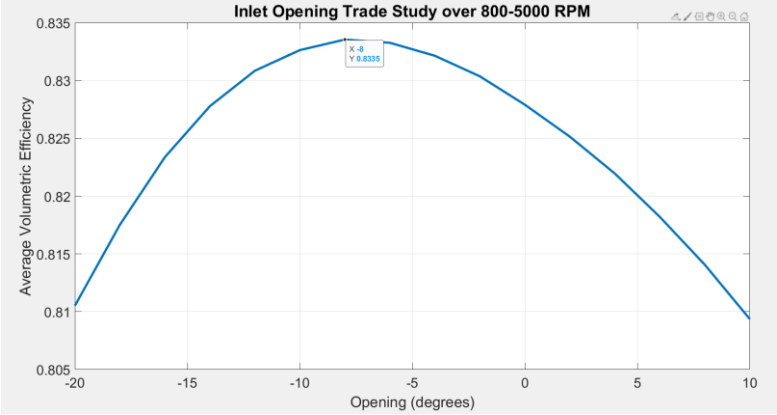

Figure C.8: Small cam opening trade study

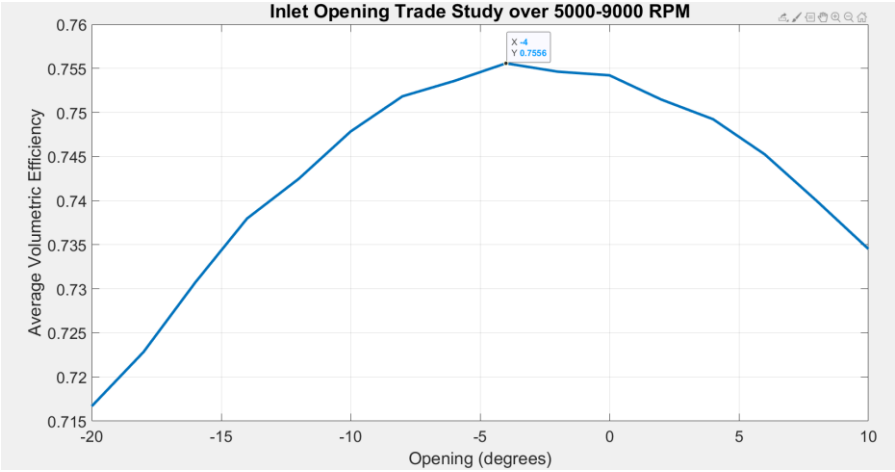

Figure C.9: Large cam opening trade study

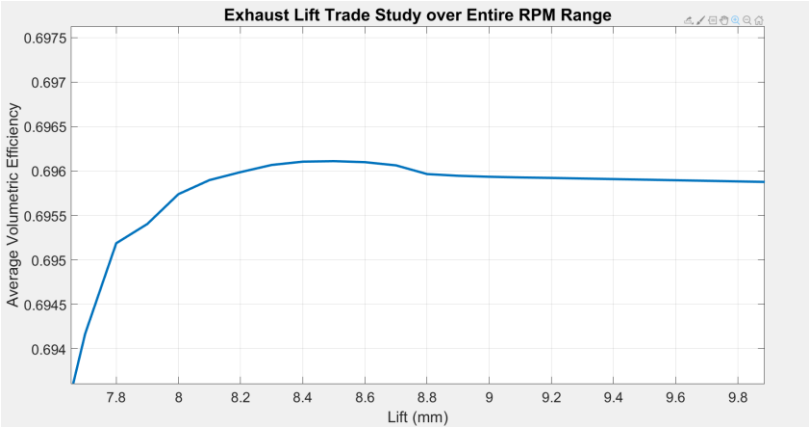

Figure C.10: Exhaust lift trade study

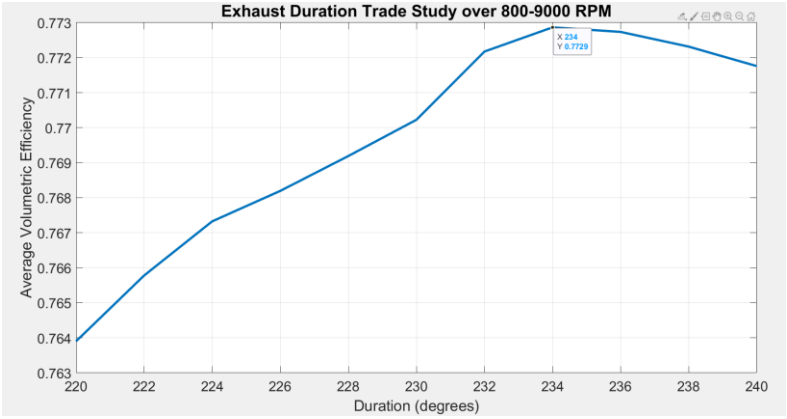

Figure C.11: Exhaust duration trade study

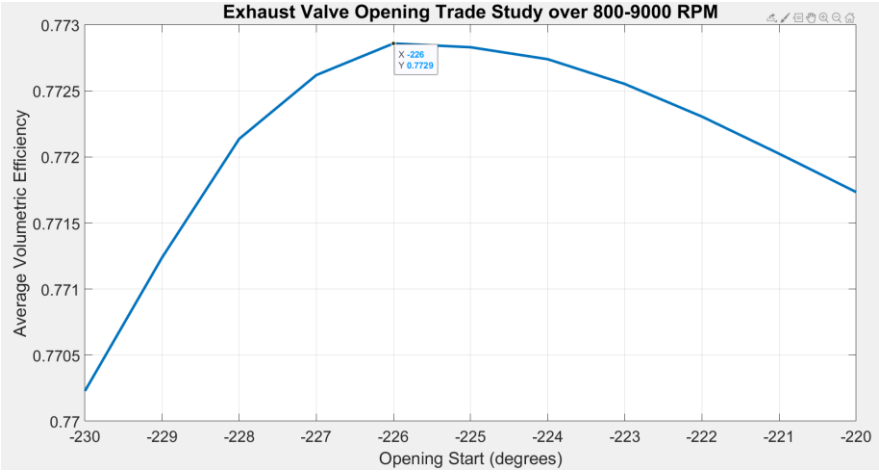

Figure C.12: Exhaust opening trade study

D - BOM

D.1 - Short Block

Part #	Part	Quan.	Purchased	Material	Manufac-turing	Secondary Process	Mass (kg)	Total Mass (kg)	Cost (USD)	Total Cost (USD)
G2P001	Crankshaft	1	No	AISI 4340 Steel	Forged	Quench and Temper, Machining	9.810	9.810	$246.40	$246.40
G2P002	Connecting Rod	3	No	AISI 4340 Steel	Forged	Quench and Temper, Machining	0.950	2.850	$78.32	$234.96
G2P003	Connecting Rod Cap	3	No	AISI 4340 Steel	Forged	-	0.280	0.840	$0.00	$0.00
G2P004	Piston	3	No	4032 Aluminum	Forged	T6 Temper, Machining, Coating	0.340	1.020	$53.68	$161.04
G2P005	Wrist pin	3	No	AISI 4340 Steel	Hydroformed	Quench and Temper, Machining	0.050	0.150	$2.61	$7.83
G2P007	Top Compression Piston Ring	3	No	Grey Nodular Cast Iron	Cast	Chromium Plating	0.001	0.003	$4.49	$13.47
G2P008	Bottom Compression Piston Ring	3	No	Grey Nodular Cast Iron	Cast	-	0.001	0.003	$4.49	$13.47
G2P009	Oil Control Piston Ring	3	No	Steel	Stamped	Nitride Coating	0.002	0.006	$4.49	$13.47
G2P010	Engine block	1	No	A356 Aluminum	Sand Cast	T6 Temper, Machining, Plasma Spray	14.120	14.120	$151.80	$151.80
G2P011	Main Cap	4	No	A356 Aluminum	Cast	T6 Temper, Machining	0.120	0.480	$9.69	$38.76
G2P012	Main bearing Alignment Dowel	8	Yes	Steel	N/A	N/A	0.010	0.080	$3.99	$31.92

G2P012	Head-Block Alignment Dowel	2	Yes	Steel	N/A	N/A	0.010	0.020	$3.99	$7.98
G2P013	Balance Shaft	1	No	AISI 4340 Steel	Cold Rolled	Quench and Temper, Machining	0.420	0.420	$2.26	$2.26
G2P017	BS Girdle	1	No	A360 Aluminum	Die Cast	T6 Temper, Machining	0.700	0.700	$58.85	$58.85
G2P018	Top Oil Pan Bolt	14	Yes	Steel	N/A	N/A	0.005	0.070	$0.14	$1.96
G2P020	Rear Main Seal	1	Yes	Rubber	N/A	N/A	0.002	0.002	$7.15	$7.15
G2P021	Timing Sprocket	1	Yes	Steel	N/A	N/A	0.130	0.130	$20.00	$20.00
G2P022	Balance Shaft Drive Sprocket	1	Yes	Steel	N/A	N/A	0.070	0.070	$10.00	$10.00
G2P025	Normal Main Bearing	8	Yes	Tri-Metal King XP	N/A	N/A	0.040	0.320	$6.25	$50.00
G2P026	Connecting Rod Bearing	6	Yes	Tri-Metal King XP	N/A	N/A	0.030	0.180	$6.25	$37.50
G2P027	Balance Shaft Idler Sprocket	2	Yes	Steel	N/A	N/A	0.070	0.140	$15.00	$30.00
G2P028	Balance Shaft Mass 1	1	No	White Cast Iron	Cast	Machining	0.220	0.220	$10.75	$10.75
G2P029	Balance Shaft Mass 2	1	No	Tungsten	Cast	Machining	0.170	0.170	$25.52	$25.52
G2P030	BS Bearings	2	Yes	Bronze	N/A	N/A	0.020	0.040	$2.36	$4.72
G2P031	BS Girdle Bolts	4	Yes	Steel	N/A	N/A	0.010	0.040	$0.30	$1.21
G2P032	Top Oil Pan	1	No	A360 Aluminum	Die Cast	T6 Temper, Machining	1.550	1.550	$65.67	$65.67
G2P033	M8 Washer	5	Yes	18-8 SS	N/A	N/A	0.002	0.010	$0.11	$0.57
G2P034	Timing Sprocket Bolt	1	Yes	12.9 Steel	N/A	N/A	0.010	0.010	$0.53	$0.53
G2P035	CS Timing Sprocket Key	1	Yes	Tool Steel	N/A	N/A	0.002	0.002	$0.25	$0.25

G2P036	BS Shaft Seal	3	Yes	Rubber	N/A	N/A	0.001	0.002	$3.51	$10.53
G2P037	Bottom Oil Pan	1	No	A360 Aluminum	Cast	T6 Temper, Machining	0.610	0.610	$49.61	$49.61
G2P038	Bottom Oil Pan Bolt	12	Yes	Steel	N/A	N/A	0.004	0.048	$0.19	$2.30
G2P039	BS Idler Bolt	2	Yes	8.8 Steel	N/A	N/A	0.009	0.018	$0.17	$0.34
G2P040	BS Mass Bolt	5	Yes	Steel	N/A	N/A	0.002	0.010	$0.11	$0.54
G2P041	BS Key	1	Yes	Tool Steel	N/A	N/A	0.002	0.002	$0.20	$0.20
G2P042	BS Sprocket Bolt	2	Yes	10.9 Steel	N/A	N/A	0.012	0.024	$0.22	$0.44
G2P043	CS Timing Sprocket	1	Yes	Steel	N/A	N/A	0.074	0.074	$15.00	$15.00
G2P044	BS Retaining Ring	2	Yes	DIN 1.4122 SS	N/A	N/A	0.001	0.002	$0.96	$1.92
G2P045	Connecting Rod Alignment Dowel	6	Yes	Steel	N/A	N/A	0.010	0.060	$3.99	$23.94
G2P046	BS Cover Bolt	6	Yes	18-8 SS	N/A	N/A	0.004	0.024	$0.15	$0.89
G2P047	BS Cover	1	No	PC Plastic	Injection Molded	-	0.150	0.150	$23.54	$23.54
G2P048	BS Chain Tensioner	1	Yes	Multiple	N/A	N/A	0.041	0.041	$25.00	$25.00
G2P049	Main Bolts	8	Yes	12.9 Steel	N/A	N/A	0.060	0.480	$1.47	$11.76
G2P050	Rod Bolts	6	Yes	12.9 Steel	N/A	N/A	0.020	0.120	$0.65	$3.90
G2P051	Head Bolts	4	Yes	12.9 Steel	N/A	N/A	0.100	0.400	$5.00	$20.00
G2P052	BS Chain Guide	1	Yes	Steel	N/A	N/A	0.058	0.058	$10.00	$10.00
G2P053	BS Chain Bolts	4	Yes	Steel	N/A	N/A	0.003	0.012	$0.12	$0.49
G2P054	Rod Nuts	6	Yes	12.9 Steel	N/A	N/A	0.010	0.060	$0.23	$1.38
G2P056	Head Studs	4	Yes	12.9 Steel	N/A	N/A	0.050	0.200	$10.00	$40.00
G2P057	Head Nuts	4	Yes	12.9 Steel	N/A	N/A	0.010	0.040	$2.00	$8.00

G2P059	Wrist Pin Clips	6	Yes	Steel	N/A	N/A	0.002	0.012	$12.00	$6.00
G2P060	Thrust Main Bearing	8	Yes	Tri-Metal King XP	N/A	N/A	0.040	0.320	$6.25	$50.00
G2P061	Head Gasket	1	No	MLS	Stamped		.020	0.020	$20.00	$20.00
N/A	Timing Chain 1	1.75	Yes	Steel	N/A	N/A		0.000	$6.19	$10.83
N/A	Timing Chain 2	1.75	Yes	Steel	N/A	N/A		0.000	$6.19	$10.83

D.2 - Cylinder Head

Part #	Part	Quan-tity	Pur-chased?	Material	Manufac-turing	Secondary Process	Mass (kg)	Total Mass (kg)	Cost (USD)	Total Cost (USD)
G1P001	Intake Valve	6	No	Sil 1 SS	Forged	Friction Welded	0.089	0.534	$12.65	$75.90
G1P002	Spring Retainer	12	No	AISI 4140 Steel	Forged	Quench and Temper, Machining	0.010	0.120	$20.13	$241.56
G1P003	Keepers	24	No	AISI 4140 Steel	Forged	Quench and Temper, Machining	0.001	0.024	$13.42	$322.08
G1P004	Intake Valve Spring	12	Yes	Chrome Silicon Steel Wire	N/A	N/A	0.038	0.456		$0.00
G1P005	Intake Valve Seat	6	No	Cast grey iron	Cast	-	0.010	0.060	$6.09	$36.54
G1P006	Valve Stem Seal Outer	6	Yes	NBR	N/A	N/A	0.000	0.002	$0.96	$5.76
G1P007	Valve Stem Seal Inner	6	Yes	NBR	N/A	N/A	0.001	0.006	$0.00	$0.00
G1P008	Valve Stem Seal Ring	6	Yes	Steel	N/A	N/A	0.000	0.002	$0.00	$0.00
G1P036	Exhaust Valve	6	No	21-4 SS	Forged	Friction Welded	0.064	0.384	$11.88	$71.28
G1P010	Bare Cylinder Head	1	No	A356 Aluminum	Sand Cast	T6 Temper, Machining	10.967	10.967	$123.20	$123.20
G1P011	Exhaust Valve Seat	6	No	Cast grey iron	Cast	-	0.010	0.060	$6.09	$36.54

G1P012	Rocker Arms	12	No	AISI 4140 Steel	Forged	Quench and Temper, Machining	0.009	0.108	$19.69	$236.28
G1P013	Intake Rocker Arm Shaft	3	No	AISI 4130 Steel	Forged	Quench and Temper, Machining	0.014	0.041	$21.45	$64.35
G1P014	Rocker Arm Upper Retainer	24	No	A356 Aluminum	Cast	T6 Temper, Machining	0.002	0.048	$4.94	$118.56
G1P016	Linear actuator shaft	2	Yes	Multiple	N/A	N/A		0.000	$64.99	$129.98
G1P017	Linear actuator housing	2	Yes	Multiple	N/A	N/A		0.000	$0.00	-
G1P018	Exhaust Camshaft	1	No	Chilled Grey Iron	Cast	Cyrotreated, Machining	1.899	1.899	$25.30	$25.30
G1P019	Intake Camshaft	1	No	Chilled Grey Iron	Cast	Cyrotreated, Machining	2.041	2.041	$26.84	$26.84
G1P020	Sprocket cover	1	No	A356 Aluminum	Cast	T6 Temper, Machining	0.031	0.031	$7.36	$7.36
G1P021	Oil Seal	6	No	FEPM	Injection Molded	-	0.001	0.006	$9.47	$56.82
G1P022	Sprocket Outer Housing	1	No	SAE 4130 Steel	Cast	Quench and Temper, Machining	0.377	0.377	$12.65	$12.65
G1P023	Plunger	1	No	AISI 4130 Steel	Forged	Quench and Temper, Machining	0.004	0.004	$16.94	$16.94
G1P024	Oil Seal Spring Steel	6	No	Spring Steel	Stamped	-	0.000	0.001	$0.35	$2.10
G1P025	Inter Shifter	1	No	AISI 4130 Steel	Forged	Quench and Temper, Machining	0.247	0.247	$48.29	$48.29
G1P026	Intake Sprocket	1	No	AISI 4130 Steel	Forged	Quench and Temper, Machining	0.330	0.330	$51.59	$51.59
G1P028	Intake Sprocket Bolt	3	Yes	Steel	N/A	N/A	0.013	0.039	$0.73	$2.20
G1P029	Thrust Bearing	1	Yes	Steel	N/A	N/A	0.030	0.030	$5.77	$5.77

G1P030	VVT to DVVL adaptor spline	1	No	AISI 4130 Steel	Forged	Quench and Temper, Machining	0.448	0.448	$55.44	$55.44
G1P031	Exhaust sprocket	1	No	AISI 4130 Steel	Forged	Quench and Temper, Machining	0.220	0.220	$47.08	$47.08
G1P035	Sprocket cover	1	No	A356 Aluminum	Cast	T6 Temper	1.229	1.229	$24.09	$24.09
G1P037	Rocker Cap Bolt	48	Yes	Steel	N/A	N/A	0.002	0.096	$0.09	$4.42
G1P038	Cam Caps	8	No	A356 Aluminum	Cast	T6 Temper, Machining	0.033	0.264	$7.44	$59.52
G1P039	Exhaust Rocker Shaft	3	No	AISI 4130 Steel	Forged	Quench and Temper, Machining	0.001	0.003	$13.42	$40.26
G1P041	Valve Cover	1	No	A356 Aluminum	Cast	T6 Temper, Machining, Painting	2.780	2.780	$40.59	$40.59
G1P042	Spark Plugs	3	Yes	Multiple - Hot Double Iridium	N/A	N/A		0.000	$5.00	$15.00
G1P043	VVT Solenoid	1	Yes	Steel	N/A	N/A		0.000	$45.85	45.85
G1P044	Cam Mount Bolts	16	Yes	Steel	N/A	N/A	0.020	0.320	$0.34	$5.36
G1P048	Exhaust Sprocket Bolt		Yes	Steel	N/A	N/A	0.020	0.000	$0.28	$0.00

D.3 - Full Assembly

Part #	Part	Quantity	Purchased?	Material	Manufacturing	Secondary Process	Mass (kg)	Total Mass (kg)	Cost (USD)	Total Cost (USD)
G0P001	Timing Chain Guide 1	1	No	PC Plastic	Injection Molded	N/A	N/A	N/A	$5.96	$5.96
G0P002	Timing Chain Tensioner	1	Yes	Multiple	N/A	N/A	N/A	N/A	$15.00	$15.00
G0P003	Timing Chain Guide 2	1	No	PC Plastic	Injection Molded	N/A	N/A	N/A	$5.96	$5.96

G0P004	Timing Chain Guide Bolt	4	Yes	Steel	N/A	N/A	N/A	N/A	$0.16	$0.62
G0P005	Timing Chain Tensioner Bolt	2	Yes	Steel	N/A	N/A	N/A	N/A	$0.10	$0.20
G0P007	Timing Cover bolt	13	Yes	Steel	N/A	N/A	N/A	N/A	$0.08	$1.06
G0P008	Catalytic Converter	1	Yes	Multiple	N/A	N/A	N/A	N/A	$291.00	$291.00
G0P009	Head Gasket	1	No	MLS	Stamping	N/A	N/A	N/A	$20.00	$20.00
G0P010	Coolant Pump	1	Yes	Multiple	N/A	N/A	N/A	N/A	$283.88	$283.88
G0P011	Injectors	3	Yes	Multiple	N/A	N/A	N/A	N/A	$10.00	$30.00

E - Matlab Code

OttoCycleI3Real.m

```
% EMAE 360 Real Otto/Atkinson Cycle Analysis Tool

%The purpose of this program is to perform a more in depth real cycle
%analysis for an Inline 3 Engine. This is the final analysis script which
%calls all other functions to complete the engine analysis.


%Author: Carter Waligura

%Date: 10/23/2019

clc
clear
close all

set(0, 'DefaultAxesFontWeight', 'normal', ...
      'DefaultAxesFontSize', 18, ...
      'DefaultAxesFontAngle', 'normal', ...
      'DefaultAxesFontWeight', 'normal', ...
      'DefaultAxesTitleFontWeight', 'bold', ...
      'DefaultAxesTitleFontSizeMultiplier', 1.2) ;
set(groot,'defaultLineLineWidth',3)
%% Simple Combustion Analysis
%Stoich balanced for .87 octane
%0.87C8H18 + 0.13C7H16 + 12.2(O2 + 3.76N2) ? 7.8CO2 + 8.86H2O + 44.63 N2
M_oct=114.2; %g/mol
M_hept=100.2; %g/mol
M_air= 29; %g/mol  O2+3.76N2
AFratio_mol= 12.2*(1+3.76)/(.87+.13);
AFratio_mass=AFratio_mol*(M_air/(.87*M_oct+.13*M_hept)); %for stoichiometry
of burning fuel
%AFratio will be less for rich mixtures and greater for lean mixtures


%% Otto Cycle
%Variable
rc=10; %compression ratio
D=.0015; %m^3
T1=294; %K
P1=101300; %Pa
C=3; %number of cylinders


%Constants
%R = 287.058; %J/kg-K for air
```

```
R= 274.05; %for air-fuel mixture 87 octane
gamma = 1.4; %Not a constant
%Cp = 1.004; %kJ/kg
%Cv = 0.718; %kJ/kg
Qlhv = 42.7e6; %j/kg
%AFratio_mass = 14.7; % air to fuel ratio
mix=1;
fuel_id=2;

%Trade Study Variables
%%%%%%%%%%%%%%%%%%%%%%%%%%%%%%%%%%%%%%%%%%%%%%%%%%%%%%%%%%%%%%%%%%%%%%%%%%%%

N =800:100:10000; % RPM range

Nredin=find(N==8800);

% phi= .974*ones(1,length(N)); %Low Load
% elseif p==2
% phi= 1.19*ones(1,length(N)); %equivalence ratio for max load
% end
phi=.974*ones(1,length(N));

open_i2 = (-4)*pi/180; %Crank angle that cam rise begins where 0 degrees is
TDC
duration_i2=235; %degrees
lift_imax2= .011; %m max lift for high cam

open_i1= -8*pi/180;
duration_i1= 220;
lift_imax1=.0085;% New low lifts for VVL


lift_emax= .0085; %m These lift values give an optimal minimum area graph


lift_RPM= 6000; %Target to switch to higher cams %make sure that this number
is a multiple of the RPM you are switching between
lift_index= find(N==lift_RPM);

open_e= -225*pi/180;
duration_e= 235;


overlap1= (open_e+ pi/180*duration_e-open_i1)*180/pi;
overlap2= (open_e+ pi/180*duration_e-open_i2)*180/pi;

% phi_RPM= 6000; %RPM at which you switch to phi_high
% phi_low=1;
```

```
% phi_high=1.1;
%Code to implement variable equivalence ratio


%Variable Valve Timing
%Phasing
phase_delta= 15*pi/180; %degrees
phase_RPM= 4000; %Shifts intake for more atkinson

phase1_index= find(N==phase_RPM);

%%%%%%%%%%%%%%%%%%%%%%%%%%%%%%%%%%%%%%%%%%%%%%%%%%%%%%%%%%%%%%%%%%%%%%%%%%%%%%%
%% Otto Cycle
%First do an ideal otto cycle calculation to get some assumptions
 [~, rho1, m_air, m_dotair, rho2, P2, T2, rho3, P3, T3, rho4, P4, T4]...
      = FourStrokeOttoBTN(N,P1,T1,rc,D,C,gamma,Qlhv, R, AFratio_mass);

m_total_full= m_air(1)*(1+phi/AFratio_mass);

D_cc=D*1000000;

%% Bore to Stroke and Piston Speed

BS=1;
bore= (D./C*4*BS/(pi))^(1/3); %for given B/S
stroke= bore/BS;%Equations given in Heywood

Sp_avg= stroke*2*N./60;
Sp_avgmax= max(Sp_avg);

crank_rad=stroke/2;

Vmin=D./(rc'-1);


%% Volume vs Crank angle

R_rodrad= 3.4; %from Design Team 2

theta=-2*pi:.03:2*pi;

[Vclear, crank_length, s, Vtheta, Sp_total] = VolumeCalc...
      (theta,D, rc,crank_rad, bore, Sp_avg,C,R_rodrad);



 %% Inefficiencies
%Mechanical
```

```
for k= 1:length(N)
%     if N(k)<=2400 can use this code for correlation from Heywood
%     mechfit= fit([N(1); 2400], [.9; .9], 'poly1');
%     Eff_mech(k)= mechfit(N(k));
%     else
%     mechfit= fit([2400; N(end)], [.90; .75], 'poly1');
%     Eff_mech(k)= mechfit(N(k));
%     end
      [W_f] = MechLosses(N,k,stroke);
      W_mech(k)=W_f(end);
end


%Combustion Eff
phi_eff = [.75; .85; 1; 1.2]; %These values were taken from Figure 3-9 in
Heywood
comb_phi = [.9; .97; .95; .79];
combfit= fit( phi_eff, comb_phi, 'poly2');


%% Air Flow Model
T0_i= T1;
P0_i=P1;

P0_e= 1e5; % Pa: Exhaust manifold pressure estimate

%In the future can try and optimize volumetric efficiency by finding the
%area below the curve
for q= 1:length(N)
%     if N(q)<phi_RPM
%           phi(q)=phi_low;
%     else
%           phi(q)=phi_high;
%     end

      Eff_comb(q)=combfit(phi(q)); %These lines change phi at the target RPM
and
      %Continually recalculate the combustion efficiency

      if N(q)<lift_RPM %VVL code
      lift_imax=lift_imax1; %Low Lift
      open_i= open_i1;
      duration_i=duration_i1;
      else

      lift_imax=lift_imax2; %High Lift
      open_i= open_i2;
      duration_i=duration_i2;
```

```
      end

      if N(q)<= phase_RPM
      open_i=open_i+phase_delta; %shifts more into the atkinson cycle
      overlap3= (open_e+ pi/180*duration_e-open_i)*180/pi;

      end

      clear m_total_loop
      m_total_loop=m_total_full;
      RPM=N(q);
   [Ev_iloop, Ev_eloop, Ev_totloop, dm_iloop, dm_eloop, m_total_loop, ...
      Pcylloop, Tcylloop, velocloop_i, Wintake, Wexhaust] = ...
      AirFlowModelBTNFinal(bore, RPM, rc,crank_rad, Sp_avg, R_rodrad,...
      C, D, T0_i,P0_i,R, phi(q), mix, P0_e,q, m_total_loop, lift_imax,...
      lift_emax, open_e, open_i, duration_i, duration_e);
      Ev_i(q)=Ev_iloop;
      Ev_e(q)=Ev_eloop;
      Ev_tot(q)=Ev_totloop;
      dm_i(q,:)=dm_iloop;
      dm_e(q,:)=dm_eloop;
      mtotal(q,:)=m_total_loop;
      Pcyl(q,:)=Pcylloop;
      Tcyl(q,:)=Tcylloop;
      Wintake_t(q)=Wintake;
      Wexhaust_t(q)=Wexhaust;

      % Cooling
   %[Flow_rate] =
Coolant_flow(Vmin,bore,stroke,Sp_avg(q),D_cc,T1,Pcyl(q,:),Tcyl(q,:),RPM);
      %Coolant_Flow(q)= Flow_rate;
      %Uncomment to get needed coolant requirements
end
 Wpump_t=Wexhaust_t+Wintake_t;

figure
pl(1)=plot(N,Ev_tot);
hold on
pl(2)=plot(N, Ev_i);
hold on
pl(3)=plot(N, Ev_e);
xlabel('RPM')
ylabel('Volumetric Efficiency')
title('RPM vs Volumetric Efficiency')

% pl(4)=xline(phase_RPM);
% text(phase_RPM, max(Ev_i)+.05, 'Atkinson Phasing')
```

```
pl(5)=xline(lift_RPM);
text(lift_RPM, max(Ev_i)+.05, 'High Power Lift Transition')

legend(pl([1 2 3]), 'Total', 'Inlet', 'Exhaust')
grid

txt = convertCharsToStrings([...
      'Inlet Max Lift (low):' num2str(lift_imax1*1000) 'mm' newline...
      'Inlet Max Lift (high):' num2str(lift_imax2*1000) 'mm' newline ...
      'Exhaust Max Lift:' num2str(lift_emax*1000) 'mm' newline...
      'Low Inlet Lift Duration:' num2str(duration_i1) ' degrees' newline...
      'Exhaust Lift Duration:' num2str(duration_e) ' degrees' newline...
      'Low Lift Overlap:' num2str(overlap1) ' degrees' newline...
      'High Inlet Lift Duration:' num2str(duration_i2) ' degrees' newline...
    'High Lift Overlap:' num2str(overlap2) ' degrees' newline ...
      'Phase Atkinson Overlap:' num2str(overlap3) ' degrees' newline]);
dim = [.2 .5 .3 .3];

annotation('textbox',dim,'String',txt,'FitBoxToText','on');


%% Real Cycle Anaysis
Vol_T= D/3+Vclear;

for j=1:length(N)
    q(j)=Qlhv*Eff_comb(j)*(m_air*Ev_tot(j)*phi(j)/AFratio_mass)/(P1*Vol_T);
      %This is where Comb and Vol Eff come in along with change in phi
      [w1,eta1,imep1, Cp, Cv, T, P, rho, theta_act,gammas]=...
      FiniteHeatReleaseBTN(rc,q(j),Vol_T, m_air, R,P1 ,phi(j));
      Eff_mech(j)= (w1*P1*Vol_T-W_mech(j))/(w1*P1*Vol_T);
      W_cycle(j)= w1*Eff_mech(j)*P1*Vol_T;
      Eff_therm(j)= eta1; %thermal eff
      IMEP_r(j)= imep1*P1; %indicated mean effective pressure
      T_comb(j,:)=T; %temperature of combustion chamber
      P_comb(j,:)=P;
end
figure
plot(N,Wpump_t)
hold on
plot(N,Wexhaust_t)
plot(N, Wintake_t)
xlabel('RPM')
ylabel('Pumping Losses per Cycle (J)')
title('Work Lost Through Simplified Pumping Losses')
legend('Total','Exhaust','Intake')

figure
```

```
plot(theta_act, T_comb(Nredin,:))
title(['Internal Temperature vs Crank Angle for ' num2str(N(Nredin)) ' RPM'])
xlabel(' Crank Angle (degrees)')
ylabel('Temperature (K)')
grid

figure
plot(theta_act, P_comb(Nredin,:)/1e6)
title(['Internal Pressure vs Crank Angle for ' num2str(N(Nredin)) ' RPM'])
xlabel(' Crank Angle (degrees)')
ylabel('Pressure (MPa)')
grid

%Incorporating Pumping Losses
Eff_pump= (W_cycle-Wpump_t)./W_cycle;
Wnet_cycle= W_cycle-Wpump_t;

figure
plot(N, Wnet_cycle)
hold on
plot(N, W_cycle)
plot(N,Wpump_t)
title('Work per Cycle vs RPM')
xlabel('RPM')
ylabel('Work Done or Lost per Cycle (J)')
legend('Net Work', 'Combustion Work', 'Pumping Losses')

P_cylinder_weib = Wnet_cycle.* N/120;
P_total_weib = P_cylinder_weib * C;
P_totalw_horse= P_total_weib*0.00134102;

torqueReal = P_totalw_horse./(N*2*pi)*33000;

%% Fuel Efficiency

Vel= [46.6 60 80];
for j= 1:length(N)
      [MPG(j,:)] = FuelEfficiencyBTN(m_air,AFratio_mass, phi(j), N(j), ...
      Wnet_cycle(j), torqueReal(j), Ev_tot(j), Vel, P_total_weib(j));
end

figure
plot(N, MPG(:,1))
hold on
plot(N, MPG(:,2))
plot(N, MPG(:,3))

title('Fuel Efficiency vs RPM at Different Speeds')
```

```
xlabel('RPM')
ylabel('MPG')
legend([num2str(Vel(1)) ' mph'],[num2str(Vel(2)) ' mph'],[num2str(Vel(3)) '
mph'])
axis([ 1000 7000 20 75])
grid

 Figure
plot(N,MPG(:,2))
axis([ 1000 7000 20 75])
hold on
fuelRPM=3500;
xline(fuelRPM);
text(fuelRPM, 60, 'Target RPM')
xlabel('RPM')
ylabel('Fuel Efficiency (MPG)')
title(['Fuel Efficiency Graph for phi= ' num2str(phi(1)) ' '])
%legend('Atkinson Phased', 'Original')
grid
%% Emissions

[NOHC_emis, CO_emis] = EmissionsBTN(phi(1), AFratio_mass, N, m_dotair, Vel,
Ev_tot);

%% Final Plotting
figure
plot(N, Eff_comb)
hold on
plot(N, Eff_mech)
plot(N, Ev_tot)
plot(N,Eff_pump)
xlabel('RPM')
ylabel('Efficiency')
title(['Engine Efficiencies for phi=' num2str(phi(1)) ''])
legend('Combustion','Mechanical', 'Volumetric', 'Pumping')


figure
pl(7)=plot(N, P_totalw_horse);
ylabel('Horsepower')
hold on
yyaxis right
pl(8)=plot(N, torqueReal);
ylabel('Torque (ft-lb)')
xlabel( 'RPM')
title('Real RPM vs Horsepower for an I3 Engine')

yyaxis left
```

```
% p(4)=xline(phase_RPM);
% text(phase_RPM, P_totalw_horse(end)/1, 'Atkinson Phasing')
pl(5)=xline(lift_RPM);
text(lift_RPM, P_totalw_horse(end)/1.1, 'High Power Lift Transition')


legend(pl([7 8]), 'Horsepower', 'Torque')

grid

dim = [.2 .4 .3 .3];

annotation('textbox',dim,'String',txt,'FitBoxToText','on');
```

FourStrokeOttoBTN.m

```
function [Cp, rho1, m_air, m_dotair, rho2, P2, T2, rho3, P3, T3, rho4,...
      P4, T4]= FourStrokeOttoBTN(N,P1,T1,rc,D,C,gamma,Qlhv, R, AFratio_mass)
   Cp = R*gamma/(gamma-1);

   %Computes simple 4 stroke otto cycle calculation for initial estimates
   %in real calculation

%Carter Waligura

% State 1
      rho1= P1/(R*T1);

      m_air = (D/C)*(rc/(rc-1)) * rho1; %per cylinder

      % Mass flow rate
      m_dotair= m_air*(N/120)*C;


      % State 2
      rho2 = rho1 *rc ;
      P2 = P1* (rho2./rho1)^gamma; %If P2>886K then 87 Octane will autoignite
      T2 = P2/(rho2* R);

      % State 3
      T3 = T2 + .8*Qlhv/(Cp* AFratio_mass); %.8 is combustion efficiency
      rho3= rho2;
      P3 = rho3 * R* T3;

      % State 4
      rho4=rho1;
      P4 = P3* (rho4/rho3)^ (gamma);
      T4 = P4/(rho4 * R);
end
```

OttoCycleTradeStudy.m (not fully necessary)

```
% EMAE 360 Ideal Otto Cycle and Combustion Tool

%The purpose of this program is to perform the simple idea otto cycle for
```

```
%a motorcycle engine in order to trade characteristics about the design


%Author: Carter Waligura

%Date: 09/09/2019

clc
clear
close all

set(0, 'DefaultAxesFontWeight', 'normal', ...
      'DefaultAxesFontSize', 18, ...
      'DefaultAxesFontAngle', 'normal', ...
      'DefaultAxesFontWeight', 'normal', ...
      'DefaultAxesTitleFontWeight', 'bold', ...
      'DefaultAxesTitleFontSizeMultiplier', 1.2) ;
set(groot,'defaultLineLineWidth',3)
%% Simple Combustion Analysis
%Stoich balanced for .87 octane
%0.87C8H18 + 0.13C7H16 + 12.2(O2 + 3.76N2) ? 7.8CO2 + 8.86H2O + 44.63 N2
M_oct=114.2; %g/mol
M_hept=100.2; %g/mol
M_air= 29; %g/mol  O2+3.76N2
AFratio_mol= 12.2*(1+3.76)/(.87+.13);
AFratio_mass=AFratio_mol*(M_air/(.87*M_oct+.13*M_hept)); %for stoichiometry
of burning fuel
%AFratio will be less for rich mixtures and greater for lean mixtures


%% Otto Cycle
%Variable
rc=9:.1:10; %compression ratio
D=.0015:.00005:.0018; %m^3
T1=300; %K
P1=101300; %Pa
C=6; %number of cylinders
N = 7500; % RPM, Max

%Constants
R = 287.058; %J/kg-K
gamma = 1.4;
C_p = 1.004; %kJ/kg
C_v = 0.718; %kJ/kg
Qlhv = 42.7e6; %j/kg
Cp = R*gamma/(gamma-1);
AFratio_mass = 14.7; % air to fuel ratio
```

```
for i=1:length(rc)
      %look at the effect of compression ratio on otto cycle
      % State 1
      rho1= P1/(R*T1);

      % State 2
      rho2(i) = rho1 *rc(i) ;
      P2(i) = P1* (rho2(i)./rho1)^gamma;
      T2(i) = P2(i)/(rho2(i)* R);

      % State 3
      T3(i) = T2(i) + .8*Qlhv/(Cp* AFratio_mass); %.8 is thermal efficiency
of combustion
      rho3(i)= rho2(i);
      P3(i) = rho3(i) * R* T3(i);

      % State 4
      rho4=rho1;
      P4(i) = P3(i)* (rho4/rho3(i))^ (gamma); %can make gamma 1.3 here to
make it more accurate
      T4(i) = P4(i)/(rho4 * R);

end

Cv = Cp-R;
for i= 1:length(rc)
      for j=1:length(D)
      % Work per cycle
      Ws(i) = Cv*((T3(i)-T2(i)) - (T4(i)-T1)); % J/kg;
      m_air(i,j) = (D(j)/C)*(rc(i)/(rc(i)-1)) * rho1; %per cylinder
      Wc(i,j) = Ws(i).*m_air(i,j); %J
      Wt(i,j) = Wc(i,j) * C;
      end
end

%Power
P_specific = Ws * N/120;
%specific power
P_cylinder = P_specific' .* m_air;
%power per cylinder
P_total = P_cylinder * C;
%total power
P_transmission = .8 * P_total;
%power given to transmission estimate


% SFC
SFC = (C * m_air/AFratio_mass)./(Wt); %kg/kj
```

```
SFC_Converted = SFC * 3.6e9; %g/Kw-hr

%Fuel Conversion Efficiency

Eff_f= 3600./(SFC_Converted*Qlhv/1000000);


%Indicated Mean Effective Pressure

IMEP= Wt./D; %Pa


%% Plotting

% Comparing Work Values for Compression Ratio and Displacement Combinations
D_cc=D*1000000;
[X,Y]=meshgrid(D_cc, rc);
P_totalhorse= P_total*0.00134102;
contourf(X,Y,P_totalhorse, 'ShowText', 'on')
title('Total Power (HP) of Engine vs Compression Ratio and Displacement')
xlabel('Displacement (cc)')
ylabel('Compression Ratio')
[A,b]=max(max(P_totalhorse));
crank_rad=find(P_totalhorse==A)/length(D);
fprintf('The greatest power produced by the engine is %.1fhp when the \n
compression ratio is %d:1 and the Displacement is %dcc \n', A, rc(crank_rad),
D_cc(b) )

%Comparing SFC to RC and D
figure
contourf(X,Y,SFC_Converted, 'showtext', 'on')

title('Specific Fuel Consumption (g/Kw-hr) of Engine vs Compression Ratio and
Displacement')
xlabel('Displacement (cc)')
ylabel('Compression Ratio')



% Mass flow rate vs rc and D

m_dot= m_air*(N/120)*C;

figure
contourf(X,Y, m_dot, 'showtext', 'on')

title('Air Flow (kg/s) into the Engine vs Compression Ratio and
Displacement')
```

```
xlabel('Displacement (cc)')
ylabel('Compression Ratio')


%DeltaTemp vs RC
figure

plot(rc, ones(1,length(rc))*T1-T1,'o-')

hold on

plot(rc, T2-T2(1),'kx-')

plot(rc, T3-T3(1),'.-')

plot(rc, T4-T4(1),'+-')

title('Change in Temperature vs Compression Ratio')
xlabel('Compression Ratio')
ylabel('Change in Temperature (K)')
legend('T1', 'T2', 'T3', 'T4')



%% Bore to Stroke and Piston Speed
%Heywood 2
Sp_avg= 25; %Max piston speed for motorcycle (m/s)
N_red=7500;

stroke= (Sp_avg*60)/(2*N_red);
crank_rad=stroke/2;

Vmin=D./(rc'-1);

bore= sqrt(D./6*4/(pi*stroke)); %Bore

BS=bore./stroke;
```

VolumeCalc.m

```
function [Vclear, crank_length, s, Vtheta, Sp_total] = VolumeCalc...
      (theta,D, rc,crank_rad, bore, Sp_avg,C, R_rodrad)
%Purpose is to calculate the volume in a singular cyclinder for any value
theta for crank angle

%Carter Waligura

   for i=1:length(theta)
      Vclear= D/((rc-1)*C); %clearance volume at bottom of cylinder
      crank_length= R_rodrad*crank_rad;

      s(i)=
crank_rad*cos(theta(i))+sqrt(crank_length^2+crank_rad^2*(sin(theta(i)))^2);

      Vtheta(i)= Vclear+ pi*bore^2/4*(crank_length+crank_rad-s(i));
      %Volume vs crank angle

      Sp_total(:,i)= Sp_avg.*pi/2*sin(theta(i))*(1+cos(theta(i))/(R_rodrad^2-
(sin(theta(i)))^2)^.5);
      %instantaneous piston speed
   end
end
```

GammaCalc.m

```
function [Cp,Cv,R,gamma] = GammaCalc(T,P, phi, mix)
fuel_id=2;
```

```
%Purpose is to take in a temperature, pressure, and phi in order to calculate
a gamma value for each step

%Carter Waligura
switch mix
      case 1 %Fuel air mixture pre combustion
      f = 0.0785; %Residual faction; estimate from research. determined
through combustion analysis
      [~, ~, ~, ~, ~, R, Cp, ~, ~, ~] = farg( T, P/1000, phi, f,
fuel_id ); %ferguson file
      Cv = Cp - R;
      gamma = Cp / Cv;
      R = R * 1000;
      case 2 %post combustion mixture
      [ierr, ~, ~, ~, ~, ~, R, Cp, ~, ~, ~] = ecp( T, P/1000, phi,
fuel_id ); %ferguson file
      if ierr ~= 0
            fprintf('Error: %d\n',ierr)
            fprintf('T = %f\n',T)
            fprintf('P = %f\n',P)
      end
      Cv = Cp - R;
      gamma = Cp / Cv;
      R = R * 1000;
 end
end
```

farg.m

From Ferguson [cite]

```
function [Y, h, u, s, v, R, Cp, MW, dvdT, dvdP] = farg( T, P, phi, f,
fuel_id )
% [y, h, s, v, r, cp, mw, dlvlt, dlvlp] = farg( T, P, phi, f, fuel_id )
%
% Subroutine for Fuel Air Residual Gas
%
% inputs:
% T - temperature (K) [ 300 --> 1000 K ]
% P - pressure (kPa)
% phi - equivalence ratio
% f - residual fraction
% fuel_id - 1=Methane, 2=Gasoline, 3=Diesel, 4=Methanol, 5=Nitromethane
%
% outputs:
% y - mole fraction of constituents
% y(1) : CO2
% y(2) : H2O
% y(3) : N2
% y(4) : O2
% y(5) : CO
% y(6) : H2
% h - specific enthalpy of mixture, kJ/kg
% u - specific internal energy of mixture, kJ/kg
% s - specific entropy of mixture, kJ/kgK
% v - specific volume of mixture, m3/kg
% r - specific ideal gas constant, kJ/kgK
% cp - specific heat at constant pressure, kJ/kgK
% mw - molecular weight of mixture, kg/kmol
% dvdt - (dv/dT) at const P, m3/kg per K
% dvdp - (dv/dP) at const T, m3/kg per kPa
[ alpha, beta, gamma, delta, h_fuel, so_fuel, cp_fuel, m_fuel ] =
fuel( fuel_id, T );
% Table C-1: curve fit coefficients for thermodynamic properties 300 < T <
1000 K
% Cp/R = a1 + a2*T + a3*T^2 + a4*T^3 + a5*T^4
% h/RT = a1 + a2/2*T + a3/3*T^2 + a4/4*T^3 + a5/5*T^4 + a6/T
% so/R = a1*ln(T) + a2*T + a3/2*T^2 + a4/3*T^3 + a5/4*T^4 + a7
A = [ [ 0.24007797e+1, 0.87350957e-2, -0.66070878e-5, 0.20021861e-8,
0.63274039e-15,-0.48377527e+5, 0.96951457e+1 ]; ... % CO2
[ 0.40701275e+1, -0.11084499e-2, 0.41521180e-5, -0.29637404e-8, 0.80702103e-
12, -0.30279722e+5, -0.32270046 ]; ... % H2O
[ 0.36748261e+1, -0.12081500e-2, 0.23240102e-5, -0.63217559e-9, -0.2257725e-
12, -0.10611588e+4, 0.23580424e+1 ]; ... % N2
```

```
[ 0.36255985e+1, -0.18782184e-2, 0.70554544e-5, -0.67635137e-8, 0.21555993e-
11, -0.10475226e+4, 0.43052778e+1 ]; ... % O2
[ 0.37100928e+1, -0.16190964e-2, 0.36923594e-5, -0.20319674e-8, 0.23953344e-
12, -0.14356310e+5, 0.2955535e+1 ]; ... % CO
[ 0.30574451e+1, 0.26765200e-2, -0.58099162e-5, 0.55210391e-8, -0.1812273e-
11, -0.98890474e+3, -0.22997056e+1 ] ]; % H2


% molar mass of constituents
% CO2 H2O N2 O2 CO H2
Mi = [ 44.01, 18.02, 28.013, 32.00, 28.01, 2.016 ];
% Calculate stoichiometric molar air-fuel ratio
a_s = alpha + beta/4 - gamma/2;
% mole fraction of fuel, O2, N2
y_1 = 1 / (1 + 4.76*a_s/phi); % mole fraction for one mole of reactant
y_fuel = y_1; % assuming 1 mole fuel
y_O2 = a_s/phi * y_1; % a_s/phi moles O2
y_N2 = a_s/phi*3.76 * y_1; % a_s/phi * 3.76 moles N2
% mass of fuel air mixture (M'')
m_fa = y_fuel*m_fuel + y_O2*32.00 + y_N2*28.013;
% default case: no residual gas
Y = zeros(6,1);
m_r = 0; % mass of residual gas
y_r = 0; % mole fraction of residual gas in mixture
n = zeros(6,1);
dcdt = 0;
if ( phi <= 1 )
% lean combustion
n(1) = alpha;
n(2) = beta/2;
n(3) = delta/2 + 3.76*a_s/phi;
n(4) = a_s*(1/phi - 1);
else
% rich combustion
d1 = 2*a_s*(1-1/phi);
z = T/1000;
K = exp( 2.743 - 1.761/z - 1.611/z^2 + 0.2803/z^3 );
a1 = 1-K;
b1 = beta/2 + alpha*K - d1*(1-K);
c1 = -alpha*d1*K;
n(5) = (-b1 + sqrt(b1^2 - 4*a1*c1))/(2*a1);
% Required derivatives for Cp calculation of mixture
% calculate dcdt = dn5/dK * dK/dT
dkdt = -K*(-1.761+z*(-3.222+z*.8409))/1000;
dn5dk = -((alpha - n(5))*(n(5) + 2*a_s*(1/phi - 1)))/(beta/2 + n(5) +
2*a_s*(1/phi -1));
dcdt = dn5dk * dkdt;
n(1) = alpha - n(5);
```

```
n(2) = beta/2 - d1 + n(5);
n(3) = delta/2 + 3.76*a_s/phi;
n(6) = d1 - n(5);
end
% total moles


N = sum(n);
% calculate mole fractions and mass of residual gas
m_r = 0;
for i=1:6
Y(i) = n(i)/N;
m_r = m_r + Y(i)*Mi(i);
end
% compute residual mole fraction
y_r = 1/(1 + m_r/m_fa * (1/f-1));
% compute total mole fractions in mixture
for i=1:6
Y(i) = Y(i)*y_r;
end
% fuel mole fraction based on all moles
y_fuel = y_fuel*(1 - y_r);
% include intake N2 and O2
Y(3) = Y(3) + y_N2*(1 - y_r);
Y(4) = Y(4) + y_O2*(1 - y_r);
% compute properties of mixture
h = h_fuel*y_fuel;
s = (so_fuel-log(max(y_fuel,1e-15)))*y_fuel;
Cp = cp_fuel*y_fuel;
MW = m_fuel*y_fuel;
% compute component properties according to curve fits
cpo = zeros(6,1);
ho = zeros(6,1);
so = zeros(6,1);
for i=1:6
cpo(i) = A(i,1) + A(i,2)*T + A(i,3)*T^2 + A(i,4)*T^3 + A(i,5)*T^4;
ho(i) = A(i,1) + A(i,2)/2*T + A(i,3)/3*T^2 + A(i,4)/4*T^3 +A(i,5)/5*T^4 +
A(i,6)/T;
so(i) = A(i,1)*log(T) + A(i,2)*T + A(i,3)/2*T^2 + A(i,4)/3*T^3 +A(i,5)/4*T^4
+A(i,7);
end
table = [-1,1,0,0,1,-1];
for i=1:6
if(Y(i)>1.e-25)
h = h + ho(i)*Y(i);
s = s + Y(i)*(so(i)-log(Y(i)));
Cp = Cp+cpo(i)*Y(i)+ho(i)*T*table(i)*dcdt*y_r/N;
MW = MW + Y(i)*Mi(i);
```

```
end
end
R = 8.31434/MW; % compute mixture gas constant
h = R*T*h; % curve fit for h is h/rt
u = h-R*T;
v = R*T/P;
s = R*(-log(P/101.325)+s);


Cp = R*Cp; % curve fit for cp is cp/r
dvdT = v/T; % derivative of volume wrt temp
dvdP = -v/P; % derivative of volume wrt pres
```

ecp.m

From Ferguson [cite]

```
function [ierr, Y, h, u, s, v, R, Cp, MW, dvdT, dvdP] = ecp( T, P, phi,
ifuel )
% Subroutine for Equilibrium Combustion Products
%
% inputs:
%   T - temperature (K)        [ 600 --> 3500 ]
%   P - pressure (kPa)         [ 20 --> 30000 ]
%   phi - equivalence ratio    [ 0.01 --> ~3 ]
%   ifuel - 1=Methane, 2=Gasoline, 3=Diesel, 4=Methanol, 5=Nitromethane
%
% outputs:
%   ierr - Error codes:
%          0 = success
%          1 = singular matrix
%          2 = maximal pivot error in gaussian elimination
%          3 = no solution in maximum number of iterations
%          4 = result failed consistency check sum(Y)=1
%          5 = failure to obtain initial guess for oxygen concentration
%          6 = negative oxygen concentration in initial guess calculation
%          7 = maximum iterations reached in initial guess solution
%          8 = temperature out of range
%          9 = pressure out of range
%          10 = equivalence ratio too lean
%          11 = equivalence ratio too rich, solid carbon will be formed for
given fuel
%
%   y - mole fraction of constituents
%     y(1)  : CO2
%     y(2)  : H2O
%     y(3)  : N2
%     y(4)  : O2
%     y(5)  : CO
%     y(6)  : H2
%     y(7)  : H
%     y(8)  : O
%     y(9)  : OH
%     y(10) : NO
%   h  - specific enthalpy of mixture, kJ/kg
%   u  - specific internal energy of mixture, kJ/kg
%   s  - specific entropy of mixture, kJ/kgK
%   v  - specific volume of mixture, m3/kg
%   R  - specific ideal gas constant, kJ/kgK
%   Cp - specific heat at constant pressure, kJ/kgK
%   MW - molecular weight of mixture, kg/kmol
```

```
%   dvdt - (dv/dT) at const P,  m3/kg per K
%   dvdp - (dv/dP) at const T,  m3/kg per kPa

% initialize outputs
Y = zeros(10,1);
h = 0;
u = 0;
s = 0;
v = 0;
R = 0;
Cp = 0;
MW = 0;
dvdT = 0;
dvdP = 0;

% solution parameters
prec = 1e-3;
MaxIter = 20;

% square root of pressure (used many times below)
PATM = P/101.325;
sqp = sqrt(PATM);

if ( T < 600 || T > 3500 )
      ierr = 8;
      return;
end

if ( P < 20 || P > 30000 )
      ierr = 9;
      return;
end

if ( phi < 0.01 )
      ierr = 10;
      return;
end


% Get fuel composition information
[ alpha, beta, gamma, delta ] = fuel( ifuel, T );


% Equilibrium constant curve fit coefficients.
% Valid in range: 600 K < T < 4000 K
%           Ai           Bi           Ci           Di           Ei
Kp = [ [  0.432168,    -0.112464e+5,  0.267269e+1, -0.745744e-4,  0.242484e-
8 ]; ...
```

```
      [  0.310805,      -0.129540e+5,  0.321779e+1, -0.738336e-4,  0.344645e-
8 ]; ...
      [ -0.141784,      -0.213308e+4,  0.853461,     0.355015e-4, -0.310227e-
8 ]; ...
      [  0.150879e-1, -0.470959e+4,  0.646096,  0.272805e-5, -0.154444e-
8 ]; ...
      [ -0.752364,      0.124210e+5, -0.260286e+1,  0.259556e-3, -0.162687e-
7 ]; ...
      [ -0.415302e-2,  0.148627e+5, -0.475746e+1,  0.124699e-3, -0.900227e-
8 ] ];

K = zeros(6,1);
for i=1:6
      log10ki = Kp(i,1)*log(T/1000) + Kp(i,2)/T  +  Kp(i,3) + Kp(i,4)*T +
Kp(i,5)*T*T;
      K(i) = 10^log10ki;
end


c1 = K(1)/sqp;
c2 = K(2)/sqp;
c3 = K(3);
c4 = K(4);
c5 = K(5)*sqp;
c6 = K(6)*sqp;

[ ierr, y3, y4, y5, y6 ] = guess( T, phi, alpha, beta, gamma, delta, c5,
c6 );

if ( ierr ~= 0 )
      return;
end

a_s = alpha + beta/4 - gamma/2;


D1 = beta/alpha;
D2 = gamma/alpha + 2*a_s/(alpha*phi);
D3 = delta/alpha + 2*3.7619047619*a_s/(alpha*phi);
A = zeros(4,4);

final = 0;

for jj=1:MaxIter,

      sqy6 = sqrt(y6);
      sqy4 = sqrt(y4);
      sqy3 = sqrt(y3);
```

```
      y7=  c1*sqy6;
      y8=  c2*sqy4;
      y9=  c3*sqy4*sqy6;
      y10= c4*sqy4*sqy3;
      y2=  c5*sqy4*y6;
      y1=  c6*sqy4*y5;

      d76 = 0.5*c1/sqy6;
      d84 = 0.5*c2/sqy4;
      d94 = 0.5*c3*sqy6/sqy4;
      d96 = 0.5*c3*sqy4/sqy6;
      d103 = 0.5*c4*sqy4/sqy3;
      d104 = 0.5*c4*sqy3/sqy4;
      d24 = 0.5*c5*y6/sqy4;
      d26 = c5*sqy4;
      d14 = 0.5*c6*y5/sqy4;
      d15 = c6*sqy4;

      % form the Jacobian matrix
      A = [ [ 1+d103,  d14+d24+1+d84+d104+d94,   d15+1,  d26+1+d76+d96 ]; ...
            [ 0,         2.*d24+d94-D1*d14,      -D1*d15-D1,
2*d26+2+d76+d96; ]; ...
            [ d103,   2*d14+d24+2+d84+d94+d104-D2*d14,  2*d15+1-D2*d15-D2,
d26+d96 ]; ...
            [ 2+d103, d104-D3*d14, -D3*d15-D3,0 ] ];

      if ( final )
      break;
      end

      B = [ -(y1+y2+y3+y4+y5+y6+y7+y8+y9+y10-1);  ...
            -(2.*y2 + 2.*y6 + y7 + y9 -D1*y1 -D1*y5); ...
            -(2.*y1 + y2 +2.*y4 + y5 + y8 + y9 + y10 -D2*y1 -D2*y5); ...
            -(2.*y3 + y10 -D3*y1 -D3*y5)  ];

      [ B, ierr ] = gauss( A, B );
      if ( ierr ~= 0 )
      return;
      end

      y3 = y3 + B(1);
      y4 = y4 + B(2);
      y5 = y5 + B(3);
      y6 = y6 + B(4);

      nck = 0;
      if ( abs(B(1)/y3) > prec )
```

```
      nck = nck+1;
      end
      if ( abs(B(2)/y4) > prec )
      nck = nck+1;
      end
      if ( abs(B(3)/y5) > prec )
      nck = nck+1;
      end
      if ( abs(B(4)/y6) > prec )
      nck = nck+1;
      end

      if( nck == 0 )
      % perform top half of loop to update remaining mole fractions
      % and Jacobian matrix
      final = 1;
      continue;
      end
end


if (jj>=MaxIter)
      ierr = 3;
      return;
end

Y = [ y1 y2 y3 y4 y5 y6 y7 y8 y9 y10 ];

% consistency check
if( abs( sum(Y)-1 ) > 0.0000001 )
      ierr = 4;
      return;
end


% constants for partial derivatives of properties
dkdt = zeros(6,1);
for i=1:6,
      dkdt(i) = 2.302585*K(i)*( Kp(i,1)/T - Kp(i,2)/(T*T) + Kp(i,4)
+2*Kp(i,5)*T );
end

dcdt = zeros(6,1);
dcdt(1) = dkdt(1)/sqp;
dcdt(2) = dkdt(2)/sqp;
dcdt(3) = dkdt(3);
dcdt(4) = dkdt(4);
dcdt(5) = dkdt(5)*sqp;
```

```
dcdt(6) = dkdt(6)*sqp;

dcdp = zeros(6,1);
dcdp(1) = -0.5*c1/P;
dcdp(2) = -0.5*c2/P;
dcdp(5) = 0.5*c5/P;
dcdp(6) =  0.5*c6/P;

x1  = Y(1)/c6;
x2  = Y(2)/c5;
x7  = Y(7)/c1;
x8  = Y(8)/c2;
x9  = Y(9)/c3;
x10 = Y(10)/c4;

dfdt(1) = dcdt(6)*x1 + dcdt(5)*x2 + dcdt(1)*x7 +dcdt(2)*x8 +dcdt(3)*x9 +
dcdt(4)*x10;
dfdt(2) = 2.*dcdt(5)*x2 + dcdt(1)*x7 + dcdt(3)*x9 -D1*dcdt(6)*x1;
dfdt(3) = 2.*dcdt(6)*x1 + dcdt(5)*x2 + dcdt(2)*x8 +dcdt(3)*x9 + dcdt(4)*x10 -
D2*dcdt(6)*x1;
dfdt(4) = dcdt(4)*x10 -D3*dcdt(6)*x1;

dfdp(1) = dcdp(6)*x1 + dcdp(5)*x2 + dcdp(1)*x7 +dcdp(2)*x8;
dfdp(2) = 2.*dcdp(5)*x2 + dcdp(1)*x7  -D1*dcdp(6)*x1;
dfdp(3) = 2.*dcdp(6)*x1 + dcdp(5)*x2 + dcdp(2)*x8  - D2*dcdp(6)*x1;
dfdp(4) = -D3*dcdp(6)*x1;

dfdphi(1) = 0;
dfdphi(2) = 0;
dfdphi(3) = 2*a_s/(alpha*phi*phi)*(Y(1)+Y(5));
dfdphi(4) = 2*3.7619047619*a_s/(alpha*phi*phi)*(Y(1)+Y(5));


% solve matrix equations for independent temperature derivatives
b = -1.0 .* dfdt'; %element by element mult.
[b, ierr] = gauss(A,b);%  solve for new b with t derivatives
if ( ierr ~= 0 )
      return;
end
dydt(3) = b(1);
dydt(4) = b(2);
dydt(5) = b(3);
dydt(6) = b(4);
dydt(1) = sqrt(Y(4))*Y(5)*dcdt(6) + d14*dydt(4) + d15*dydt(5);
dydt(2) = sqrt(Y(4))*Y(6)*dcdt(5) + d24*dydt(4) + d26*dydt(6);
dydt(7) = sqrt(Y(6))*dcdt(1) + d76*dydt(6);
dydt(8) = sqrt(Y(4))*dcdt(2) + d84*dydt(4);
dydt(9) = sqrt(Y(4)*Y(6))*dcdt(3) + d94*dydt(4) + d96*dydt(6);
```

```
dydt(10) = sqrt(Y(4)*Y(3))*dcdt(4) + d104*dydt(4) + d103*dydt(3);


% solve matrix equations for independent pressure derivatives
b = -1.0 .* dfdp'; %element by element mult.
[b,ierr] = gauss(A,b); %  solve for new b with p derivatives
if ( ierr~=0 )
      return;
end
dydp(3) = b(1);
dydp(4) = b(2);
dydp(5) = b(3);
dydp(6) = b(4);
dydp(1) = sqrt(Y(4))*Y(5)*dcdp(6) + d14*dydp(4) + d15*dydp(5);
dydp(2) = sqrt(Y(4))*Y(6)*dcdp(5) + d24*dydp(4) + d26*dydp(6);
dydp(7) = sqrt(Y(6))*dcdp(1) + d76*dydp(6);
dydp(8) = sqrt(Y(4))*dcdp(2) + d84*dydp(4);
dydp(9) = d94*dydp(4) + d96*dydp(6);
dydp(10)= d104*dydp(4) + d103*dydp(3);

% molecular weights of constituents (g/mol)
%     CO2     H2O       N2          O2       CO       H2    H        O
      OH          NO
Mi = [ 44.01,  18.02,   28.013,   32.00,   28.01,   2.016,   1.009,   16.,
17.009,   30.004];

if ( T > 1000 )
      % high temp curve fit coefficients for thermodynamic properties 1000 <
T < 3000 K
      AAC = [ ...
       [.446080e+1,.309817e-2,-.123925e-5,.227413e-9, -.155259e-
13,-.489614e+5,-.986359 ]; ...
       [.271676e+1,.294513e-2,-.802243e-6,.102266e-9, -.484721e-
14,-.299058e+5,.663056e+1 ]; ...
      [.289631e+1,.151548e-2,-.572352e-6,.998073e-10,-.652235e-
14,-.905861e+3,.616151e+1 ]; ...
       [.362195e+1,.736182e-3,-.196522e-6,.362015e-10,-.289456e-
14,-.120198e+4,.361509e+1 ]; ...
       [.298406e+1,.148913e-2,-.578996e-6,.103645e-9, -.693535e-
14,-.142452e+5,.634791e+1 ]; ...
      [.310019e+1,.511194e-3, .526442e-7,-.349099e-10,.369453e-
14,-.877380e+3,-.196294e+1 ]; ...
      [.25e+1,0,0,0,0,.254716e+5,-.460117 ]; ...
       [.254205e+1,-.275506e-4,-.310280e-8,.455106e-11,-.436805e-
15,.292308e+5,.492030e+1 ]; ...
       [.291064e+1,.959316e-3,-.194417e-6,.137566e-10,.142245e-
15,.393538e+4,.544234e+1 ]; ...
```

```
      [.3189e+1  ,.133822e-2,-.528993e-6,.959193e-10,-.648479e-
14,.982832e+4,.674581e+1 ]; ];
elseif ( T <= 1000 )
      % low temp curve fit coefficients for thermodynamic properties, 300 < T
<= 1000 K
      AAC = [ ...
      [ 0.24007797e+1,  0.87350957e-2, -0.66070878e-5,  0.20021861e-8,
0.63274039e-15, -0.48377527e+5,  0.96951457e+1 ]; ... % CO2
      [ 0.40701275e+1, -0.11084499e-2,  0.41521180e-5, -0.29637404e-8,
0.80702103e-12, -0.30279722e+5, -0.32270046     ]; ... % H2O
      [ 0.36748261e+1, -0.12081500e-2,  0.23240102e-5, -0.63217559e-9, -
0.22577253e-12, -0.10611588e+4,  0.23580424e+1 ]; ... % N2
      [ 0.36255985e+1, -0.18782184e-2,  0.70554544e-5, -0.67635137e-8,
0.21555993e-11, -0.10475226e+4,  0.43052778e+1 ]; ... % O2
      [ 0.37100928e+1, -0.16190964e-2,  0.36923594e-5, -0.20319674e-8,
0.23953344e-12, -0.14356310e+5,  0.2955535e+1  ]; ... % CO
      [ 0.30574451e+1,  0.26765200e-2, -0.58099162e-5,  0.55210391e-8, -
0.18122739e-11, -0.98890474e+3, -0.22997056e+1 ]; ... % H2
      [ 0.25000000e+1,  0,                0,                0,
      0,                0.25471627e+5, -0.46011762e+0 ]; ... % H
      [ 0.29464287e+1, -0.16381665e-2,  0.24210316e-5, -0.16028432e-8,
0.38906964e-12,  0.29147644e+5,  0.29639949e+1 ]; ... % O
      [ 0.38375943e+1, -0.10778858e-2,  0.96830378e-6,  0.18713972e-9, -
0.22571094e-12,  0.36412823e+4,  0.49370009e+0 ]; ... % OH
      [ 0.40459521e+1, -0.34181783e-2,  0.79819190e-5, -0.61139316e-8,
0.15919076e-11,  0.97453934e+4,  0.29974988e+1 ]; ... % H2
      ];
end

% compute cp,h,s
% initialize h, etc to zero
MW = 0;
Cp = 0;
h = 0;
s = 0;
dMWdT = 0;
dMWdP = 0;

for i=1:10,
      cpo = AAC(i,1) + AAC(i,2)*T + AAC(i,3)*T^2 + AAC(i,4)*T^3 +
AAC(i,5)*T^4;
      ho = AAC(i,1) + AAC(i,2)/2*T + AAC(i,3)/3*T^2 + AAC(i,4)/4*T^3
+AAC(i,5)/5*T^4 + AAC(i,6)/T;
      so = AAC(i,1)*log(T) + AAC(i,2)*T + AAC(i,3)/2*T^2 + AAC(i,4)/3*T^3
+AAC(i,5)/4*T^4 +AAC(i,7);

      h = h + ho*Y(i); % h is h/rt here
      MW = MW + Mi(i)*Y(i);
```

```
      dMWdT = dMWdT + Mi(i)*dydt(i);
      dMWdP = dMWdP + Mi(i)*dydp(i);
      Cp = Cp+Y(i)*cpo + ho*T*dydt(i);

      if (Y(i)> 1.0e-37)
      s = s + Y(i)*(so - log(Y(i)));
      end
end

R = 8.31434/MW;
v = R*T/P;
Cp = R*(Cp - h*T*dMWdT/MW);
h = h*R*T;
s = R*(-log(PATM) + s);
u=h-R*T;
dvdT = v/T*(1 - T*dMWdT/MW);
dvdP = v/P*(-1 + P*dMWdP/MW);

ierr = 0;
return;


      function [ierr, y3, y4, y5, y6] = guess( T, phi, alpha, beta, gamma,
delta, c5, c6 )
      ierr = 0;
      y3 = 0;
      y4 = 0;
      y5 = 0;
      y6 = 0;

      % estimate number of total moles produced, N
      n = zeros(6,1);

      % Calculate stoichiometric molar air-fuel ratio
        a_s = alpha + beta/4 - gamma/2;

      if ( phi <= 1 )
            % lean combustion
            n(1) = alpha;
            n(2) = beta/2;
            n(3) = delta/2 + 3.76*a_s/phi;
            n(4) = a_s*(1/phi - 1);
      else
            % rich combustion
            d1 = 2*a_s*(1-1/phi);
            z = T/1000;
            KK = exp( 2.743 - 1.761/z - 1.611/z^2 + 0.2803/z^3 );
```

```
            aa = 1-KK;
            bb = beta/2 + alpha*KK - d1*(1-KK);
            cc = -alpha*d1*KK;
            n(5) = (-bb + sqrt(bb^2 - 4*aa*cc))/(2*aa);

            n(1) = alpha - n(5);
            n(2) = beta/2 - d1 + n(5);
            n(3) = delta/2 + 3.76*a_s/phi;
            n(6) = d1 - n(5);
      end

      % total product moles per 1 mole fuel
      N = sum(n);

      % try to get close to a reasonable value of ox mole fraction
      % by finding zero crossing of 'f' function
      ox = 1;
      nIterMax=40;
      for ii=1:nIterMax,
            f = 2*N*ox - gamma - (2*a_s)/phi + (alpha*(2*c6*ox^(1/2) +
1))/(c6*ox^(1/2) + 1) + (beta*c5*ox^(1/2))/(2*c5*ox^(1/2) + 2);
            if ( f < 0 )
                  break;
            else
                  ox = ox*0.1;
                  if ( ox < 1e-37 )
                  ierr = 5;
                  return;
                  end
            end
      end

      % now zero in on the actual ox mole fraction using Newton-Raphson
iteration
      for ii=1:nIterMax,
            f = 2*N*ox - gamma - (2*a_s)/phi + (alpha*(2*c6*ox^(1/2) +
1))/(c6*ox^(1/2) + 1) + (beta*c5*ox^(1/2))/(2*c5*ox^(1/2) + 2);
            df = 2*N - (beta*c5^2)/(2*c5*ox^(1/2) + 2)^2 +
(alpha*c6)/(ox^(1/2)*(c6*ox^(1/2) + 1)) +
(beta*c5)/(2*ox^(1/2)*(2*c5*ox^(1/2) + 2)) - (alpha*c6*(2*c6*ox^(1/2) +
1))/(2*ox^(1/2)*(c6*ox^(1/2) + 1)^2);
            dox = f/df;
            ox = ox - dox;
            if ( ox < 0.0 )
                  ierr = 6;
                  return;
            end
            if ( abs(dox/ox) < 0.001 )
```

```
            break;
      end
end

if( ii == nIterMax )
      ierr = 7;
      return;
end

y3 = 0.5*(delta + a_s/phi*2*3.76)/N;
y4 = ox;
y5 = alpha/N/(1+c6*sqrt(ox));
y6 = beta/2/N/(1+c5*sqrt(ox));

end % guess

function [B, IERQ] = gauss( A, B )
% maximum pivot gaussian elimination routine adapted
% from FORTRAN in Olikara & Borman, SAE 750468,  1975
% not using built-in MATLAB routines because they issue
% lots of warnings for close to singular matrices
% that haven't seemed to cause problems in this application
% routine below does check however for true singularity

IERQ = 0;

for N=1:3,
      NP1=N+1;
      BIG = abs( A(N,N) );
      if ( BIG < 1.0e-05)
      IBIG=N;

      for I=NP1:4,
            if( abs(A(I,N)) <= BIG )
                  continue;
            end
            BIG = abs(A(I,N));
            IBIG = I;
      end

      if(BIG <= 0.)
            IERQ=2;
            return;
      end

      if( IBIG ~= N)
            for J=N:4,
                  TERM = A(N,J);
```

```
                        A(N,J) = A(IBIG,J);
                        A(IBIG,J) = TERM;
                  end

                  TERM = B(N);
                  B(N) = B(IBIG);
                  B(IBIG) = TERM;
            end
            end

            for I=NP1:4,
            TERM = A(I,N)/A(N,N);

            for J=NP1:4,
                  A(I,J) = A(I,J)-A(N,J)*TERM;
            end

            B(I) = B(I)-B(N)*TERM;
            end
      end

      if( abs(A(4,4)) > 0.0 )
            B(4) = B(4)/A(4,4);
            B(3) = (B(3)-A(3,4)*B(4))/A(3,3);
            B(2) = (B(2)-A(2,3)*B(3)-A(2,4)*B(4))/A(2,2);
            B(1) = (B(1)-A(1,2)*B(2)-A(1,3)*B(3)-A(1,4)*B(4))/A(1,1);
      else
            IERQ=1; % singular matrix
            return;
      end
      end % gauss()


end % ecp()
```

FiniteHeatReleaseBTN.m

Code Adapted from Ferguson [source]

```
function [w1,eta1,imep1, Cp, Cv, T, P, rho,
theta_act,gammas]=FiniteHeatReleaseBTN(rc,q,Vol_T, m_air, R,P1 ,phi)
%Outputs net specific work, thermal efficiency, specific mean effective
pressure,
%Originally from Ferguson
%Edited to make use in EMAE 360 BTN Performance


% Gas cycle heat release code for two engines

% engine parameters

%CHANGE THETA START AND DURATION TO RELATE TO RPM

thetas(1,1)= -20; % Engine1 start of heat release (deg)
%thetas(2,1)= -10;   % Engine2 start of heat release (deg)
thetad(1,1) = 30; % Engine1 duration of heat release (deg)
%thetad(2,1) = 10; % Engine2 duration of heat release (deg)

% rc=10;
% q=34.1;
gamma= 1.4; %gas const

a= 5;  %weibe parameter a
n= 3; %weibe exponent n

step=1;     % crankangle interval for calculation/plot
NN=360/step; % number of data points

% initialize the results data structure
save.theta=zeros(NN,1); % crankangle
save.vol=zeros(NN,1);   % volume
save.press=zeros(NN,2); % pressure
save.work=zeros(NN,2);  % work

pinit(1) = 1; % Engine 1 initial dimensionless pressure P/P1
pinit(2) = 1; % Engine 2 initial dimensionless pressure P/P1

% for loop for engine1 and engine2
for j=1
theta = -180;           %initial crankangle
thetae = theta + step; %final crankangle in step
fy(1) = pinit(j); % assign initial pressure to working vector
```

```
fy(2) =0.;         % reset work vector

  % for loop for pressure and work calculation
  for i=1:NN
      [fy, vol] = integrate(theta,thetae,fy);

      % reset to next interval
      theta = thetae;
      thetae = theta+step;

      % copy results to output vectors
      save.theta(i)=theta;
      save.vol(i)=vol;
      save.press(i,j)=fy(1);
      save.work(i,j)=fy(2);
%%%%%%%%%%%%%%%%%%%%%%%%%%%%%%%%%%%%%%%%%%%%%%%%%%%%%%%%%%%%%%%%
%Main Addition
      theta_act(i)=theta;
      P(i)=fy(1)*P1;
      Vol=vol*Vol_T;
      rho(i)= m_air/(Vol);
      T(i)= P(i)/(rho(i)* R);
   if T(i)<1000
      mix(i)=1;
      else
      mix(i)=2;
      end

      [Cp(i),Cv(i),R,gamma] = GammaCalc(T(i),P(i), phi, mix(i));
      %gamma=1.4;
      gammas(i)= gamma;

%%%%%%%%%%%%%%%%%%%%%%%%%%%%%%%%%%%%%%%%%%%%%%%%%%%%%%%%%%%%%%%%

  end %end of pressure and work iteration loop
end %end of engine iteration loop

[pmax1, id_max1] = max(save.press(:,1)); %Engine 1 max pressure
[pmax2, id_max2] = max(save.press(:,2)); %Engine 2 max pressure
thmax1=save.theta(id_max1);%Engine 1 crank angle
thmax2=save.theta(id_max2);%Engine 2 crank angle

w1=save.work(NN,1);
w2=save.work(NN,2);
eta1= w1./q; % thermal efficiency
eta2= w2./q;
imep1 = eta1.*q*(rc/(rc -1)); %imep
imep2 = eta2.*q*(rc/(rc -1));
```

```
eta_rat1 = eta1/(1-rc^(1-gamma));
eta_rat2 = eta2/(1-rc^(1-gamma));

% output overall results
% fprintf('                    Engine 1          Engine 2  \n');
% fprintf(' Theta_start       %5.2f             %5.2f \n', thetas(1,1),
thetas(2,1));
% fprintf(' Theta_dur         %5.2f             %5.2f \n', thetad(1,1),
thetad(2,1));
% fprintf(' P_max/P_1         %5.2f             %5.2f \n', pmax1, pmax2);
% fprintf(' Theta_max         %7.1f             %7.1f \n',thmax1,thmax2);
% fprintf(' Net Work/P1V1   %7.2f               %7.2f \n', w1,w2);
% fprintf(' Efficiency        %5.3f                 %5.3f  \n', eta1, eta2);
% fprintf(' Eff. Ratio        %5.3f             %5.3f  \n', eta_rat1,
eta_rat2);
% fprintf(' Imep/P1           %5.2f             %5.2f  \n', imep1, imep2);

%plot results

%set(gcf,'Units','pixels','Position', [50,50,1200,600]);
%subplot(1,2,1);

% Figure();
% %subplot(1,2,2);
% plot(save.theta,save.work(:,1),'-',save.theta,save.work(:,2),'--',
'linewidth',2)
% set(gca, 'fontsize', 18,'linewidth',2);
% %grid
% title('Dimensionless Work for One Cylinder Cycle')
% xlabel('Theta (deg)','fontsize', 18)
% ylabel('Work','fontsize', 18)


function[fy,vol] = integrate(theta,thetae,fy)
%  ode23 integration of the pressure differential equation
%  from theta to thetae with current values of fy as initial conditions
[tt, yy] = ode23(@rates, [theta thetae], fy);
%put last element of yy into fy vector
 for k=1:2
  fy(k) = yy(length(tt),k);
 end
%pressure differential equation
      function [yprime] = rates(theta,fy)
      vol=(1.+ (rc -1)/2.*(1-cosd(theta)))/rc;
      dvol=(rc - 1)/2.*sind(theta)/rc*pi/180.; %dvol/dtheta
      dx=0.; %set heat release to zero
      if(theta > thetas(j)) % then heat release dx  > 0
      dum1=(theta -thetas(j))/thetad(j);
```

```
      x=1.- exp(-(a*dum1^n));
      dx=(1-x)*a*n*dum1^(n-1)/thetad(j); %dx/dthetha
      end
      term1= -gamma*fy(1)*dvol/vol;
      term2= (gamma-1).*q*dx/vol;
      yprime(1,1)= term1 + term2;
      yprime(2,1)= fy(1)*dvol;
      end %end of function rates
end  %end of function integrate2
end
```

AirFlowModelBTNFinal.m

```
function  [Ev_iloop, Ev_eloop, Ev_totloop, dm_iloop, dm_eloop,
m_total_loop, ...
      Pcylloop, Tcylloop, velocloop_i, Wintake, Wexhaust] = ...
      AirFlowModelBTNFinal(bore, RPM, rc,crank_rad, Sp_avg, R_rodrad,...
      C, D, T0_i,P0_i,R, phi, mix,P0_e,q, m_total_loop, lift_imax,...
      lift_emax, open_e, open_i, duration_i, duration_e)
% EMAE 360 Air Flow Model Tool
clear Ev_iloop Ev_eloop Ev_totloop dm_iloop dm_eloop
%The purpose of this program is to model the air flow within an I3 motorcycle
engine

%Author: Carter Waligura

%Date: 10/22/2019


set(0, 'DefaultAxesFontWeight', 'normal', ...
      'DefaultAxesFontSize', 18, ...
      'DefaultAxesFontAngle', 'normal', ...
      'DefaultAxesFontWeight', 'normal', ...
      'DefaultAxesTitleFontWeight', 'bold', ...
      'DefaultAxesTitleFontSizeMultiplier', 1.2) ;
set(groot,'defaultLineLineWidth',3)

close_e= open_e+duration_e*pi/180;
close_i = open_i+(duration_i)*pi/180; %crank angle that cam closes the valve

overlap= (open_e+ pi/180*duration_e-open_i)*180/pi;

thetas= -2*pi;
thetae= 2*pi;
theta=thetas:.01:thetae;

Tcylloop= 1000; %Temperature at the end of a cycle in the cylinder
PPP=4.5e5;%Pressure at end of cycle
Pcylloop=PPP*ones(1,length(theta));
%These are the temp and pressure for inside the cylinder at the beginning of
exhaust



rho0_i= P0_i/(T0_i*R);
[~,~,~,gamma0_i] = GammaCalc(T0_i,P0_i, phi, mix);
c0_e= sqrt(gamma0_i*R*T0_i); %speed of sound
```

```
%% Valve Dimensions

% D_intake= .33*bore;
% D_exhaust=.29*bore; %ferguson estimations 5.11
D_exhaust=.029; %These values were supplied from Group 1
D_intake=.0375;


%from Heywood page 221 we can get valve geometry
Ds_i= .25*D_intake; %stem diameter
Dv_i= 1.1*D_intake; %head diameter
w_i= (Dv_i-D_intake)/2; %seat width
Dm_i = Dv_i-w_i; %mean seat diameter

Ds_e= .25*D_exhaust; %stem diameter
Dv_e= 1.1*D_exhaust; %head diameter
B= 45*pi/180; %seat angle
w_e= (Dv_e-D_exhaust)/2; %seat width
Dm_e = Dv_e-w_e; %mean seat diameter

%% Valve Lift vs Angle


for i=1:length(theta) %intake
      if theta(i)>=open_i && theta(i)<close_i
      %lift_inb(i)= -(theta(i)-open_i)*(theta(i)-close_i);
      [s] = Cam_Profile_Function_I(lift_imax, duration_i,theta(i), open_i);
      lift_inb(i)=s;
      else
      lift_inb(i)=0;
      end
end
maxyi= max(lift_inb);
lift_i= lift_inb.*lift_imax/maxyi;

for i=1:length(theta) %exhaust
      if theta(i)>=open_e && theta(i)<close_e
      %lift_eb(i)= -(theta(i)-open_e)*(theta(i)-close_e);
      [s] = Cam_Profile_Function_E(lift_emax, duration_e,theta(i), open_e);
      lift_eb(i)=s;
      else
      lift_eb(i)=0;
      end
end
maxye= max(lift_eb);
lift_e= lift_eb.*lift_emax/maxye;
```

```
%plot
if q==1
      figure
      plot(theta*180/pi, lift_i*1000)
      hold on
      plot(theta*180/pi, lift_e*1000)
      xlabel('Crank Angle (degrees)')
      ylabel('Valve Lift (mm)')
      title(['Valve Lift vs Crank Angle at ' num2str(RPM) ' RPM'])
      legend('Intake Lift', 'Exhaust Lift')
      txt = convertCharsToStrings([...
      'Inlet Max Lift:' num2str(lift_imax*1000) 'mm' newline...
      'Exhaust Max Lift:' num2str(lift_emax*1000) 'mm' newline...
      'Overlap:' num2str(overlap) ' degrees']);
      dim = [.2 .5 .3 .3];
      annotation('textbox',dim,'String',txt,'FitBoxToText','on');
    grid
end


%% Minimum Valve Area
%Equations 6.7-6.9 in Heywood
%Assume Dp=D_intake for full port design

%Intake
for j=1:length(theta)
      if w_i/(sin(B)*cos(B)) > lift_i(j)
      Amin_i(j) = pi * lift_i(j) * cos(B) * (Dv_i - 2*w_i + lift_i(j)/2 *
sin(2*B));
      %disp('low')
      elseif ((((D_intake^2-Ds_i^2)/(4*Dm_i))^2 - w_i^2)^(1/2) + w_i *
tan(B) >= lift_i(j)) && (lift_i(j) > w_i / (sin(B) *cos(B)))
      Amin_i(j) = pi * Dm_i * ((lift_i(j) - w_i * tan(B))^2 + w_i^2)^(1/2);
      % disp('med')
      elseif lift_i(j) > ((((D_intake^2 - Ds_i^2)/(4*Dm_i))^2 - w_i^2)^(1/2)
+ w_i * tan(B))
      Amin_i(j) = pi / 4 * (D_intake^2 - Ds_i^2);
      %disp('high')
      else
      Amin_i(j)=0;
      end
end



%Exhaust
for j=1:length(theta)
      if w_e/(sin(B)*cos(B)) > lift_e(j)
```

```
      Amin_e(j) = pi * lift_e(j) * cos(B) * (Dv_e - 2*w_e + lift_e(j)/2 *
sin(2*B));
      %disp('low')
      elseif ((((D_exhaust^2-Ds_e^2)/(4*Dm_e))^2 - w_e^2)^(1/2) + w_e *
tan(B) >= lift_e(j)) && (lift_e(j) > w_e / (sin(B) *cos(B)))
      Amin_e(j) = pi * Dm_e * ((lift_e(j) - w_e * tan(B))^2 + w_e^2)^(1/2);
      % disp('med')
      elseif lift_e(j) > ((((D_exhaust^2 - Ds_e^2)/(4*Dm_e))^2 - w_e^2)^(1/2)
+ w_e * tan(B))
      Amin_e(j) = pi / 4 * (D_exhaust^2 - Ds_e^2);
      %disp('high')
      else
      Amin_e(j)=0;
      end
end

%plotting
if q==1
      figure

      plot(theta*180/pi, Amin_i)
      hold on
      plot(theta*180/pi, Amin_e)
      legend('Intake', 'Exhaust')
      xlabel('Crank Angle')
      ylabel('Valve Flow Area (m^2)')
      title(['Minimum Valve Flow Area vs Crank Angle at ' num2str(RPM) '
RPM'])
      grid
  txt = convertCharsToStrings([...
      'Inlet Max Lift:' num2str(lift_imax*1000) 'mm' newline...
      'Exhaust Max Lift:' num2str(lift_emax*1000) 'mm' newline...
      'Overlap:' num2str(overlap) ' degrees' newline]);
      annotation('textbox',dim,'String',txt,'FitBoxToText','on');
end


%% Cd Trends
%Trends from Figures 6.18 and 6.16 in Heywood Respectively

%Exhaust
Cd_fit_e = [.68; .695; .75; .685; .65; .595];
LvDv_fit_e = [.025; .1; .15; .225; .28; .325];
sf_e = fit(LvDv_fit_e, Cd_fit_e, 'poly3');
for i=1:length(lift_e)
      if lift_e(i)==0
      LvDv_e(i) =  lift_e(i)/ Dv_e;
      Cd_e(i)=0;
```

```
      else
      LvDv_e(i) =  lift_e(i)/ Dv_e;
      Cd_e(i) = sf_e(LvDv_e(i));
      end
end


% Intake
LvDv_i = lift_i./Dv_i;
for j=1:length(lift_i)
      if LvDv_i(j)==0
      Cd_i(j)=0;
      stage(j)=0;
      % Stage 1
      elseif LvDv_i(j) >0 && LvDv_i(j) <= .08
        Cd_fit_i = [.52; .595; .62; .64];
      LvDv_fit_i = [0; 0.055; .07; .08];
      sf_i = fit(LvDv_fit_i, Cd_fit_i, 'poly2');
      stage(j)=1;
      Cd_i(j) = sf_i(LvDv_i(j));

      % Connection between 1-2
      elseif LvDv_i(j) > .08 && LvDv_i(j) <= .105
      Cd_fit_i = [.65 ;.56];
      LvDv_fit_i = [0.085; .105];
      sf_i = fit(LvDv_fit_i, Cd_fit_i,'poly1');
      stage(j)=1.5;
      Cd_i(j) = sf_i(LvDv_i(j));

      % Stage 2
      elseif LvDv_i(j) > .105 && LvDv_i(j) <= .17
      Cd_fit_i = [.56; .565;.585; .625;.65];
      LvDv_fit_i = [.105; .11;.135 ;.15; .17];
      sf_i = fit(LvDv_fit_i, Cd_fit_i,'poly2');
      stage(j)=2;
      Cd_i(j) = sf_i(LvDv_i(j));

      % Stage 3
      elseif LvDv_i(j) > .17
      %&& LvDv_i(j) <= .25 can put this back in if statement and add
      %other if statement at the top
      Cd_fit_i = [.65; .625;.605; .49];
      LvDv_fit_i = [.17; .18; .19; .25];
      sf_i = fit(LvDv_fit_i, Cd_fit_i, 'poly2');
      stage(j)=3;
      Cd_i(j) = sf_i(LvDv_i(j));
```

```
        else
        Cd_i(j) = 0.6;
        stage(j)=4;

        end
end

%plotting
if q==1
        figure
        plot(theta*180/pi, Cd_i)
        hold on
        plot(theta*180/pi,Cd_e)
        legend('Inlet Cd', 'Exhaust Cd')
        xlabel('Crank Angle (degrees')
        ylabel('Cd')
        title(['Flow Coefficient vs Crank Angle at ' num2str(RPM) ' RPM'])
        grid
        txt = convertCharsToStrings([...
        'Inlet Max Lift:' num2str(lift_imax*1000) 'mm' newline...
        'Exhaust Max Lift:' num2str(lift_emax*1000) 'mm' newline...
        'Overlap:' num2str(overlap) ' degrees']);
        annotation('textbox',dim,'String',txt,'FitBoxToText','on');

        figure
        plot(LvDv_i, Cd_i, 'b*')
        hold on
        plot(LvDv_e, Cd_e, 'r*')
        xlabel('Lift/Diameter')
        ylabel('Flow Coefficient (Cd)')
        title('Flow Coefficient vs Lift/Bore')
        grid
end


%% Mass Flows with Respect to Time:
% Intake and Exhaust

disp(RPM)
T= 60/RPM; %seconds per revolution;
Ra= 2*pi; %radians per revolution
TR=T/Ra; %seconds per radian
Time= theta*TR;
dt=Time(2)-Time(1);

[~,~,~, Vtheta, ~] = ...
VolumeCalc(theta,D, rc,crank_rad, bore, Sp_avg,C, R_rodrad);
```

```
clear conte countmix counti countnone1 countnone2
counte=0;
countmix=0;
counti=0;
countnone1=0;
countnone2=0;

dm_eloop=zeros(1,length(theta)-1);
dm_iloop=zeros(1,length(theta)-1);

for i=1:length(theta)-1

  [~,~,R,gamma(i)] = GammaCalc(Tcylloop(i),Pcylloop(i), phi, mix);
  c(i)= sqrt(gamma(i)*R*Tcylloop(i)); %speed of sound


  rhocyl(i)= Pcylloop(i)/(Tcylloop(i)*R);

      if theta(i)<open_e %Nothing open
      countnone1=countnone1+1;

      m_total_loop(i+1)=m_total_loop(i);
      Pcylloop(i+1)=Pcylloop(i);
      Tcylloop(i+1)=Tcylloop(i);

      elseif theta(i)>close_i %Nothing open
      countnone2=countnone2+1;

      m_total_loop(i+1)=m_total_loop(i);
      Pcylloop(i+1)=Pcylloop(i);
      Tcylloop(i+1)=Tcylloop(i);

      elseif theta(i)>=open_e && theta(i)<=open_i %exhaust open
      counte=counte+1;

       if P0_e<Pcylloop(i) %Normal Flow
            %Note that dm is mass flow leaving the piston
      dm_eloop(i)= -
2*Cd_e(i)*Amin_e(i)*Pcylloop(i)/(R*Tcylloop(i))^.5*(P0_e/Pcylloop(i))^(1/gamm
a(i))*(2*gamma(i)...
            /(gamma(i)-1)*(1-(P0_e/Pcylloop(i))^((gamma(i)-
1)/gamma(i))))^.5; %Heywood
      direction(i)=1;

      %CHOKED
      if P0_e/Pcylloop(i)<= ((gamma(i)+1)/2)^-(gamma(i)/(gamma(i)-1))/10
            disp([ ' ' num2str(P0_e/Pcylloop(i)) '<'
num2str(((gamma(i)+1)/2)^-(gamma(i)/(gamma(i)-1))) ' '])
```

```
            choked(i)=1;
            dm_eloop(i)= -
2*Cd_e(i)*rhocyl(i)*Amin_e(i)/c(i)*gamma(i)*(2/(gamma(i)+1))^...
                  ((gamma(i)+1)/(2*(gamma(i)-1))); %From Heywood
      else
            choked(i)=0;
      end
      if imag(dm_eloop(i))~=0
            disp(1)
            return
      end


      else %Reverse Flow
      dm_eloop(i)=
2*Cd_e(i)*Amin_e(i)*P0_e/(R*Tcylloop(i))^.5*(P0_e/Pcylloop(i))^-
(1/gamma(i))*(2*gamma(i)...
            /(gamma(i)-1)*(1-(P0_e/Pcylloop(i))^-((gamma(i)-
1)/gamma(i))))^.5; %Heywood
      direction(i)=2;
      %disp([ ' ' num2str(P0_e) '>' num2str(Pcyl(i))])
      if imag(dm_eloop(i))~=0
            disp(2)
            return
            end
      end
        veloc_e(i)=abs(real(dm_eloop(i)))/(rhocyl(i)*Amin_e(i));
      %exhaust flow velocity

      dt=Time(2)-Time(1); %time step

        m_total_loop(i+1)=m_total_loop(i)+dm_eloop(i)*dt;
      %new total mass in engine
      if m_total_loop(i+1) <0
            m_total_loop(i+1)=0.000001;
      end

        rhocyl(i+1)=m_total_loop(i+1)/Vtheta(i+1);
      %cylinder density

      Tcylloop(i+1)=Tcylloop(i);
      if dm_eloop(i)~=0
        Pcylloop(i+1)=rhocyl(i+1)*R*Tcylloop(i+1);
      %Cylinder pressure
      end


      elseif theta(i)>open_i && theta(i)<close_e %Both valves open
```

```
      countmix=countmix+1;

      if P0_i>Pcylloop(i) %Intake Flow

            dm_iloop(i)=
2*Cd_i(i)*Amin_i(i)*P0_i/(R*Tcylloop(i))^.5*(Pcylloop(i)/P0_i)^(1/gamma(i))*(
2*gamma(i)...
                /(gamma(i)-1)*(1-(Pcylloop(i)/P0_i)^((gamma(i)-
1)/gamma(i))))^.5; %Heywood

            Tcylloop(i+1)= (m_total_loop(i)*Tcylloop(i)+T0_i*dm_iloop(i)*dt)/
(m_total_loop(i)+dm_iloop(i)*dt);
            %Simplified T change

            direction_i(i)=1;
      else %reverse flow into intake
            dm_iloop(i)= -2*Cd_i(i)*Amin_i(i)*Pcylloop(i)/(R*Tcylloop(i))
^.5*(P0_i/Pcylloop(i))^(1/gamma(i))*(2*gamma(i)                /(gamma(i)-
1)*(1-(P0_i/Pcylloop(i))^((gamma(i)-1)/gamma(i))))^.5; %Heywood
            Tcylloop(i+1)=Tcylloop(i);
                  direction_i(i)=2;
                 % disp([ ' ' num2str(P0_i) '<' num2str(Pcyl(i))])
            if imag(dm_iloop(i))~=0
                  disp(2)
                  return
            end
      end

      if P0_e<Pcylloop(i) %Exhaust Flow
            dm_eloop(i)= -
2*Cd_e(i)*Amin_e(i)*Pcylloop(i)/(R*Tcylloop(i))^.5*(P0_e/Pcylloop(i))^(1/gamm
a(i))*(2*gamma(i)                /(gamma(i)-1)*(1-
(P0_e/Pcylloop(i))^((gamma(i)-1)/gamma(i))))^.5; %Heywood
            direction(i)=1;
      else %Reverse Flow from exhaust
             dm_eloop(i)=
2*Cd_e(i)*Amin_e(i)*P0_e/(R*Tcylloop(i))^.5*(P0_e/Pcylloop(i))^-
(1/gamma(i))*(2*gamma(i)/(gamma(i)-1)*(1-(P0_e/Pcylloop(i))^- ((gamma(i)-
1)/gamma(i))))^.5; %Heywood
            direction(i)=2;
            %disp([ ' ' num2str(P0_e) '>' num2str(Pcyl(i))])
            if imag(dm_eloop(i))~=0
                  disp(2)
                  return
            end
      end

        m_total_loop(i+1)=m_total_loop(i)+dm_iloop(i)*dt+dm_eloop(i)*dt;
```

```
      Tcylloop(i+1)=
(m_total_loop(i)*Tcylloop(i)+T0_i*dm_iloop(i)*dt+dm_eloop(i)*dt*Tcylloop(i))/
(m_total_loop(i)+dm_iloop(i)*dt+dm_eloop(i)*dt); %Simplified T change

      Pcylloop(i+1)= m_total_loop(i+1)*R*Tcylloop(i+1)/Vtheta(i+1);


      elseif theta(i)>=close_e && theta(i)<=close_i %Intake Open
      %  Intake
      counti=counti+1;

      if P0_i>Pcylloop(i) %Normal Flow
      %Equations from ferguson 5.1
      dm_iloop(i)=
2*Cd_i(i)*Amin_i(i)*P0_i/(R*Tcylloop(i))^.5*(Pcylloop(i)/P0_i)^(1/gamma(i))*(
2*gamma(i)/(gamma(i)-1)*(1-(Pcylloop(i)/P0_i)^((gamma(i)-1) /gamma(i))))^.5;

      Tcylloop(i+1)=
(m_total_loop(i)*Tcylloop(i)+T0_i*dm_iloop(i)*dt)/(m_total_loop(i)+dm_iloop(i
)*dt); %Simplified T change
      direction_i(i)=1;

      %CHOKED
      if Pcylloop(i)/P0_i<= ((gamma(i)+1)/2)^-(gamma(i)/(gamma(i)-1))/10
            disp([ ' ' num2str(P0_i/Pcylloop(i)) '<'
num2str(((gamma(i)+1)/2)^-(gamma(i)/(gamma(i)-1))) ' '])
            choked_i(i)=1;
            dm_iloop(i)=
2*Cd_i(i)*rhocyl(i)*Amin_i(i)/c(i)*gamma(i)*(2/(gamma(i)+1))^...
                ((gamma(i)+1)/(2*(gamma(i)-1))); %From Heywood
            Tcylloop(i+1)=
(m_total_loop(i)*Tcylloop(i)+T0_i*dm_iloop(i)*dt)/(m_total_loop(i)+dm_iloop(i
)*dt); %Simplified T change

      else
            choked_i(i)=0;
      end
            if imag(dm_iloop(i))~=0
                  disp(3)
                  return
            end

            else %Reverse Flow
                  dm_iloop(i)= -
2*Cd_i(i)*Amin_i(i)*Pcylloop(i)/(R*Tcylloop(i))^.5*(P0_i/Pcylloop(i))^(1/gamm
a(i))*(2*gamma(i/(gamma(i)-1)*(1-(P0_i/Pcylloop(i))^( (gamma(i)-
1)/gamma(i)))) ^.5; %Heywood
            Tcylloop(i+1)=Tcylloop(i);
```

```
                direction_i(i)=2;
                %disp([ ' ' num2str(P0_i) '<' num2str(Pcyl(i))])

            if imag(dm_iloop(i))~=0
                disp(2)
                return
            end
      end
        velocloop_i(i)=abs(real(dm_iloop(i)))/(rhocyl(i)*Amin_i(i));

        m_total_loop(i+1)=m_total_loop(i)+dm_iloop(i)*dt;
      if m_total_loop(i+1) <0
          m_total_loop(i+1)=0.000001;
      end
        rhocyl(i+1)=m_total_loop(i+1)/Vtheta(i+1);

      if dm_iloop(i)~=0
      Pcylloop(i+1)=rhocyl(i+1)*R*Tcylloop(i+1);
      end
      end
end

Ev_eloop= 1-m_total_loop(counte+countnone1)/m_total_loop(1);
% exhaust volumetric efficicncy

Ev_iloop= m_total_loop(end)/m_total_loop(1);
%intake volumetric efficiency

Ev_totloop= Ev_eloop*Ev_iloop;
%total volumetric efficiency

%% Pumping Losses Estimate
% W=PdV
Wexhaust=0;
Wintake=0;
for z=1:length(theta)
      if theta(z)>-pi && theta(z)<0 %Exhaust pumping
    Wexhaust=Wexhaust+abs(Pcylloop(z)-P0_e)*(Vtheta(z-1)-Vtheta(z));

      elseif theta(z)>0 && theta(z)<pi
      Wintake= Wintake+abs(Pcylloop(z)-P0_i)*(Vtheta(z)-Vtheta(z-1));
      end
end

end
```

Cam_Profile_Function_I.m

```
function [s] = Cam_Profile_Function_I(lift_imax, duration_i,theta, open_i)
% Equations taken from Design of Machinery
%This program outputs a polynomial for a more accurate lift curve for the
intake cam
% Alex Kushner and Carter Waligura
h = lift_imax; %
beta = duration_i*180/pi;% degrees- enter desired value: Inlet 70, Exhaust 65
d1=20; % base circle diameter
%%coef=[a b c d]'
x=beta;
x1=beta/2;
l=[x^3 x^4 x^5 x^6;
      3*x^2 4*x^3 5*x^4 6*x^5;
      6*x 12*x^2 20*x^3 30*x^4;
      x1^3 x1^4 x1^5 x1^6];
w=[0 0 0 h]';
coef=linsolve(l,w);
a=coef(1);
b=coef(2);
c=coef(3);
d=coef(4);
q=theta*180/pi-open_i*180/pi;
s=a*q^3+b*q^4+c*q^5+d*q^6;
end
```

Cam_Profile_Function_E.m

```
function [s] = Cam_Profile_Function_E(lift_emax, duration_e,theta, open_e)
% Equations taken from Design of Machinery -
%This program outputs a polynomial for a more accurate lift curve for the
%exhaust cam
%Alex Kushner and Carter Waligura
h = lift_emax; % maximum lift in mm
beta = duration_e*180/pi;% degrees- enter desired value: Inlet 70, Exhaust 65
d1=20; % base circle diameter
x=beta;
x1=beta/2;
l=[x^3 x^4 x^5 x^6;
      3*x^2 4*x^3 5*x^4 6*x^5;
      6*x 12*x^2 20*x^3 30*x^4;
      x1^3 x1^4 x1^5 x1^6];
w=[0 0 0 h]';
coef=linsolve(l,w);
a=coef(1);
b=coef(2);
c=coef(3);
d=coef(4);
q=theta*180/pi-open_e*180/pi;
s=a*q^3+b*q^4+c*q^5+d*q^6
end
```

Cooling.m

```
function [Flow_rate] = Coolant_flow
(Vmin,bore,stroke,Sp_avg,D_cc,T1,Pcyl,Tcyl,RPM,theta,q)
%Heat transfer out of cylinder take 2
%Specify coolant temp 90 degrees c
%Run AirFlowModelBTNtest

% for Count= 1:length(N)
%Need air flow through cylinder
Cyl_air = zeros(1,361);
V1=((D_cc/3/100^3)+Vmin);

Swirl_ratio = 3; %approximated from Heywood
Paddle_velocity = 2*pi()*RPM*Swirl_ratio/60; %rad/s, paddle velocity
Swirl_velocity = bore*Paddle_velocity/2; %m/s, swirl velocity
pressure_max =10733000*ones(length(theta)); %maximum pressure (pa)
P1=101300;

for z= 1: length(theta)
      if z <(length(theta)-1)/4+1
      C_1 = 6.18 + 0.417*Swirl_velocity/Sp_avg(q);
      C_2 = 0;
      w(z) = C_1*Sp_avg(q) + C_2*(D_cc/3/100^3*T1*(-
Pcyl(q,z))+pressure_max(z))/(P1*V1);
      end

      if z >= (length(theta)-1)/4+1 && z < ((length(theta)-1)/2)+1
      C_1 = 2.28 + 0.308*Swirl_velocity/Sp_avg(q);
      C_2 = 0;
      w(z) = C_1*Sp_avg(q) + C_2*(D_cc/3/100^3*T1*(-
Pcyl(q,z)+pressure_max(z)))/(P1*V1);
      end

      if z >= ((length(theta)-1)/2)+1 && z < (3*(length(theta)-1)/4)+1
      C_1 = 2.28 + 0.308*Swirl_velocity/Sp_avg(q);
      C_2 = 3.24*10^-3;
      w(z) = C_1*Sp_avg(q) + C_2*(D_cc/3/100^3*T1*((-
Pcyl(q,z)+pressure_max(z))))/(P1*V1);
      end

      if  z >= (3*(length(theta)-1)/4)+1 && z < length(theta)
      C_1 = 6.18 + 0.417*Swirl_velocity/Sp_avg(q);
      C_2 = 0;
      w(z) = C_1*Sp_avg(q) + C_2*(D_cc/3/100^3*T1*(-
Pcyl(q,z))+pressure_max(z))/(P1*V1);
      end
end



T_ave=(1/length(Tcyl))*trapz(Tcyl(q,:));
Cyl_heatTransfer = 3.26*bore^-0.2*(((Pcyl(q,z))./1000)^0.8).*(T_ave^-
0.55).*(w.^0.8);
Cyl_heatTransfer_ave = (1/length(Cyl_heatTransfer))*trapz(Cyl_heatTransfer);
```

```
%Coolant properties 50/50 ethylene glycol water
T_coolant=80+273.15; % degrees celsius coolant
k_c = 0.47; %W/m-K, thermal conductivity of coolant, 50/50 Mix, Pulkabrek
c_p_c = 3.74*10^3; %J/mol-K, specific heat of coolant, 50/50 Mix, Pulkabrek
mu_water = 1.13*10^-5; %kg/m-s, dynamic viscosity of water @90degC
mu_ethyleneglycol = .0162; %kg/m-s, dynamic viscosity of ethylene glycol
rho_water = 977; %kg/m^3, density of water @90degC
rho_ethyleneglycol = 1109; %kg/m^3, density of ethylene glycol @20degC
mu_coolant = .5*mu_water+.5*mu_ethyleneglycol; %kg/m-s approx dynamic
viscosity of mix
rho_coolant = .5*rho_water+.5*rho_ethyleneglycol; %kg/m^3, estimated density
of mix
nu_coolant = mu_coolant/rho_coolant; %m^2/s, kinematic viscosity of coolant

%Engine properties
Thickness_S=.0045; %sleeve thickness m
K_S=148; %Thermal conductivity of sleeve W/m*k
Thickness_W=.0045; %Wall thickness m
K_W=148; %Thermal conductivity of Wall W/m*k
T_desired=55+273.15; %desired engine surface temperature

%Flow properties
L=.075; %M
Perimeter=.75; %M
Aext=Perimeter*L; %M^2
ChannelW=.005; %M
Section_perimeter=2*ChannelW+2*L; %M
Xarea=L*ChannelW; %M^2
VolumeCool=Xarea*Perimeter; %M^3
Dia_hydro= 4*((Xarea)/Section_perimeter); %Hydraulic Diameter of
channel=4*A/P

%Initial guesses
Flow_rate=.001; %L/s
T_outside_calc_avg=2000;

while  T_outside_calc_avg>T_desired
      Cool_flow=Flow_rate/1000; %coolant flow m/s
      Rey_coolant=Cool_flow*Dia_hydro/nu_coolant;
      Pr_coolant=mu_coolant*c_p_c/k_c;

      Nu_coolant=(.3387*Pr_coolant^(1/3)*Rey_coolant^0.5)/((1+(0.0468/Pr_cool
ant)^(2/3))^0.25);

      H_coolant=Nu_coolant* k_c/Dia_hydro;

    Q_tot=(Tcyl(q,:)-
T_coolant)*(((1./Cyl_heatTransfer_ave)+(Thickness_S/K_S)+(Thickness_W/K_W)+(1
/H_coolant))^-1);
      Q_tot_avg = (1/360)*trapz(Q_tot);

      A = .242; %m^2 surface area of external cooling
```

```
      Acyl=(stroke*bore*pi())+(pi()*(bore^2)/2);

      R_1 = 1/(Cyl_heatTransfer_ave*Acyl) + + Thickness_S/(K_S*Aext) +
(Thickness_W/(K_W*Aext));
      R_c = 3/(H_coolant*Aext) + ChannelW/(k_c*Aext);
      R_m = ChannelW/(K_W*Aext);
      R_2 = (1/R_c + 1/R_m)^-1;
      R_3 = Thickness_W/(K_W*Aext);
      R_th = R_1 + R_2 + R_3;

      T_outside_calc = Tcyl(q,:) - Q_tot.*R_th.*A;
      T_outside_calc_avg = (1/360)*trapz(T_outside_calc);

      Flow_rate = Flow_rate + .01;

end
Rey_coolant
Flow_rate = Flow_rate - .01;

end
```

MechanicalEff.m

```
function [W_f] = losses(N,k,stroke)
%Mechanical Inefficiencies
%In cylinder conditions
%Inefficiency versus RPM
%Look at friction on cylinder walls how that changes with piston speed
%Approximate range should be between 75 and 90%


%Need to download airflow modelbtn and OttoCycleI3Real

%Energy loss = Force*Distance
%Force= Force of Friction= Mu_c*Fnormal
Scc=.8; %Surface Contact Constant
Mu_s=.17; %Friction metal
Mu_l=.03; %Friction oil

Mu_c=Scc*Mu_s+(1-Scc)*Mu_l;

%Curve fit U must be from 1-17
U=linspace(1,17,length(N));
P_total(k)=-111.61*U(k)^2+3683.9*U(k)+37056;
%P_ringTot= [29999.75, 34031, 37874.75, 41531, 44999.75, 48281, 51374.75,
54281,...
%     56999.75, 59531, 61874.75, 64031, 65999.75, 67781, 69374.75, 70781,
71999.75,];%Pa 28000 suggested by haywood
%P_ringTot= [33999.75,37781,41374.75,44781,47999.75,51031,53874.75,56531,...
%
58999.75,61281,63374.75,65281,66999.75,68531,69874.75,71031,71999.75];

A_ring=.001*3*.086; %Surface area of 3 rings

F_n(k)=P_total(k)*A_ring; %Normal forces in piston

F_f(k)=F_n(k)*Mu_c; %Friction force on wall

RPS(k)=N(k)/60; %Revolutions each second
D_pistons(k)=2*stroke*RPS(k); %total distance per second

W_f(k)=2*F_f(k)*D_pistons(k); %Work of Friction *2 for full system

%W_mechloss(k)=Wnet_cycle(k)-W_f(k); %total work accounting for friction loss

%Mech_eff(k)=W_mechloss(k)/Wnet_cycle(k); %Percentage efficiency
end
```

EmissionsBTN.m

```
function [NOHC_emis, CO_emis] = EmissionsBTN(phi, AFratio_mass, N, m_dotair,
Vel, Ev_tot)
%This function's purpose is to calculate the g/km emissions of a few
%important exhaust gases and to export these values to the main script for
%analysis

%Carter Waligura

EmissionsMat= CEAEmissions();

AFtarget=AFratio_mass/phi;

[~,closestIndex] = min(abs(AFtarget-EmissionsMat(:,1)));
closestValue = EmissionsMat(closestIndex,1);
CO= EmissionsMat(closestIndex,2);
NOHC= EmissionsMat(closestIndex,3);

figure
plot(EmissionsMat(:,1), EmissionsMat(:,2)*100)
ylabel('CO Mass Percentage')
hold on
yyaxis right
plot(EmissionsMat(:,1), EmissionsMat(:,3)*100)
ylabel('NO+HC Mass Percentage')
title('Emissions Data Varying with AFR from CEA')
xlabel('Air to Fuel Ratio')
legend('CO', 'NO+HC')
grid


m_dotfuel=m_dotair.*phi/AFratio_mass;

m_dottot= (m_dotfuel+m_dotair).*Ev_tot;


m_dotCO= CO*m_dottot;
m_dotNOHC=NOHC*m_dottot;

Speedkm= Vel* 0.00044704; %mi/hr to km/s

CO_emis= m_dotCO./Speedkm';
NOHC_emis= m_dotNOHC./Speedkm';

figure
plot(N,NOHC_emis(1,:)*1000)
hold on
```

```
plot(N, CO_emis(1,:)*1000)
hold on
xlabel('RPM')
ylabel('Emissions (g/km)')
title(['Emissions for an I3 Engine at phi=' num2str(phi) ''])
legend('NO+HC', 'CO')
grid
end
```

CEAEmissions.m

```
function EmissionsMat= CEAEmissions()
%Tabulated emissions data for BTN engine from CEA
%Data is in for: Fuel grade, CO, COOH, HCN, HCO, HNCO, HCOOH, NO
% Carter Waligura and Joel Hauerwas
EmissionsR=[12.6, 0.064632, 0.0000020189, 0.00000014682, 0.00000083826,...
      0.00000058726, 0.00000058858, 0.0025057;12.7, 0.062448,
0.0000020194,...
      0.0000001317, 0.00000079747, 0.00000055367, 0.00000056799,
0.0026928;...
      12.8, 0.060306, 0.0000020167, 0.00000011807, 0.00000075754,...
      0.00000052164, 0.00000054766, 0.0028881;12.9, 0.058208,
0.0000020107,...
      0.00000010578, 0.00000071856, 0.00000049112, 0.00000052762,...
      0.0030913;13, 0.056154, 0.0000020015, 0, 0.00000068062,...
      0.00000046209, 0.00000050791, 0.0033023;13.1, 0.054147,
0.0000019892,...
      0, 0.00000064377, 0.00000043451, 0.00000048855, 0.0035204;13.2,...
      0.052187, 0.0000019739, 0, 0.0000006081, 0.00000040833,
0.00000046958,...
      0.0037453;13.3, 0.050277, 0.0000019557, 0, 0.00000057365,...
      0.00000038352, 0.00000045102, 0.0039765;13.4, 0.048415,
0.0000019347,...
      0, 0.00000054047, 0.00000036004, 0.0000004329, 0.0042133;13.5,...
      0.046605, 0.000001911, 0, 0.00000050858, 0.00000033783,
0.00000041523,...
      0.0044551;13.6, 0.044845, 0.000001885, 0, 0.00000047801,...
      0.00000031686, 0.00000039804, 0.0047012;13.7, 0.043136,...
      0.0000018566, 0, 0.00000044878, 0.00000029706, 0.00000038134,...
      0.004951;13.8, 0.04148, 0.0000018261, 0, 0.00000042088, ...
      0.00000027841, 0.00000036514, 0.0052037;13.9, 0.039874,...
      0.0000017938, 0, 0.00000039432, 0.00000026084, 0.00000034944,...
      0.0054587;14, 0.03832, 0.0000017597, 0, 0.00000036908,
0.00000024431,...
      0.00000033426, 0.005715;14.1, 0.036817, 0.0000017241, 0,
0.00000034513,...
      0.00000022876, 0.00000031959, 0.0059722;14.2, 0.035365,
0.0000016872,...
      0, 0.00000032247, 0.00000021416, 0.00000030544, 0.0062294;14.3,...
      0.033963, 0.0000016492, 0, 0.00000030105, 0.00000020046,...
      0.00000029181, 0.006486;14.4, 0.032609, 0.0000016103, 0,...
      0.00000028083, 0.00000018759, 0.00000027868, 0.0067413;14.5,...
    0.031305, 0.0000015705, 0, 0.00000026179, 0.00000017553,...
      0.00000026605, 0.0069947;14.6, 0.030047, 0.0000015303, 0,...
      0.00000024388, 0.00000016423, 0.00000025393, 0.0072456;14.7,...
      0.028836, 0.0000014896, 0, 0.00000022705, 0.00000015364,...
      0.00000024228, 0.0074936;14.8, 0.02767, 0.0000014486,...
```

```
      0, 0.00000021126, 0.00000014372, 0.00000023112, 0.007738;...
      14.9, 0.026549, 0.0000014075, 0, 0.00000019646, 0.00000013444,...
      0.00000022042, 0.0079785;15, 0.02547, 0.0000013665, 0,...
      0.00000018261, 0.00000012575, 0.00000021017, 0.0082147;15.1, ...
      0.024433, 0.0000013255, 0, 0.00000016965, 0.00000011762, ...
      0.00000020036, 0.0084461;15.2, 0.023436, 0.0000012849, 0,...
      0.00000015755, 0.00000011002, 0.00000019097, 0.0086724;15.3,...
      0.022478, 0.0000012446, 0, 0.00000014625, 0.00000010291,...
      0.000000182, 0.0088934;15.4, 0.021559, 0.0000012047, 0,...
      0.00000013571, 0, 0.00000017343, 0.0091088];

NOEmis= EmissionsR(:, 3:8);
NOCEmis= sum(NOEmis,2);
EmissionsMat= [EmissionsR(:,1:2) NOCEmis]; %AFR; CO, NO and HC
end
```

FuelEfficiencyBTN.m

```
function [MPG] = FuelEfficiencyBTN(m_air,AFratio_mass, phi, N, Wnet_cycle,
torqueReal, Ev_tot, Vel, P_total_weib)
% Program used to determine fuel efficiency through incorporating specific
% fuel consumption and road load power.

%Carter Waligura

% %Road Load Power
 M=400; %kg
 Cd=.45; %drag coefficient
 A= .9; %m^2
 Cr= .015; %road drag coef
 g=9.81; %m/s^2

S=Vel*1.60934; %get in km/hr

Pr=(2.73*Cr*M*g+.0126*Cd*A*S.^2).*S*10^-3;
P_weib=P_total_weib/1000; %kW
Pratio= 1-Pr./P_weib;

trans_scaling= .8;

W_tot_cycle= Wnet_cycle.*Pratio*trans_scaling;
SFC = m_air*Ev_tot*phi/(AFratio_mass)./(W_tot_cycle); %kg/kj
SFC_conv = SFC * 3.6e6; %g/Kw-hr

rho_fuel= 6.30*754.906; %kg/m^3)
torqueReal= torqueReal*1.3558179483314; %Nm
Tr= torqueReal*N*2*pi/60/1000;
mpg= S./(Tr*SFC_conv); %in km/kg
MPG= mpg*rho_fuel*0.00235215; %in mi/gal;
end
```

ConRodForcesBTN.m

```
% Program used to calculate the forces acting on the connecting rod
% Jackson White

% values from SolidWorks, as well as givens from earlier determinations
```

```
ConRodLength = .146; % meters
redline = 8750*pi/30; % rad/s
% redline = 8750*6; % deg/s
ConrodMass = 1.2332; % kg
PistonMass = .32258; % kg
PistonSA = .005268+.0005263; % m^2 piston surface area
Pmax = 10000000; % Pa
Fcombustion = Pmax*PistonSA; % N
ycentmass = .04903; % position of the center of mass along conrod

% represent conrod as rotating(1) and oscillating(2) mass
A = [ycentmass -(ConRodLength-ycentmass); 1 1];
B = [0; ConrodMass];
C= A\B;
m1 = C(1);
m2 = C(2);
mtau = m2+PistonMass; % total reciprocating mass

hold on;
xlim([-180 180])
fv = @(x) (mtau*(redline^2)*.043*(cosd(x)+(.043/.146)*cosd(2*x))); %
calculating the vertical inertial forces
vert = fv(-179:180);
comb = [101309.7207… …509845.0086];
comb = comb.*(-1*PistonSA);% determining vertical combustion forces
% from thermo combustion pressures
vert = -vert+comb; % total vertical forces
plot(-179:180,vert,'r'); % plotting vertical forces
fh = @(x) -m2*(redline^2)*.043*sind(x); % Determining Horizontal
(inertial)   % forces
fplot(fh, [-180 180], 'b'); % plotting horizontal forces
ylabel('Force(N)');
xlabel('Crank Angle(Degrees)');
title('Horizontal and Vertical Forces on Connecting Rod');
hold off;
```

Balanceshaft.m

```
r=.086/2; %crank throw diam (m)
mcon=.80832+.23592;
mpis=.346;
mwp=.059;
mp=mcon+mpis+mwp;
la=.104;
rb=.025;
l3=.273;
mb=.433*mp*r*(la/l3)/rb;
```

Unbalance.m

```
r=.086/2; %crank throw diam (m)
mcon=.80832+.23592;
mpis=.346;
mwp=.059;
mp=mcon+mpis+mwp;
la=.104;
w=9000*pi()/30;
alpha=(0:360);
m=[]
m1=[]
for a=(0:360)
      m(end+1)=.5*sqrt(3)*mp*r*w^2*la*(cos((a-210)*pi()/180));
end
for a=(0:360)
      m1(end+1)=.5*sqrt(3)*mp*r^2*w^2*(la/.270)*cos((2*a-150)*pi()/180);
end
mt=m+m1;
figure
plot(alpha,mt)
hold on
plot(alpha,-1*m)
plot(alpha,mt-m)
legend('Rocking Moment w/o BS','BS Momement','Rocking Moment w/
BS','FontSize', 12)
title('Inline 3 Cylinder Rocking Moment','FontSize', 20)
xlabel('Crankshaft Angle (Deg)','FontSize', 20)
ylabel('Moment (Nm)','FontSize', 20)
grid on


xlim([0 360])
```

Cam.m

```
% Equations taken from Design of Machinary - Norton and

h = 12; % maximum lift in mm
beta = 230/2;% degrees- enter desired value: Inlet 70, Exhaust 65
d1=30; % base circle diameter
%%coef=[a b c d]'
x=1;
x1=.5;
q=[x^4 x^5 x^6 x^7;
      4*x^3 5*x^4 6*x^5 7*x^6;
      12*x^2 20*x^3 30*x^4 42*x^5;
      x1^4 x1^5 x1^6 x1^7];
w=[0 0 0 12]';
coef=linsolve(q,w);
a=coef(1);
b=coef(2);
c=coef(3);
d=coef(4);
syms q
s=a*q^3+b*q^4+c*q^5+d*q^6;
v=diff(s);
a=diff(v);
j=diff(a);
% figure
% fplot(s,[0 1])
% title("s")
% figure
% fplot(v,[0 1])
% title("v")
% figure
% fplot(a,[0 1])
% title("a")
% figure
% fplot(j,[0 1])
% title("j")
%%
x = [0:1:beta];
for  theta = [0:1:beta]
p=theta;
s1(theta+1) = subs(s,q,p);
v1(theta+1) = subs(v,q,p);
a1(theta+1) = subs(a,q,p);
j1(theta+1) = subs(j,q,p);
end
%svaj plots in degrees x = [0:1:beta];
figure
plot(x,s1)
```

```
title('Displacement')
xlabel('Cam Angle (deg)')
ylabel('Lift (mm)')
xlim([0 beta])

figure
plot(x,v1)
title('Velocity')
xlabel('Cam Angle (deg)')
ylabel('Velocity (mm/deg)')
xlim([0 beta])

figure
plot(x,a1)
title('Acceleration')
xlabel('Cam Angle (deg)')
ylabel('Acceleration (mm/deg^2)')
xlim([0 beta])

figure
plot(x,j)
title('Jerk')
xlabel('Cam Angle (deg)')
ylabel('Jerk (mm/deg^3)')
%%
u=d1*ones(1,length(s1))+s1;
s2=flip(s1);
%figure
%polarplot(x*pi/180,u)

x1=beta*ones(1,length(x))+x;
%figure
%polarplot(x1*pi/180,u1)

cx=(beta:1:360);
cu=d1*ones(1,length(cx));
ccu=zeros(1,length(cx));

xt=[x,cx];
ut=[u,cu];
zt=[s1,s2,ccu]';
z=double(s1');
zx=(0:1:beta)';
figure
polarplot(xt*pi/180,ut)

[xf,yf]=pol2cart(xt*pi/180,ut)
grid off
```

F - FMEA

Subsystem	Part Name	Failure Mode	Failure Effects	Potential Causes	Detection	S	O	D	RPN	Recommended Action	S	O	D	RPN
Crank Train	**Piston**	Crown Break-Through	Loss of Compression	Fatigue, Thin wall	Less power	3.5	1.5	1	5.25	Use FEA	3.5	1	1	3.5
		Cracking	Eventual failure	Fatigue	Undetectable before failure	3	2	5	30	Use FEA	3	1	5	15
		Seizure	Loss of power	Piston expands more rapidly than walls of cylinder causing jamming	Smoke, strange noise	3.5	1.5	1	5.25	Check that spark plug temperature is not too high	3.5	1	1	3.5
	Wrist Pin	Fracture	Loss of Compression	Fatigue, excessive force	Eventual loss of compression change in noise	3	2	2	12	Change material	3	1	2	6
		Retaining ring failure	Shifting of wrist pin could cause excessive forces on weaker portions and eventually lead to fracture	Wear, improper retaining ring installation, lack of concentricity	Undetectable before failure	2	2	5	20	Creation of tools to ensure proper alignment of wrist pin in piston	2	1	5	10
	Connecting Rod	Fracture	Decreased Engine performance, Possible engine failure, noise	Fatigue, Overload, lack of lubrication	Surface Inspections	3	2	2	12	Quality assurance in manufacturing	3	1.5	1.5	6.75
	Crankshaft	Fracture	Engine Failure	Fatigue, Material Defects	Surface Inspection	5	2.5	2	25	Quality assurance in manufacturing	5	1.5	1.5	11.25

	Crankshaft Timing Sprocket	Breaks	Valve Collision	Fatigue, Weak Chain	Engine shuts off	4	2	1	8	Use larger chain and sprocket	4	1.5	1	6
Cylinder Head	**Camshaft**	Lobes wear off	Lack of valve opening	Improper wear behavior	Loss in performance	3	2.5	2	15	Cyrotreat Camshaft	3	1	2	6
	Rocker arms	Fracture	Ineffective valve opening	Fatigue, Excessive Stress Concentrations	Loss in performance, Engine failure	3	2	3	18	Choose suitable material and appropriate factor of safety	3	1	2	6
		Mechan-ical Failure	Ineffective valve opening	Improper heat treatment	Loss in performance, Engine failure	3	1.5	3	13.5	Conduct proper heat treatment processes	3	1	2	6
	Keepers	Groove failure	Valve spring unretained, valve can drop into cylinder	Excess spring pressure/incorrect installed height induces excess stress in groove area	Loss in performance	3.5	1.5	2.5	13.125	Test load of springs once installed Groove rolled instead of machined	3	1	2.5	7.5
	Retainers	Flange yielding	Valve spring unretained, valve no longer able to close	Excess spring pressure, incorrect installed height of springs	Loss in performance	2	2	3	12	Test load of springs once installed	2	1	3	6
	Inlet Valve	Valve tip wears down	Valve lift reduced, can lead to valve not opening	Excess force on valve tip from rocker arm, incorrect installation of rocker arms	Loss in performance	2	2	3	12	Use hardened valve tips	2	1	3	6
		Chan-neling	Can lead to portion of valve melting/warping. Improper valve seal	Excessive temperatures on valve face created by peening (excess temp causes expansion, induces compressive stresses)	oval shaped heat discoloration on bottom face of valve, loss in performance	2	1.5	3	9	Sodium filled hollow stem to further improve cooling	2	1	3	6
		Off-Square seating	Subjects valve stem to large side loading, valve stem breakage	Valve face and guide not aligned concentrically	Loss in performance	2.5	2	3.5	17.5	Assembly drawings should make use of GD&T to specify concentricity to 0.002" per 1.5" of valve diameter	2.5	1	3.5	8.75

	Ex-haust Valve	Valve tip wears down	Valve lift reduced, can lead to valve not opening	Excess force on valve tip from rocker arm, incorrect instalation of rocker arms, poor afr, inadequate cooling	Loss in performance, engine failure	3	2	3	18	Use hardened valve tips	3	1	3	9
		Chan-neling	Can lead to portion of valve melting/warping. Improper valve seal	Excessive temperatures on valve face created by peening, poor afr, inadequate cooling	oval shaped heat discoloration on bottom face of valve, loss in performance	2	3	3	18	Sodium filled hollow stem to further improve cooling	2	1	3	6
		Off-Square seating	Subjects valve stem to large side loading, valve stem breakage	Valve face and guide not aligned concentrically	Loss in performance	2.5	2	3.5	17.5	Assembly drawings should make use of GD&T to specify concentricity to 0.002" per 1.5" of valve diameter	2.5	1	3.5	8.75
	Valve Seat	Valve mating surface wears down	Improper valve seal	Excess spring forces cause higher impact with seat	Loss in performance	2	1.5	4	12	Have adjustable valve lash to reduce closing speeds. Use wear resistant, hardened valve seat	2	1	4	8
	VVT	Shifting sprocket fails fails to shift	Excessive oil pressure or low oil pressure through the sprocket	Oil solenoid fails to actuate	Loss in efficiency	1	1	1	1	Replace oil solenoid	1	1	1	1
	DVVL	Shift cam fails to shift	Loss of high end performance gain	Linear actuators fail to move	Loss in performance	1	1	1	1	Replace linear actuators	1	2	2	4
	Combustion Cham-ber	Cracked	Lost of compression	Excess pressure in chamber	Loss in performance	3	1.5	3	13.5	Do FEA to improve strength				0
En-gine Block	**Cool-ant Chan-nels**	Cracks	Engine overheats	Thin walls, bad casting	Engine fails to operate	4	2	3	24	Use coolant temp & pressure sensors	2	2	1	4
	Oil Chan-nels	Lubrication leak	Loss of oil supply to components	Thin walls, bad casting	Loss of efficiency, increased engine noise	4	1.5	3.5	21	Use oil pressure sensor	2	1.5	1.5	4.5

	Cylinder Wall	Fracturing/ Cracking	Loss of combustion	Thin walls, bad casting	Engine fails to operate	5	1	1	5	FEA for cylinder walls	2	1	1	2
	Head Gasket	Bursting	Loss of combustion, burning of oil and/or coolant	Misalignment	Engine fails to operate, blue/white smoke out of exhaust	3	1.5	3	13.5	Use dowels to align gasket	3	1	3	9
	Main Bearing	Wear	Decrease in Engine performance	Insufficient lubrication	Inspection, increased engine noise	3	2	2	12	Implement oil buffer	3	1	2	6
	Main Cap	Fracturing/ Cracking	Engine Failure	Fatigue	Engine Fails to operate	4	2	1	8	Fatigue FEA	4	1	1	4
	Oil Pan Gasket	Leaking	Loss of oil	Improper application of gasket compound	inspection, noise	2	3	2	12	Engine oil level sensor, detailed application guide	2	1	2	4
	Balance Shaft	Sprocket fails	Engine unbalanced	Fatigue, Weak Chain	Increased vibration	2	2	3	12	Use larger chain and sprocket	2	1	3	6
		Weights come loose	Engine unbalanced, component collision	Poor installation, improper bolt selection	Increased vibration/noise	3	2.5	1.5	11.25	Fine pitch bolts, threadlocker	3	1	1.5	4.5
	Oil Pan	Fracturing/ Cracking	Loss of Oil	Fatigue, thermal cycling	increased noise, engine siezure	4.5	2	3	27	Engine oil level sensor, thermal fea	4.5	1	1.5	6.75

G - Professional Meme Section

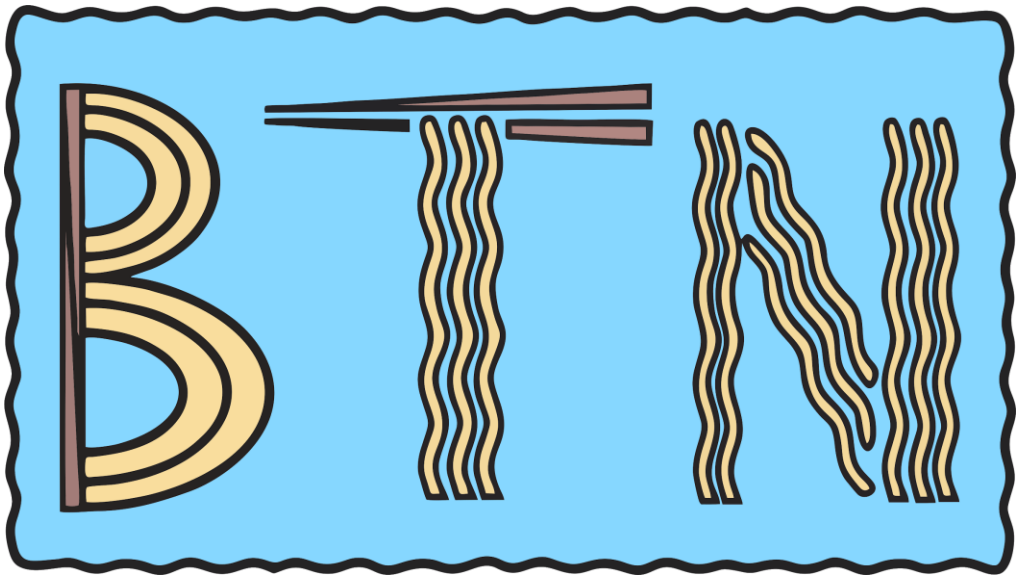

Figure L.1: Original Team Logo

Figure L.2: California compliant Cat

Figure L3: Thermo Team Meeting November, 2019 Colorized